

[Co(TPP)]-Catalyzed Formation of Substituted Piperidines

Bas de Bruin, Marianne Lankelma, Astrid M. Olivares

Submitted date: 07/02/2019 • Posted date: 08/02/2019

Licence: CC BY-NC-ND 4.0

Citation information: de Bruin, Bas; Lankelma, Marianne; Olivares, Astrid M. (2019): [Co(TPP)]-Catalyzed Formation of Substituted Piperidines. ChemRxiv. Preprint.

Radical cyclization via cobalt(III)–carbene radical intermediates is a powerful method for the synthesis of (hetero)cycles. Building on the recently reported synthesis of N-heterocyclic pyrrolidines catalyzed by Co(II) porphyrins, we herein report the [Co(TPP)]-catalyzed formation of desirable six membered N heterocyclic piperidines, directly from linear aldehydes. Piperidines were obtained in overall high yields, with linear alkenes being formed as side products in small amounts. A DFT study was performed to gain a deeper mechanistic understanding of the cobalt(II)-porphyrin-catalyzed formation of pyrrolidines, piperidines and linear alkenes. The calculations show that the alkenes are unlikely to be formed through 1,2-HAT. Instead, the calculations are consistent with a pathway involving benzyl radical formation followed by radical rebound ring-closure to form the piperidines. Competitive 1,5-HAT from the beta-position to the benzyl radical explains the formation of linear alkenes.

File list (2)

De Bruin_piperidines_article_plus_ESI_ChemRxiv.pdf (15.06 MiB)	view on ChemRxiv • download file
De Bruin_piperidines_raw data_7_2_2019.zip (577.49 KiB)	view on ChemRxiv • download file

[Co(TPP)]-catalyzed formation of substituted piperidines

Marianne Lankelma[†],^[a] Astrid M. Olivares[†],^[b] and Bas de Bruin^{*[a]}

Abstract: Radical cyclization via cobalt(III)–carbene radical intermediates is a powerful method for the synthesis of (hetero)cyclic structures. Building on the recently reported synthesis of five-membered *N*-heterocyclic pyrrolidines catalyzed by Co(II) porphyrins, we herein report the [Co(TPP)]-catalyzed formation of desirable six-membered *N*-heterocyclic piperidines, directly from linear aldehydes. Piperidines were obtained in overall high yields, with linear alkenes being formed as side products in small amounts. A DFT study was performed to gain a deeper mechanistic understanding of the cobalt(II)-porphyrin-catalyzed formation of pyrrolidines, piperidines and linear alkenes. The calculations show that the alkenes are unlikely to be formed through an expected 1,2-hydrogen atom transfer to the carbene carbon. Instead, the calculations are consistent with a pathway involving benzyl radical formation followed by radical rebound ring-closure to form the piperidines. Competitive 1,5-hydrogen atom transfer from the β -position to the benzyl radical explains the formation of linear alkenes as side products.

Considerable efforts have been directed towards the synthesis of nitrogen-based heterocycles because of their importance in medicinal chemistry.^[1] The most prevalent *N*-heterocycles in U.S. FDA-approved drugs are piperidines (Figure 1).^[2] Common synthetic routes to the piperidine motif include hydroamination and ring-closing metathesis.^[3] An attractive alternative strategy for the formation of piperidines could be ring-closing C–C bond formation catalyzed by complexes based on earth-abundant transition metals.^[4]

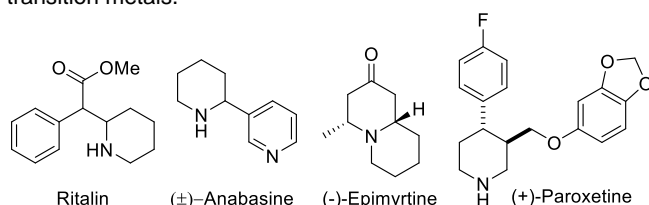
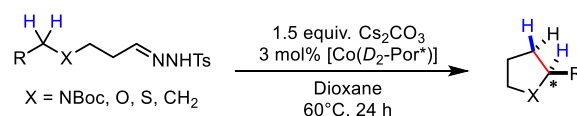


Figure 1. A few examples of piperidine-based drugs and natural products.

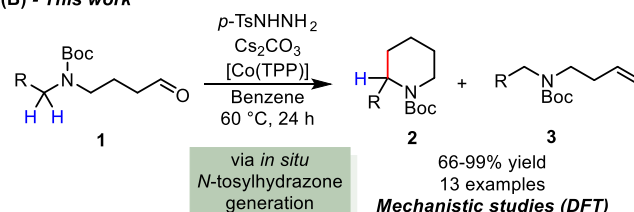
In recent years, our group and others have demonstrated that low-spin d^7 cobalt(II) porphyrin complexes are excellent catalysts for C–C bond formation through radical-type carbene-transfer. In these reactions, the cobalt(II) porphyrin reacts with a carbene precursor (usually a diazo compound or *N*-tosylhydrazone) to form a Co(III)–carbene radical, which can engage in controlled radical addition or hydrogen atom transfer (HAT). Cobalt(III)–carbene radical chemistry has been successfully applied in the

synthesis of carbo- and heterocyclic structures, including cyclopropanes,^[5] chromenes,^[6] furans,^[7] indenenes,^[8] indolines,^[9] ketenes,^[10] butadienes & dihydronaphthalenes,^[11] dibenzocyclooctenes^[12] and phenylindolines.^[13] Recently, the group of Zhang reported the synthesis of chiral pyrrolidines and related five-membered ring compounds, starting from *N*-tosylhydrazones and catalyzed by cobalt(II) complexes of D_2 -symmetric chiral amidoporphyrins (Scheme 1A).^[14] Related reactions leading to five-membered *N*-heterocycles via carbene insertion into activated C–H bonds, mediated by Grubbs-type catalysts, were recently disclosed by the group of Fernández.^[15]

(A) - Previous work, Zhang et al.



(B) - This work



Scheme 1. (A) Formation of chiral pyrrolidines and other five-membered hetero- or carbocycles from *N*-tosylhydrazones, catalyzed by cobalt(II) complexes of D_2 -symmetric chiral amidoporphyrins. (B) [Co(TPP)]-catalyzed one-pot synthesis of six-membered piperidine rings directly from linear aldehydes (this work).

As part of our ongoing exploration of the reactivity of cobalt(III)–carbene radicals, and in view of the importance of six-membered *N*-heterocycles in medicinal chemistry, we sought to explore the feasibility of this approach for the development of a novel method to synthesize substituted piperidines (Scheme 1B, compounds 2). Furthermore, instead of starting from *N*-tosylhydrazones, we opted for *in situ* formation of *N*-tosylhydrazones from aldehydes, followed by *in situ* deprotonation of the hydrazones to form the necessary diazo compounds. This one-pot approach reduces the number of synthetic steps and would thereby provide accelerated access to the desired products. The potential of *in situ* *N*-tosylhydrazone formation in other reactions was briefly illustrated in 2014 by the group of Che^[16] and more recently by Chattopadhyay and co-workers.^[13]

Initial screening proved this approach to be successful, yielding the targeted piperidines 2 in overall high yields. Linear alkenes 3 were obtained as side products, in most instances in small amounts (Scheme 1B). In this paper we describe the details of the catalytic reactions, including optimization studies, substrate screening and mechanistic investigations aimed at understanding the formation of both ring products and linear alkenes.

[a] Marianne Lankelma,[†] Prof. dr. B. de Bruin
Van 't Hoff Institute for Molecular Sciences (HIMS)
Homogeneous, Supramolecular & Bio-Inspired Catalysis
University of Amsterdam, Science Park 904
1098 XH, Amsterdam, The Netherlands
E-mail: b.debruin@uva.nl

[b] Astrid M. Olivares[†]
Department of Chemistry, University of Rochester
404 Hutchison Hall, Rochester, NY 14627-0216 (USA)

[†] These authors contributed equally to this work.

Supporting information and the ORCID identification number(s) for the author(s) of this article can be found under: DOI

The reaction parameters involved in the conversion of **1a** to **2a** and **3a** were screened in an effort to optimize product ratio and yield (Table 1; R = Ph). Without [Co(TPP)] (entry 0), only the diazo compound was formed. The use of 5 mol% [Co(TPP)], 1.2 equivalents of *p*-TsNHNH₂, 2 equivalents of Cs₂CO₃, benzene (1 or 2 mL) and 60 °C (entries 1 and 2) resulted in a quantitative combined yield and a **2a/3a** ratio of ca. 1 : 0.10. Increasing the catalyst loading (entry 3) did not have a beneficial influence. Addition of more than 1.2 equivalents of *p*-TsNHNH₂ (entry 4) or >2 equivalents Cs₂CO₃ (entry 5) was disadvantageous for both yield and product ratio. Elevated temperatures (entries 6 and 7) promoted alkene formation, possibly due to an increased entropy contribution to ΔG^\ddagger .

Exclusion of light (entry 8) did not affect the yield or product ratio. The use of solvents with reduced ability to π -stack (vs. benzene) (entries 9–11) did not improve the yield or product ratio either, and in the case of toluene the product ratio was even negatively affected. Notably, use of the isolated *N*-tosylhydrazone provided effectively the same results as *in situ* generation from **1a**, with the latter approach giving faster access to the same products in the same yield and product ratio.

Next we investigated the scope of the reaction (Table 2), applying the reaction conditions of entry 1 of Table 1. The reaction proved to be compatible with a wide range of substituents (13 examples, Table 2). We observed the relative amount of alkene to be dependent on the substitution of the substrate.

Table 1. Screening of conditions to optimize the yield and product ratio of the conversion of **1a** to **2a** and **3a**.

Entry	[Co(TPP)] (mmol)	<i>p</i> -TsNHNH ₂ (mmol)	Cs ₂ CO ₃ (mmol)	Solvent	Volume (mL)	Temperature (°C)	Time (h)	Yield (%)	Piperidine : alkene ratio
0 ^{a, b}	0	0.12	0.20	Benzene	2	60	24	0	N/A
1 ^a	0.005	0.12	0.20	Benzene	2	60	24	Quant.	1 : 0.10
2 ^a	0.005	0.12	0.20	Benzene	1	60	24	Quant.	1 : 0.08
3 ^a	0.015	0.12	0.20	Benzene	2	60	24	Quant.	1 : 0.14
4 ^a	0.005	0.15	0.20	Benzene	2	60	24	78	1 : 0.40
5 ^a	0.005	0.12	0.22	Benzene	2	60	24	92	1 : 0.42
6 ^a	0.005	0.12	0.20	Benzene	2	80	24	Quant.	1 : 0.28
7 ^a	0.005	0.12	0.20	Toluene	2	105	24	96%	1 : 0.59
8 ^{a, c}	0.005	0.12	0.20	Benzene	1	60	24	Quant.	1 : 0.07
9 ^a	0.005	0.12	0.20	<i>o</i> -dichlorobenzene	2	60	24	85%	1 : 0.11
10 ^a	0.005	0.12	0.20	Toluene	2	60	24	Quant.	1 : 0.51
11 ^a	0.005	0.12	0.20	Cyclohexane	2	60	24	85%	1 : 0.16

^a 0.1 mmol substrate, 24h. ^b Only the corresponding diazo compound formed. ^c Excluded from light.

Table 2. Investigation of the substrate scope of [Co(TPP)]-catalyzed piperidine formation.

formation.

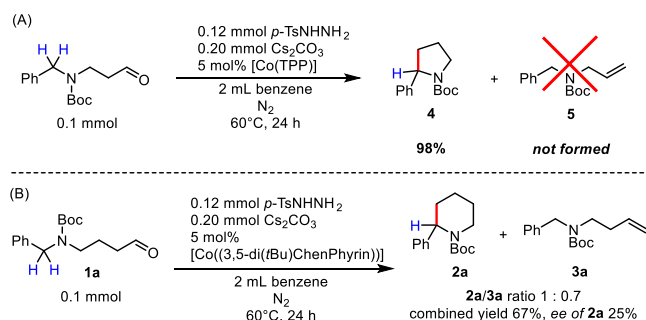
1 (0.1 mmol) $\xrightarrow[2 \text{ mL benzene, } N_2, 60^\circ\text{C, 24 h}]{0.12 \text{ mmol } p\text{-TsNHNH}_2, 0.20 \text{ mmol } \text{Cs}_2\text{CO}_3, 5 \text{ mol\% } [\text{Co}(\text{TPP})]}$ 2 + 3

		Combined isolated yield (%)	Product 2 : 3			Combined isolated yield (%)	Product 2 : 3
a		quant.	1 : 0.11	h		77%	1 : 0.07
b		96%	1 : 0.23	i		66%	1 : 0.10
c		quant.	1 : 1.55	j		98%	1 : 0.07
d		84%	ca. 1 : 1 ^a	k		quant.	1 : 0.09
e		92%	1 : 0.16	l		99%	1 : 0.19
f		71%	1 : 0.22	m		94%	1 : 0.08
g		quant.	1 : 0.28				

^a The overlap of the signals of **2d** and **3d** in ¹H-NMR complicates proper determination of their ratio.

In most instances, piperidine and alkene formed in a ratio varying between 1 : 0.07 and 1 : 0.28, but there seems to be a delicate balance between the product ratio and the stability of the proposed benzylic radical intermediate (*vide infra*). Considerable stability of this intermediate appears to induce substantial alkene formation (entries c and d), whereas absence of radical-stabilizing substituents seems to favour ring closure. Density functional theory (DFT) calculations support these observations (Scheme S4 and S16).

Notably, in reactions leading to formation of five-membered *N*-heterocyclic pyrrolidines, no linear alkenes were formed as side products.^[14] We wondered if this is due to a beneficial effect of the D_2 -symmetric Co(II) amidoporphyrins used by Zhang and co-workers, or rather due to five-membered ring formation being substantially more favorable than linear alkene formation. We therefore investigated formation of pyrrolidine **4** using [Co(TPP)] and the above described *in situ* approach (Scheme 2A). Interestingly, as in the report of Zhang and co-workers, this led to clean pyrrolidine formation without detectable amounts of linear alkene.



Scheme 2. (A) [Co(TPP)]-catalyzed formation of pyrrolidine **4** via *in situ* generation of the *N*-tosylhydrazone. (B) Formation of piperidine **2a** and alkene **3a** catalyzed by [Co(3,5-di(*t*Bu)ChenPhyrin)].

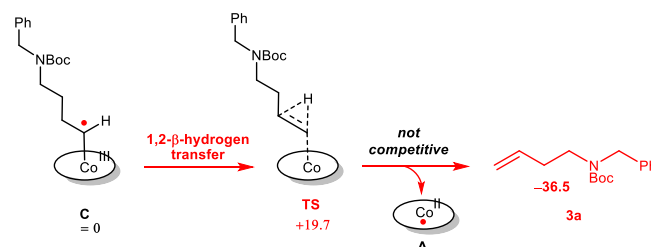
Furthermore, when using Zhang's D_2 -symmetric chiral catalyst [Co(3,5-di(*t*Bu)ChenPhyrin)] to synthesize six-membered *N*-heterocyclic piperidine **2a** (Scheme 2B), we observed a *higher* amount of linear alkene than with [Co(TPP)]. With this catalyst, piperidine **2a** and alkene **3a** were formed in an almost equimolar ratio (1 : 0.70), which might be attributed to the formation of hydrogen bonds between the substrate and amide substituents of the porphyrin.^[17] The products were obtained in poor combined yield (67%) compared to [Co(TPP)], and chirality transfer proved inefficient (ee of **2a**: 25%). Optimization of chirality transfer is beyond the scope of this paper, but would be of interest for subsequent studies.

The above observations show that six-membered ring formation and linear alkene production are competitive, while linear alkenes are not formed in the synthesis of five-membered pyrrolidine rings, irrespective of the type of cobalt(II)-porphyrin used. Such behaviour is not easy to understand in terms of a mechanism involving linear alkene formation via a commonly accepted 1,2-hydrogen shift (Scheme 3).^[18]

Therefore, to gain a better understanding of the mechanisms of cobalt(II)-porphyrin-catalyzed formation of pyrrolidines, piperidines and alkenes, the reactions were investigated using DFT. To reduce computation time, a simplified

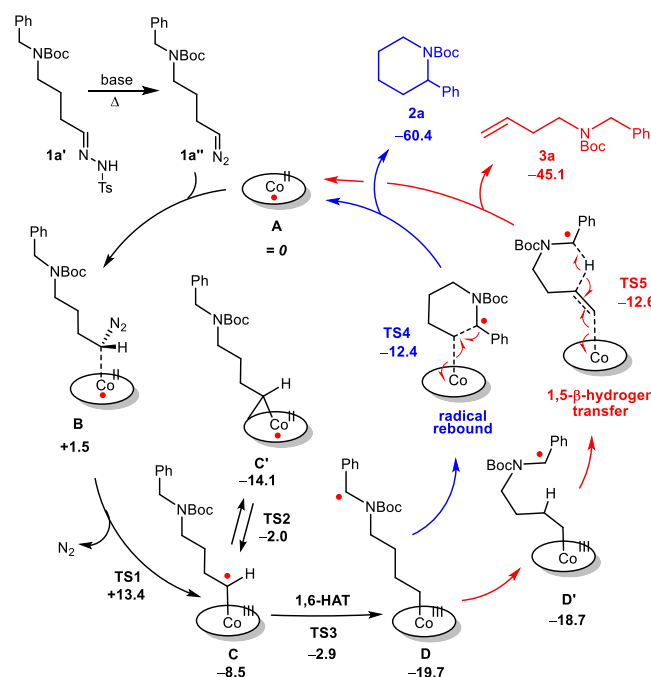
porphyrin without phenyl substituents on the *meso*-positions was used, abbreviated as [Co(por)].

A first important observation is that alkene formation via the expected 1,2-HAT from the β -position to the carbene-radical carbon of the proposed intermediate **C** has a high computed free energy barrier of +20 kcal mol⁻¹ (Scheme 3). This barrier is too high to compete with radical rebound ring-closure to form **2a** (barrier: +7 kcal mol⁻¹; Scheme 4).



Scheme 3. Linear alkene formation from cobalt(III)-carbene radical intermediate **C** via 1,2-HAT from the β - to the α -position has a rather high energy barrier.

However, we found an alternative pathway for linear alkene formation, involving 1,5-HAT from the β -position to the benzylic radical carbon of **D** over **TS5**, which has a similar barrier as radical rebound ring-closure over **TS4**. As such, the DFT calculations point in the direction of the two competitive pathways depicted in Scheme 4.

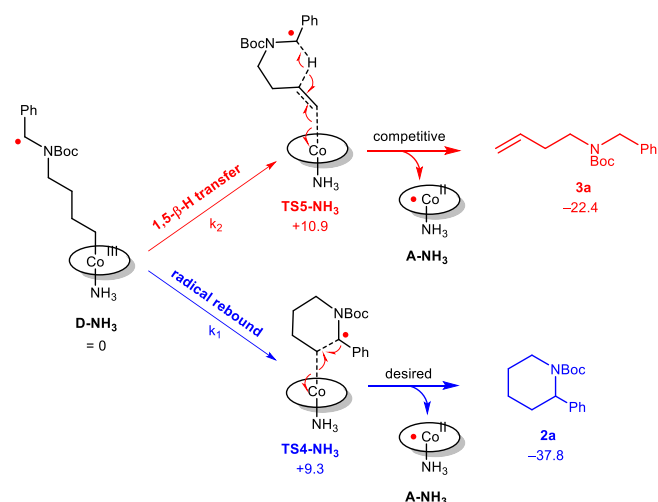


Scheme 4. Proposed mechanisms for [Co(TPP)]-catalyzed competitive formation of piperidines and alkenes. All Gibbs free energies (ΔG°_{333K} , in kcal mol⁻¹) including those of **TS1**-**TS5**, are reported relative to the energy of intermediate **A**.

The catalytic cycle is preceded by the (presumably) uncatalyzed formation of diazo compound **1a''** from *N*-tosylhydrazone **1a'** which is in turn *in situ* generated from aldehyde **1a**. Coordination of diazo compound **1a''** to the cobalt(II) porphyrin generates intermediate **B**. Dinitrogen loss from diazo adduct **B** over **TS1** to form cobalt(III)-carbene radical intermediate **C** is an exergonic,

low-barrier process (+13.4 kcal mol⁻¹). Similar to previously reported cobalt(III)–carbene radical species, intermediate **C** carries most of its spin density localized at the carbene carbon.^[19,20] An intramolecular 1,6-HAT process then relocates the radical character from the α -position to the ζ -position to yield benzyl-radical intermediate **D** or its bent analogue **D'**. Intramolecular ring-closure (effectively involving radical combination of the α - and ζ -positions) over **TS4** yields piperidine **2a**, while a 1,5- β -HAT over **TS5** leads to formation of alkene **3a**. The almost identical **TS4** and **TS5** barriers suggest that these two pathways should be in close competition (see also Scheme S1, S3 and S15). While these DFT results explain the formation of both **2a** and **3a**, the computed barriers are too similar to explain the experimentally observed **2a/3a** ratio of 1 : 0.10. Therefore we also explored alternative pathways involving six-coordinate intermediates.

Insertion of the carbene carbon of intermediate **C** into the bond between the metal and a pyrrolato nitrogen of the porphyrin can cause the carbene to adopt a bridging position (Scheme 4, **C'**).^[20, 21] One could also envision a hexacoordinate species bearing both a bridging carbene and a terminal carbene (**D_{bridged}**). When the pathways toward products **2a** and **3a** are computed starting from **D_{bridged}** and passing through **TS4_{bridged}** and **TS5_{bridged}**, the radical rebound and 1,5- β -HAT pathways remain too similar (see Scheme S8 and S20). For that reason we also computed the energy barriers (from **D** onwards) for six-coordinated cobalt complexes formed upon coordination of a few different nitrogen-donor ligands at the axial position *trans* to the substrate. Ammonia, methylimidazole and pyridine were used as simplified computational models to study the effects of different axial ligands coordinated to cobalt under the applied reaction conditions.^[22] Indeed axial coordination to cobalt(III)–alkyl radical intermediate **D** changes the selectivity in favour of ring closure, and the different donors were found to have different degrees of influence on the product ratio (Scheme 5 and S9–S12).^[23]



Scheme 5. The computed effect of coordination of NH₃ (as a simplified model for a variety of possible ligands)^[22] on the energy barriers for [Co(TPP)]-catalyzed piperidine and alkene formation. All Gibbs free energies (ΔG°_{333K} , in kcal mol⁻¹), including those of **TS4** and **TS5**, are reported relative to the energy of intermediate **D-NH₃**.

Coordination of ammonia resulted in a computed k_1/k_2 value of 10.4 (k_1 for piperidine formation, k_2 for alkene formation) at 60 °C, which is in accord with the experimentally observed **2a/3a** ratio of 1 : 0.10.^[24] The other axial ligand donors give rise to slightly different k_1/k_2 values (pyridine: 14.4; methylimidazole: 5.9), suggesting that changes in the composition of the reaction mixture over time could indeed lead to a change in product ratio. This was experimentally confirmed. Monitoring the reaction of **1a** by ¹H-NMR over time indeed showed that the **2a/3a** ratio gradually shifts from 1 : 0.33 toward 1 : 0.10. We interpret this behaviour as the result of a changing composition of the reaction mixture over the course of the reaction, with (on average) different axial ligands being coordinated to cobalt (*vide supra*).^[22]

The absolute amounts of piperidine and alkene formed over time clearly indicate that alkenes **3** are not converted to piperidines **2** (Figure 2). More details on the monitoring experiments can be found in the Supporting Information.

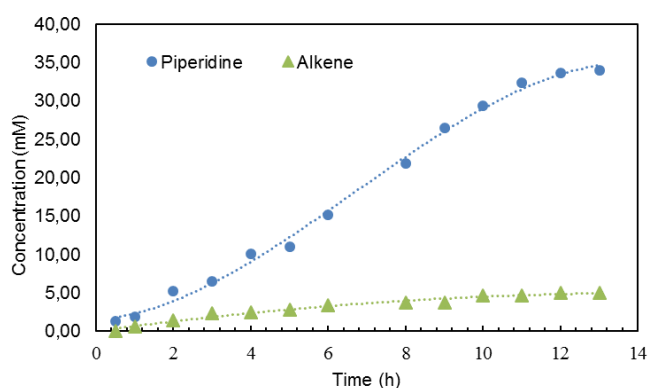


Figure 2. Monitoring piperidine and alkene formation over time.

To fully exclude the possibility that alkenes **3** could be converted to piperidines **2**, aldehyde **1a** was subjected to the general reaction conditions (Table 1, entry 1) in presence of an equimolar amount of alkene **3h**. From all alkenes formed from the substrates enumerated in Table 2, **3h** was selected based on its ¹H-NMR signature, which was most distinct from the ¹H-NMR signatures of **2a** and **3a**. Based on ¹H-NMR analysis, it was clear that no piperidine **2h** had formed from alkene **3h**; only piperidine **2a** and alkenes **3a** and **3h** were detected in the crude reaction mixture.

Lastly, we also computed the reaction pathway leading to five-membered pyrrolidines, in order to explain why alkene formation is not in competition with this reaction. The results are detailed in the Supporting Information (Scheme S5–7 and S17–19) and are in excellent agreement with the experimental results. The DFT calculations confirm that [Co(por)]-catalyzed ring-closure toward pyrrolidines has a much lower transition state barrier than pathways leading to alkene formation. Neither alkene formation through 1,4- β -HAT nor through 1,2- β -HAT is competitive, with the computed barriers being respectively 8 and 11 kcal mol⁻¹ higher in energy than the barrier for radical rebound ring-closure.

In conclusion, we developed a new base-metal-catalyzed synthetic route toward six-membered piperidine rings, which are important substructures of various medicinal compounds. In contrast to the cobalt(II)porphyrin-catalyzed synthesis of five-membered pyrrolidines, the cobalt(II)porphyrin-catalyzed

construction of piperidines is accompanied by formation of (generally small amounts of) olefinic side products. Overall, the reaction is high-yielding and compatible with a wide range of functional groups. The relative amount of alkene was found to be dependent on the substitution of the substrate. DFT calculations indicate a mechanism involving 1,6-HAT from the carbene radical carbon to the benzylic position of intermediate **C**, to form benzyl radical intermediate **D**. The latter can undergo radical rebound ring-closure to form piperidines. Competitive 1,5-HAT from the β -position to the benzylic radical carbon explains the formation of linear alkenes as side products. DFT and ^1H -NMR monitoring experiments suggest that axial ligand coordination influences the product ratio.

Acknowledgements

The work described in this paper was financially supported by the Netherlands Organization for Scientific Research (NWO TOP-Grant 716.015.001), the University of Amsterdam (Research Priority Area Sustainable Chemistry) and the National Science Foundation (Graduate Research Fellowship Program, NSF-NWO-GROW-project, no. DGE-1419118). We thank Prof. dr. Joost N.H. Reek for a valuable suggestion, Ed Zuidinga for HRMS measurements and Dylan E. Parsons (University of Rochester) for helpful scientific discussions.

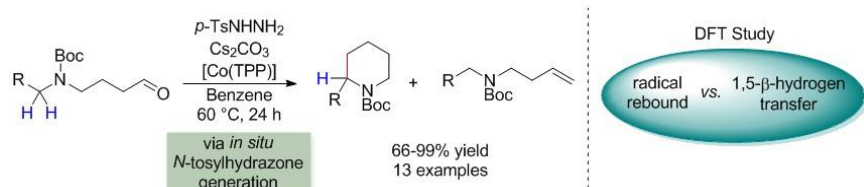
Conflict of interest

The authors declare no conflict of interest.

Keywords: Homogeneous catalysis • Radicals • Nitrogen heterocycles • C-H activation • C-C coupling

- [1] (a) A.L. Mndzhoian, in *Synthesis of Heterocyclic Compounds*, Springer, **1959**. (b) C.W. Bird, in *Comprehensive Heterocyclic Chemistry II*, Pergamon: Oxford, **1996**.
- [2] (a) E. Vitaku, D.T. Smith, J.T. Njardarson, *J. Med. Chem.* **2014**, *57*, 10257. (b) R.D. Tylor, M. MacCoss, A.D.G. Lawson, *J. Med. Chem.* **2014**, *57*, 5845.
- [3] I. Nakamura, Y. Tamamoto, *Chem. Rev.* **2004**, *104*, 2127.
- [4] (a) P. Chirik, R. Morris (Ed.) *Earth Abundant Metals in Homogeneous Catalysis* (special issue), *Acc. Chem. Res.* **2015**. (b) R.J.M. Klein Gebbink & M.-E. Moret (Ed.) *Non-Noble Metal Catalysis: Molecular Approaches and Reactions*, Wiley, **2019**, ISBN: 978-3-527-34061-3.
- [5] (a) L. Huang, Y. Chen, G.Y. Gao, X. P. Zhang, *J. Org. Chem.* **2003**, *68*, 8179. (b) S. Zhu, J.V. Ruppel, H. Lu, L. Wojtas, X.P. Zhang, *J. Am. Chem. Soc.* **2008**, *130*, 5042. (c) D. Intrieri, A. Caselli, E. Gallo, *Eur. J. Inorg. Chem.* **2011**, 5071. (d) A. Chirila, B.G. Das, N.D. Paul, B. de Bruin, *ChemCatChem* **2017**, *9*, 1413. (e) M. Goswami, B. de Bruin, W.I. Dzik, *Chem. Commun.* **2017**, 53, 4382.
- [6] (a) N.D. Paul, S. Mandal, M. Otte, X. Cui, X. P. Zhang, B. de Bruin, *J. Am. Chem. Soc.* **2014**, *136*, 1090. (b) N. Mujumdar, N. D. Paul, S. Mandal, B. de Bruin, W.D. Wulff, *ACS Catal.* **2015**, *5*, 2329.
- [7] X. Cui, X. Xu, L. Wojtas, M. M. Kim, X.P. Zhang, *J. Am. Chem. Soc.* **2012**, *134*, 19981.
- [8] B.G. Das, A. Chirila, M. Tromp, J.N.H. Reek, B. de Bruin, *J. Am. Chem. Soc.* **2016**, *138*, 8968.
- [9] A.S. Karns, M. Goswami, B. de Bruin, *Chem. Eur. J.* **2018**, *24*, 5253. For the synthesis of enantioselective indolines, see: X. Wen, Y. Wang, X.P. Zhang *Chem. Sci.* **2018**, *9*, 5082.
- [10] N.D. Paul, A. Chirila, H. Lu, X.P. Zhang, B. de Bruin, *Chem. Eur. J.* **2013**, *19*, 12953.
- [11] C. te Grotenhuis, B.G. Das, P.F. Kuijpers, W. Hageman, M. Trouwborst, B. de Bruin, *Chem. Sci.* **2017**, *8*, 8221.
- [12] C. te Grotenhuis, N. Heuvel, J.I. van der Vlugt, B. de Bruin, *Angew. Chem. Int. Ed.* **2018**, *57*, 140.
- [13] S. Roy, S.K. Das, B. Chattopadhyay, *Angew. Chem. Int. Ed.* **2018**, *57*, 2238.
- [14] Y. Wang, X. Wen, X. Cui, X.P. Zhang, *J. Am. Chem. Soc.* **2018**, *140*, 4792.
- [15] D. Solé, A. Amenta, M.-L. Bennasar, I. Fernández, *Chem. Commun.*, **2019**, 55, 1160.
- [16] A.R. Reddy, C. Zhou, Z. Guo, J. Wei, C. Che *Angew. Chem. Int. Ed.* **2014**, *53*, 14175.
- [17] Y. Wang, X.P. Zhang, "[Co(3,5-Di-*t*-Bu-ChenPhyrin)]" e-EROS, John Wiley & Sons, **2018**.
- [18] (a) M.P. Doyle, M.A. McKerver, T. Ye, *Modern Catalytic Methods for Organic Synthesis with Diazo Compounds*, Wiley-Interscience, New York, **1998**. (b) G. Bertrand, *Carbene Chemistry*, Fontis Media, Lausanne, Switzerland, **2002**.
- [19] (a) H. Lu, W. I. Dzik, X. Xu, L. Wojtas, B. de Bruin and X. P. Zhang, *J. Am. Chem. Soc.*, **2011**, *133*, 8518. (b) W. I. Dzik, X. P. Zhang and B. de Bruin, *Inorg. Chem.*, **2011**, *50*, 9896. (c) W. I. Dzik, J. N. H. Reek and B. de Bruin, *Chem.-Eur. J.* **2008**, *14*, 7594. (d) V. Lyaskovskyy and B. de Bruin, *ACS Catal.*, **2012**, *2*, 270.
- [20] W.I. Dzik, X. Xu, X.P. Zhang, J.N.H. Reek, B. de Bruin *J. Am. Chem. Soc.* **2010**, *132*, 10891.
- [21] Involvement of a bis-carbene species was considered unlikely, based on previously published calculations. See reference [20]
- [22] Under catalytic conditions the reaction medium changes, and various different donors could be coordinated to cobalt, not necessarily the same in the beginning and end of the reaction: e.g. *p*-TsNHNH₂, the oxygen atoms of the base, the terminal nitrogen atom of the *N*-tosylhydrazone, the internal nitrogen atom of the deprotonated *N*-tosylhydrazone and the terminal nitrogen atom of the diazo compound could all act as axial ligands.
- [23] Only the relative energy barriers were significantly affected by these nitrogen-donor ligands. The absolute energy barriers remained similar.
- [24] Note that these DFT calculations were performed in the gas phase and were simplified in several ways. Furthermore, the product ratio is calculated based on very small energy differences between the transition states of the *k*₁ and *k*₂ pathways, close to the accuracy of the calculations. The effects of axial ligand coordination on the computed *k*₁/*k*₂ ratios should therefore not be over-interpreted.

Entry for the Table of Contents



Marianne Lankelma, Astrid M. Olivares,
and Bas de Bruin*

Page No. – Page No.

**[Co(TPP)]-catalyzed formation of
substituted piperidines**

Radical cyclization via cobalt(III)–carbene radical intermediates is a powerful method for the synthesis of (hetero)cyclic structures. Building on the recently reported synthesis of five-membered pyrrolidine rings catalyzed by Co(II) amidoporphyrins, we herein report the [Co(TPP)]-catalyzed formation of six-membered piperidine rings, which was found to be accompanied by formation of small amounts of linear alkenes. A DFT study was performed to gain a deeper mechanistic understanding.

TOC Keyword: Nitrogen heterocycles

[Co(TPP)]-catalyzed formation of substituted piperidines

Marianne Lankelma^{†, [a]} Astrid M. Olivares^{†, [b]} and Bas de Bruin^{*, [a]}

^[a]University of Amsterdam, Science Park 904, 1098 XH, Amsterdam, The Netherlands.

^[b]University of Rochester, Rochester, NY USA 14627-0216.

[†]These authors contributed equally to this work.

Supporting Information

Table of Contents

1. List of abbreviations	S3
2. General information	S4
3. Substrate synthesis	
3.1 General procedure A	S5
3.2 Substrate characterization	S7
3.3 Copies of ^1H -, ^{13}C - and ^{19}F -NMR spectra of all substrates	S12
4. Catalysis	
4.1 General procedure B	S41
4.2 Product characterization	S42
4.3 Copies of ^1H -, ^{13}C - and ^{19}F -NMR spectra of the functional group screening	S51
4.4 Copies of ^1H -NMR spectra of the conditions screening and experiments mentioned in the main text	S96
5. Control experiments	
5.1 Addition of alkene 3h to the reaction of aldehyde 1a	S112
5.2 Monitoring the conversion of 1a to 2a and 3a over time by ^1H -NMR	S117
5.3 Copies of the ^1H -NMR spectra of the monitoring experiments	S118
6. Computational methods	S131
7. Computational studies	S132
8. References	S148

1. List of abbreviations

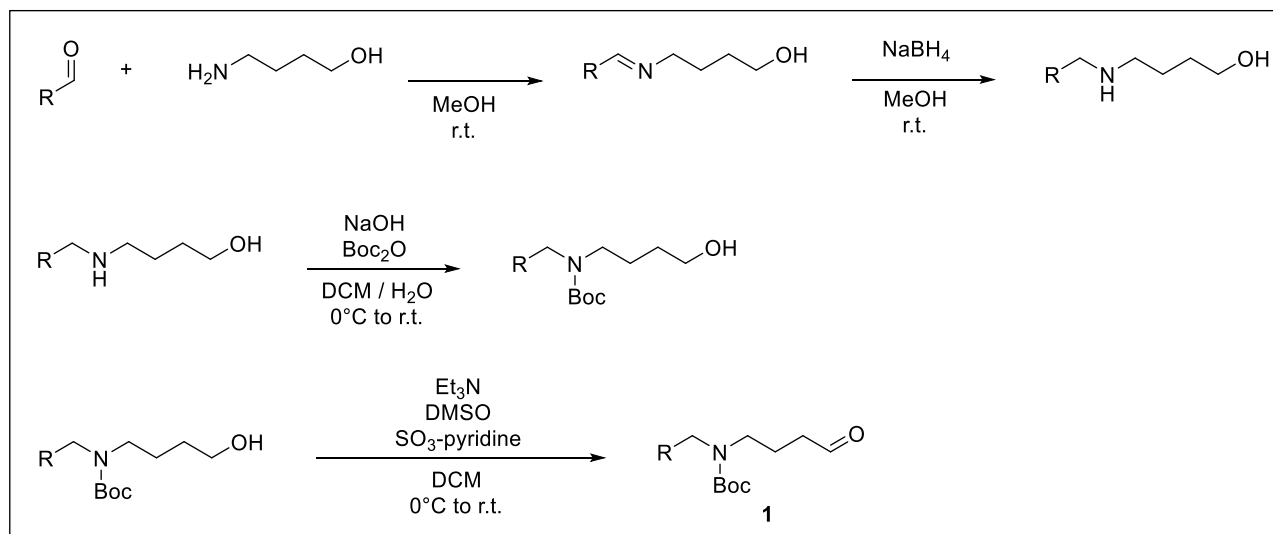
aq	aqueous
Boc	<i>tert</i> -butyloxycarbonyl
BP86	a GGA functional composed of the Becke 1988 exchange functional and the Perdew 86 correlation functional
br	broad
[Co(TPP)]	5,10,15,20-tetraphenyl-21 <i>H</i> ,23 <i>H</i> -porphine cobalt(II)
d	doublet
DCM	dichloromethane
DMSO	dimethyl sulfoxide
def2-tzvp	default basis set, second generation, triple zeta valence plus polarization
DFT	density functional theory
equiv	equivalents
ESI	electrospray ionization
FD	field desorption
GC	gas chromatography
HAT	hydrogen atom transfer
HRMS	high resolution mass spectrometry
<i>J</i>	coupling constant
LC	liquid chromatography
m	multiplet
M	mol liter ⁻¹
m/z	mass-to-charge ratio
NMR	nuclear magnetic resonance
por	porphyrin
ppm	parts per million
PQS	parallel quantum solutions
PTFE	polytetrafluoroethylene (Teflon)
q	quartet
R _f	retention factor
rpm	rotations per minute
s	singlet
sat	saturated
t	triplet
TLC	thin layer chromatography
TOF	time of flight
TS	transition state
UV	ultraviolet
v/v	volumetric ratio

2. General information

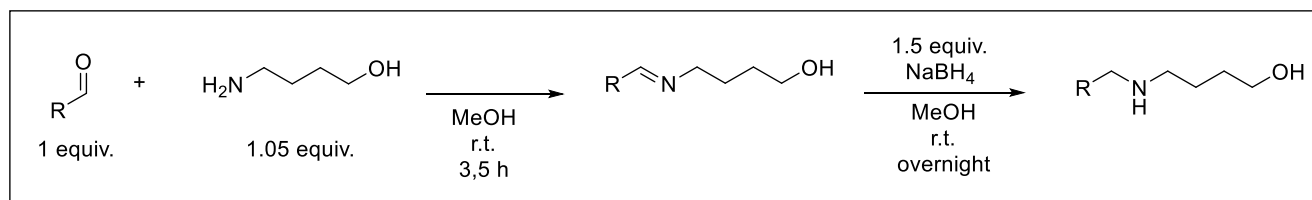
Substrate syntheses were carried out open to air. Catalytic reactions were set up in a nitrogen-filled glove box. Starting materials were purchased from commercial suppliers (Sigma Aldrich or TCI) and used without further purification. Solvents used for substrate synthesis were used as received. Anhydrous benzene (Sigma Aldrich) used for catalysis was degassed by three freeze-pump-thaw cycles and stored over activated molecular sieves (3 Å, 3-4 mm) inside a nitrogen-filled glove box. *p*-TsNHNH₂ and Cs₂CO₃ were dried overnight under vacuum at 85°C and 120°C respectively. Flash column chromatography was performed with silica gel (Screening Devices, 60Å, particle size 0.040-0.063 µm). Eluent mixtures are reported as v/v%. Products were visualized by UV light or by staining with ninhydrin in the case of all aldehydes and all catalysis products. ¹H-, ¹³C- and ¹⁹F-NMR spectra were acquired at room temperature on Bruker DRX 400 and 300 MHz instruments. NMR chemical shifts are reported in ppm and are referenced internally to the residual solvent peak of CDCl₃ (¹H NMR: δ = 7.26 ppm, ¹³C NMR: δ = 77.16 ppm). Coupling constants (*J*) are reported in Hz. High resolution mass spectra were recorded on a JEOL AccuTOF GC v 4G, JMS-T100GCV mass spectrometer equipped with a field desorption (FD) probe fitted with an FD emitter (Carbotec or Linden (Germany)), 13 µm tungsten wire, current rate 51.2 mA/min over 1.2 min. Only the HRMS spectra of [**2c**+**3c**] and **3n** could not be recorded with FD and were recorded on a JEOL AccuTOF LC, JMS-T100LP mass spectrometer with electrospray ionization (ESI). Chiral GC analysis was performed on a Shimadzu GC-2010 Plus equipped with a CP-ChiraSil-Dex CB column (25 m x 0.32 mm x 0.25 µm, film thickness 0.25 µm) and helium as a carrier gas.

3. Substrate synthesis

3.1 General Procedure A: Synthesis of *tert*-butyl benzyl(4-oxobutyl)carbamate derivatives **1**

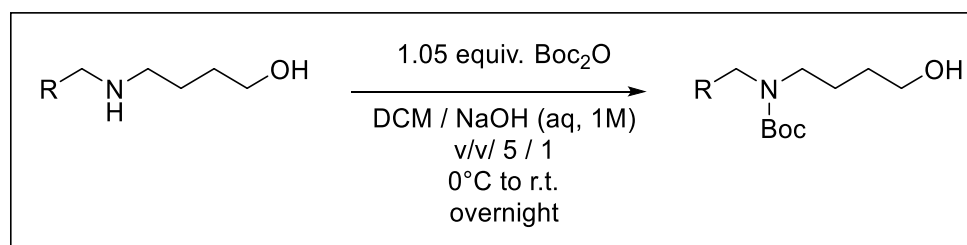


Reductive amination



According to Widenhoefer's procedure,^[1] a solution of a benzaldehyde derivative (1.0 equiv) and 4-amino-1-butanol (1.05 equiv) in methanol (0.5 M) was stirred at room temperature for 3.5 h. NaBH₄ (1.5 equiv) was added and the reaction mixture was stirred overnight. The reaction mixture was treated with water (0.13 M) and 1 M NaOH (0.42 M with respect to benzaldehyde) and then three times extracted into DCM. The combined organic extracts were dried over MgSO₄, filtered, and the solvent was removed under vacuum. Formation of the product was confirmed by ¹H-NMR spectroscopy and the crude was used without further purification.

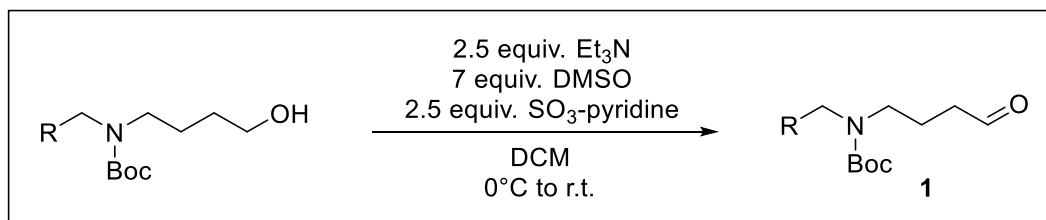
Amine protection



According to Thomson's procedure,^[2] Boc anhydride (1.05 equiv) was added to a stirred solution of 4-(benzylamino)butan-1-ol derivative (1 equiv) in DCM/NaOH (aq, 1 M) (v/v 5:1, 0.34 M) at

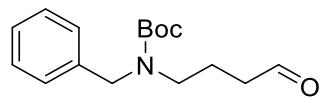
0°C. After stirring at room temperature overnight, the reaction mixture was washed with water, dried over MgSO₄, filtered, and DCM was evaporated under vacuum. Formation of the product was confirmed by ¹H-NMR spectroscopy and the crude was used without further purification.

Alcohol oxidation



Following the procedure described by Parikh & Doering,^[3] Et₃N (2.5 equiv), DMSO (7.0 equiv) and sulfur trioxide pyridine complex (2.5 equiv) were added to a 0°C solution of *tert*-butyl benzyl(4-hydroxybutyl)carbamate derivate (1 equiv) in DCM (0.5 M). After ca. 5 minutes, the reaction was allowed to warm up to room temperature. Reaction progress was monitored by TLC. Upon completion, the reaction mixture was diluted with DCM and washed with HCl (aq, 1M), followed by NaHCO₃ (aq, sat.) and brine. The organic layer was dried over Na₂SO₄, filtered, and DCM was removed under vacuum. The resulting aldehyde was purified by flash column chromatography (eluent compositions indicated below) and visualized by staining the TLC-plates with a solution of 1.5 g ninhydrin in 100 mL *n*-butanol and 3 mL acetic acid.

3.2 Substrate characterization



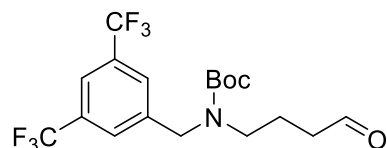
tert-butyl benzyl(4-oxobutyl)carbamate^[4] (1a)

General procedure A was followed, starting from benzaldehyde. Flash column chromatography (gradient towards 7/3 hexanes/ethyl acetate, $R_f = 0.76$) afforded **1a** as a colorless liquid (72% yield over three steps).

^1H NMR (500 MHz, CDCl_3) δ 9.61 (br, 1H), 7.37–6.98 (m, 5H), 4.37 (br s, 2H), 3.15 (br, 2H), 2.30 (br s, 2H), 1.74 (br s, 2H), 1.43 (br s, 9H). (Mixture of rotamers)

^{13}C NMR (126 MHz, CDCl_3) δ 200.84, 155.32, 138.04, 128.07, 127.27, 126.77, 79.40, 50.10, 45.17, 40.46, 27.97, 20.06.

HRMS (FD, m/z): Calculated for $\text{C}_{16}\text{H}_{23}\text{NO}_3$: 277.1678, found: 277.1679.



tert-butyl (3,5-bis(trifluoromethyl)benzyl)(4-oxobutyl)carbamate (1b)

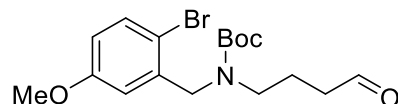
General procedure A was followed, starting from 3,5-bis(trifluoromethyl)benzaldehyde. Flash column chromatography (gradient towards 7/3 hexanes/ethyl acetate, $R_f = 0.50$) afforded **1b** as a very pale yellow liquid (68% yield over three steps).

^1H NMR (500 MHz, CDCl_3) δ 9.70 (s, 1H), 7.79–7.56 (m, 3H), 4.48 (br s, 2H), 3.25 (br s, 2H), 2.43 (br s, 2H), 1.82 (br s, 2H), 1.40 (br s, 9H). (Mixture of rotamers)

^{13}C NMR (126 MHz, CDCl_3) δ 201.28, 155.87, 141.57, 131.90 (q, $J = 33.3$ Hz), 127.42, 124.42, 122.26, 121.24, 80.78, 50.19, 46.64, 40.93, 28.24, 20.61.

^{19}F NMR (282 MHz, CDCl_3) δ -63.08.

HRMS (FD, m/z): Calculated for $\text{C}_{18}\text{H}_{21}\text{F}_6\text{NO}_3$: 413.1426, found: 413.1444.



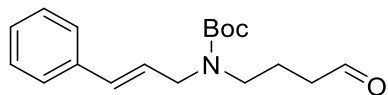
tert-butyl (2-bromo-5-methoxybenzyl)(4-oxobutyl)carbamate (1c)

General procedure A was followed, starting from 2-bromo-5-methoxybenzaldehyde. Flash column chromatography (gradient towards 7/3 hexanes/ethyl acetate, $R_f = 0.50$) afforded **1c** as a very pale yellow liquid (59% yield over three steps).

^1H NMR (500 MHz, CDCl_3) δ 9.67 (br, 1H), 7.46–7.13 (m, 1H), 6.81–6.44 (m, 2H), 4.40 (s, 2H), 3.68 (br, 3H), 3.18 (br s, 2H), 2.38 (br s, 2H), 1.79 (br s, 2H), 1.51–1.02 (m, 9H). (Mixture of rotamers)

^{13}C NMR (126 MHz, CDCl_3) δ 201.20, 159.21, 155.60, 138.27, 133.24, 114.15, 80.04, 55.30, 50.64, 49.79, 46.08, 40.87, 28.29, 20.57.

HRMS (FD, m/z): Calculated for $\text{C}_{17}\text{H}_{24}\text{BrNO}_4$: 385.0889, found: 385.0902.



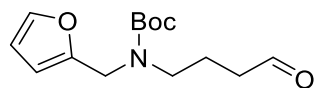
tert-butyl cinnamyl(4-oxobutyl)carbamate (1d)

General procedure A was followed, starting from cinnamaldehyde. Flash column chromatography (gradient towards 7/3 hexanes/ethyl acetate, $R_f = 0.56$) afforded **1d** as a colorless liquid (39% yield over three steps).

^1H NMR (500 MHz, CDCl_3) δ 9.73 (s, 1H), 7.41–7.14 (m, 5H), 6.44 (br s, 1H), 6.13 (br s, 1H), 3.93 (br s, 2H), 3.24 (br s, 2H), 2.42 (br s, 2H), 1.84 (br s, 2H), 1.47 (s, 9H). (Mixture of rotamers)

^{13}C NMR (126 MHz, CDCl_3) δ 201.45, 155.36, 136.56, 128.46, 127.49, 126.23, 125.41, 79.59, 49.12, 48.64, 45.57, 40.88, 28.32, 20.70.

HRMS (FD, m/z): Calculated for $\text{C}_{18}\text{H}_{25}\text{NO}_3$: 303.1834, found: 303.1829.



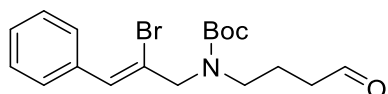
tert-butyl (furan-2-ylmethyl)(4-oxobutyl)carbamate (1e)

General procedure A was followed, starting from furan-2-carbaldehyde. Flash column chromatography (gradient towards 7/3 hexanes/ethyl acetate, $R_f = 0.60$) afforded **1e** as a colorless liquid (73% yield over three steps).

^1H NMR (500 MHz, CDCl_3) δ 9.63 (s, 1H), 6.22 (s, 1H), 6.13 (br s, 1H), 4.30 (br m, 2H), 3.19 (br s, 2H), 2.30 (s, 2H), 1.72 (br s, 2H), 1.39 (s, 9H). (Mixture of rotamers)

^{13}C NMR (126 MHz, CDCl_3): δ 200.98, 154.99, 151.57, 141.56, 110.02, 107.71, 107.15, 79.54, 45.57, 43.46, 42.67, 40.45, 27.99, 20.26.

HRMS (FD, m/z): Calculated for $\text{C}_{14}\text{H}_{21}\text{NO}_4$: 267.1471, found: 267.1470.



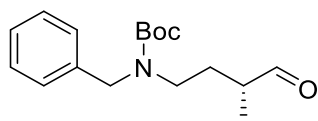
tert-butyl (Z)-(2-bromo-3-phenylallyl)(4-oxobutyl)carbamate (1f)

General procedure A was followed, starting from (Z)-2-bromo-3-phenylacrylaldehyde.^[5] Flash column chromatography (gradient towards 6/4 hexanes/ethyl acetate, $R_f = 0.61$) afforded **1f** as a yellow liquid (42% yield over three steps).

^1H NMR (300 MHz, CDCl_3) δ 9.78 (d, $J = 17.0$ Hz, 1H), 7.62 (d, $J = 7.3$ Hz, 1H), 7.45–7.16 (m, 5H), 4.53–4.17 (m, 2H), 3.44–3.12 (m, 2H), 2.57–2.36 (m, 2H), 1.99–1.75 (m, 2H), 1.50 (s, 9H). (Mixture of rotamers)

^{13}C NMR (75 MHz, CDCl_3) δ 201.78, 155.51, 135.18, 129.09, 128.63, 128.31, 128.25, 127.35, 122.89, 80.50, 80.05, 56.50, 50.61, 46.05, 45.73, 41.19, 28.54, 28.50, 20.65.

HRMS (FD, m/z): Calculated for $\text{C}_{18}\text{H}_{24}\text{BrNO}_3$: 381.0940, found: 381.0943.



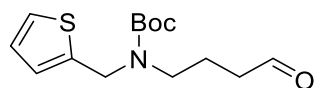
tert-butyl (S)-benzyl(3-methyl-4-oxobutyl)carbamate (1g)

General procedure A was followed, starting from benzaldehyde and (*R*)-4-amino-2-methyl-1-butanol (TCI Chemicals). Flash column chromatography (gradient towards 7/3 hexanes/ethyl acetate, $R_f = 0.87$) afforded **1g** as a colorless liquid (58% yield over three steps).

^1H NMR (500 MHz, CDCl_3) δ 9.42 (s, 1H), 7.32–6.90 (m, 5H), 4.32 (br s, 2H), 3.12 (br, 2H), 2.17 (br s, 1H), 1.82 (br s, 1H), 1.36 (br s, 10H), 0.95 (s, 3H). (Mixture of rotamers)

^{13}C NMR (126 MHz, CDCl_3): δ 203.15, 155.33, 138.06, 128.11, 127.36, 126.83, 79.33, 50.24, 49.50, 44.03, 43.39, 28.00, 12.97.

HRMS (FD, m/z): Calculated for $\text{C}_{17}\text{H}_{25}\text{NO}_3 + [\text{H}^+]$: 292.1913, found: 292.1920.



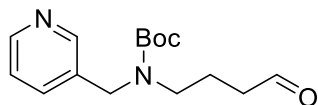
tert-butyl (4-oxobutyl)(thiophen-2-ylmethyl)carbamate (1h)

General procedure A was followed, starting from thiophene-2-carbaldehyde. Flash column chromatography (gradient towards 7/3 hexanes/ethyl acetate, $R_f = 0.66$) afforded **1h** as a colorless liquid (56% yield over three steps).

^1H NMR (500 MHz, CDCl_3) δ 9.70 (s, 1H), 7.18 (s, 1H), 6.90 (s, 2H), 4.50 (s, 2H), 3.23 (s, 2H), 2.39 (s, 2H), 1.80 (s, 2H), 1.47 (s, 9H). (Mixture of rotamers)

^{13}C NMR (126 MHz, CDCl_3) δ 201.59, 155.38, 155.11, 141.17, 126.39, 125.99, 125.20, 80.17, 45.54, 40.98, 28.38, 20.51.

HRMS (FD, m/z): Calculated for $\text{C}_{14}\text{H}_{21}\text{NO}_3\text{S}$: 283.1242, found: 283.1259.



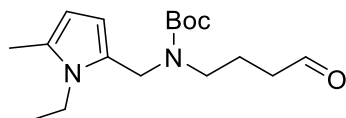
tert-butyl 2-(pyridine-3-yl)piperidine-1-carboxylate (1i)

General procedure A was followed, starting from 3-pyridinecarboxaldehyde. Flash column chromatography (gradient towards 8/2 ethyl acetate/dichloromethane, $R_f = 0.23$) afforded **1i** as a yellow liquid (14% yield over three steps).

^1H NMR (300 MHz, CDCl_3) δ 9.46 (s, 1H), 8.29–8.16 (m, 2H), 7.40–7.25 (m, 1H), 7.04–6.93 (m, 1H), 4.16 (br s, 2H), 2.96 (br s, 2H), 2.17 (br s, 2H), 1.56 (s, 2H), 1.18 (br s, 9H). (Mixture of rotamers)

^{13}C NMR (126 MHz, CDCl_3) δ 200.93, 175.14, 155.44, 155.00, 148.20, 147.91, 147.73, 135.56, 134.92, 133.90, 123.32, 79.91, 79.71, 47.92, 47.19, 45.72, 40.48, 31.11, 28.14, 27.99, 27.83, 23.14, 20.19.

HRMS (FD, m/z): Calculated for $\text{C}_{15}\text{H}_{22}\text{N}_2\text{O}_3$: 278.1630, found: 278.1619.



tert-butyl ((1-ethyl-5-methyl-1H-pyrrol-2-yl)methyl)(4-oxobutyl)carbamate (1j)

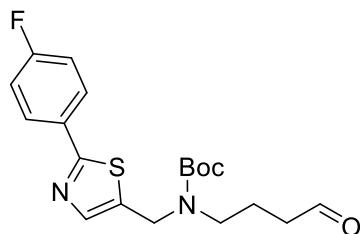
General procedure A was followed, starting from 1-ethyl-5-methyl-1H-pyrrole-2-carbaldehyde.

Flash column chromatography (gradient towards 6/4 hexanes/ethyl acetate, $R_f = 0.78$) afforded **1j** as an orange liquid (51% yield over three steps).

^1H NMR (300 MHz, CDCl_3) δ 9.71 (s, 1H), 5.97–5.90 (m, 1H), 5.82–5.75 (m, 1H), 4.43 (br s, 2H), 3.87 (q, $J = 7.3$ Hz, 2H), 3.12 (t, $J = 6.7$ Hz, 2H), 2.33 (t, $J = 7.1$ Hz, 2H), 2.22 (br s, 3H), 1.73 (q, $J = 7.3$ Hz, 2H), 1.48 (s, 9H), 1.26–1.03 (m, 3H). (Mixture of rotamers)

^{13}C NMR (75 MHz, CDCl_3) δ 201.78, 155.29, 129.62, 126.50, 109.14, 105.72, 80.04, 43.68, 41.14, 38.56, 28.63, 20.20, 16.42, 12.35, 1.17.

HRMS (FD, m/z): Calculated for $\text{C}_{17}\text{H}_{28}\text{N}_2\text{O}_3$: 308.2100, found: 308.2106.



tert-butyl ((2-(4-fluorophenyl)thiazol-5-yl)methyl)(4-oxobutyl)carbamate (1k)

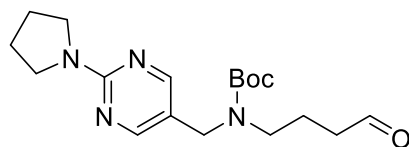
General procedure A was followed, starting from 2-(4-fluorophenyl)thiazole-5-carbaldehyde. Flash column chromatography (gradient towards 6/4 hexanes/ethyl acetate, $R_f = 0.48$) afforded **1k** as a colorless liquid (73% yield over three steps).

^1H NMR (300 MHz, CDCl_3) δ 9.77 (s, 1H), 7.90 (td, $J = 5.5, 2.3$ Hz, 2H), 7.64 (s, 1H), 7.12 (t, $J = 8.6$ Hz, 2H), 4.55 (s, 2H), 3.27 (br s, 2H), 2.46 (br s, 2H), 1.95–1.78 (br m, 2H), 1.51 (s, 9H). (Mixture of rotamers)

^{13}C NMR (75 MHz, CDCl_3) δ 201.34, 165.56, 162.24, 142.24, 135.58, 130.09, 128.40, 128.29, 116.21, 115.92, 80.74, 45.86, 43.23, 40.97, 28.50, 20.75.

^{19}F NMR (282 MHz, CDCl_3) δ -110.36.

HRMS (FD, m/z): Calculated for $\text{C}_{19}\text{H}_{23}\text{FN}_2\text{O}_3\text{S}$: 378.1413, found: 378.1413.



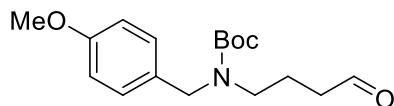
tert-butyl (4-oxobutyl)((2-(pyrrolidin-1-yl)pyrimidin-5-yl)methyl)carbamate (1l)

General procedure A was followed, starting from 2-(pyrrolidin-1-yl)pyrimidine-5-carbaldehyde. Flash column chromatography (gradient towards 8/2 ethyl acetate/dichloromethane, $R_f = 0.46$) afforded **1l** as a colorless liquid (51% yield over three steps).

^1H NMR (300 MHz, CDCl_3) δ 9.76 (s, 1H), 8.25 (s, 2H), 4.21 (br s, 2H), 3.65–3.49 (br m, 4H), 3.17 (br s, 2H), 2.44 (br t, $J = 6.5$ Hz, 2H), 2.09–1.91 (br m, 4H), 1.83 (br m, 2H), 1.47 (s, 9H). (Mixture of rotamers)

^{13}C NMR (75 MHz, CDCl_3) δ 201.05, 159.70, 157.45, 118.07, 79.87, 46.43, 45.11, 40.72, 28.22, 25.31, 20.34.

HRMS (FD, m/z): Calculated for $\text{C}_{18}\text{H}_{28}\text{N}_4\text{O}_3$: 348.2161, found: 348.2155.



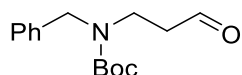
***tert*-butyl (4-methoxybenzyl)(4-oxobutyl)carbamate (**1m**)**

General procedure A was followed, starting from 4-methoxybenzaldehyde. Flash column chromatography (gradient towards 8/2 cyclohexane/ethyl acetate, $R_f = 0.17$) afforded **1m** as a colorless liquid (29% yield over three steps).

^1H NMR (400 MHz, CDCl_3) δ 9.56 (s, 1H), 7.05 (s, 2H), 6.72 (d, $J = 8.1$ Hz, 2H), 4.24 (br s, 2H), 3.63 (s, 3H), 3.17–2.95 (br m, 2H), 2.26 (br s, 2H), 1.67 (br s, 2H), 1.36 (br s, 9H). (Mixture of rotamers)

^{13}C NMR (126 MHz, CDCl_3) δ 201.08, 158.56, 155.36, 130.03, 128.73, 128.27, 113.55, 79.35, 54.75, 49.50, 48.83, 45.03, 40.54, 28.07, 20.10.

HRMS (FD, m/z): Calculated for $\text{C}_{17}\text{H}_{25}\text{NO}_4$: 307.1784, found: 307.1798.



***tert*-butyl benzyl(3-oxopropyl)carbamate (**1n**)**

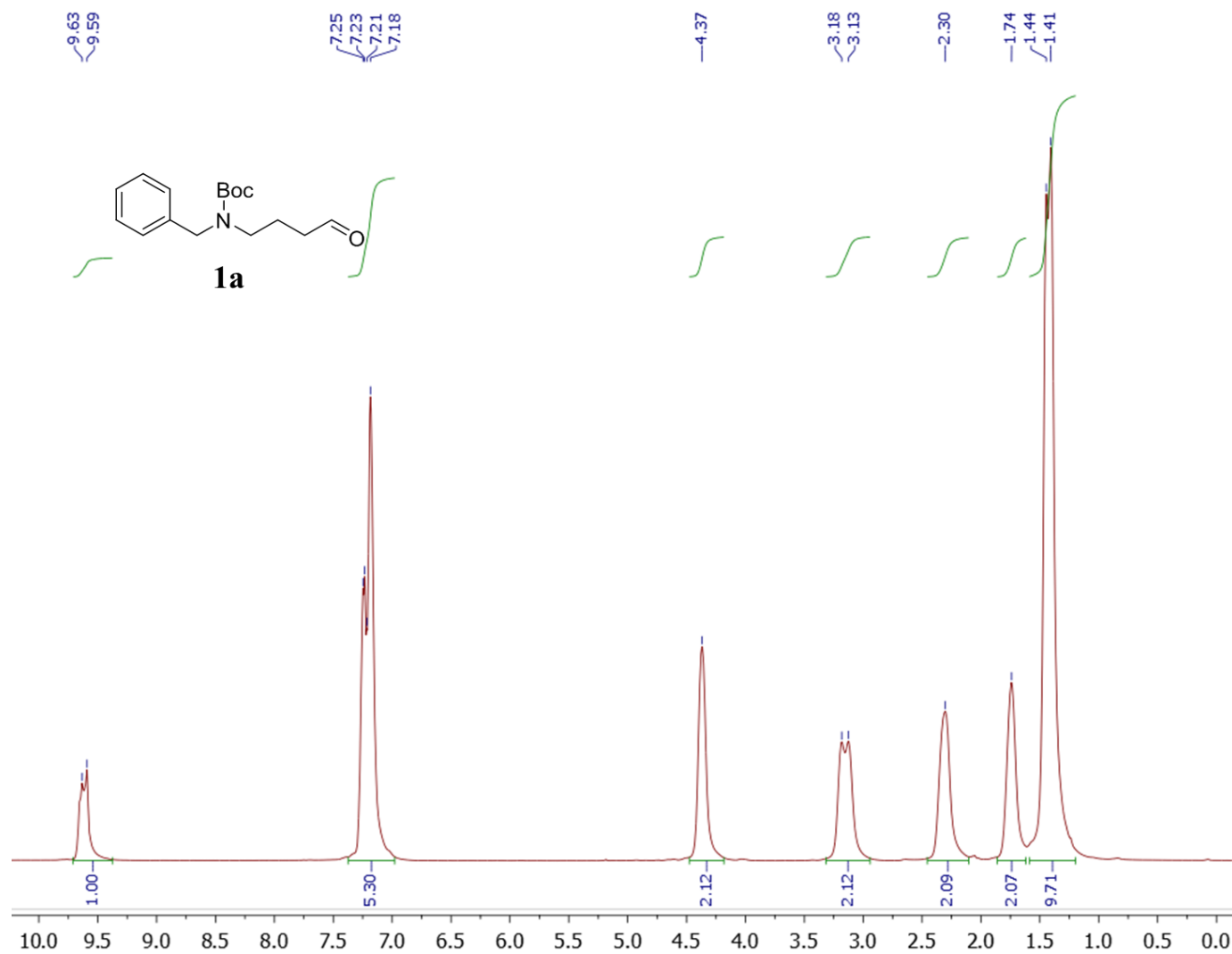
General procedure A was followed, starting from benzaldehyde and 3-aminopropan-1-ol. NMR data were in correspondence with those reported by for instance Zhang and co-workers.^[6]

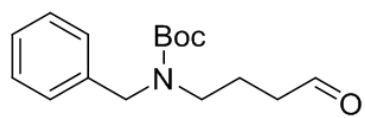
^1H NMR (400 MHz, CDCl_3) δ 9.74 (br s, 1H), 7.38–7.04 (m, 5H), 4.45 (br s, 2H), 3.60–3.32 (br m, 2H), 2.74–2.45 (br m, 2H), 1.46 (s, 9H). (Mixture of rotamers)

HRMS (FD, m/z): Calculated for $\text{C}_{15}\text{H}_{21}\text{NO}_3$: 263.1521, found: 263.1510.

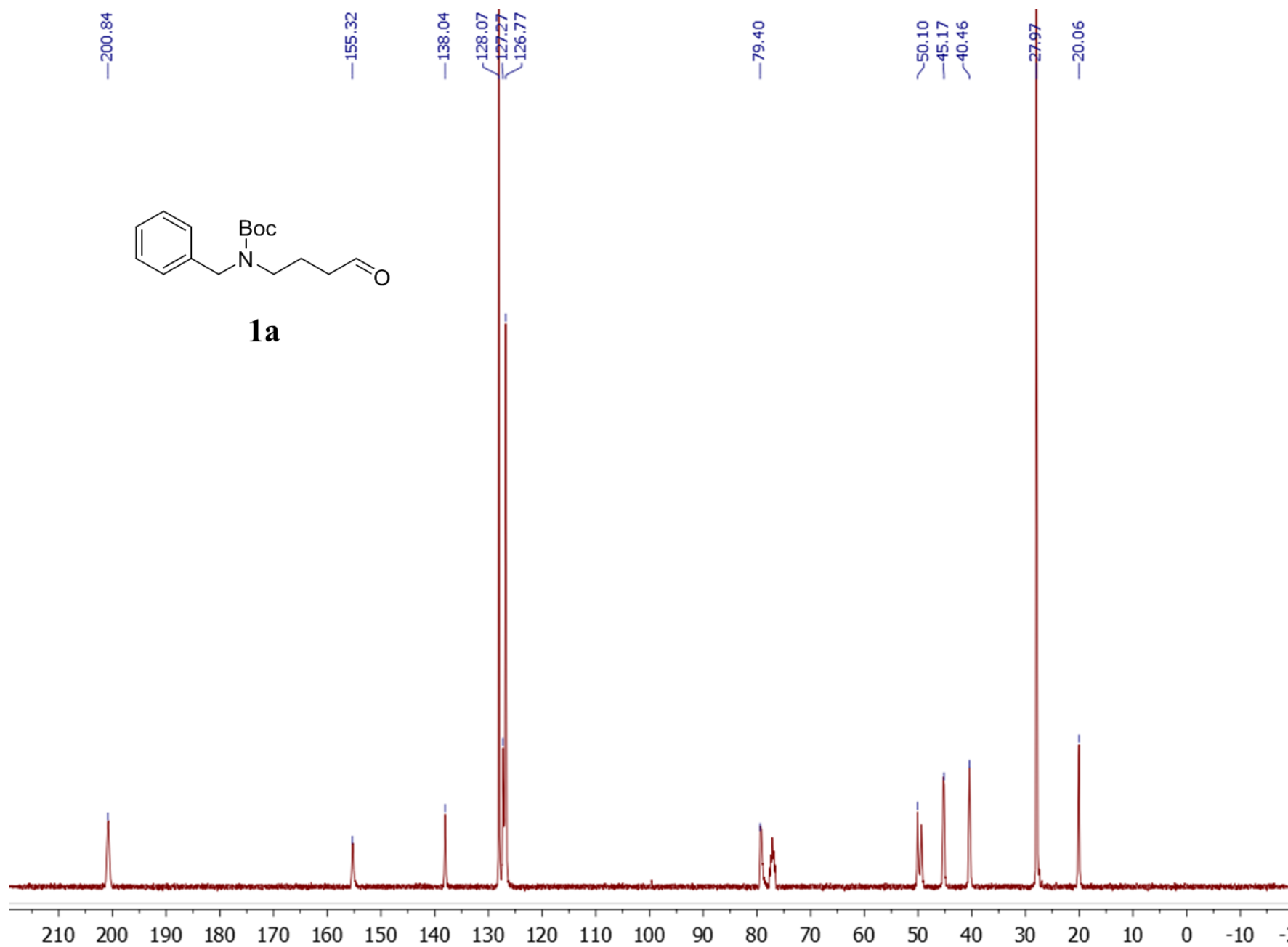
3.3 Copies of ^1H -, ^{13}C - and ^{19}F -NMR spectra

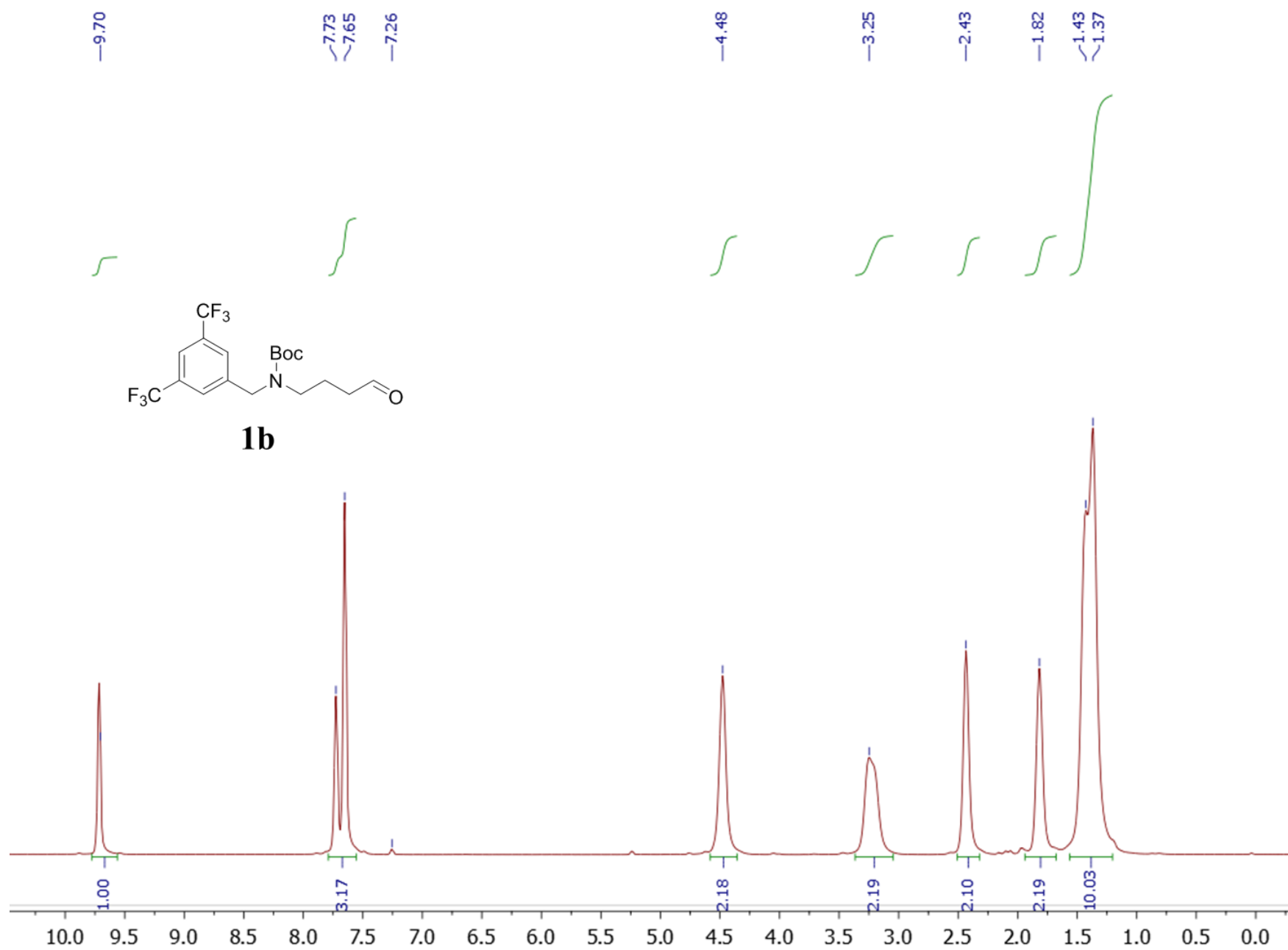
Note: most of the following compounds exhibit restricted bond rotation and therefore show broadened and/or overlapping signals due to presence of different rotamers.

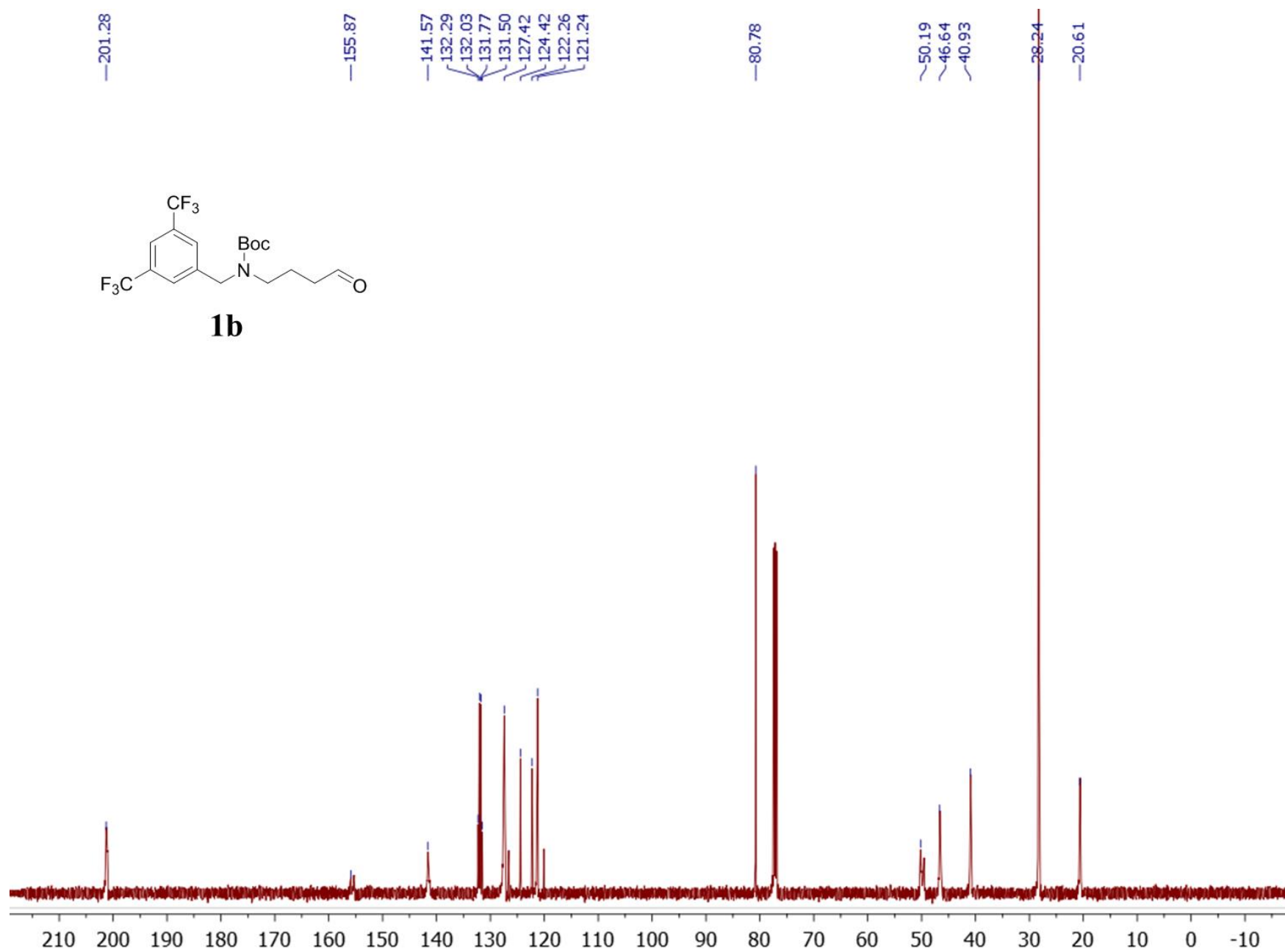
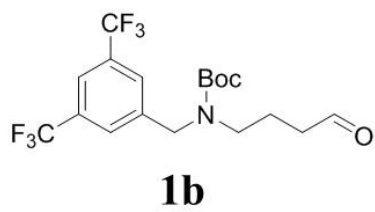


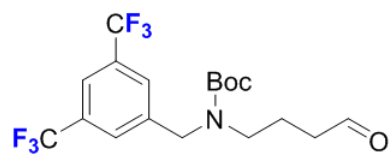


1a

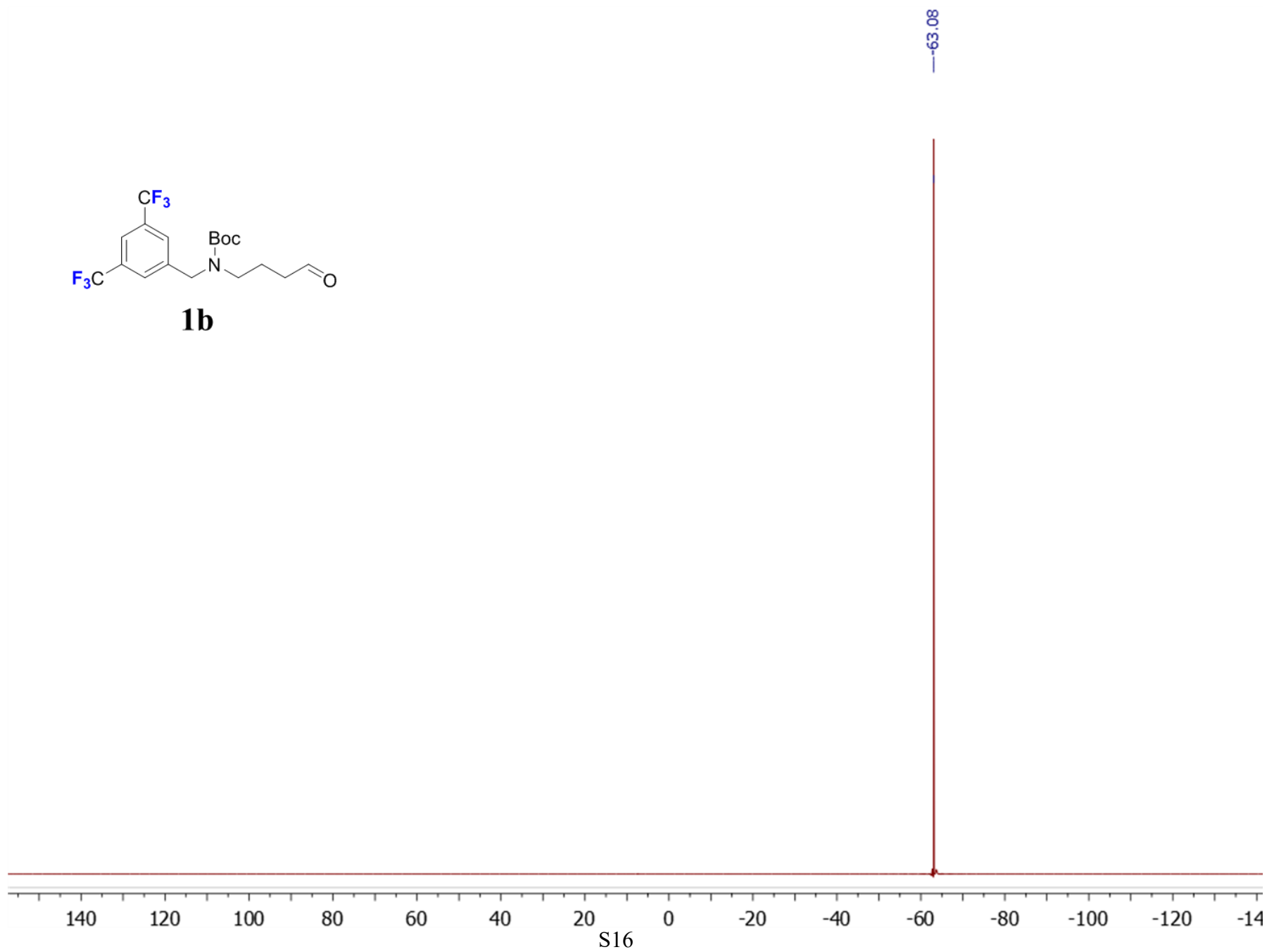


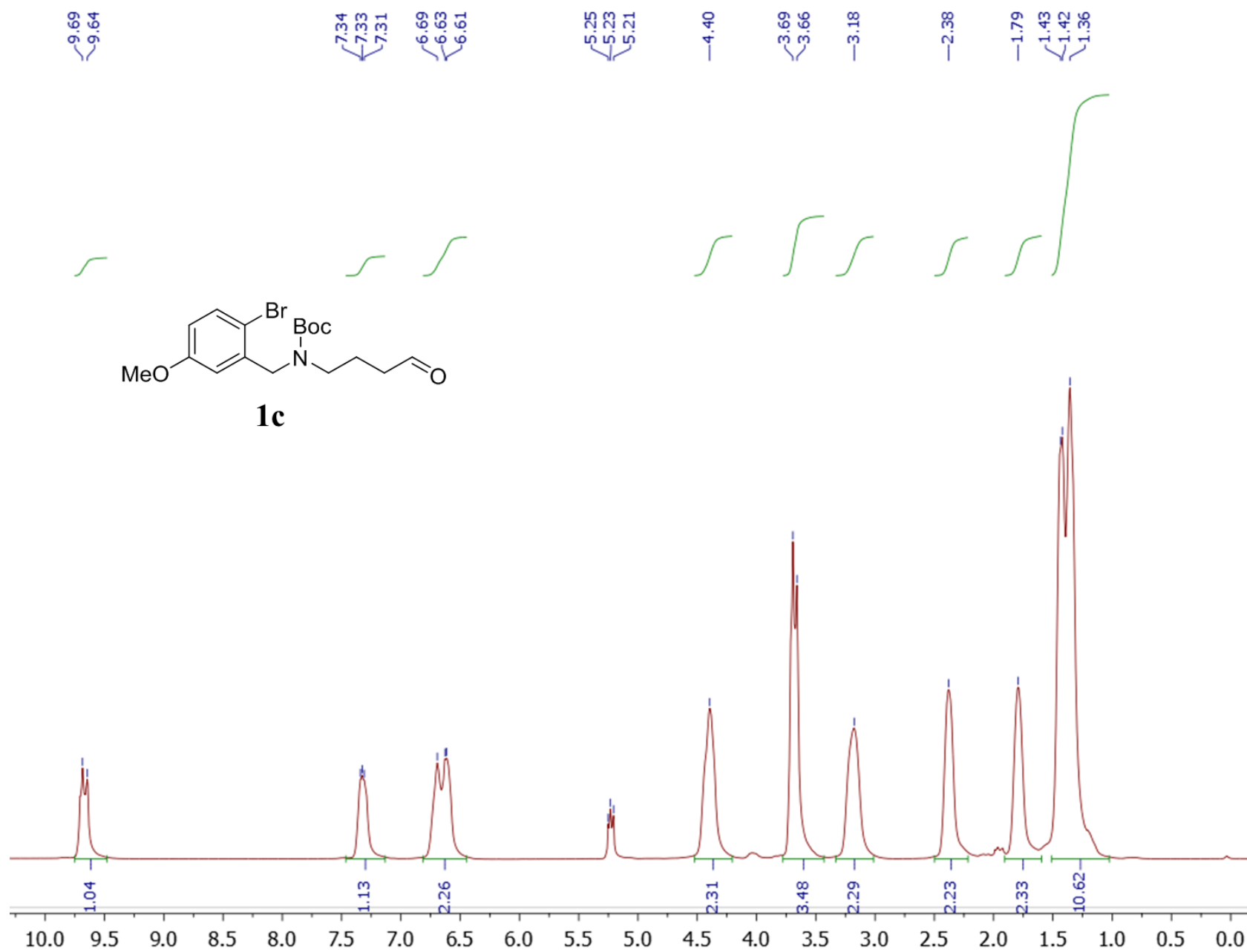


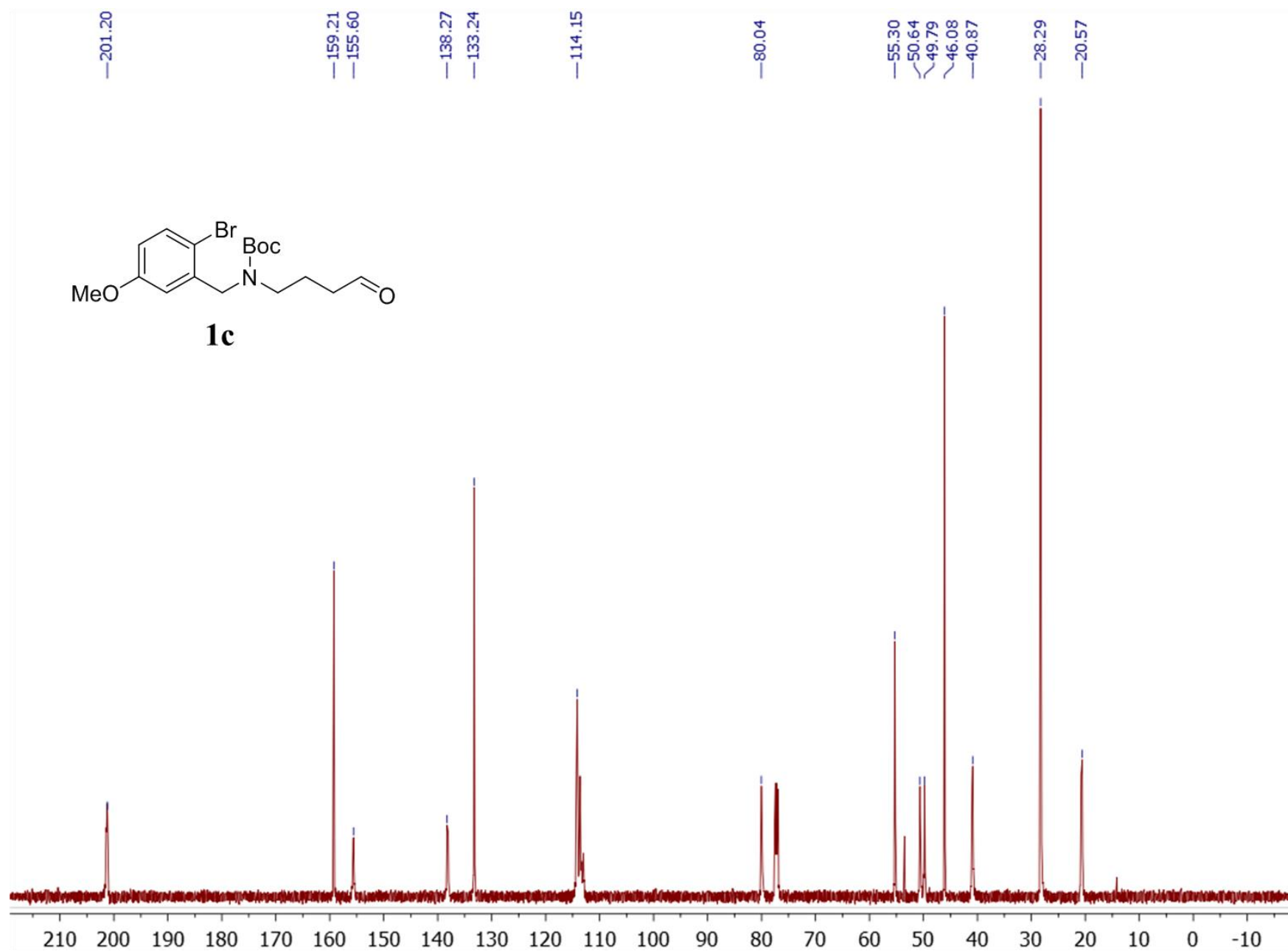


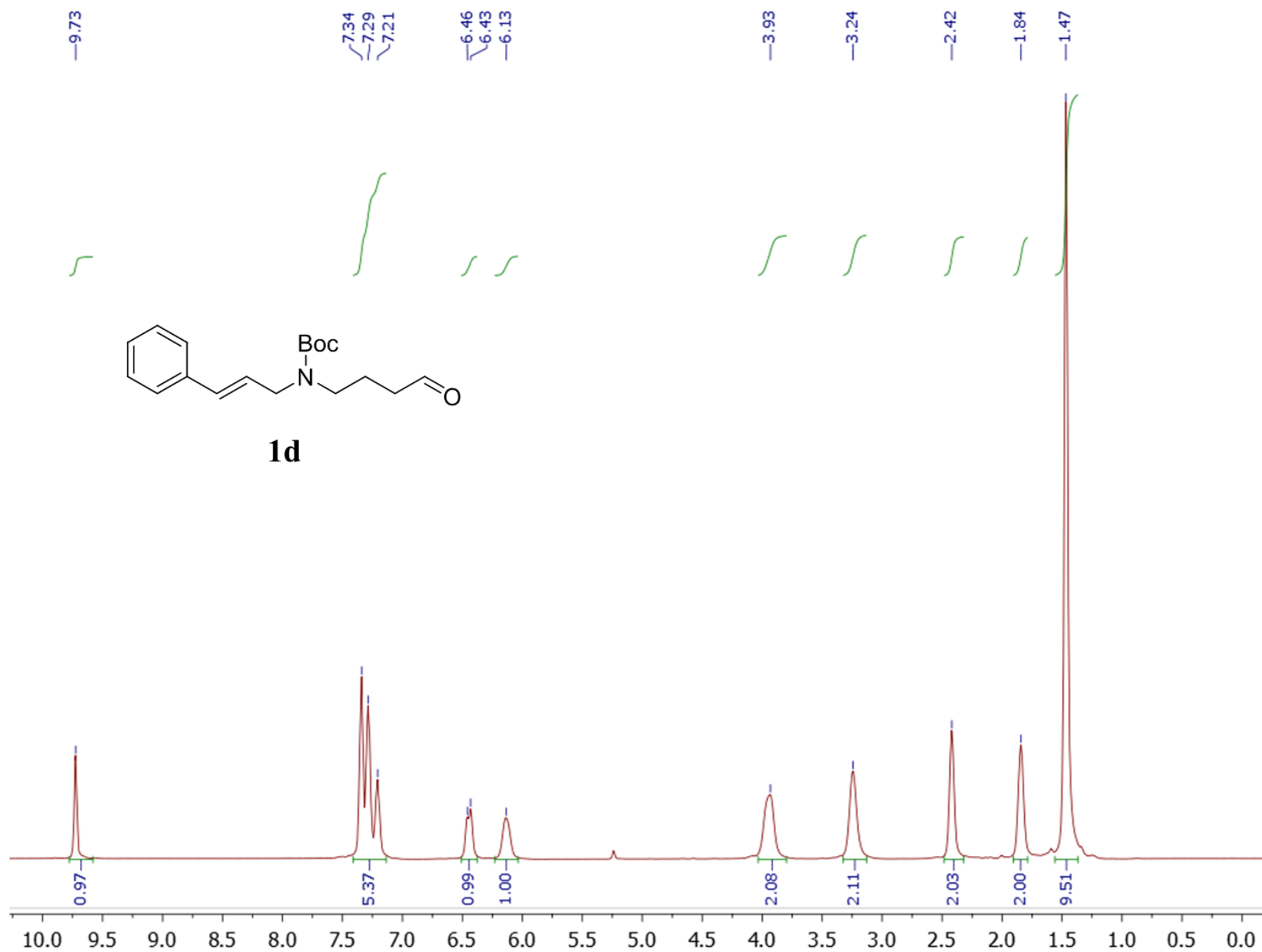


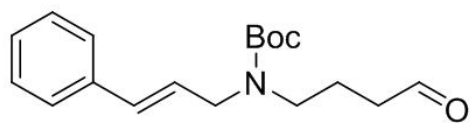
1b



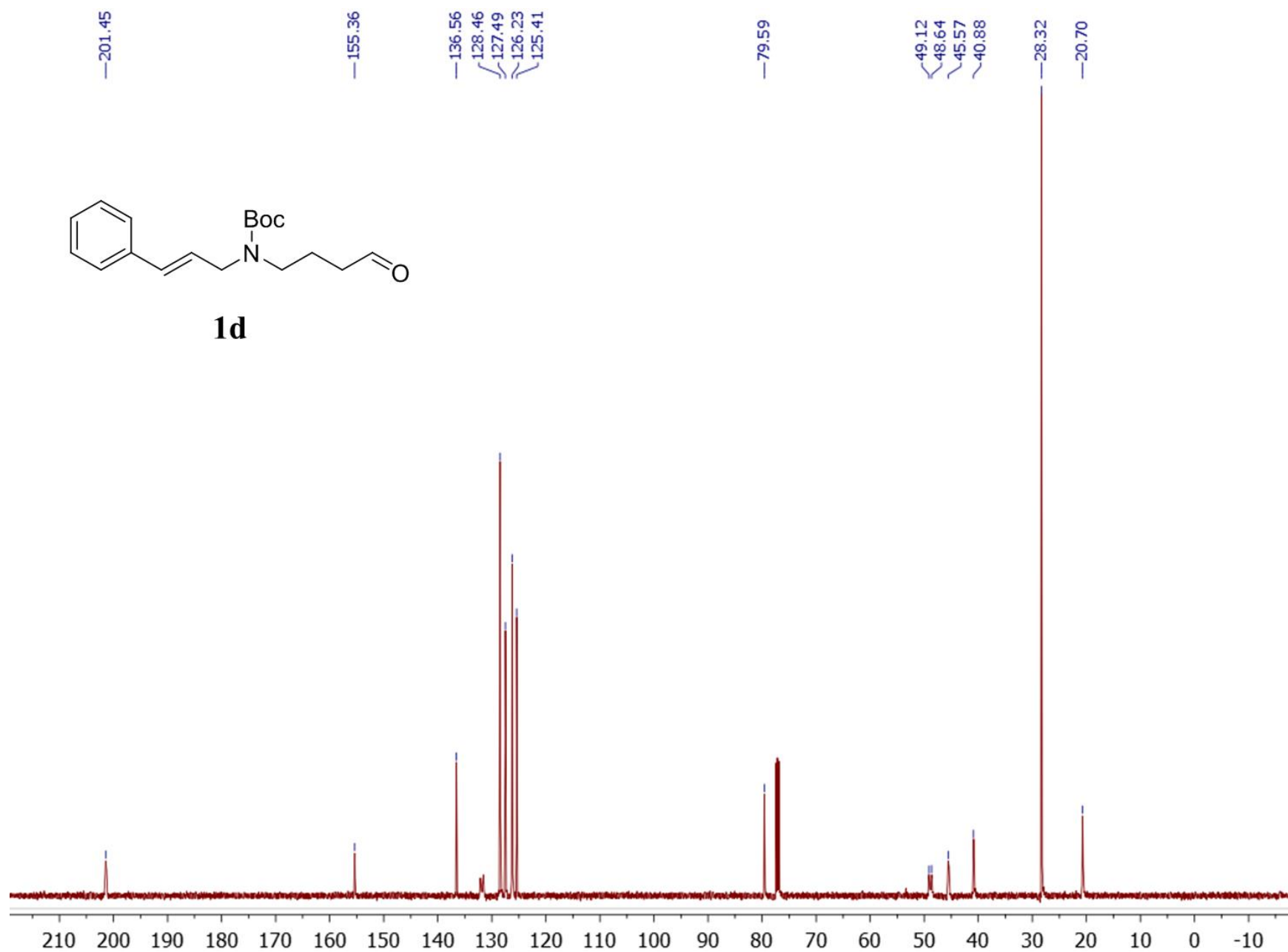


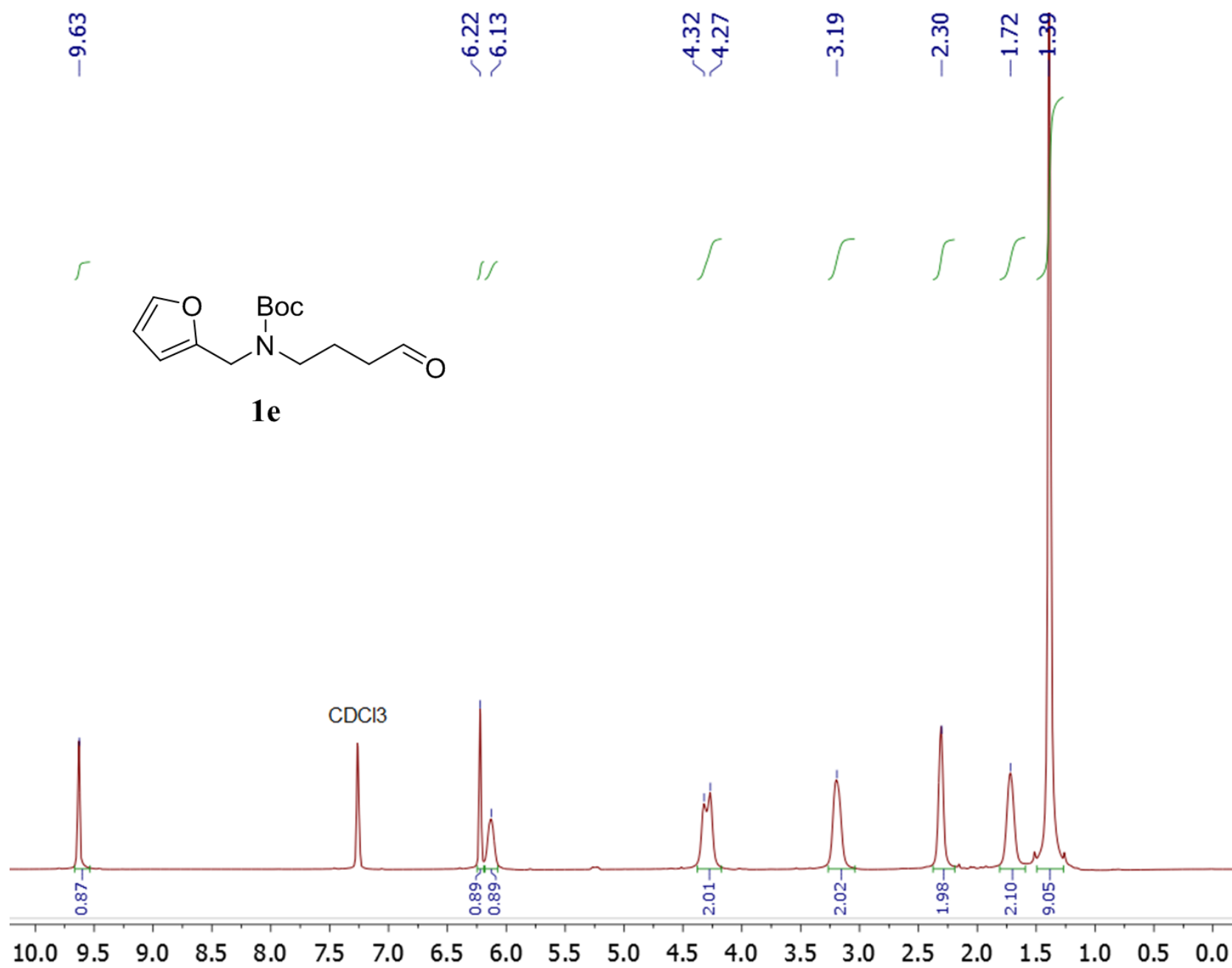


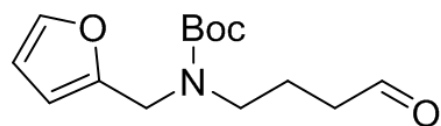




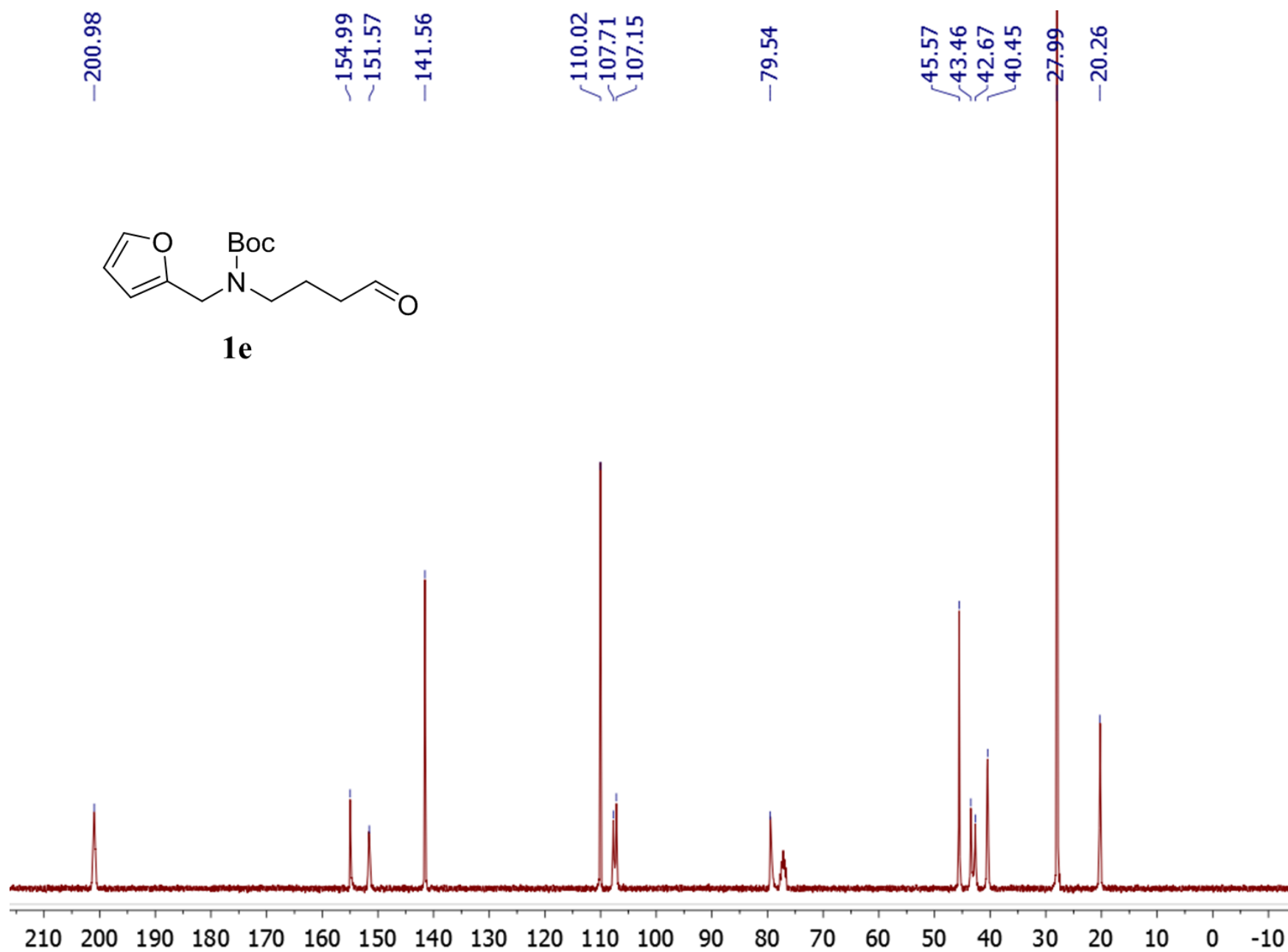
1d

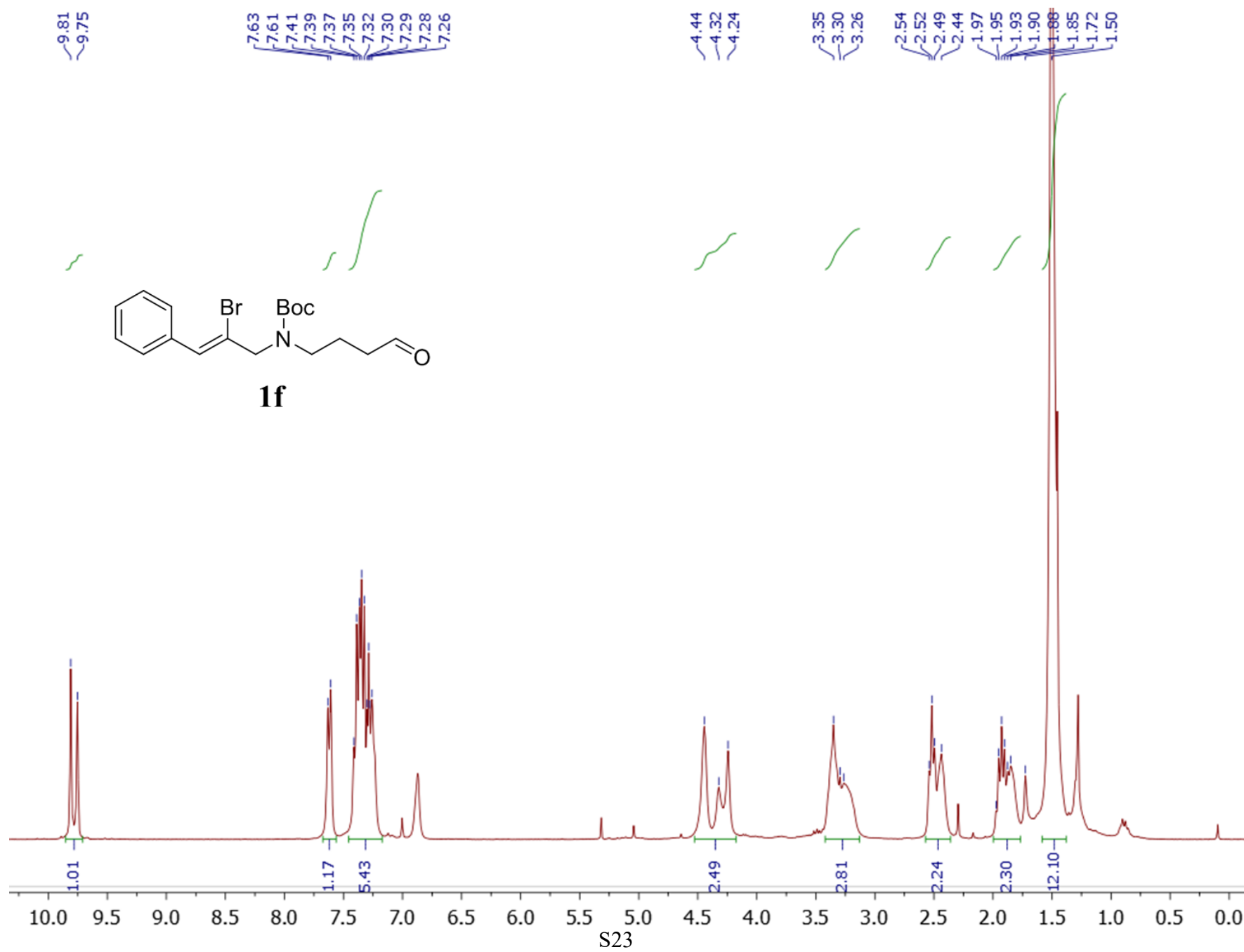


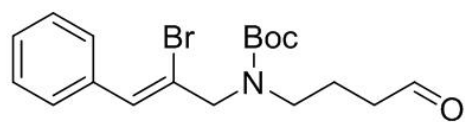




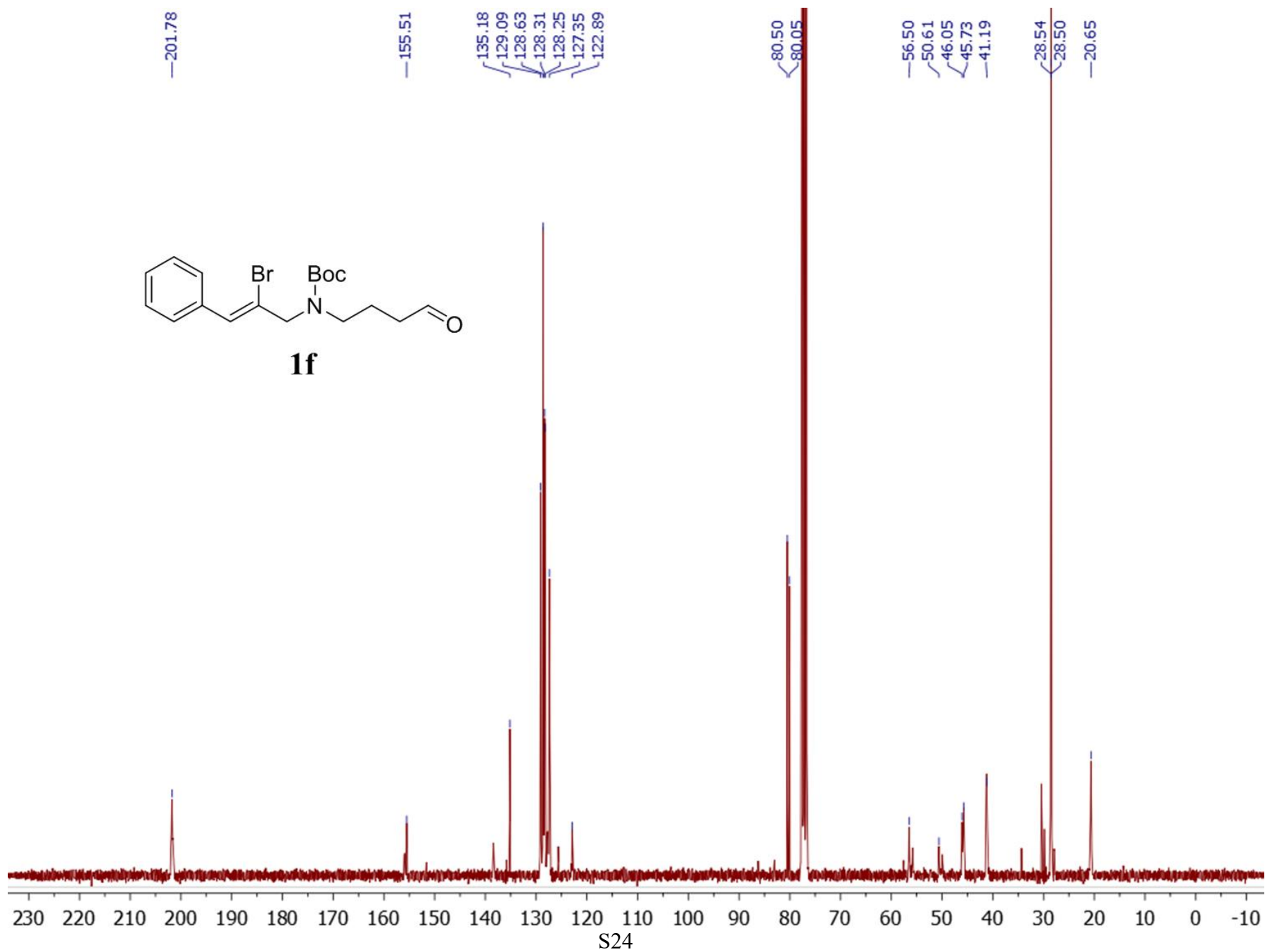
1e

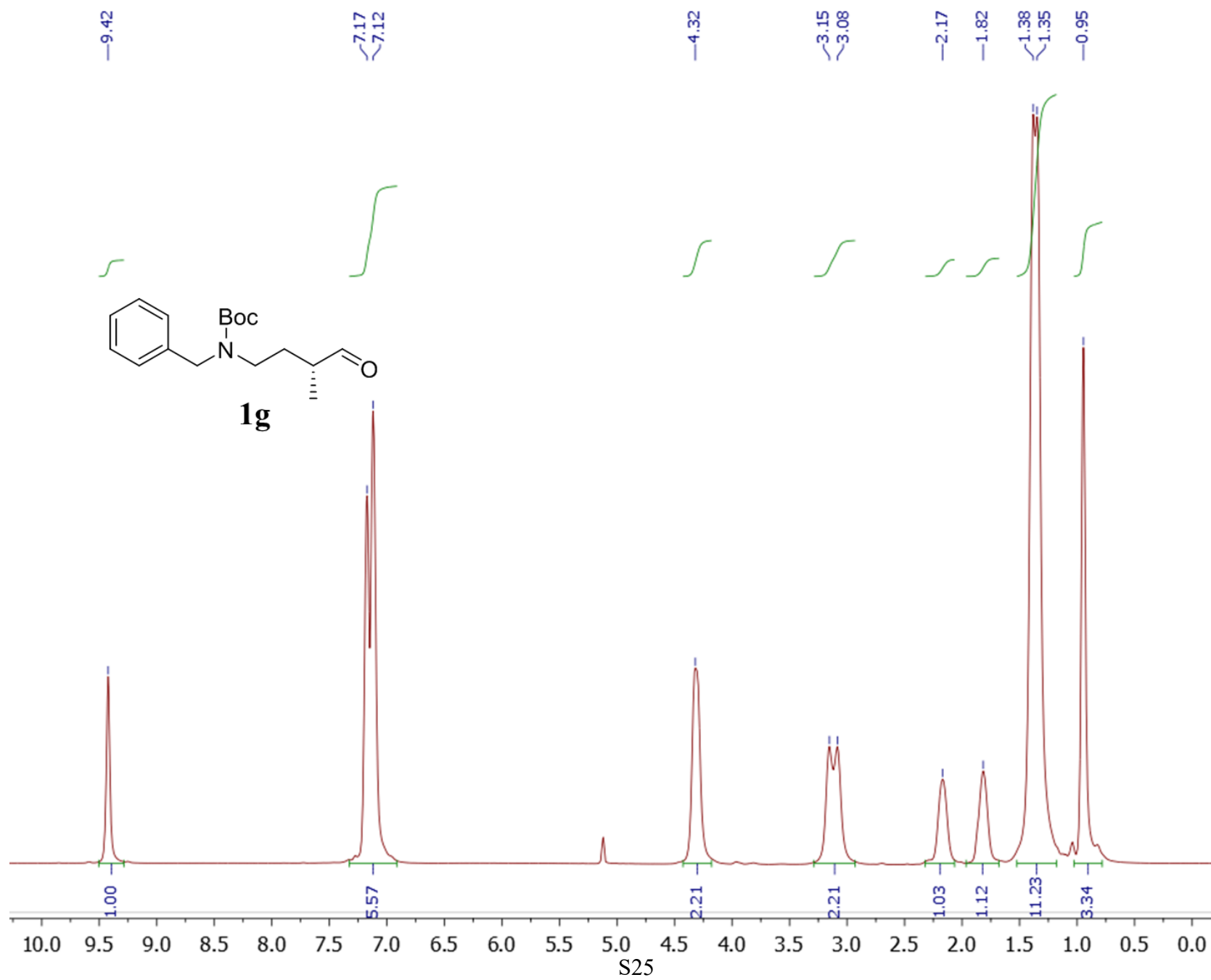


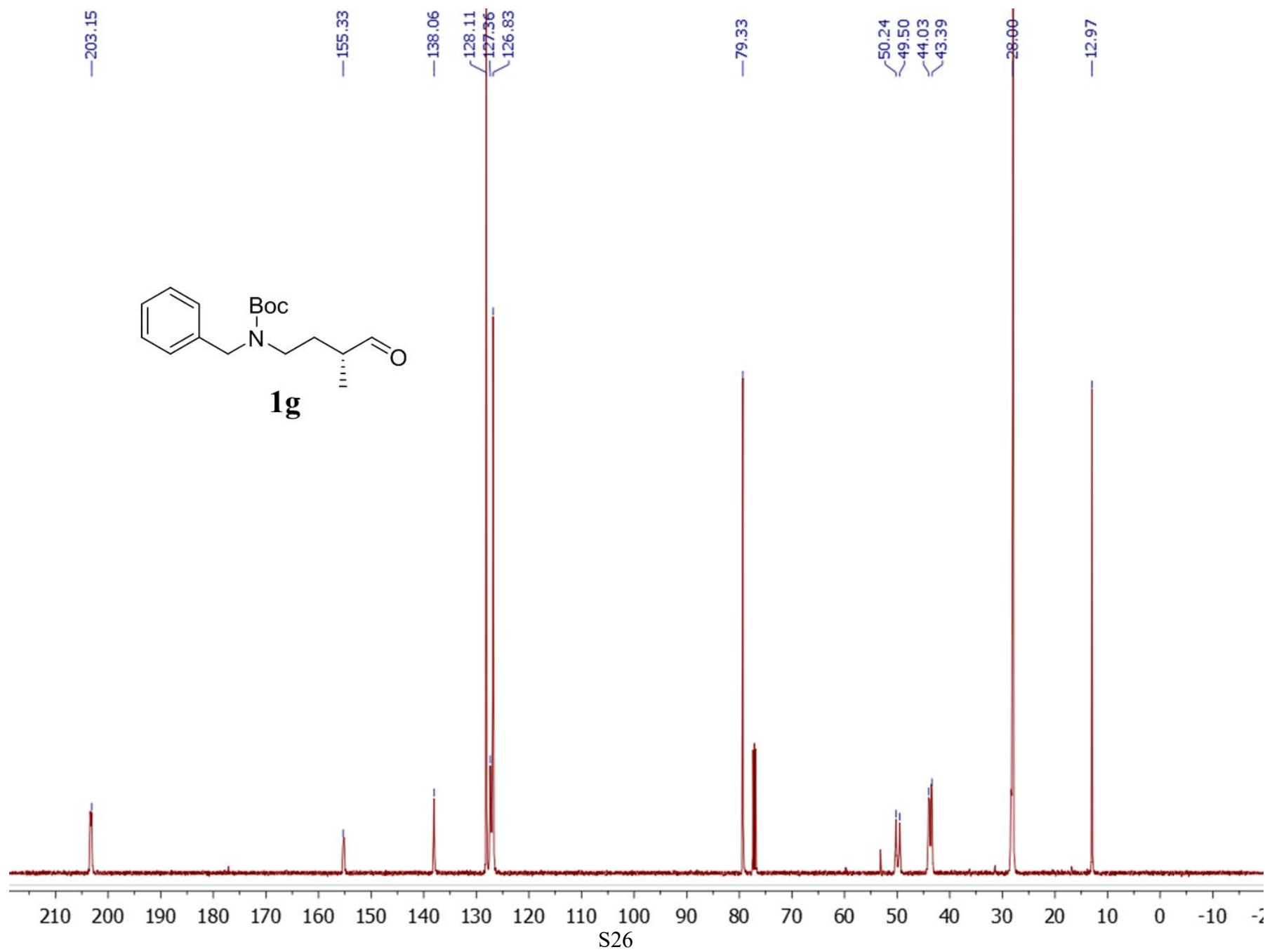
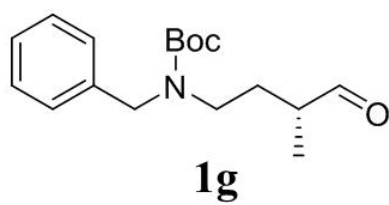


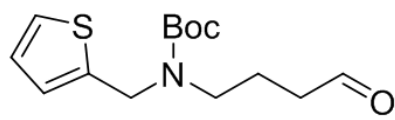


1f

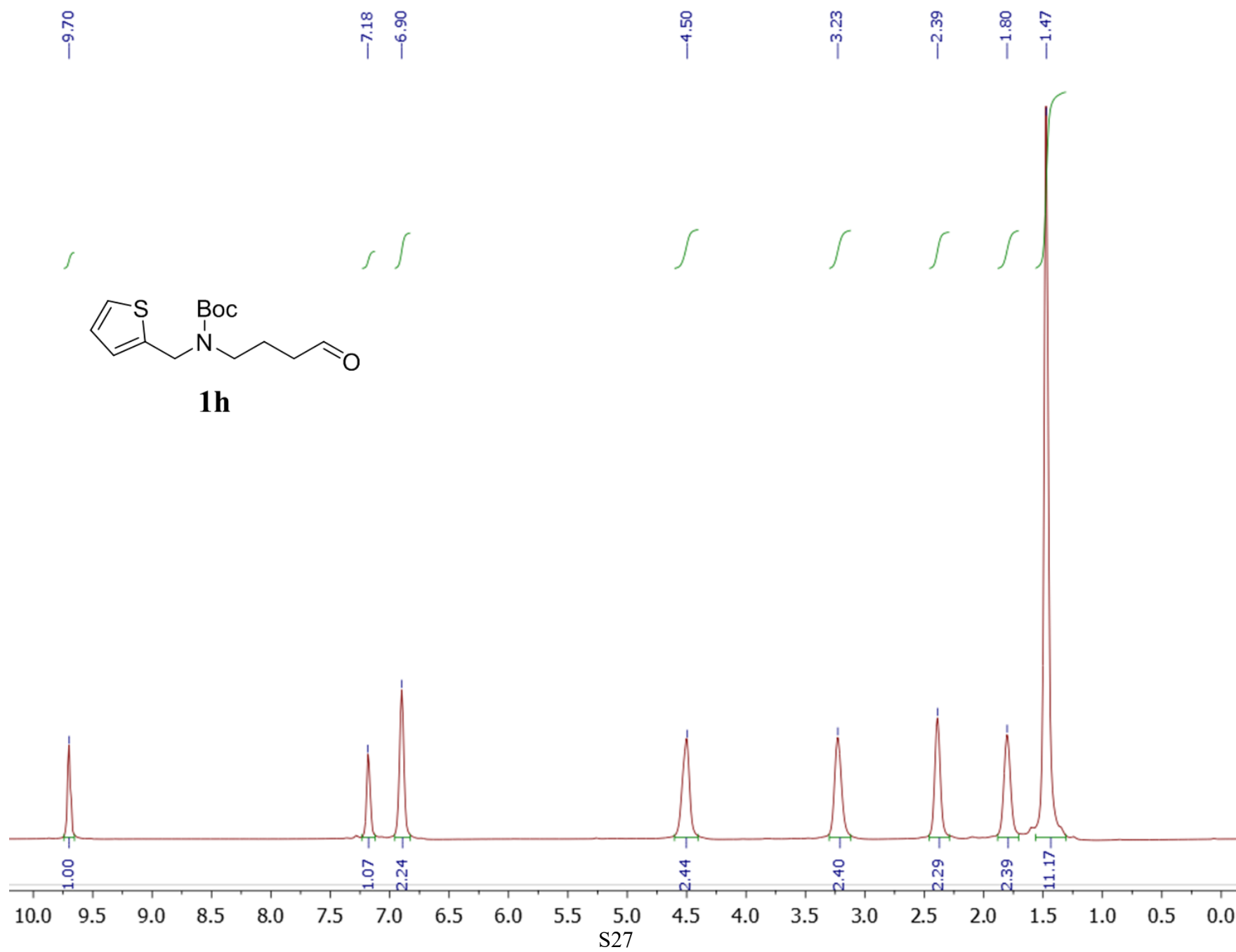


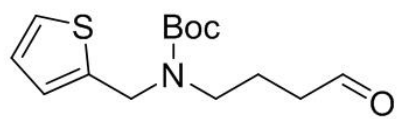




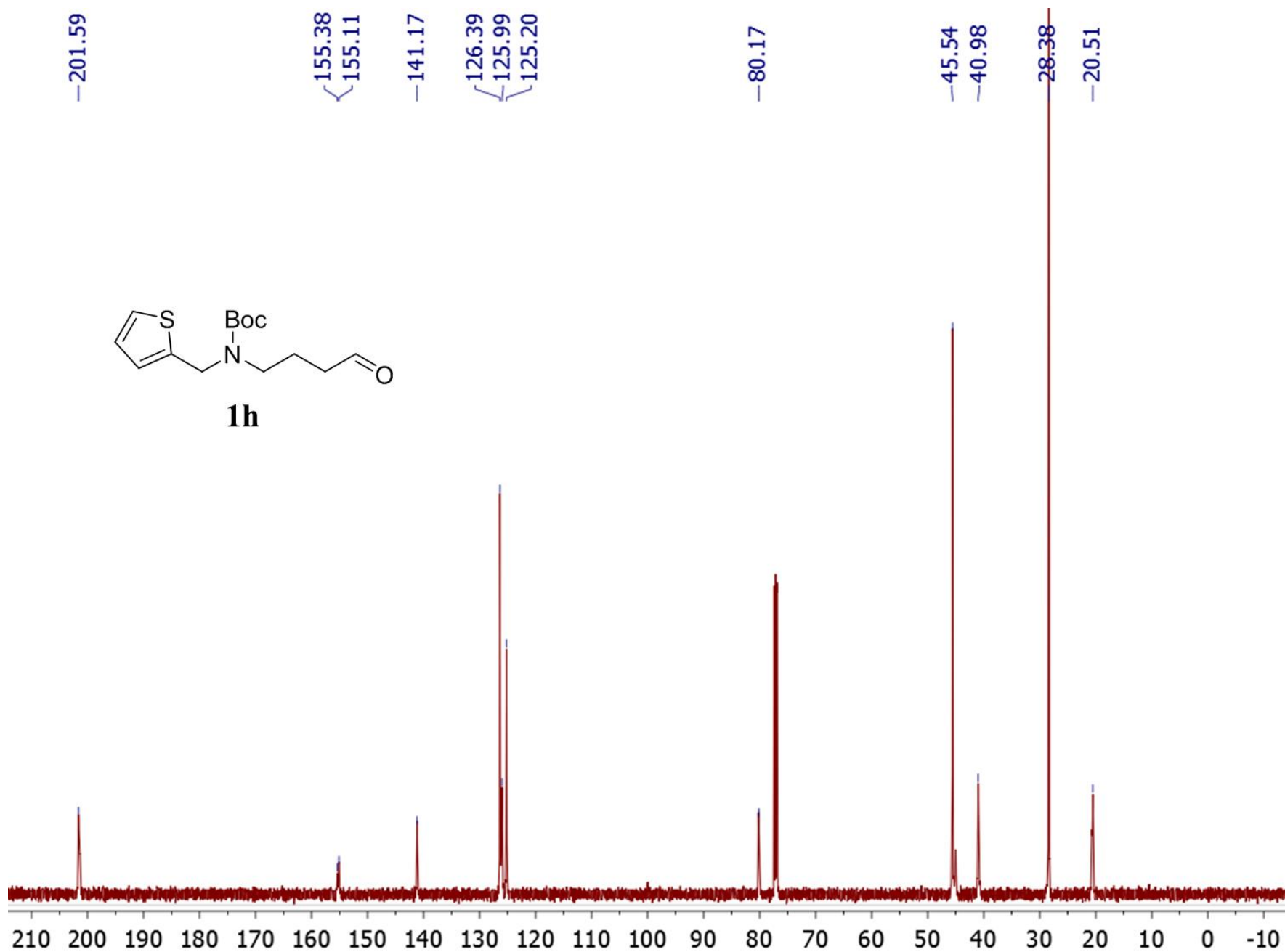


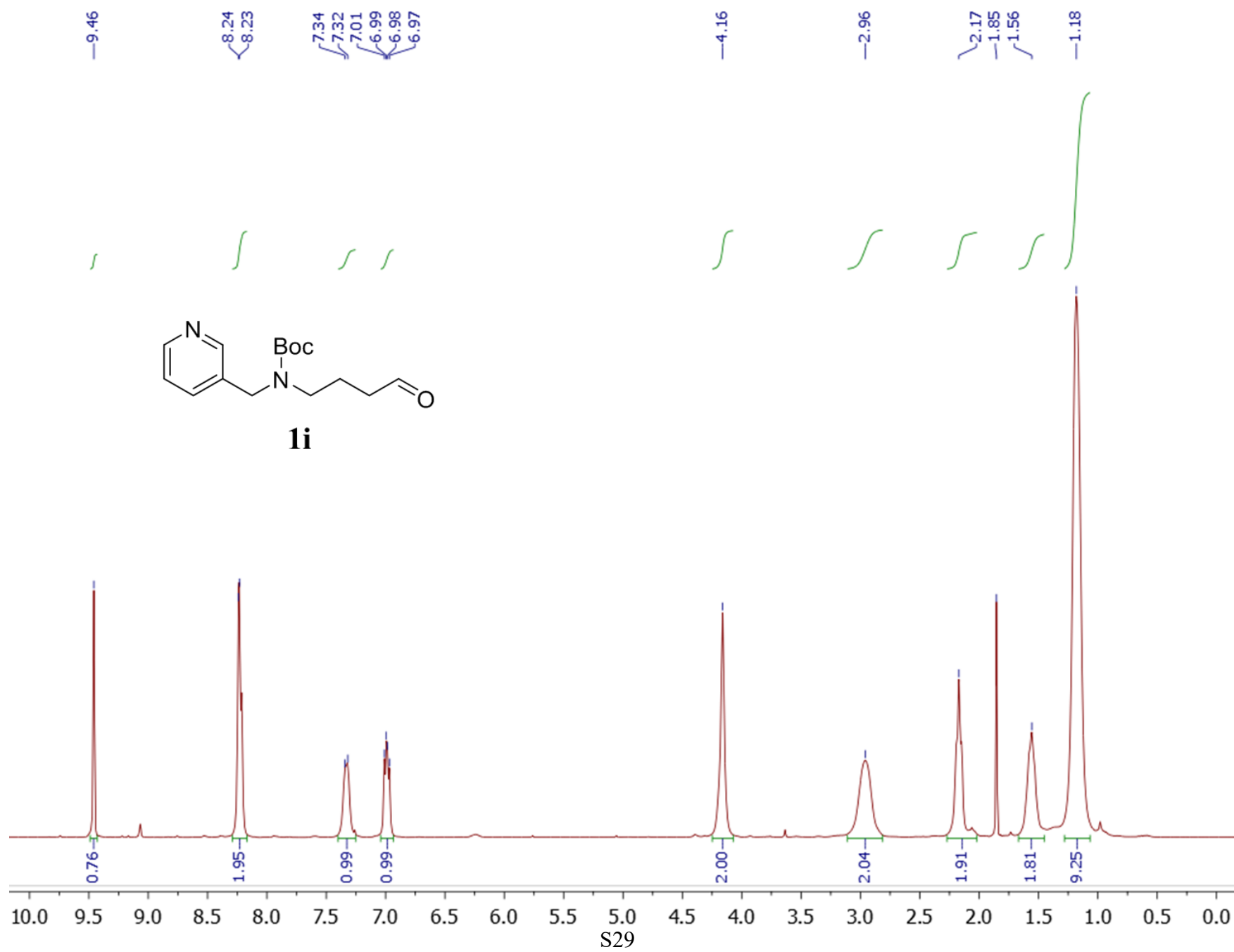
1h

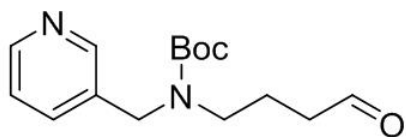




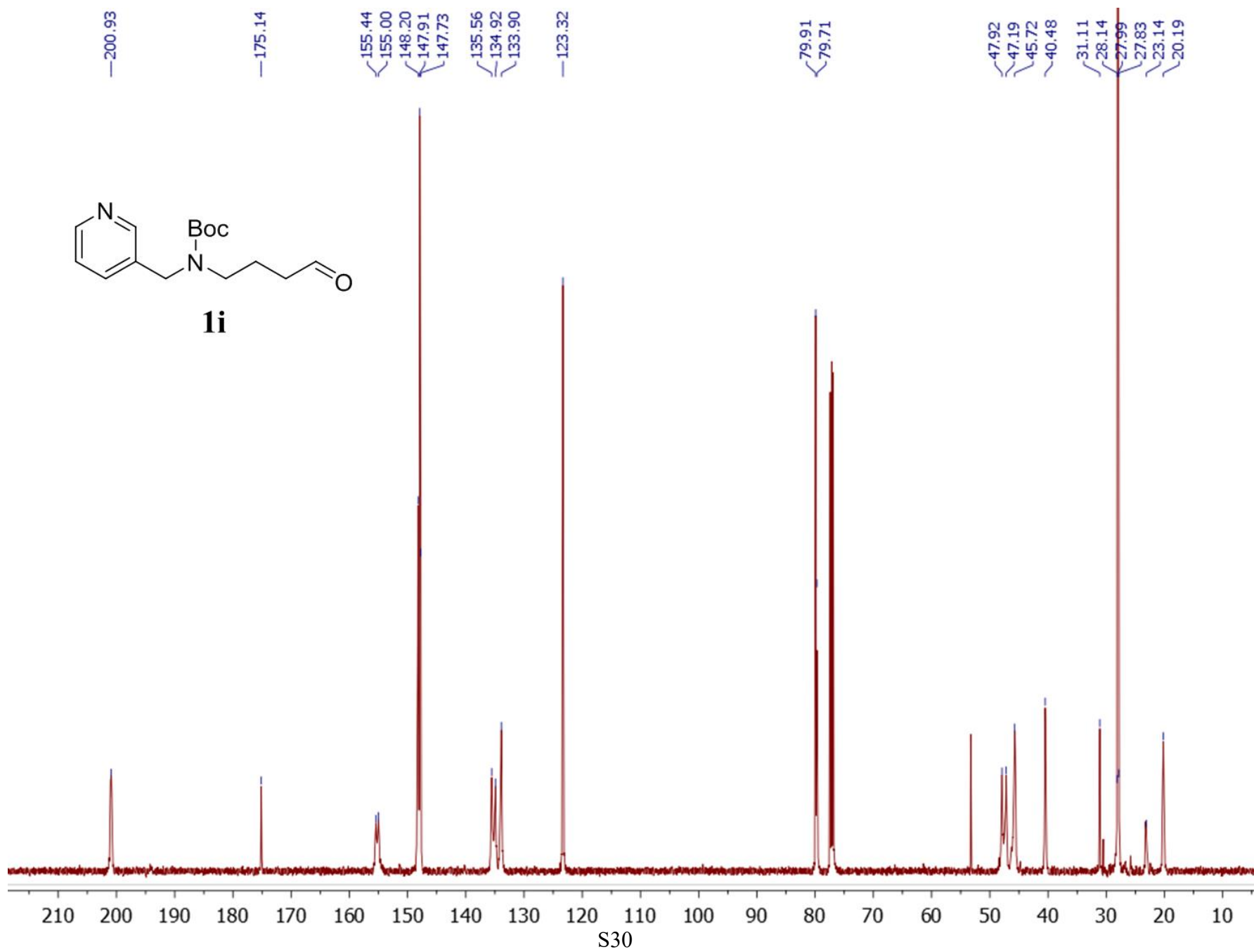
1h

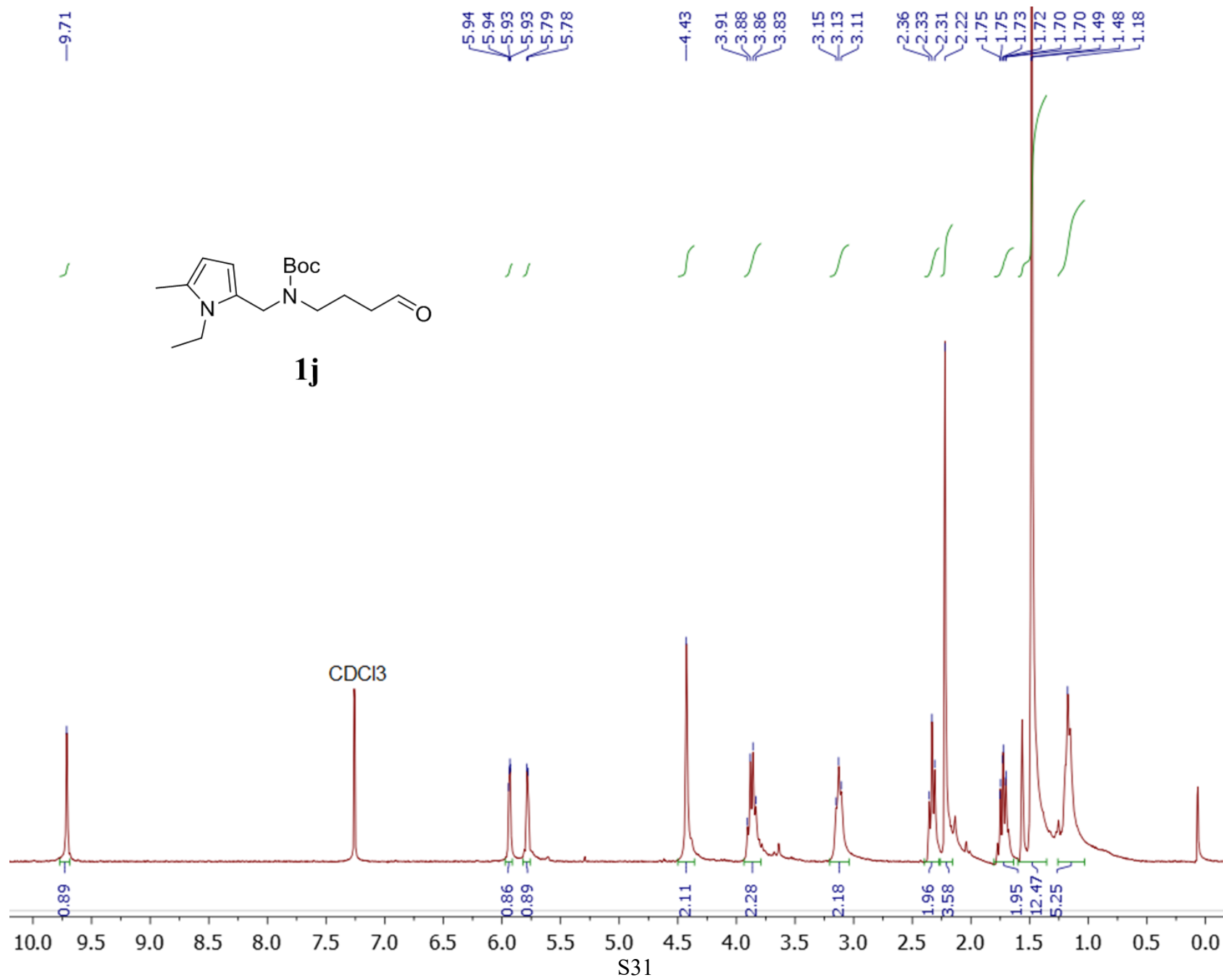


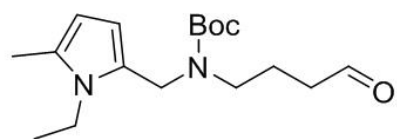




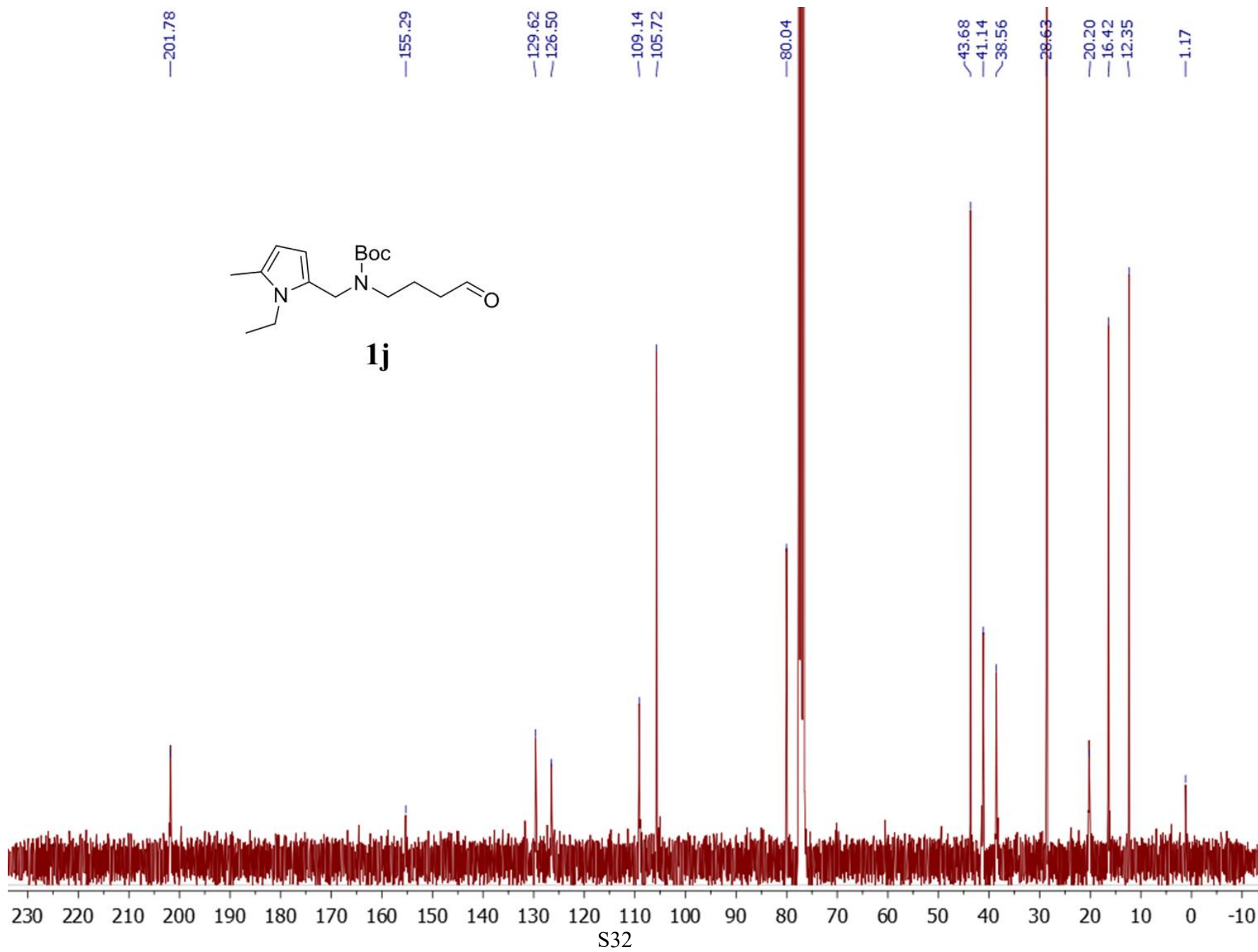
1i

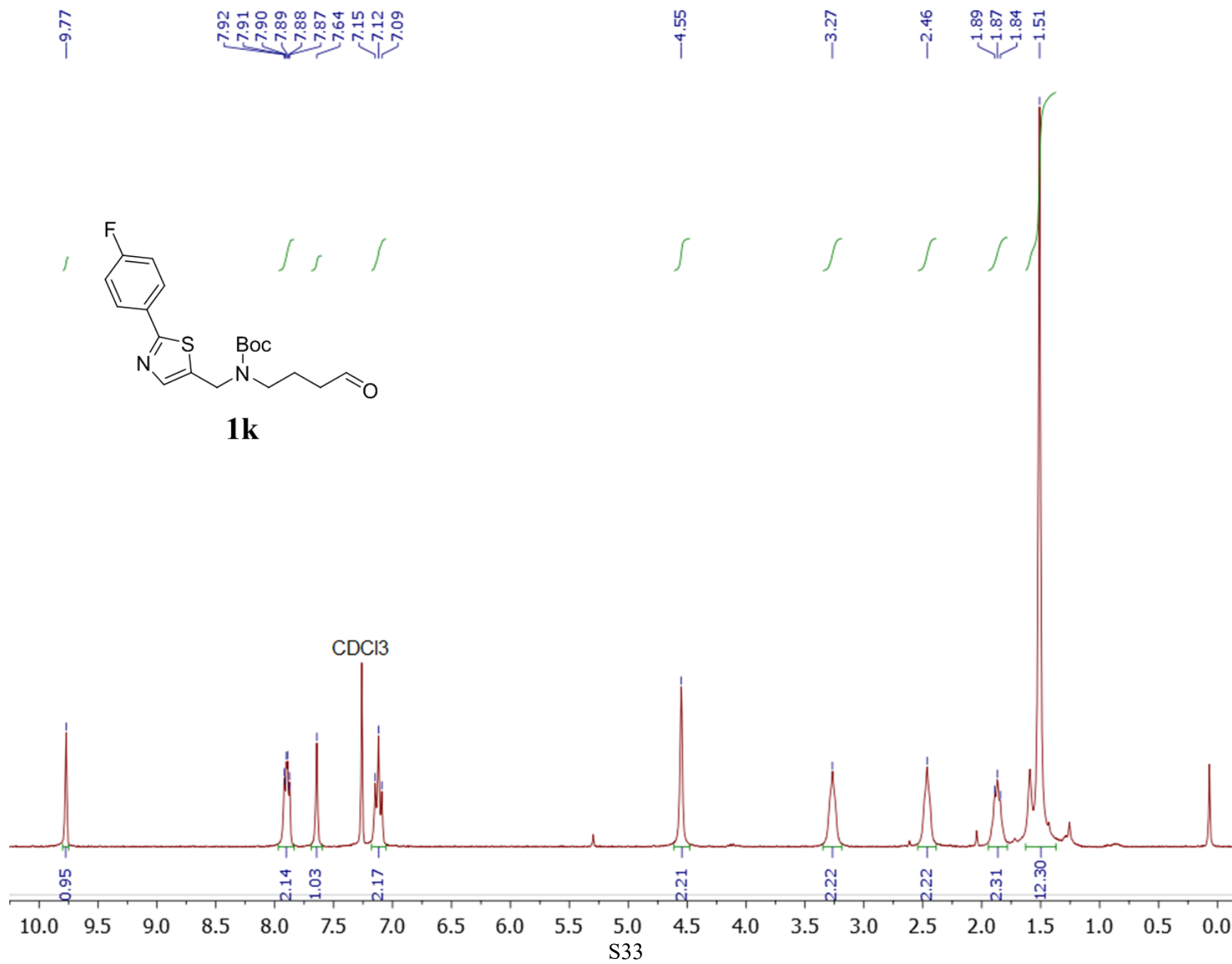


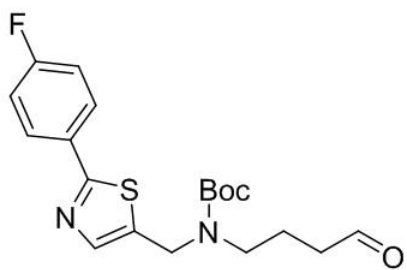




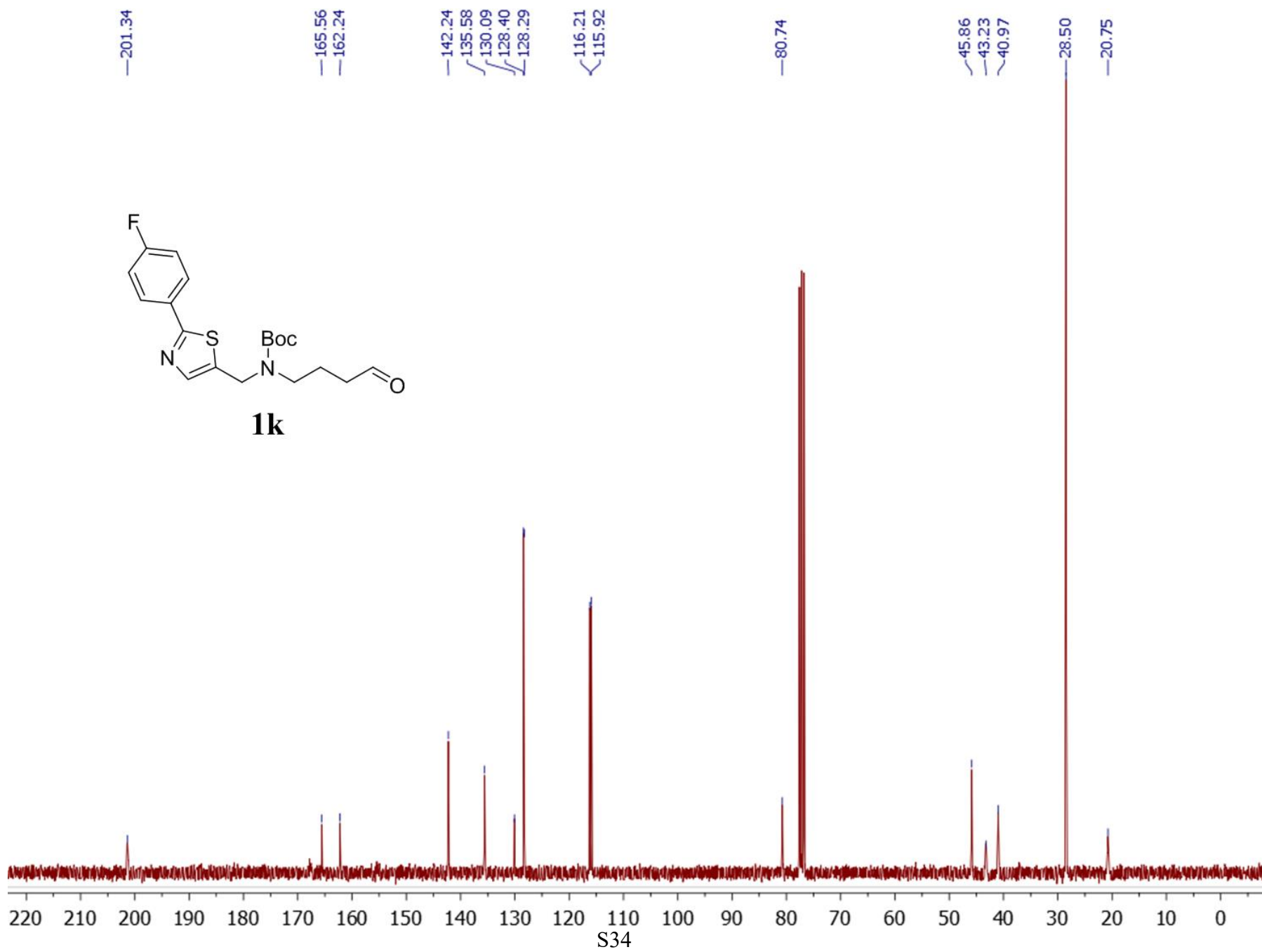
1j

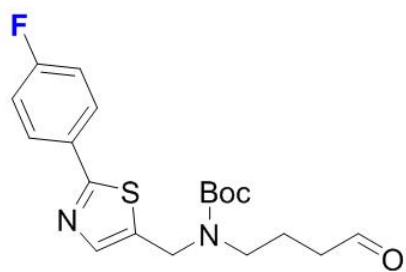




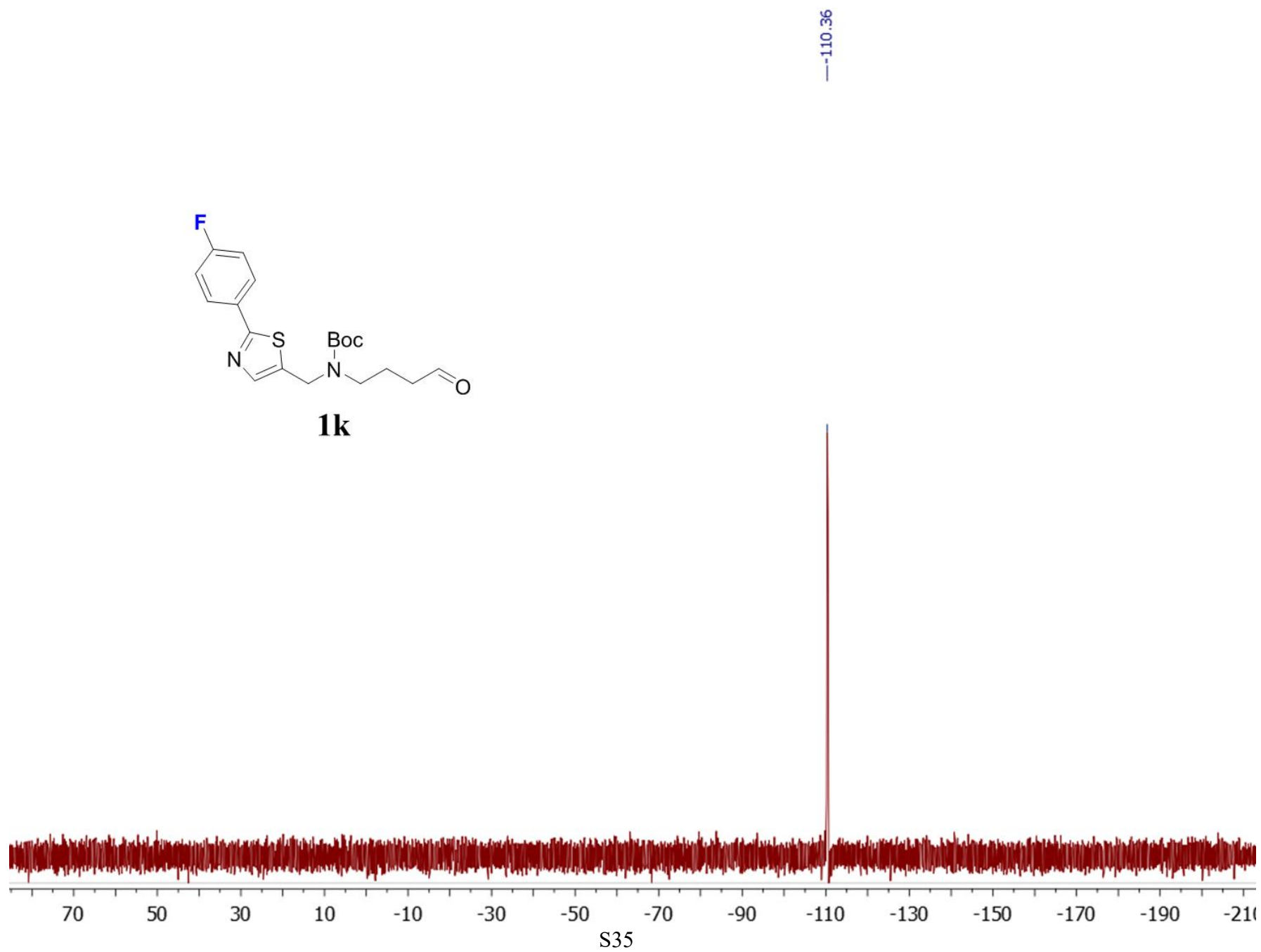


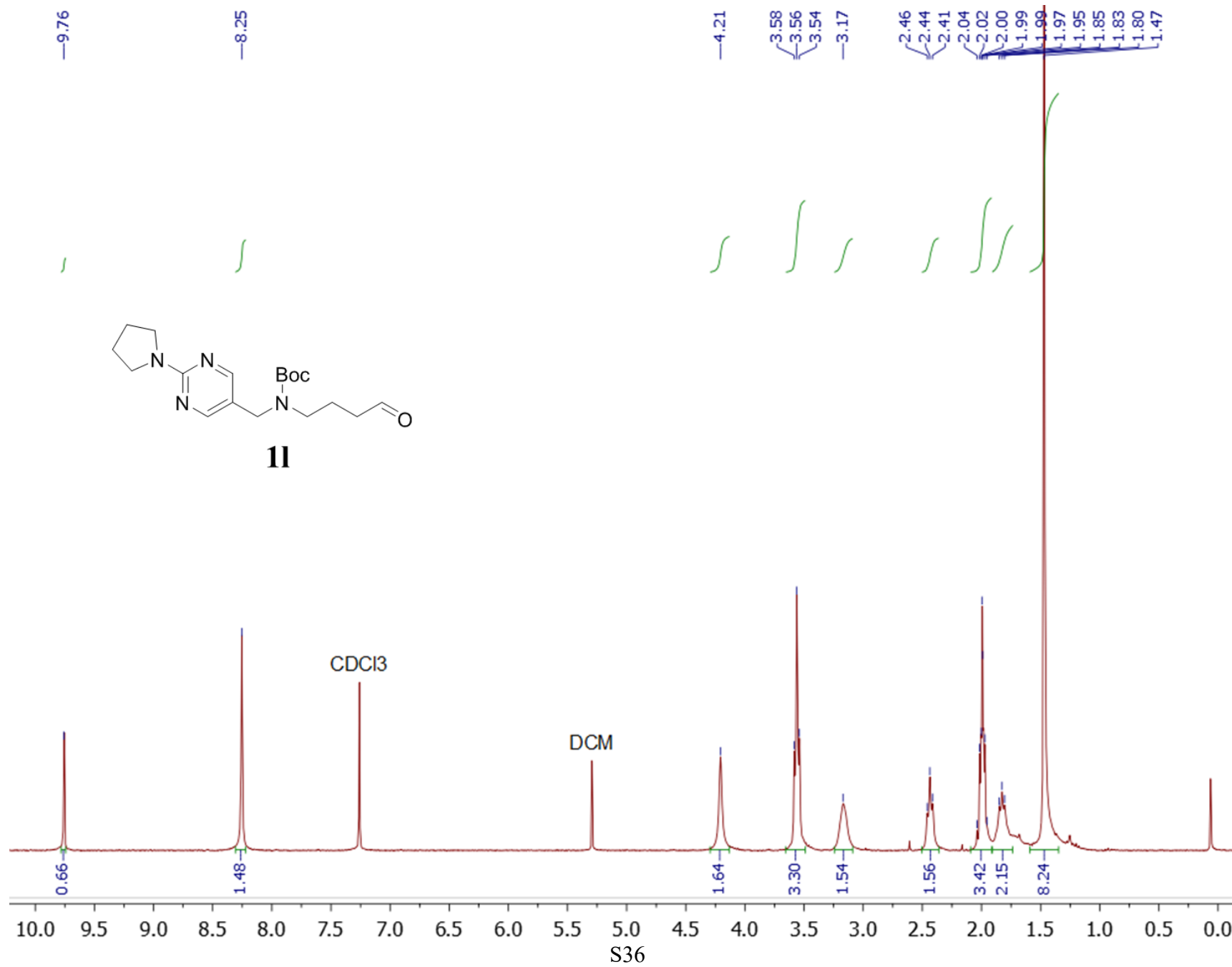
1k

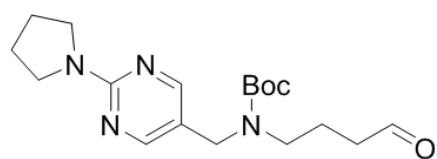




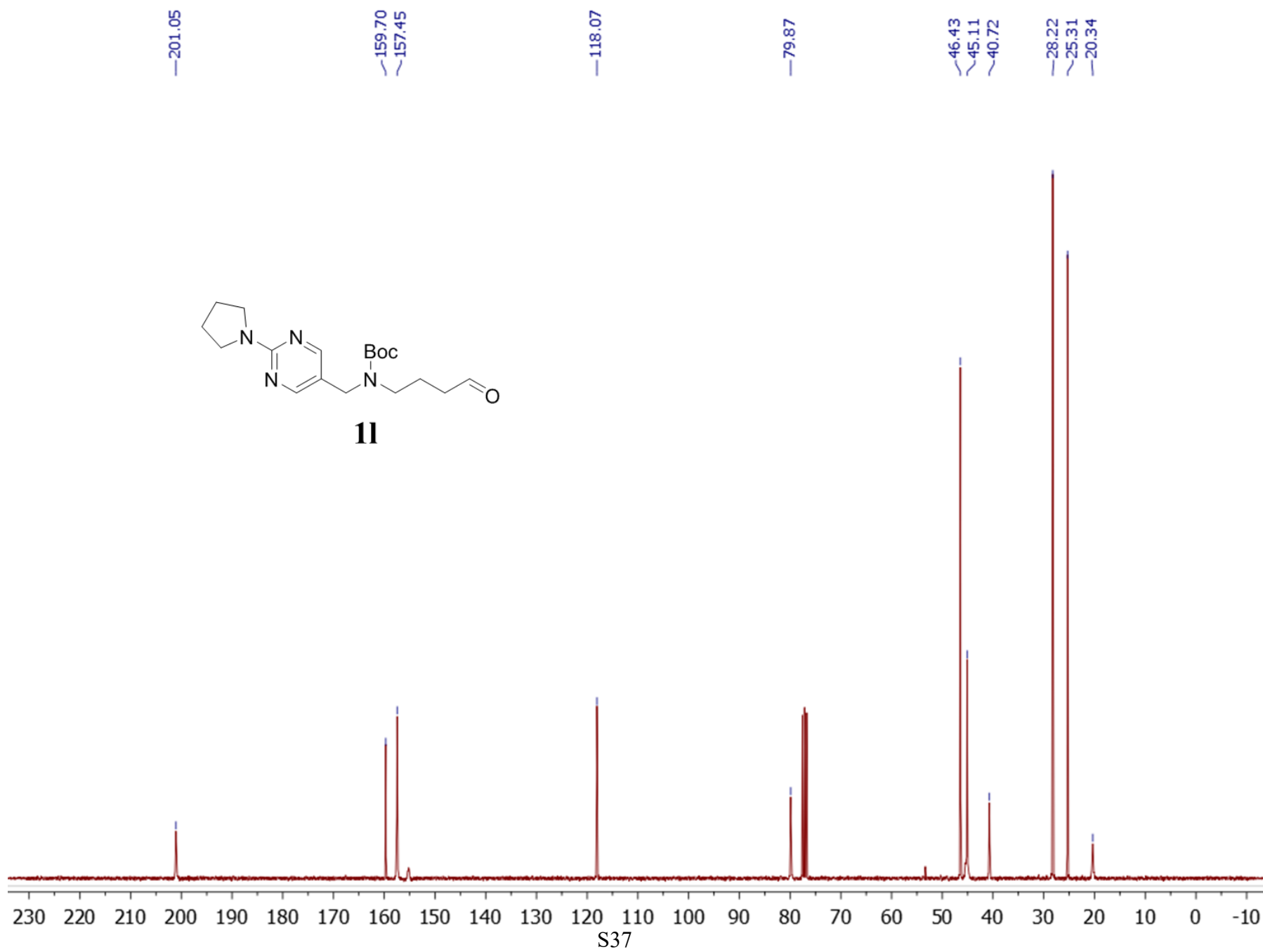
1k

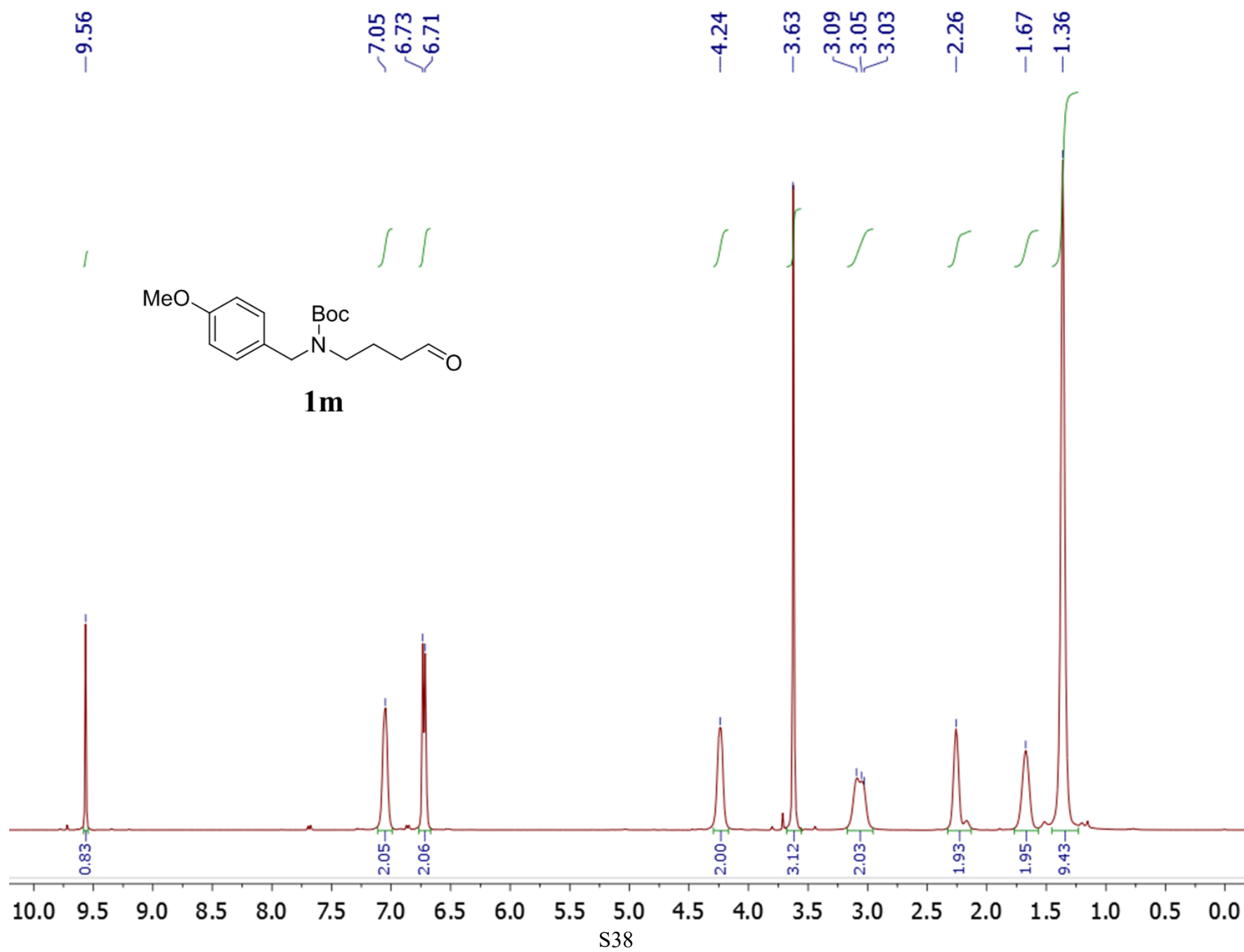


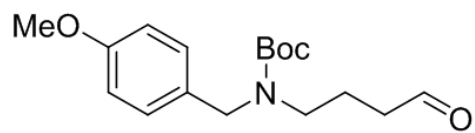




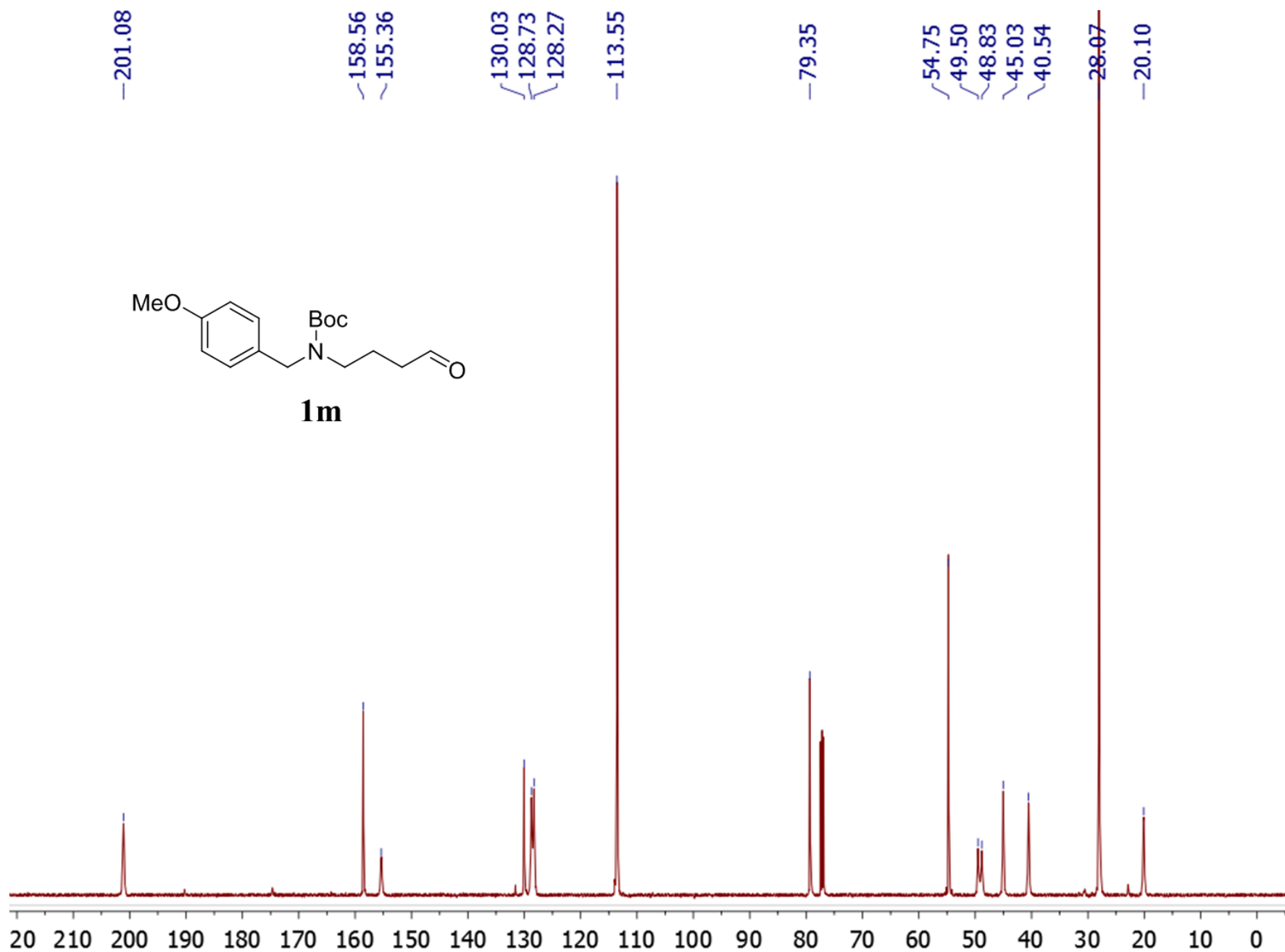
11

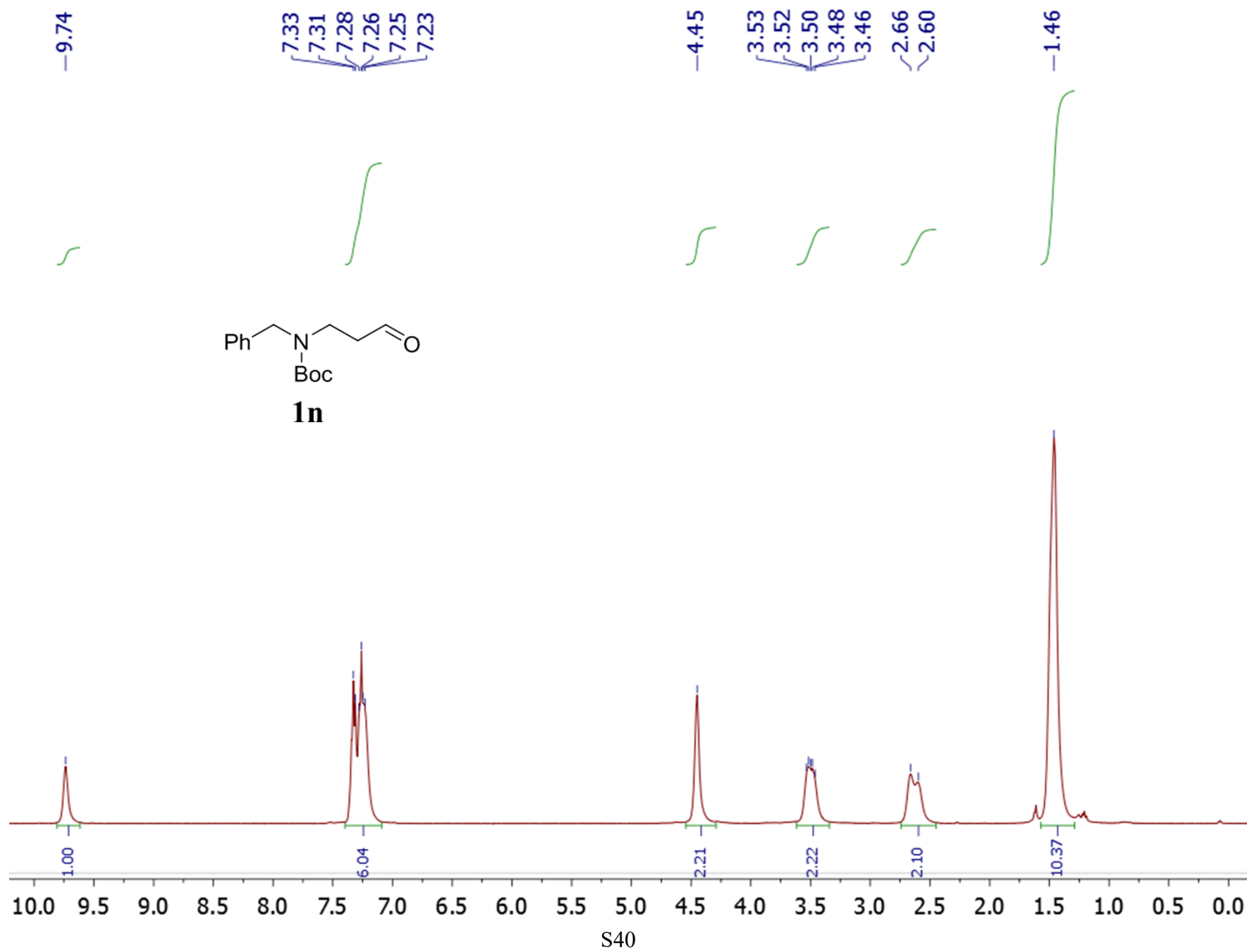






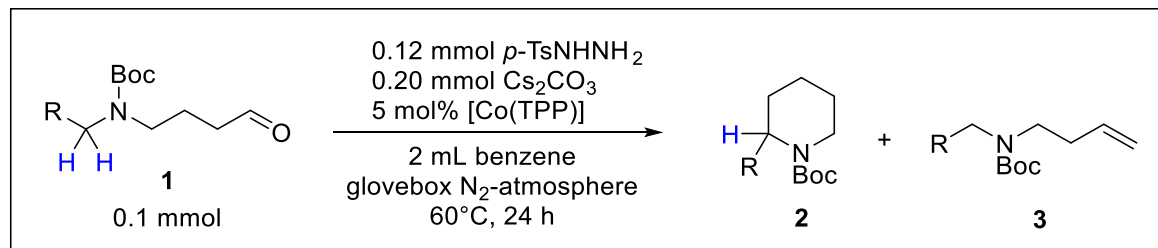
1m





4. Catalytic reactions

4.1 General procedure B



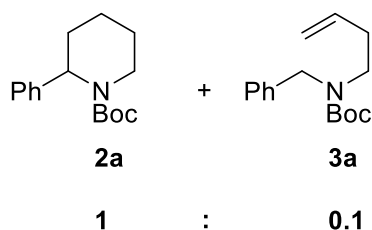
Inside a nitrogen-filled glove box, an oven-dried 4 mL vial fitted with an oven-dried Teflon-coated stir bar was charged with [Co(TPP)] (0.005 mmol, 3.4 mg), *p*-TsNHNH₂ (0.12 mmol, 22.3 mg), Cs₂CO₃ (0.20 mmol, 65.2 mg). The liquid substrate (0.10 mmol) was pre-weighed into a 1 mL syringe and then weighed into the tared vial by careful deposition onto the inner rim of the vial, thereby avoiding direct solid-liquid contact between the powders and the substrate. Then benzene (2 mL) was quickly added. The vial was tightly capped with a screw cap fitted with a PTFE-faced silicone septum, immediately brought to a pre-heated 60°C metal plate and stirred at 1100 rpm for 24h.

The reaction mixture was transferred to a 10 mL vial and the vial used for catalysis was rinsed with DCM (6 × ca. 0.25 mL). Benzene was removed under vacuum. The resulting residue was deposited on a column (ca. 30 cm of silica gel, Ø ca. 6,5 cm) and purified with an eluent gradient from 100% (cyclo)hexane (or pentane) to (cyclo)hexane/ethyl acetate in a ratio X/Y (specified for each product) in steps of 2 mL and portions of 100 mL. The mixture of piperidine and alkene (which co-eluted despite the large column and slow gradient - except for **2h** and **3h**) was visualized by staining the TLC-plates with a solution of 1.5 g ninhydrin in 100 mL *n*-butanol and 3 mL acetic acid. Usually a small amount of [Co(TPP)] co-eluted. This amount was generally sufficient to color the product mixture slightly red, but not sufficient to appear in NMR.

4.2 Product characterization

Notes:

- All yields are the combined isolated yield of piperidine and alkene, as these always co-eluted from the column, except for **2g** and **3g** (although diastereomer **2g'** did co-elute with **3g**).
- ^{13}C -signatures could not be properly assigned to all alkene side products, due to low concentration in which most alkenes were present.



tert-butyl 2-phenylpiperidine-1-carboxylate^[7] and *tert*-butyl benzyl(but-3-en-1-yl)carbamate (**2a** + **3a**)

General procedure B was followed with *tert*-butyl benzyl(4-oxobutyl)carbamate **1a** (0.10 mmol). The products were isolated by flash column chromatography (above described gradient towards 8/2 hexanes/ethyl acetate, $R_f = 0.65$) to afford **2a** and **3a** (quantitative combined isolated yield).

2a:

^1H NMR (300 MHz, CDCl_3) δ 7.47–7.13 (m, 5H), 5.45 (s, 1H), 4.07 (d, $J = 13.6$ Hz, 1H), 2.85–2.72 (m, 1H), 2.34 (d, $J = 13.9$ Hz, 1H), 1.99–1.83 (m, 1H), 1.67–1.39 (m and s overlapping, 4H + 9H respectively).

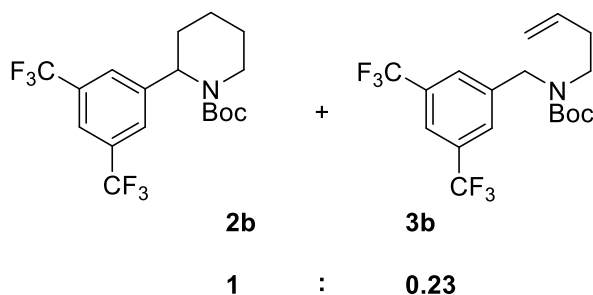
^{13}C NMR (75 MHz, CDCl_3) δ 155.79, 140.51, 128.64, 126.62, 126.44, 79.66, 53.35, 40.21, 28.58, 28.20, 25.60, 19.50.

These data are in correspondence with the literature.^[8]

3a:

^1H NMR (300 MHz, CDCl_3) δ 5.77 (br s, 1H), 5.12–4.97 (m, 2H), 4.45 (br s, 2H), 3.38–3.09 (br m, 2H), 2.40–2.27 (m, 2H, overlaps with 1H of **2a**). Aromatic protons overlap with **2a**.

HRMS (FD, m/z): Calculated for $\text{C}_{16}\text{H}_{23}\text{NO}_2 + [\text{H}^+]$: 262.1807, found: 262.1798.



tert-butyl 2-(3,5-bis(trifluoromethyl)phenyl)piperidine-1-carboxylate^[9] and *tert*-butyl (3,5-bis(trifluoromethyl)benzyl)(but-3-en-1-yl)carbamate (**2b** + **3b**)

General procedure B was followed with *tert*-butyl (3,5-bis(trifluoromethyl)benzyl)(4-oxobutyl)carbamate **1b** (0.10 mmol). The products were isolated by flash column chromatography (above described gradient towards 9/1 hexanes/ethyl acetate, $R_f = 0.41$) to afford **2b** and **3b** (96% combined isolated yield).

2b:

^1H NMR (500 MHz, CDCl_3) δ 7.76 (s, 1H), 7.70–7.63 (m, 2H), 5.46 (s, 1H), 4.10 (br d, 1H), 2.77–2.67 (m, 1H), 2.29 (br d, 1H), 2.05–1.93 (m, 1H), 1.69 (br d, 1H), 1.65–1.55 (m, 2H), 1.47 (s, 9H), 1.37–1.32 (d, J = 8.6 Hz, 2H).

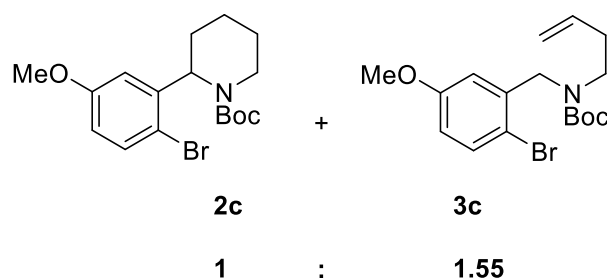
^{13}C NMR (126 MHz, CDCl_3) δ 155.60, 144.03, 132.09 (q, J = 33.1 Hz), 126.93, 124.56 (d, J = 12.8 Hz), 120.78, 80.54, 53.22, 40.51, 29.85, 28.45, 25.13, 19.38.

^{19}F NMR (282 MHz, CDCl_3) δ –62.85.

3b:

^1H NMR (500 MHz, CDCl_3) δ 5.74 (br s, 1H), 5.09–4.99 (m, 2H), 4.58–4.41 (m, 2H), 3.43–3.12 (m, 2H). The aromatic protons, the Boc-group and the methylene adjacent to the olefin overlap with **2b**.

HRMS (FD, m/z): Calculated for $\text{C}_{18}\text{H}_{21}\text{F}_6\text{NO}_2$: 397.1476, found: 397.1498.



***tert*-butyl 2-(2-bromo-5-methoxyphenyl)piperidine-1-carboxylate and *tert*-butyl (2-bromo-5-methoxybenzyl)(but-3-en-1-yl)carbamate (**2c** + **3c**)**

General procedure B was followed with *tert*-butyl (2-bromo-5-methoxybenzyl)(4-oxobutyl)carbamate **1c** (0.10 mmol). The products were isolated by flash column chromatography (above described gradient towards 8/2 hexanes/ethyl acetate, R_f = 0.51) to afford **2c** and **3c** (quantitative combined isolated yield).

2c:

^1H NMR (300 MHz, CDCl_3) δ 7.46–7.36 (m, 1H), 6.85–6.59 (br m, 2H), 6.23–6.10 (br m, 1H), 5.20–4.98 (br m, 2H), 4.57–4.37 (br m, 2H, overlapping with **3c**), 3.76 (s, 3H), 3.39–3.10 (br m, 2H), 2.30 (br s, 1H), 1.75–1.62 (br m, 1H), 1.46 (br d, J = 29.3 Hz, 9H).

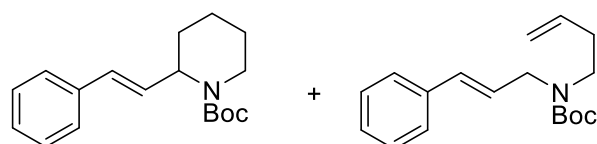
2c + **3c:**

^{13}C NMR (75 MHz, CDCl_3) δ 159.38, 135.42, 133.38, 131.04, 116.88, 114.35, 80.16, 55.54, 53.56, 29.85, 28.54.

3c:

^1H NMR (300 MHz, CDCl_3) δ 5.88–5.66 (br m, 1H), 5.20–4.98 (br m, 2H, overlapping with **2c**), all other signals overlapping with **2c**.

HRMS (ESI, m/z): Calculated for $[\text{C}_{17}\text{H}_{24}\text{BrNO}_3 + \text{Na}]^+$: 392.0832, found: 392.0833.



2d

3d

ca. 1 : 1
***tert*-butyl (E)-2-styrylpiperidine-1-carboxylate^[10] and *tert*-butyl but-3-en-1-yl(cinnamyl)carbamate (2d + 3d)**

General procedure B was followed with *tert*-butyl cinnamyl(4-oxobutyl)carbamate **1d** (0.10 mmol). The products were isolated by flash column chromatography (above described gradient towards 8/2 hexanes/ethyl acetate, $R_f = 0.65$) to afford **2d** and **3d** (84% combined isolated yield). Note: the overlap of the signals of **2d** and **3d** in ^1H -NMR complicates proper determination of their ratio.

2d:

^1H NMR (400 MHz, CDCl_3) δ 7.45–7.16 (m, 5H, overlapping with **3d**), 6.52–6.35 (m, 1H, overlapping with **3d**), 6.26–6.09 (m, 1H, overlapping with **3d**), 5.13–4.90 (m, 1H, overlapping with **3d**), 2.91 (t, $J = 12.8$ Hz, 1H), 1.90–1.67 (m, 3H), 1.68–1.57 (m, 4H), 1.48 (s, 9H, overlapping with **3d**).

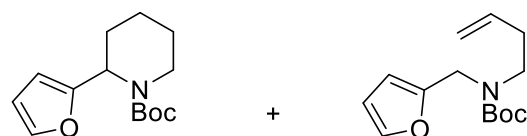
2d + 3d:

^{13}C NMR (75 MHz, CDCl_3) δ 155.55, 137.22, 135.71, 130.88, 128.69, 127.50, 126.38, 79.59, 52.37, 40.02, 29.66, 28.62, 25.71, 19.85.

3d:

^1H NMR (400 MHz, CDCl_3) δ 7.45–7.16 (m, 5H, overlapping with **2d**), 6.52–6.35 (m, 1H, overlapping with **2d**), 6.26–6.09 (m, 1H, overlapping with **2d**), 5.87–5.67 (m, 1H), 5.13–4.90 (m, 2H, overlapping with **2d**), 4.13–3.82 (m, 2H), 3.27 (br s, 2H), 2.37–2.23 (m, 2H), 1.48 (s, 9H, overlapping with **2d**).

HRMS (FD, m/z): Calculated for $\text{C}_{18}\text{H}_{25}\text{NO}_2$: 287.1885, found: 287.1887.



2e

3e

1

:

0.16

***tert*-butyl 2-(furan-2-yl)piperidine-1-carboxylate and *tert*-butyl but-3-en-1-yl(furan-2-ylmethyl)carbamate (2e + 3e)**

General procedure B was followed with *tert*-butyl (furan-2-ylmethyl)(4-oxobutyl)carbamate **1e** (0.10 mmol). The products were isolated by flash column chromatography (above described gradient towards 7/3 hexanes/ethyl acetate, $R_f = 0.74$) to afford **2e** and **3e** (92% combined isolated yield).

2e:

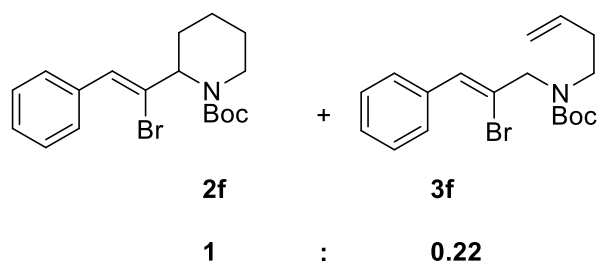
^1H NMR (300 MHz, CDCl_3) δ 7.34 (s, 1H), 6.34–6.28 (m, 1H), 6.08 (br d, 1H), 5.43–5.31 (m, 1H), 3.98 (d, $J = 13.4$ Hz, 1H), 2.84–2.70 (m, 1H), 2.16 (d, $J = 13.6$ Hz, 1H), 1.85–1.71 (m, 1H), 1.68–1.51 (m, 3H), 1.46 (m, 1H + 9H overlapping).

^{13}C NMR (75 MHz, CDCl_3) δ 155.48, 154.34, 141.57, 110.25, 106.60, 79.86, 49.37, 40.42, 28.55, 27.47, 25.46, 20.10.

3e:

^1H NMR (300 MHz, CDCl_3) δ 6.24–6.12 (m, 2H), 5.75 (br s, 1H), 5.08–4.95 (m, 2H), 4.45–4.29 (m, 2H), 3.26 (br s, 2H), 2.07–1.96 (m, 1H). The aromatic protons, a methylene proton and the Boc-group overlap with **2e**.

HRMS (FD, m/z): Calculated for $\text{C}_{14}\text{H}_{21}\text{NO}_3$: 251.1521, found: 251.1532.



***tert*-butyl (Z)-2-(1-bromo-2-phenylvinyl)piperidine-1-carboxylate and *tert*-butyl (Z)-(2-bromo-3-phenylallyl)(but-3-en-1-yl)carbamate (2f + 3f)**

General procedure B was followed with *tert*-butyl (Z)-(2-bromo-3-phenylallyl)(4-oxobutyl)carbamate **1f** (0.10 mmol). The products were isolated by flash column chromatography (above described gradient towards 8/2 hexanes/ethyl acetate, R_f = 0.38) to afford **2f** and **3f** (71% combined isolated yield).

2f:

^1H NMR (500 MHz, CDCl_3) δ 7.39–7.13 (m, 5H), 6.76 (br s, 1H), 5.41 (br s, 1H), 4.06 (br s, 2H), 3.01–2.87 (m, 1H), 2.81–2.70 (m, 1H), 2.42–2.18 (m, 2H), 1.94–1.80 (m, 1H), 1.80–unknown (m, 1H) 1.46 (br s, 9H). (Accompanied by a second set of signals due to presence of two rotamers because of hindered rotation of the C-C bond between the piperidine ring and the vinyl group)

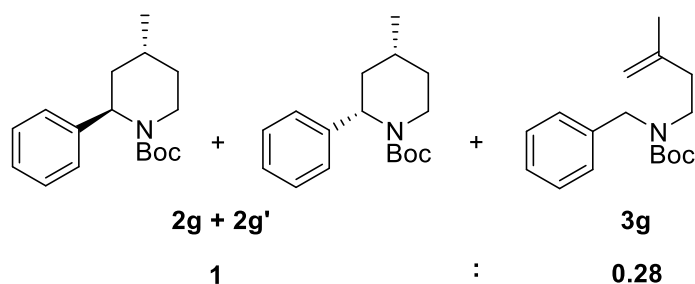
2f + 3f:

^{13}C NMR (126 MHz, CDCl_3): δ 155.80, 155.38, 140.56, 136.06, 129.16, 128.64, 128.21, 126.63, 126.44, 80.18, 79.67, 58.35, 53.38, 40.56, 40.23, 28.59, 28.56, 28.23, 27.53, 25.61, 24.91, 19.52, 19.15.

3f:

^1H NMR (500 MHz, CDCl_3) δ 5.75 (br s, 1H), 5.13–5.00 (m, 2H), 4.50–4.14 (m, 2H + 1H), 3.44–3.03 (m, 2H + 1H). All other peaks overlapping with **2f**.

HRMS (FD, m/z): Calculated for $\text{C}_{18}\text{H}_{24}\text{BrNO}_2$: 365.0990, found: 365.1006.



***tert*-butyl (4*R*)-4-methyl-2-phenylpiperidine-1-carboxylate and *tert*-butyl benzyl(3-methylbut-3-en-1-yl)carbamate (2g + 2g' + 3g)**

General procedure B was followed with *tert*-butyl (*S*)-benzyl(3-methyl-4-oxobutyl)carbamate **1g** (0.10 mmol). The products, which consisted of the two diastereoisomers **2g** and **2g'** and alkene **3g**, were isolated by flash column chromatography (above described gradient towards 8/2 hexanes/ethyl acetate, R_f = 0.42 for **2g** and 0.51 for [**2g'** + **3g**]) to afford **2g** in 64% isolated yield and [**2g'** + **3g**] in 36% isolated yield. Since the $^1\text{H-NMR}$ of the [**2g'** + **3g**] mixture shows a **2g'**/**3g** ratio of 0.4/0.6, **2g'** makes up for $0.4 \times 36 = 14.4\%$ of the total [**2g**+**2g'**+**3g**] mixture, and **3g** makes up for $0.6 \times 36 = 21.6\%$ of the total [**2g**+**2g'**+**3g**] mixture. Therefore, the combined [**2g** + **2g'**] yield is $64 + 14.4 \approx 78\%$, and hence the [**2g**+**2g'**]/**3g** ratio is 1/0.28.

2g:

$^1\text{H NMR}$ (500 MHz, CDCl_3) δ 7.43–7.08 (m, 5H), 4.85 (br s, 1H), 3.99 (br s, 1H), 3.34 (br s, 1H), 2.01 (br s, 2H), 1.84 (br s, 1H), 1.68–1.41 (m, 2H), 1.30 (br s, 9H), 0.93 (br s, 3H).

$^{13}\text{C NMR}$ (126 MHz, CDCl_3) δ 156.09, 144.96, 128.41, 126.41, 125.34, 79.54, 57.04, 38.65, 31.26, 28.39, 26.67, 21.72.

2g' (diastereoisomer of 2g):

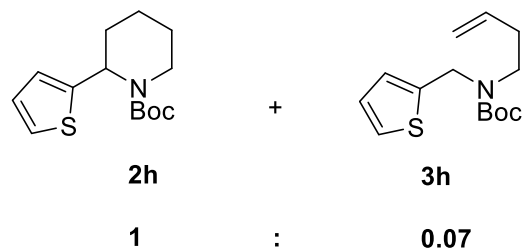
$^1\text{H NMR}$ (300 MHz, CDCl_3) δ 7.37–7.14 (m, 5H, overlapping with **3g**), 5.45 (br s, 1H), 4.15–3.88 (m, 1H), 2.76 (td, J = 13.4, 2.8 Hz, 1H), 2.37–2.09 (m, 1H, overlapping with **3g**), 2.06–1.88 (m, 1H), 1.71 (s, 3H), 1.46 (s, 9H, overlapping with **3g**), 1.01–0.78 (m, 3H, overlapping with **3g**).

3g:

$^1\text{H NMR}$ (300 MHz, CDCl_3) δ 7.37–7.14 (m, 5H, overlapping with **2g'**), 4.76–4.60 (m, 2H), 4.49–4.35 (m, 2H), 3.42–3.09 (m, 2H), 2.37–2.09 (m, 2H, overlapping with **2g'**), 1.46 (s, 9H, overlapping with **2g'**), 1.01–0.78 (m, 3H, overlapping with **2g'**).

$^{13}\text{C NMR}$ (126 MHz, CDCl_3) δ 128.63, 128.60, 127.26, 126.55, 126.43, 112.03, 111.72, 79.82, 79.76, 45.50, 31.08, 29.85, 28.59, 22.36.

HRMS (FD, m/z): Calculated for $\text{C}_{17}\text{H}_{25}\text{NO}_2$: 275.1885, found: 275.1884.



***tert*-butyl 2-(thiophen-2-yl)piperidine-1-carboxylate⁷ and *tert*-butyl but-3-en-1-yl(thiophen-2-ylmethyl)carbamate (2h + 3h)**

General procedure B was followed with *tert*-butyl (thiophen-2-ylmethyl)(4-oxobutyl)carbamate **1h** (0.10 mmol). The products were isolated by flash column chromatography (above described

gradient towards 8/2 hexanes/ethyl acetate, $R_f = 0.68$) to afford **2h** and **3h** (77% combined isolated yield).

2h:

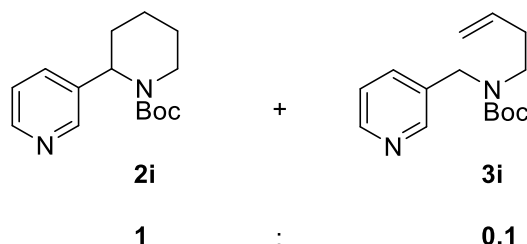
^1H NMR (300 MHz, CDCl_3) δ 7.20 (d, $J = 4.9$ Hz, 1H), 6.99–6.92 (m, 1H), 6.85–6.79 (m, 1H), 5.59 (br, 1H), 4.01 (d, $J = 13.3$ Hz, 1H), 2.91–2.73 (m, 1H), 2.18 (br d, 1H), 2.00–1.82 (m, 1H), 1.71–1.51 (m, 4H, overlapping with the singlet at 1.49 ppm), 1.49 (s, 9H).

^{13}C NMR (75 MHz, CDCl_3) δ 155.09, 145.54, 126.94, 124.36, 124.29, 79.96, 50.84, 39.85, 29.71 (d, $J = 18.5$ Hz), 28.57, 25.47, 19.69.

3h:

NMR data match with those of isolated **3h** described in section 5.1.

HRMS (FD, m/z): Calculated for $\text{C}_{14}\text{H}_{21}\text{NO}_2\text{S}$: 267.1293, found: 267.1289.



***tert*-butyl 2-(pyridine-3-yl)piperidine-1-carboxylate^[11] and *tert*-butyl but-3-en-1-yl(pyridine-3-ylmethyl)carbamate (**2i** + **3i**)**

General procedure B was followed with *tert*-butyl (pyridine-3-ylmethyl)(4-oxobutyl)carbamate **1i** (0.10 mmol). The products were isolated by flash column chromatography (above described gradient towards 6/4 hexanes/ethyl acetate, $R_f = 0.23$) to afford **2i** and **3i** (66% combined isolated yield).

2i:

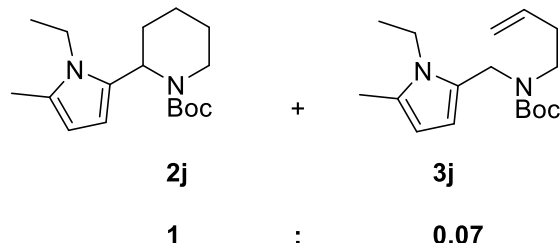
^1H NMR (300 MHz, CDCl_3) δ 8.55 (br s, 2H), 7.52 (d, $J = 7.8$ Hz, 1H), 7.30 (br s, 1H), 5.46 (br s, 1H), 4.06 (d, $J = 13.5$ Hz, 1H), 2.83–2.64 (m, 1H), 2.37–2.15 (m, 1H), 2.02–1.83 (m, 1H), 1.70–1.48 (m, 4H), 1.46 (s, 9H).

^{13}C NMR (75 MHz, CDCl_3) δ 155.54, 148.48, 147.83, 135.28, 134.61, 123.84, 80.12, 51.74, 40.29, 29.83, 28.54, 25.40, 19.38.

3i:

^1H NMR (300 MHz, CDCl_3) δ 8.55 (br s, 2H, overlapping with **2i**), 7.52 (d, $J = 7.8$ Hz, 1H, overlapping with **2i**), 7.30 (br s, 1H, overlapping with **2i**), 5.89–5.62 (m, 1H), 5.10–4.87 (m, 2H), 4.43 (br s, 2H), 3.37–3.06 (m, 2H). The peaks belonging to the Boc-group and the methylene adjacent to the olefin overlap with **2i**.

HRMS (FD, m/z): Calculated for $\text{C}_{15}\text{H}_{22}\text{N}_2\text{O}_2$: 262.1681, found: 262.1684.



***tert*-butyl 2-(1-ethyl-5-methyl-1H-pyrrol-2-yl)piperidine-1-carboxylate and *tert*-butyl but-3-en-1-yl((1-ethyl-5-methyl-1H-pyrrol-2-yl)methyl)carbamate (**2j** + **3j**)**

General procedure B was followed starting from *tert*-butyl ((1-ethyl-5-methyl-1H-pyrrol-2-yl)methyl)(4-oxobutyl)carbamate **1j** (0.10 mmol). The products were isolated by flash column chromatography (above described gradient towards 9/1 pentane/ethyl acetate, $R_f = 0.83$) to afford **2j** and **3j** (98% combined isolated yield).

2j:

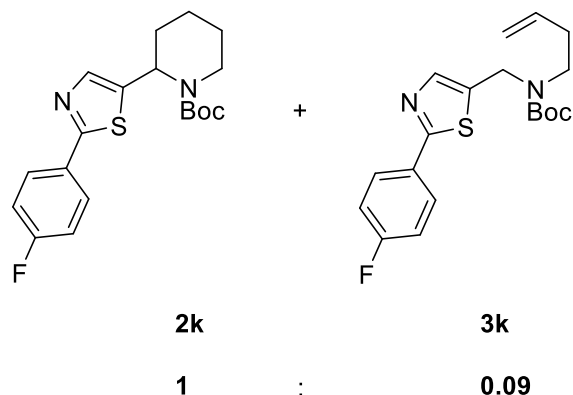
^1H NMR (300 MHz, CDCl_3) δ 6.13–6.06 (m, 1H), 5.87–5.80 (m, 1H), 5.49–5.36 (m, 1H), 3.97–3.75 (m, 2H + 1H), 2.84–2.69 (m, 1H), 2.23 (s, 3H), 2.18–2.05 (m, 2H), 1.93–1.78 (m, 1H), 1.78–1.64 (m, 1H), 1.63–1.53 (m, 2H), 1.50 (s, 9H), 1.16 (t, $J = 7.1$ Hz, 3H).

^{13}C NMR (75 MHz, CDCl_3) δ 154.68, 129.86, 128.78, 107.57, 105.25, 79.59, 40.19, 38.56, 28.67, 28.04, 25.94, 20.83, 16.21, 12.29.

3j:

^1H NMR (300 MHz, CDCl_3) δ 5.69–5.62 (m, 1H), 5.08–4.94 (m, 2H), 4.44 (s, 2H + 1H), 3.74–3.58 (m, 2H), 3.25–3.01 (m, 2H + 1H). All remaining protons overlap with **2j**.

HRMS (FD, m/z): Calculated for $\text{C}_{17}\text{H}_{28}\text{N}_2\text{O}_2$: 292.2151, found: 292.2138.



tert-butyl ((2-(4-fluorophenyl)thiazol-5-yl)methyl)(4-oxobutyl)carbamate and *tert*-butyl but-3-en-1-yl((2-(4-fluorophenyl)thiazol-5-yl)methyl)carbamate (**2k** + **3k**)

General procedure B was followed with *tert*-butyl ((2-(4-fluorophenyl)thiazol-5-yl)methyl)(4-oxobutyl)carbamate **1k** (0.10 mmol). The products were isolated by flash column chromatography (above described gradient towards 9/1 pentane/ethyl acetate, $R_f = 0.55$) to afford **2k** and **3k** in quantitative combined isolated yield).

2k:

^1H NMR (300 MHz, CDCl_3) δ 7.95–7.82 (m, 2H), 7.54 (s, 1H), 7.11 (t, $J = 8.5$ Hz, 2H), 5.64 (br s, 1H), 4.03 (d, $J = 13.4$ Hz, 1H), 2.82 (t, $J = 12.8$ Hz, 1H), 2.20–2.08 (m, 1H), 2.06–1.89 (m, 1H), 1.77–1.59 (m, 4H), 1.50 (s, 9H).

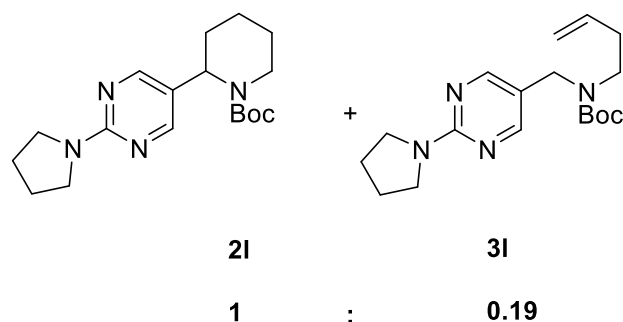
^{13}C NMR (75 MHz, CDCl_3) δ 166.60, 165.55, 162.23, 154.78, 140.49 (d, $J = 69.1$ Hz), 130.22 (d, $J = 3.3$ Hz), 128.29 (d, $J = 8.4$ Hz), 116.11 (d, $J = 22.1$ Hz), 80.40, 49.01, 40.00, 29.50, 28.56, 25.32, 19.72.

^{19}F NMR (282 MHz, CDCl_3) δ –110.71.

3k:

^1H NMR (300 MHz, CDCl_3) δ 5.29 (s, 1H), 5.11–4.97 (m, 1H), 4.55 (br s, 1H), 4.18–4.08 (m, 2H), 3.28 (br s, 1H), 2.28 (br s, 1H). All aromatic protons, one methylene group and the Boc-group overlap with **2k**.

HRMS (FD, m/z): Calculated for $\text{C}_{19}\text{H}_{23}\text{FN}_2\text{O}_2\text{S}$: 362.1464, found: 362.1456.



***tert*-butyl 2-(2-(pyrrolidine-1-yl)pyrimidin-5-yl)piperidine-1-carboxylate and *tert*-butyl but-3-en-1-yl((2-(pyrrolidin-1-yl)pyrimidin-5-yl)methyl)carbamate (2l + 3l)**

General procedure B was followed with *tert*-butyl (4-oxobutyl)((2-(pyrrolidine-1-yl)pyrimidin-5-yl)methyl)carbamate **1l** (0.10 mmol). The products were isolated by flash column chromatography (above described gradient towards 6/4 hexanes/ethyl acetate, $R_f = 0.42$) to afford **2l** and **3l** (99% combined isolated yield).

2l:

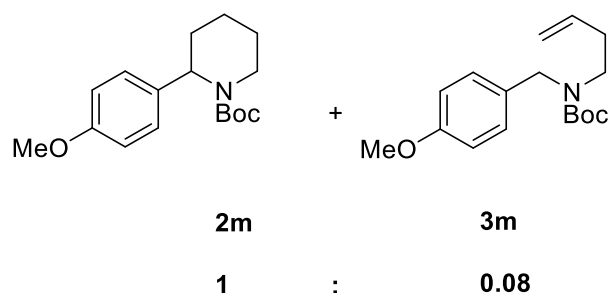
^1H NMR (500 MHz, CDCl_3) δ 8.19 (s, 2H), 5.34 (br s, 1H), 3.99 (d, $J = 13.2$ Hz, 1H), 3.59–3.50 (m, 5H), 2.67 (t, $J = 12.6$ Hz, 1H), 2.13 (d, $J = 14.3$ Hz, 1H), 2.01–1.94 (m, 5H), 1.90–1.79 (m, 1H), 1.66–1.60 (m, 1H), 1.60–1.54 (m, 1H), 1.45 (s, 9H).

^{13}C NMR (126 MHz, CDCl_3) δ 159.55, 156.89, 155.29, 119.71, 79.92, 49.42, 46.75 (d, $J = 5.4$ Hz), 39.79, 28.58, 27.50, 25.68 (d, $J = 3.6$ Hz), 25.56, 19.33.

3l:

^1H NMR (500 MHz, CDCl_3) δ 8.23 (s, 2H), 5.72 (br s, 1H), 5.28 (s, 2H), 5.07–4.96 (m, 2H), 4.21 (br s, 3H), 4.13–4.03 (m, 2H), 3.28–3.02 (m, 2H), 2.23 (br s, 2H), 2.02 (s, 3H). Boc signal (9H) overlapping with **2l**.

HRMS (FD, m/z): Calculated for $\text{C}_{18}\text{H}_{28}\text{N}_4\text{O}_2$: 332.2212, found: 332.2226.



***tert*-butyl 2-(4-methoxyphenyl)piperidine-1-carboxylate and *tert*-butyl but-3-en-1-yl(4-methoxybenzyl)carbamate (2m + 3m)**

General procedure B was followed with *tert*-butyl (4-methoxybenzyl)(4-oxobutyl)carbamate **1m** (0.10 mmol). The products were isolated by flash column chromatography (above described gradient towards 85/15 cyclohexane/ethyl acetate, $R_f = 0.53$) to afford **2m** and **3m** (94% combined isolated yield).

2m:

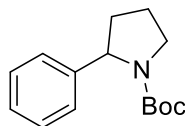
^1H NMR (400 MHz, CDCl_3) δ 7.13 (d, $J = 8.3$ Hz, 2H), 6.87 (d, $J = 8.3$ Hz, 2H), 5.37 (br s, 1H), 4.02 (d, $J = 13.6$ Hz, 1H), 3.80 (s, 3H), 2.73 (t, $J = 12.5$ Hz, 1H), 2.26 (d, $J = 14.1$ Hz, 1H), 1.91–1.80 (m, 1H), 1.71–1.49 (m, 4H, overlapping with the adjacent singlet), 1.47 (s, 9H).

^{13}C NMR (101 MHz, CDCl_3) δ 158.21, 155.76, 132.42, 127.77, 114.01, 79.59, 55.37, 52.79, 40.04, 28.61, 28.20, 25.69, 19.48.

3m:

^1H NMR (400 MHz, CDCl_3) δ 5.74 (br s, 1H), 5.07–4.94 (m, 2H), 4.37 (br s, 3H), 3.30–3.04 (m, 1H). All other signals overlap with **2m**.

HRMS (FD, m/z): Calculated for $\text{C}_{17}\text{H}_{25}\text{NO}_3$: 291.1834, found: 291.1842.



***tert*-butyl 2-phenylpyrrolidine-1-carboxylate (**4**)**

General procedure B was followed with *tert*-butyl benzyl(3-oxopropyl)carbamate **1n** (0.10 mmol). The product was isolated by flash column chromatography (above described gradient towards 8/2 pentane/ethyl acetate, R_f = 0.62) to afford **4** (98% isolated yield).

^1H NMR (400 MHz, CDCl_3) δ 7.38–7.11 (m, 5H), 5.10–4.62 (m, 1H), 3.73–3.37 (br m, 2H), 2.40–2.19 (br m, 1H), 2.00–1.72 (br m, 3H), 1.48 (br s, 3H), 1.19 (br s, 6H).

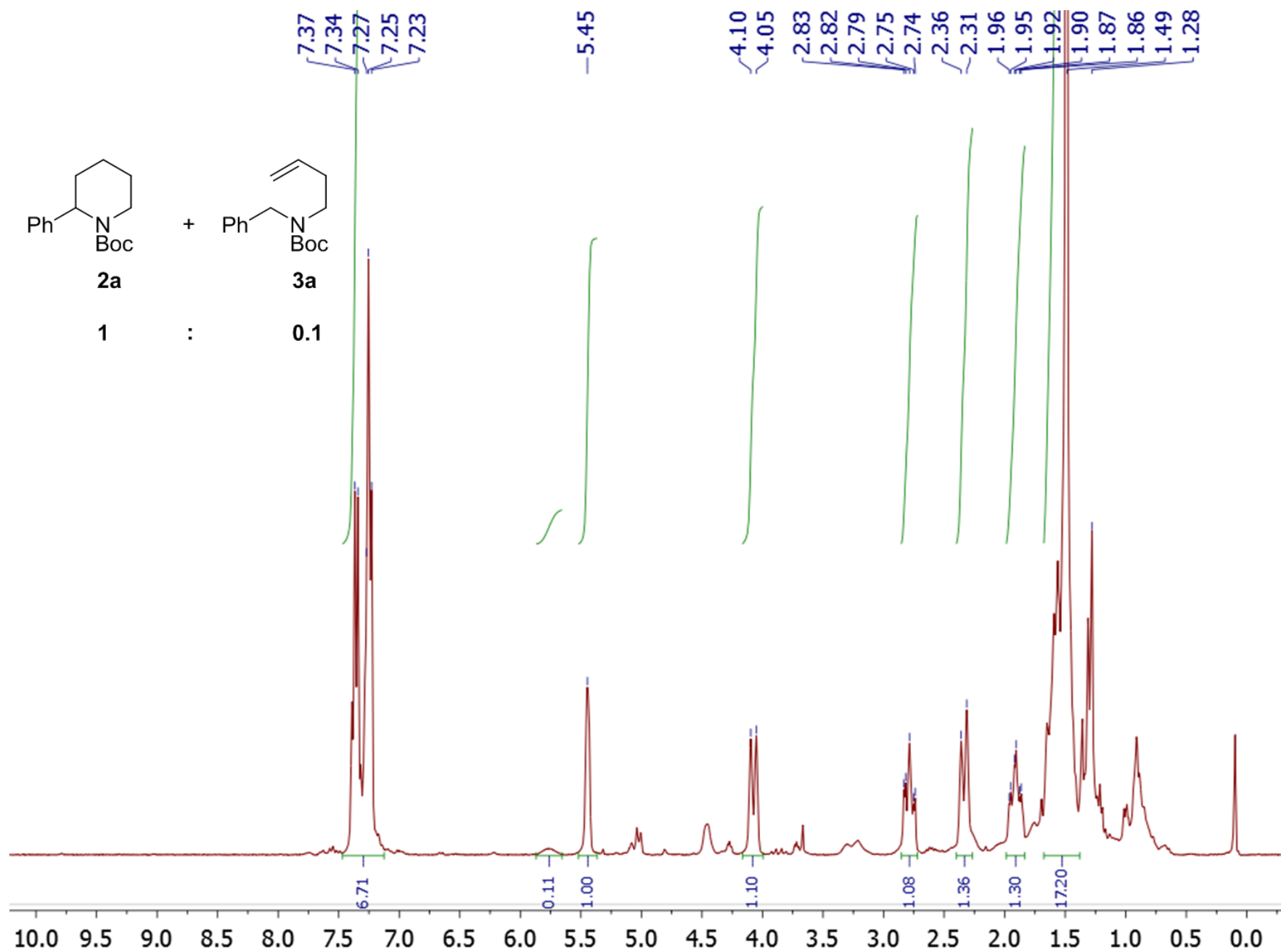
^{13}C NMR (75 MHz, CDCl_3) δ 154.68, 129.86, 128.78, 107.57, 105.25, 79.59, 47.77, 40.19, 38.56, 28.67, 28.04, 25.94, 20.83, 16.21, 12.29.

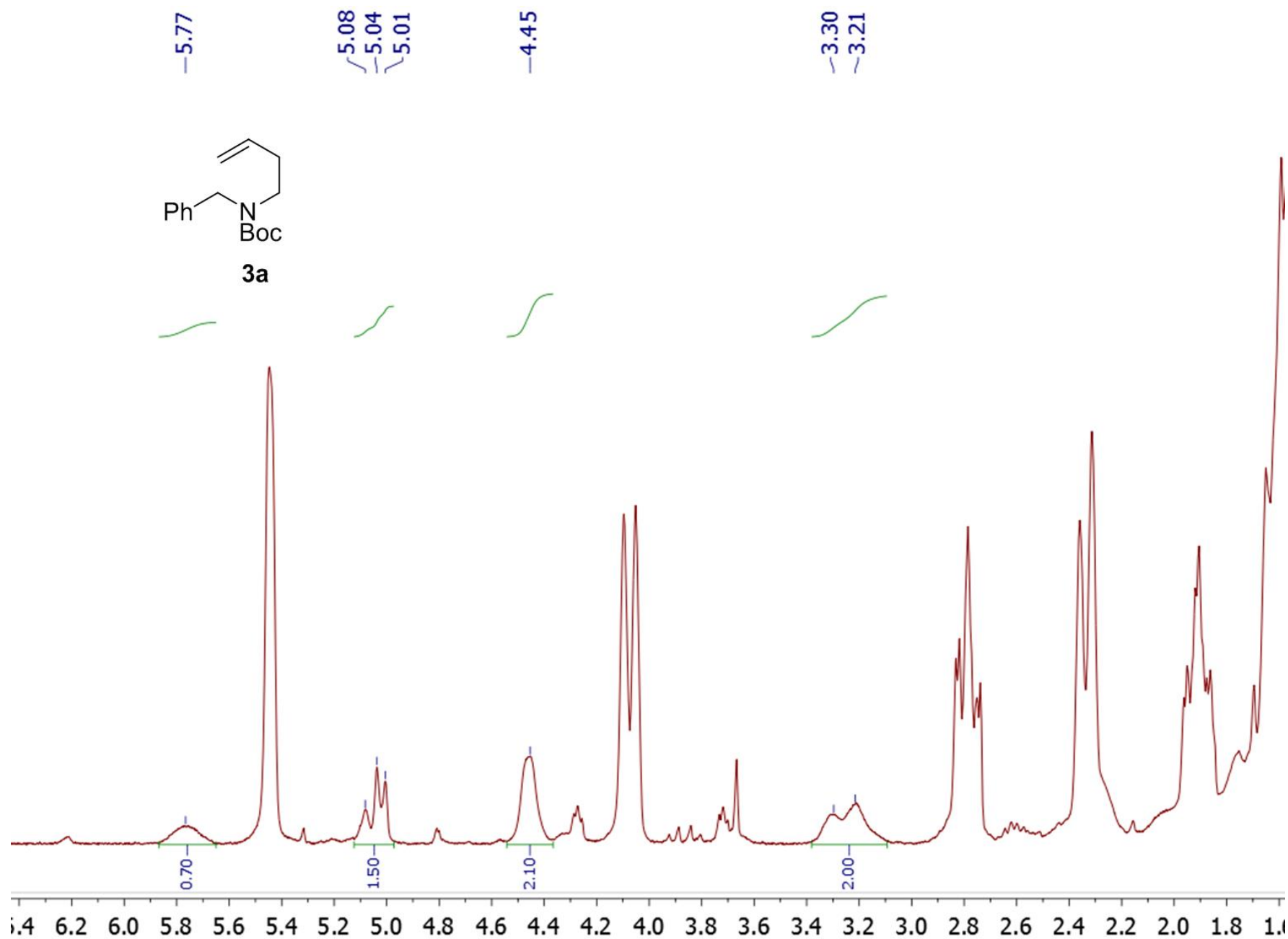
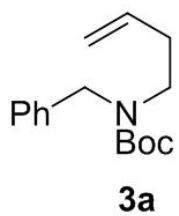
These data are in correspondence with those reported by Zhang and co-workers.⁶

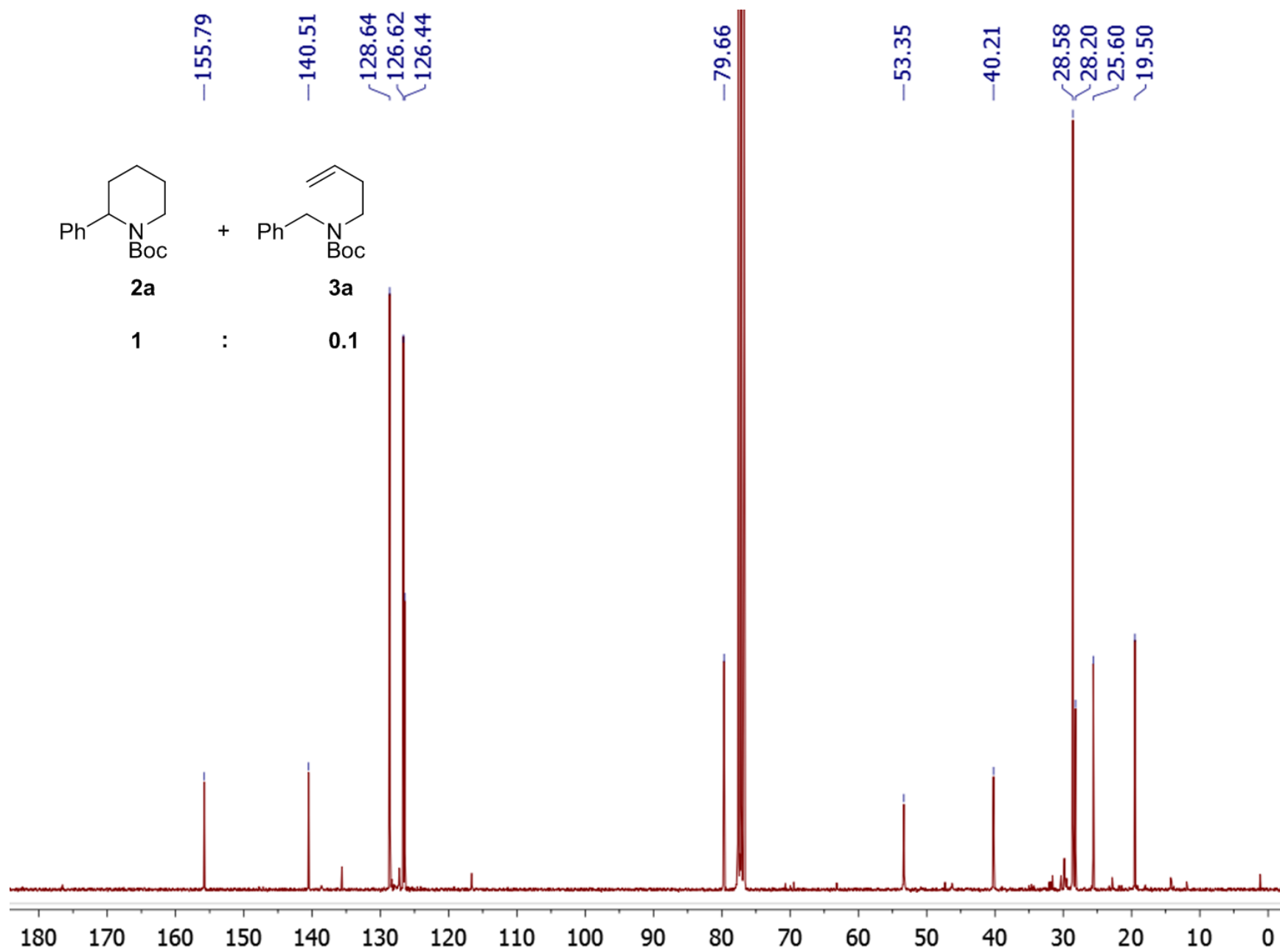
4.3 Copies of ^1H -, ^{13}C - and ^{19}F -NMR spectra

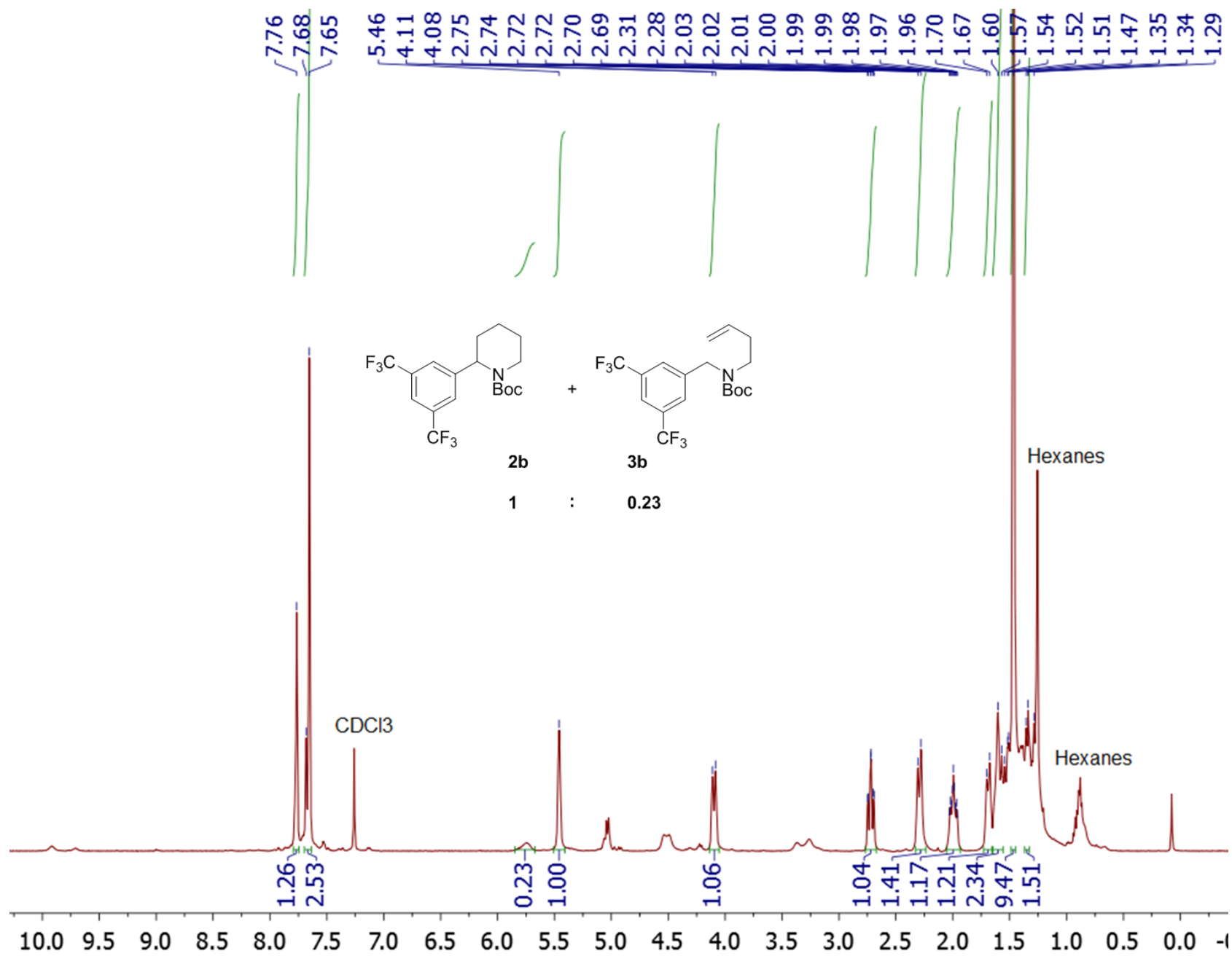
Notes:

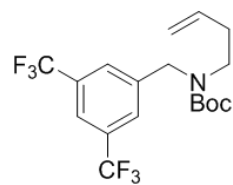
- Several of the following compounds exhibit restricted bond rotation, and therefore show broadened and/or overlapping signals and/or two sets of signals corresponding to different rotamers.
- Every first of two ^1H -NMR spectra displays the assignment of peaks belonging to product **2**, as well as ratio between products **2** and **3** (shown by setting the signal belonging to the proton of the central tertiary carbon of product **2** at 1H and integrating the peak belonging to $\text{RCH}=\text{CH}_2$ of product **3**). Only in the case of **2c** + **3c**, the ratio is shown in the second of the two ^1H -NMR spectra. In the case of **2d** + **3d**, the complete overlap of product peaks complicated proper determination of their ratio.



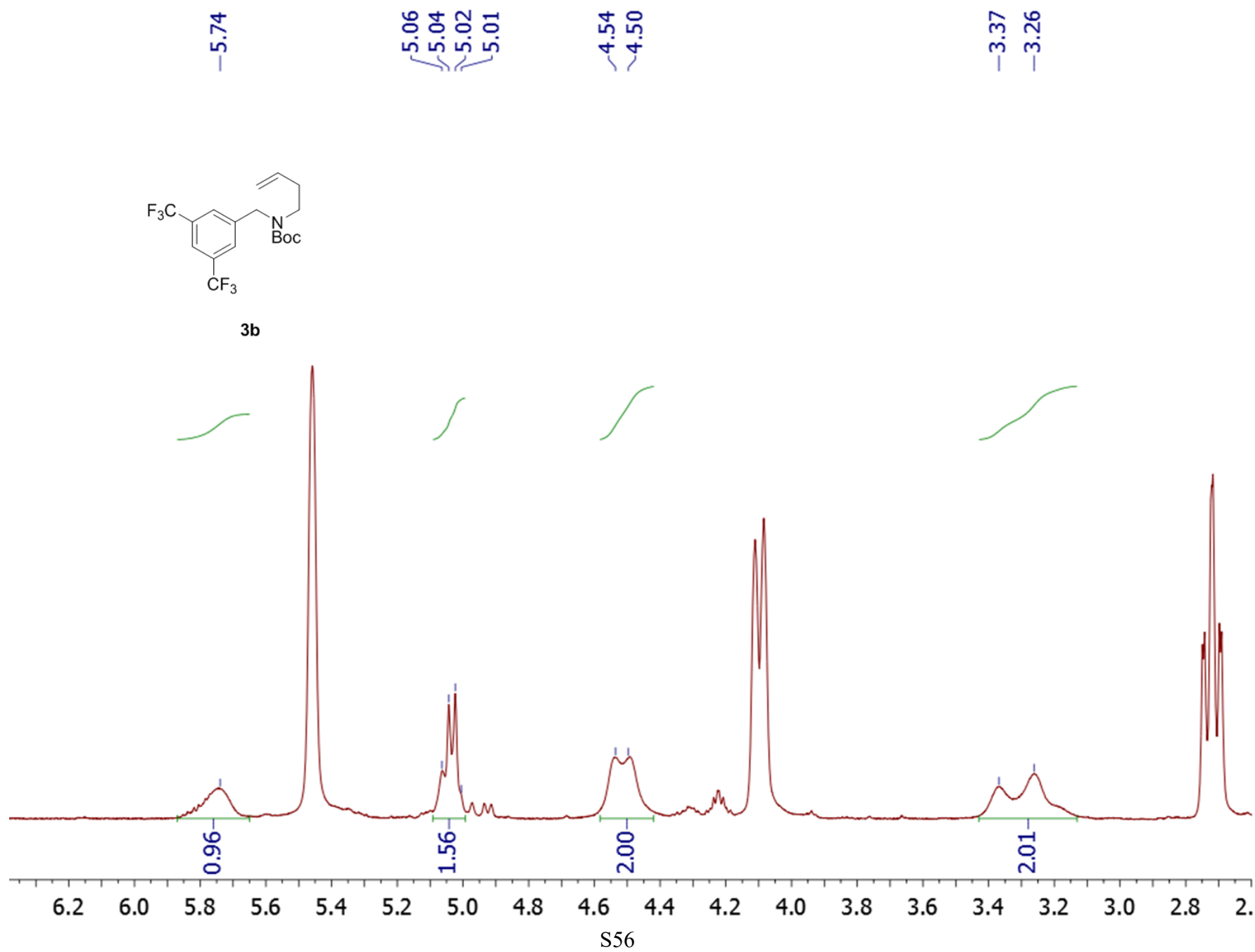


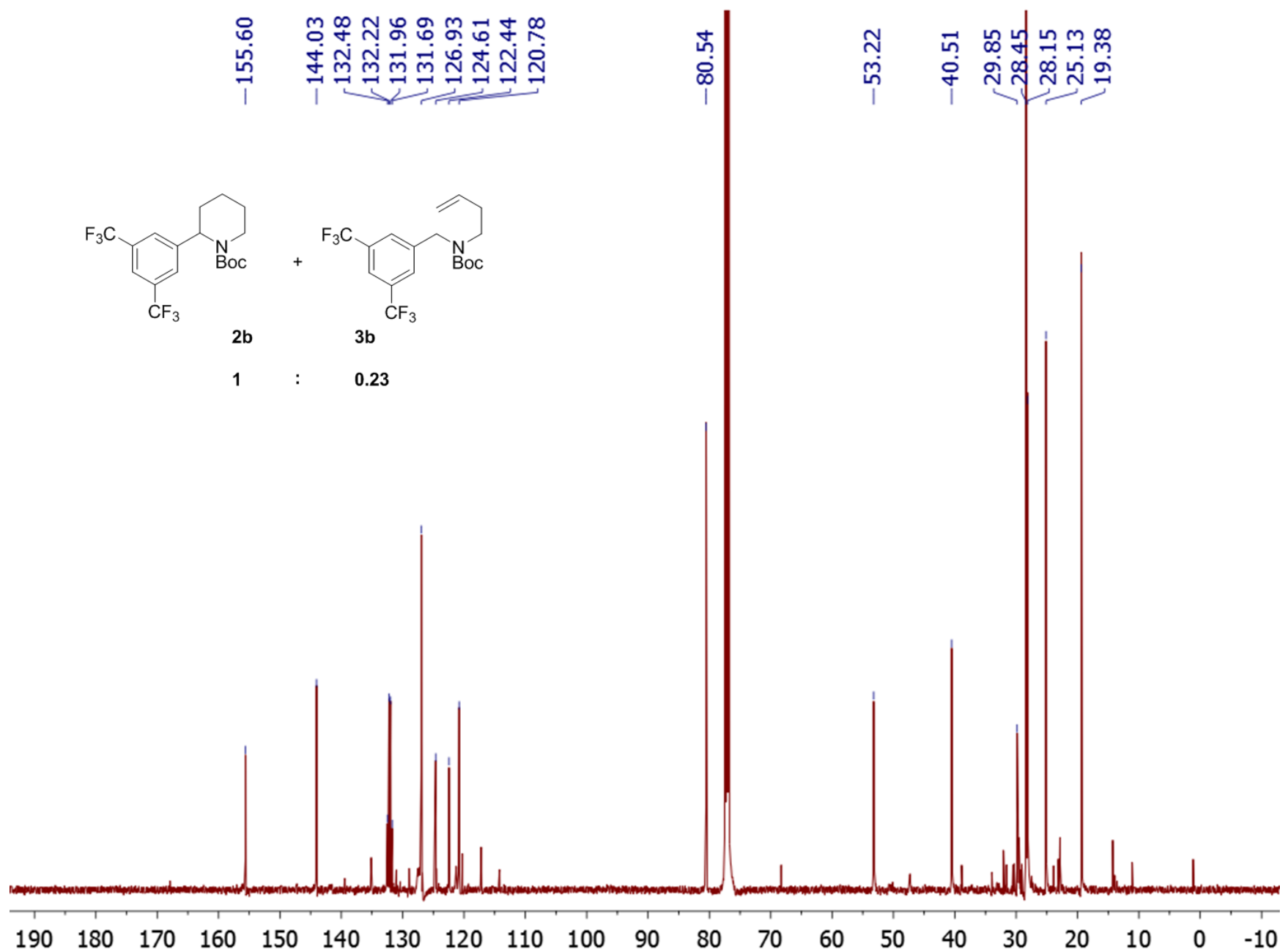


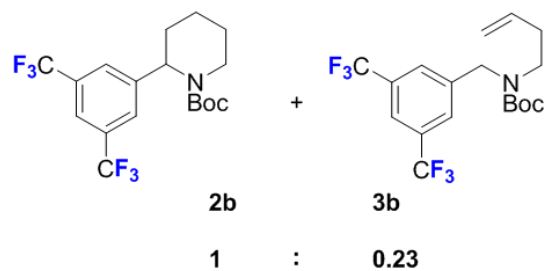




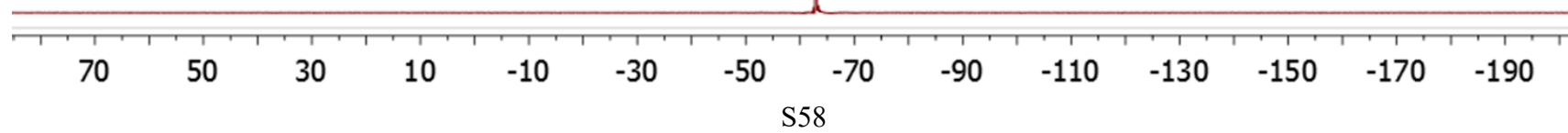
3b

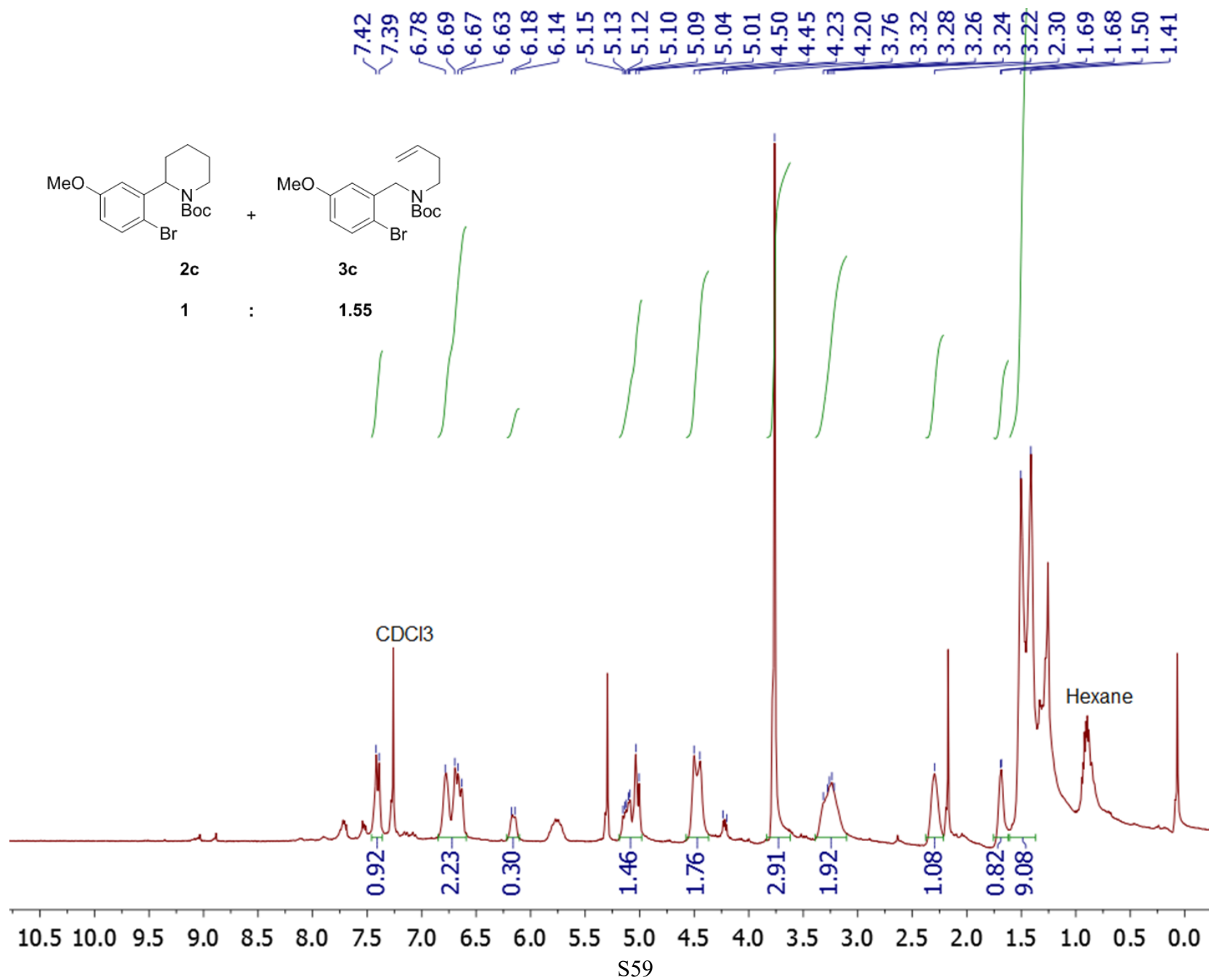


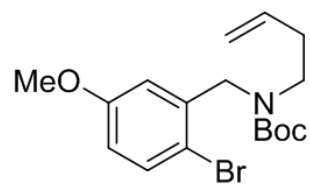




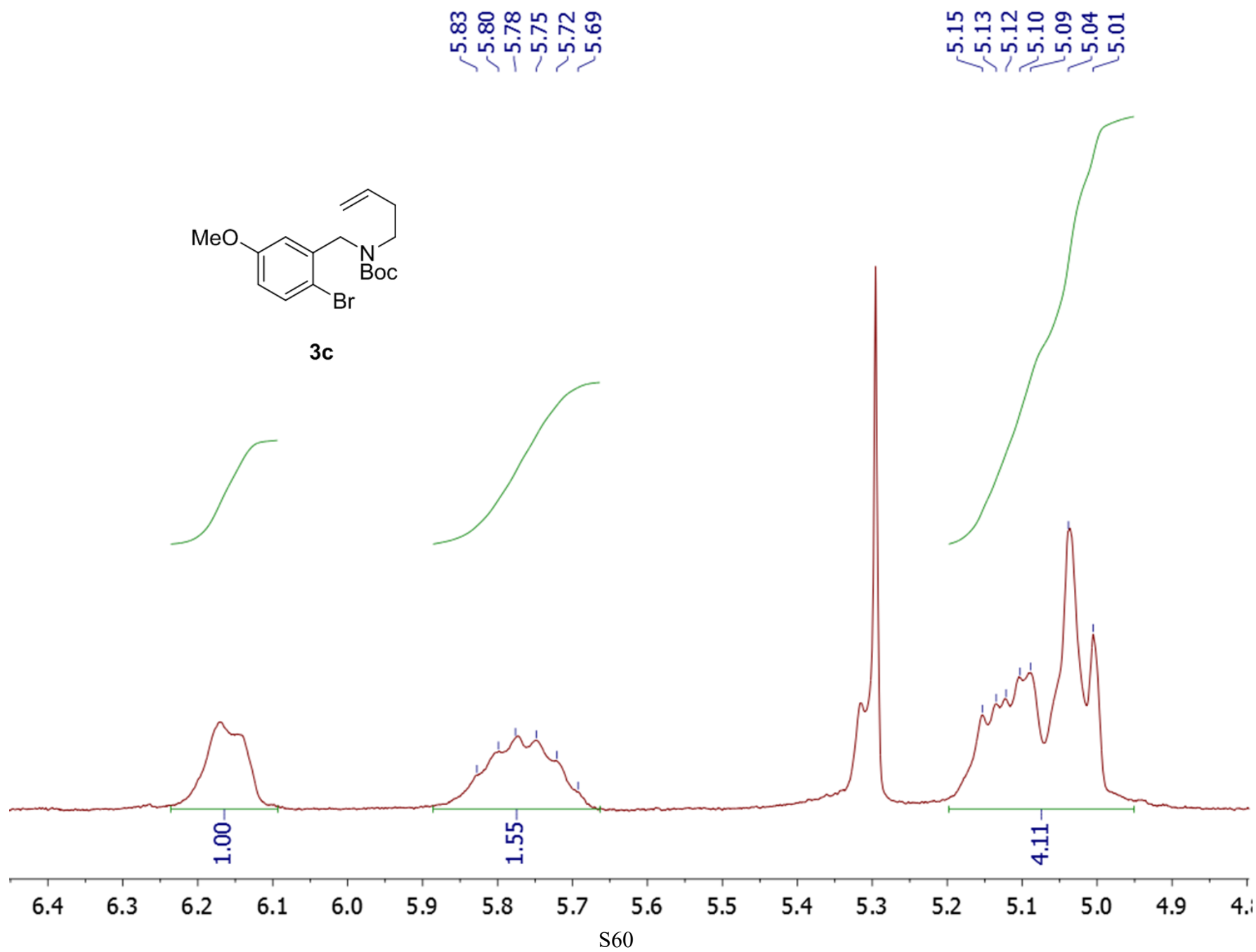
--62.85

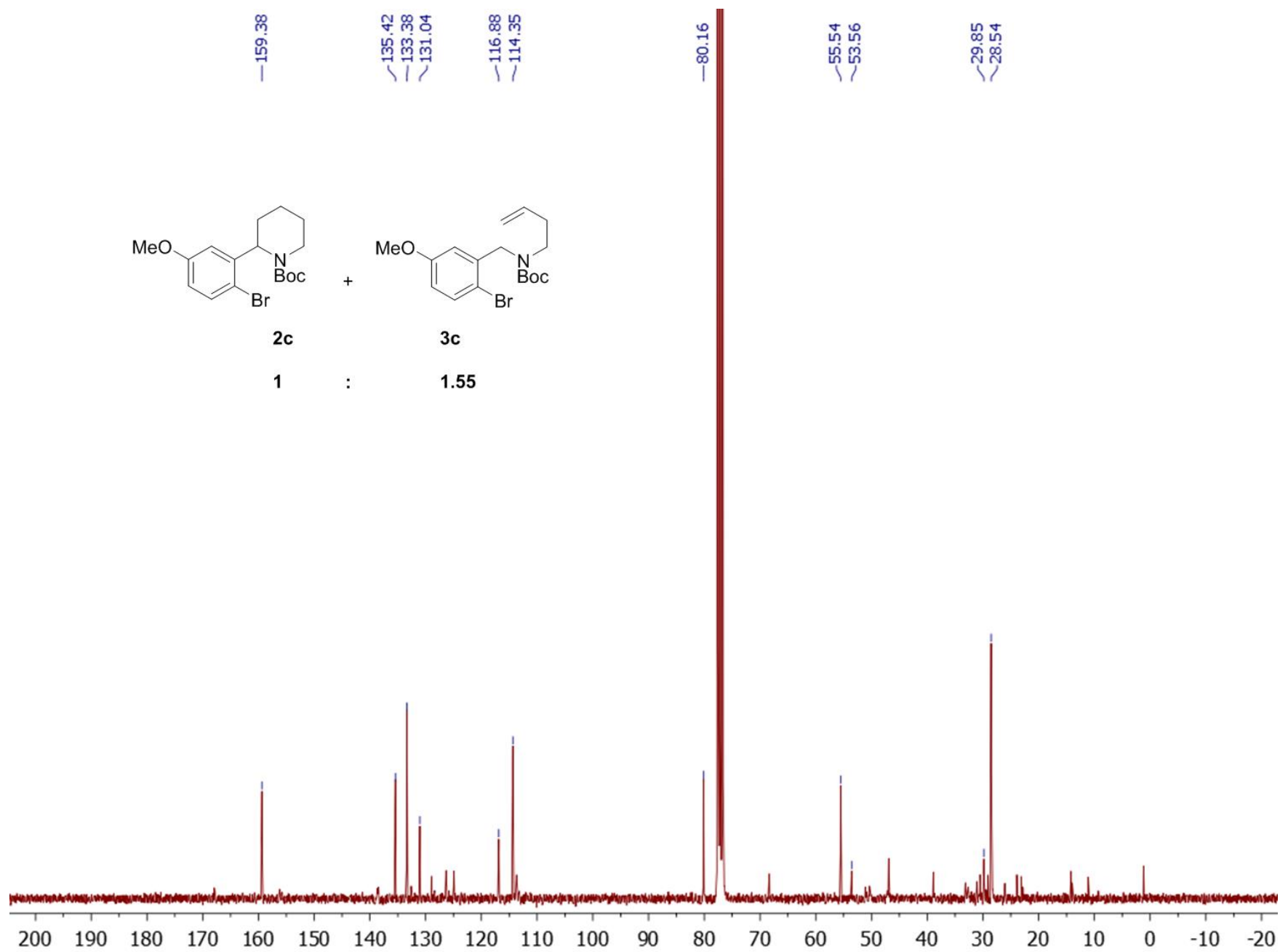


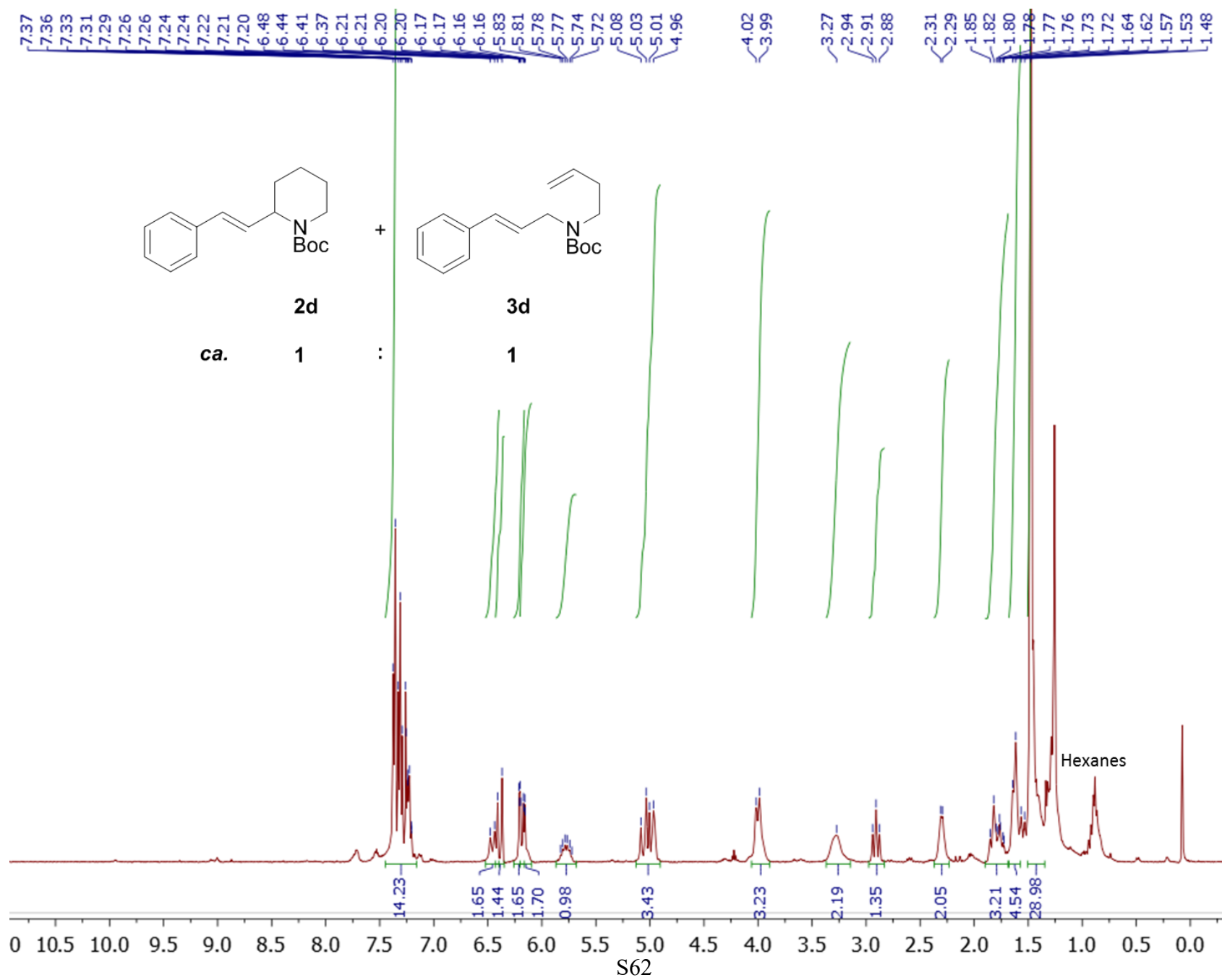


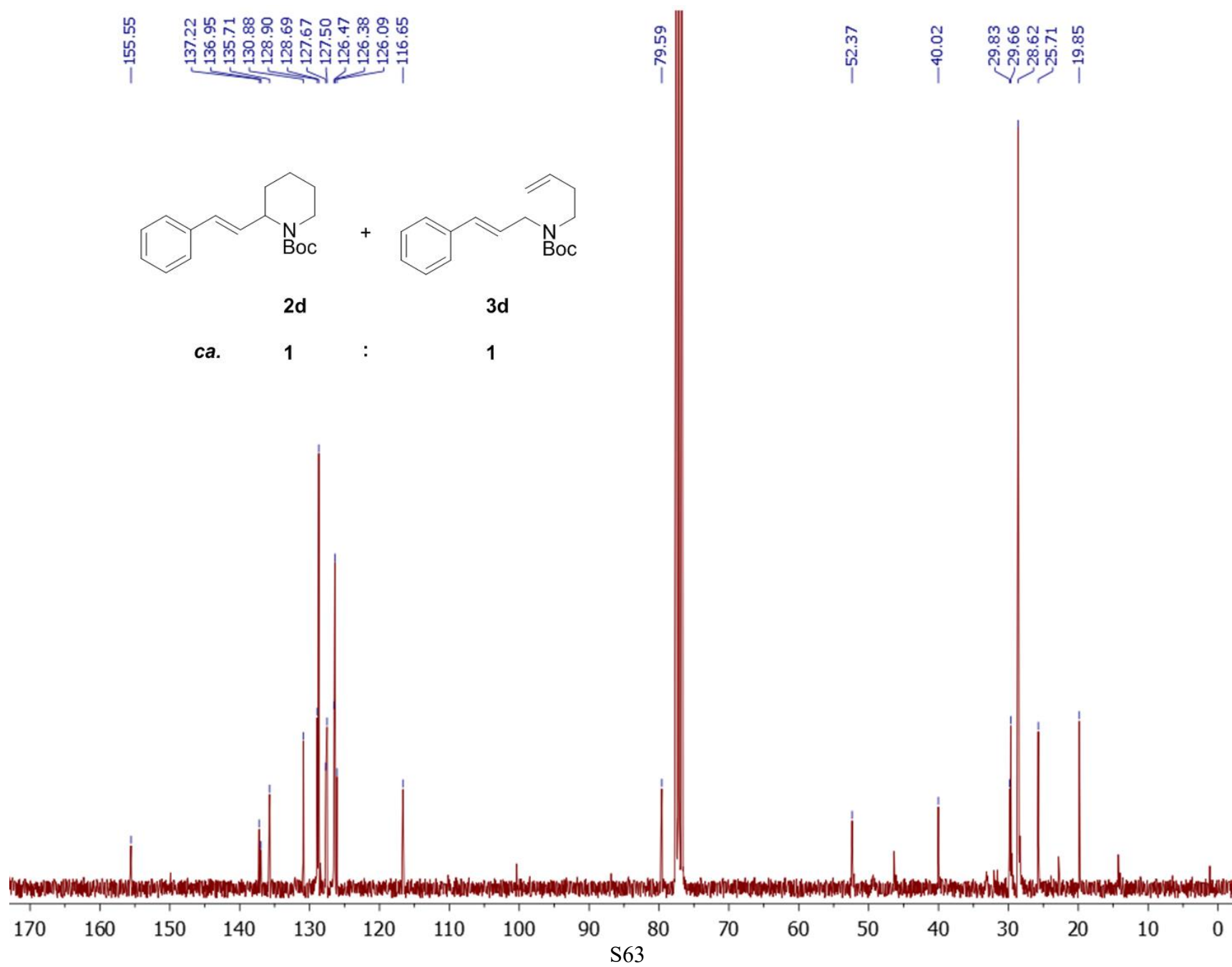


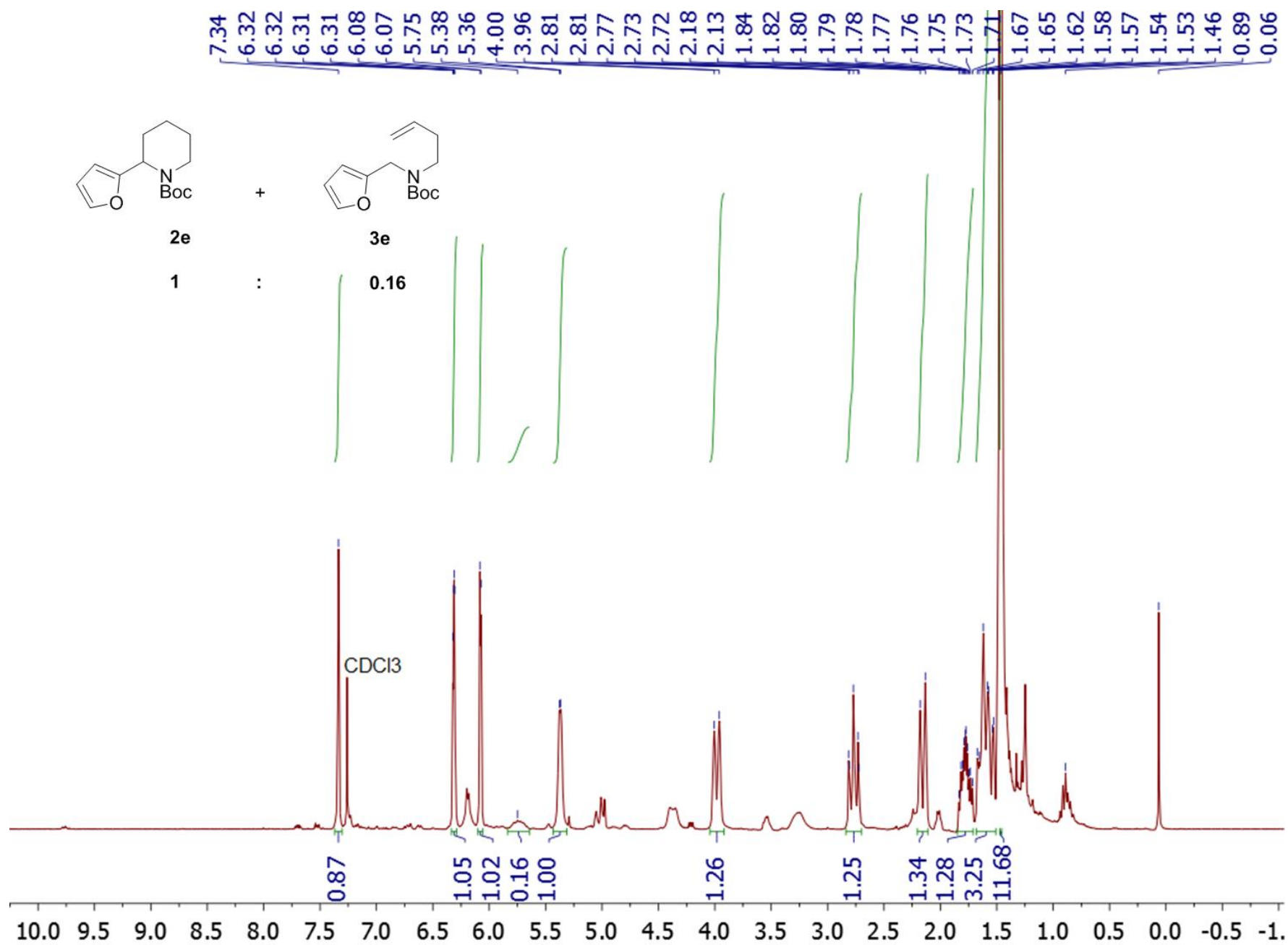
3c

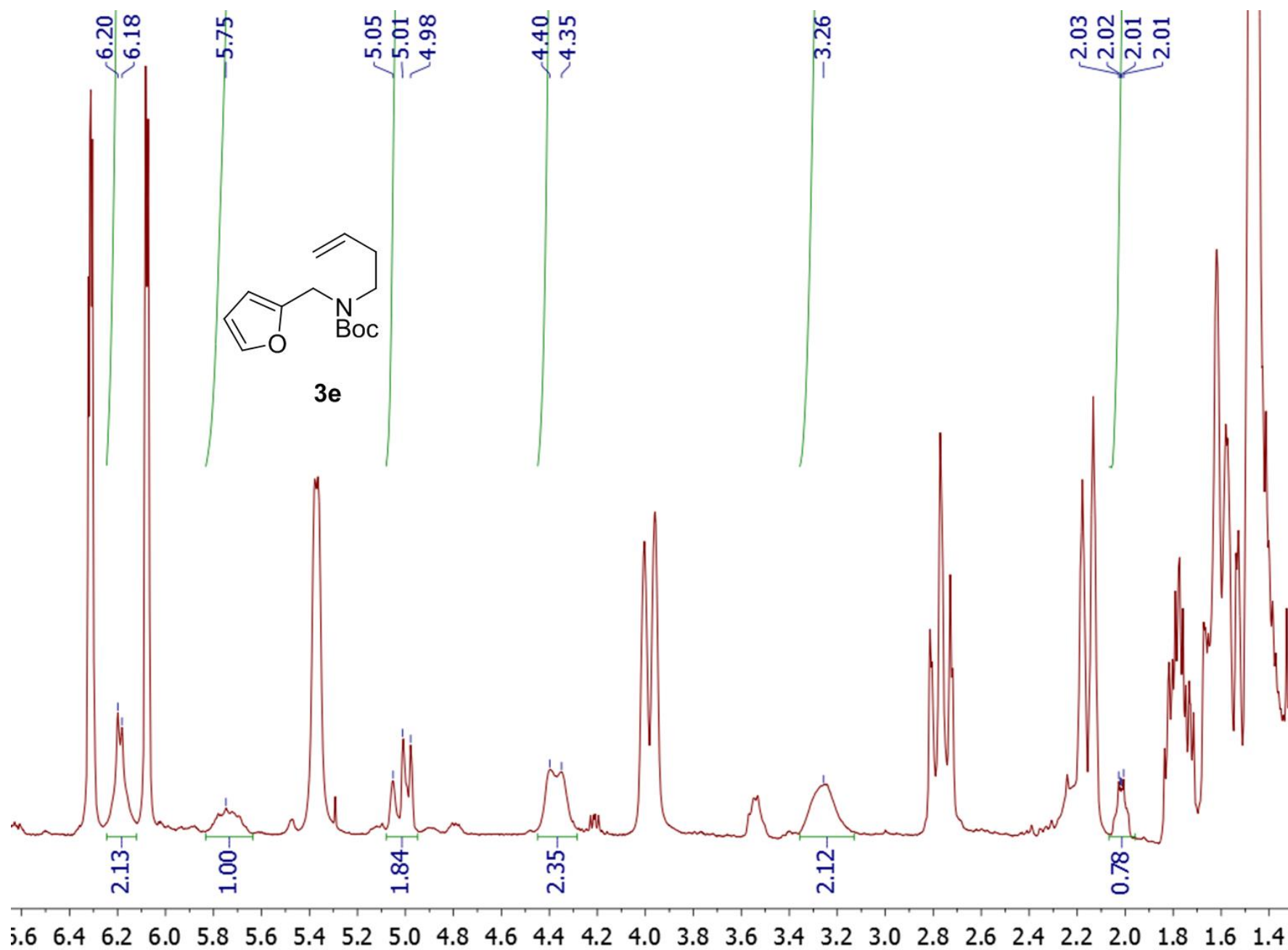


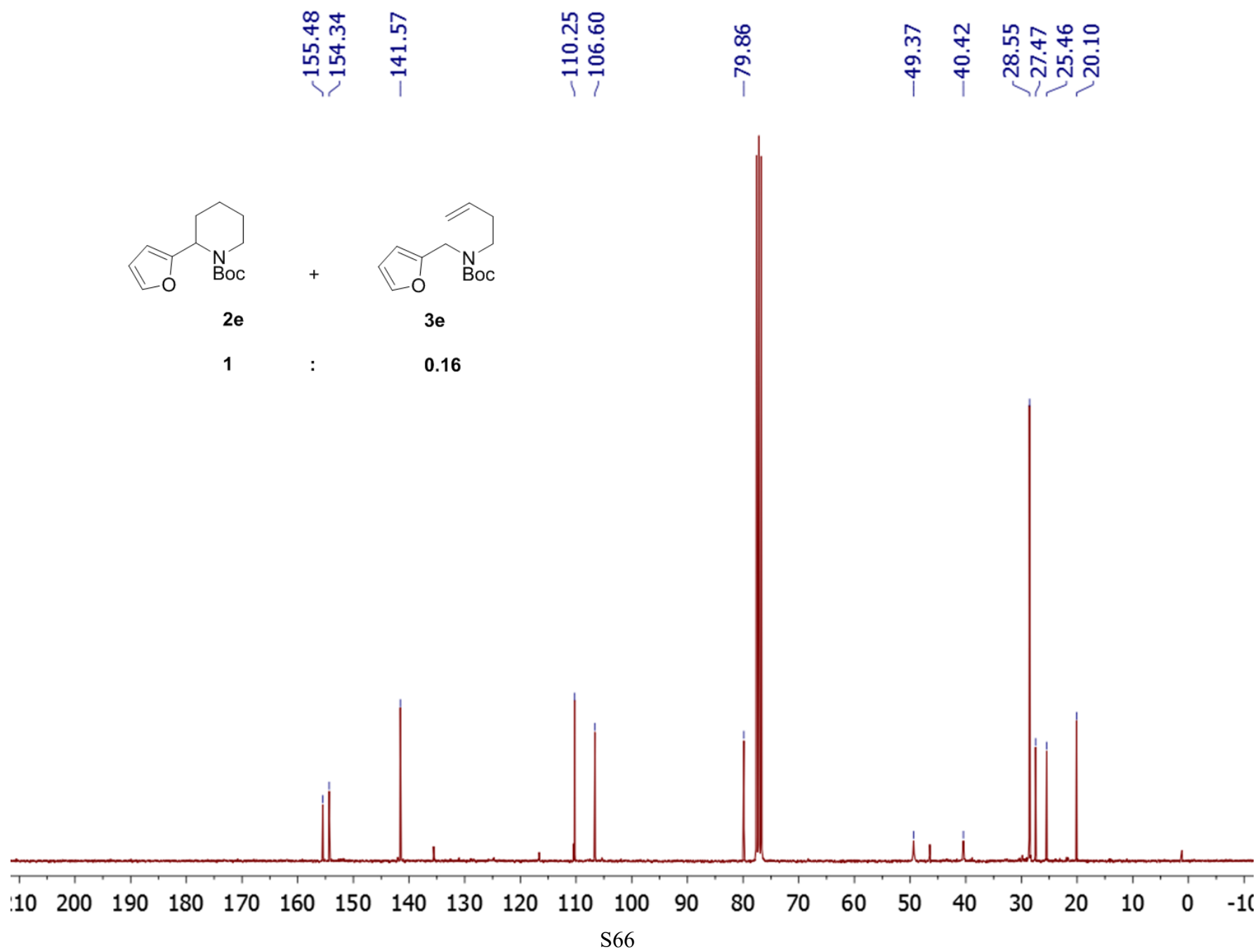


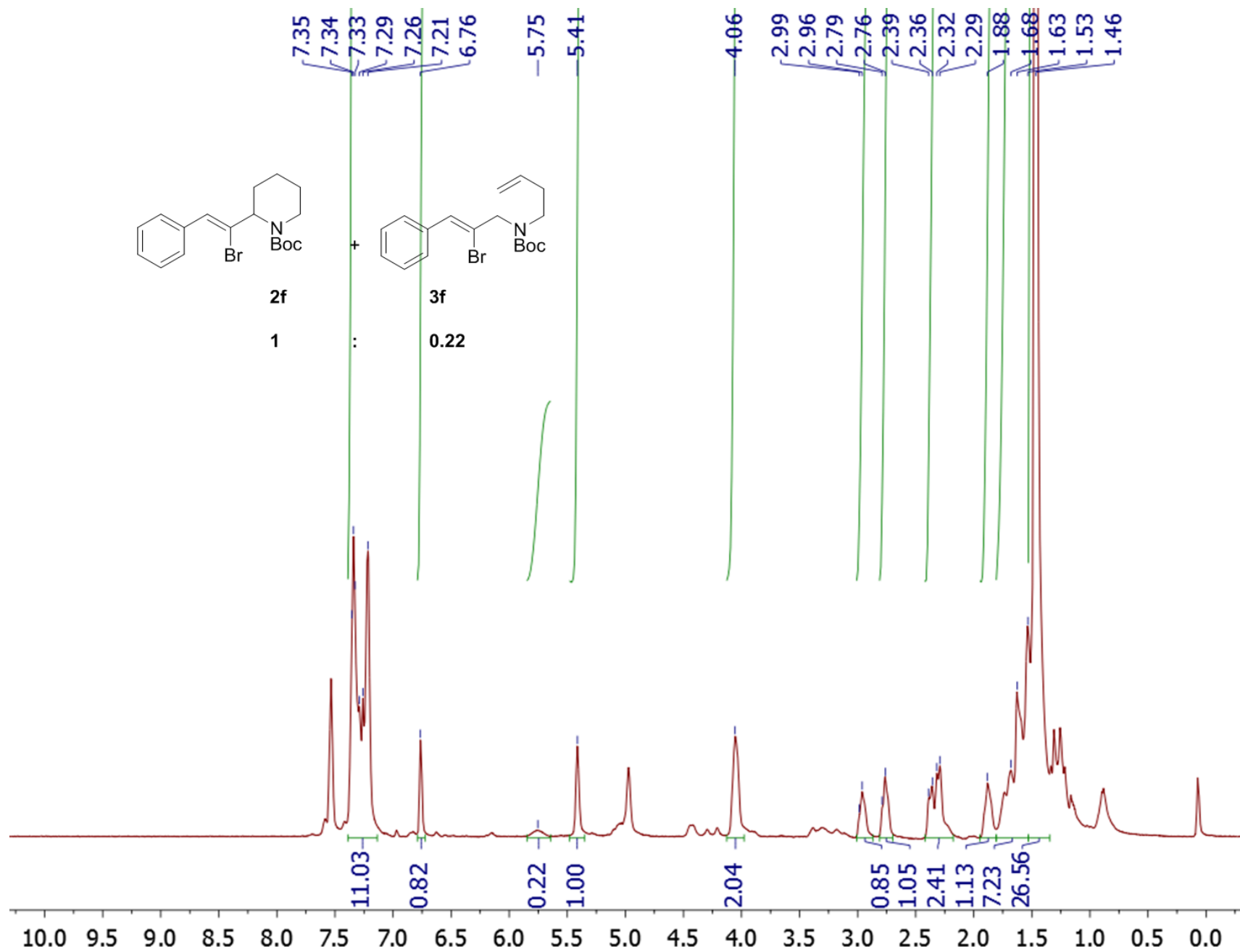


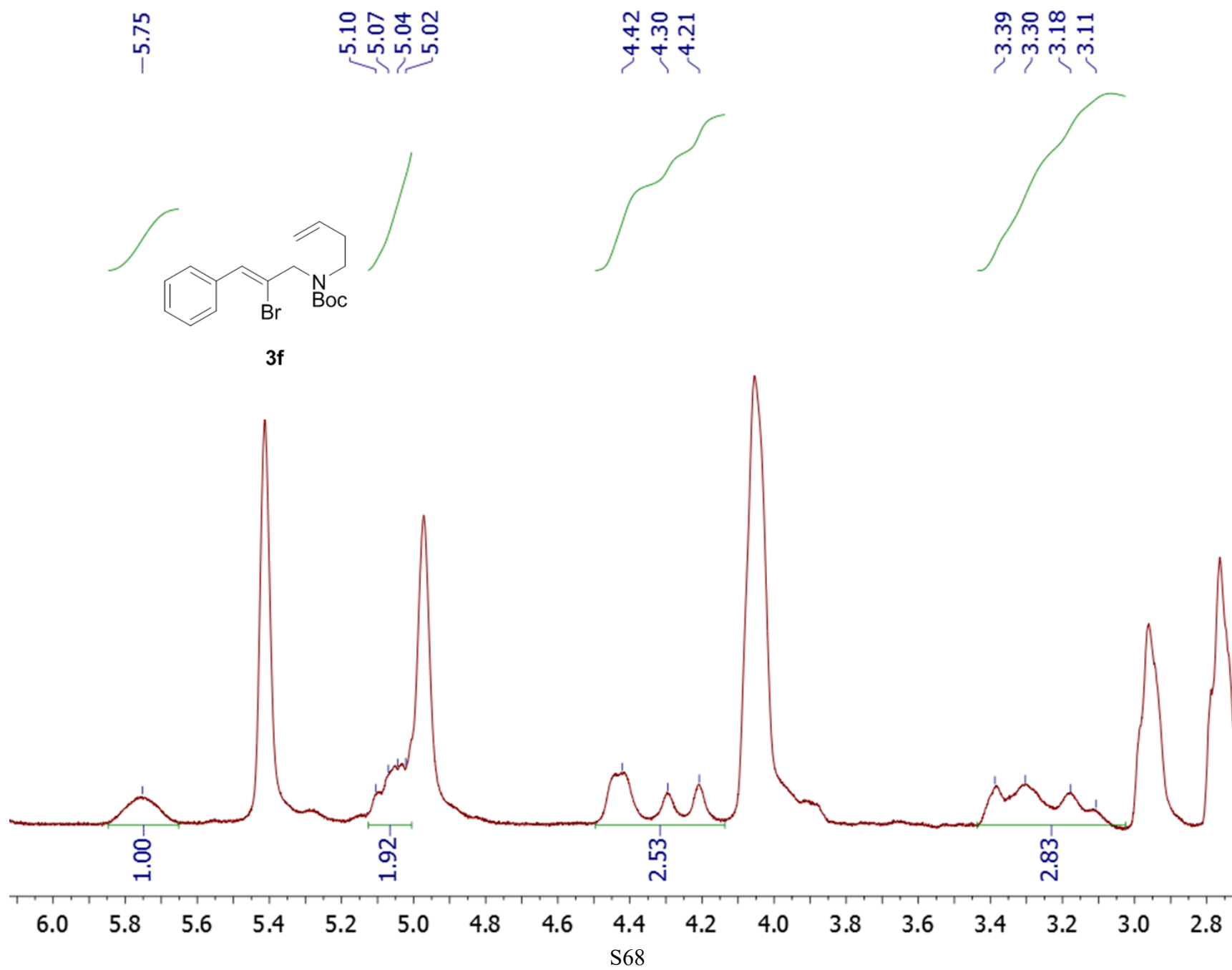


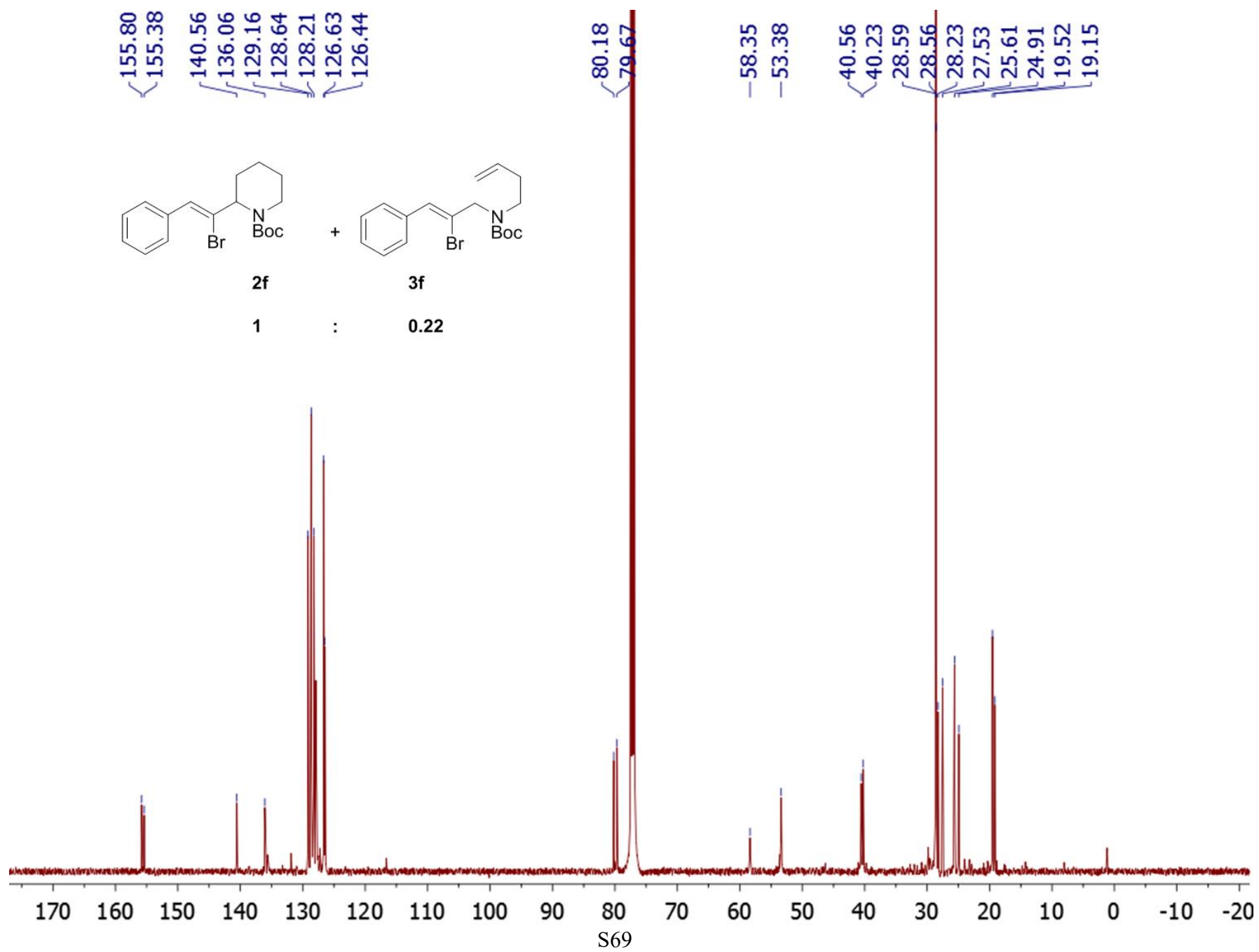


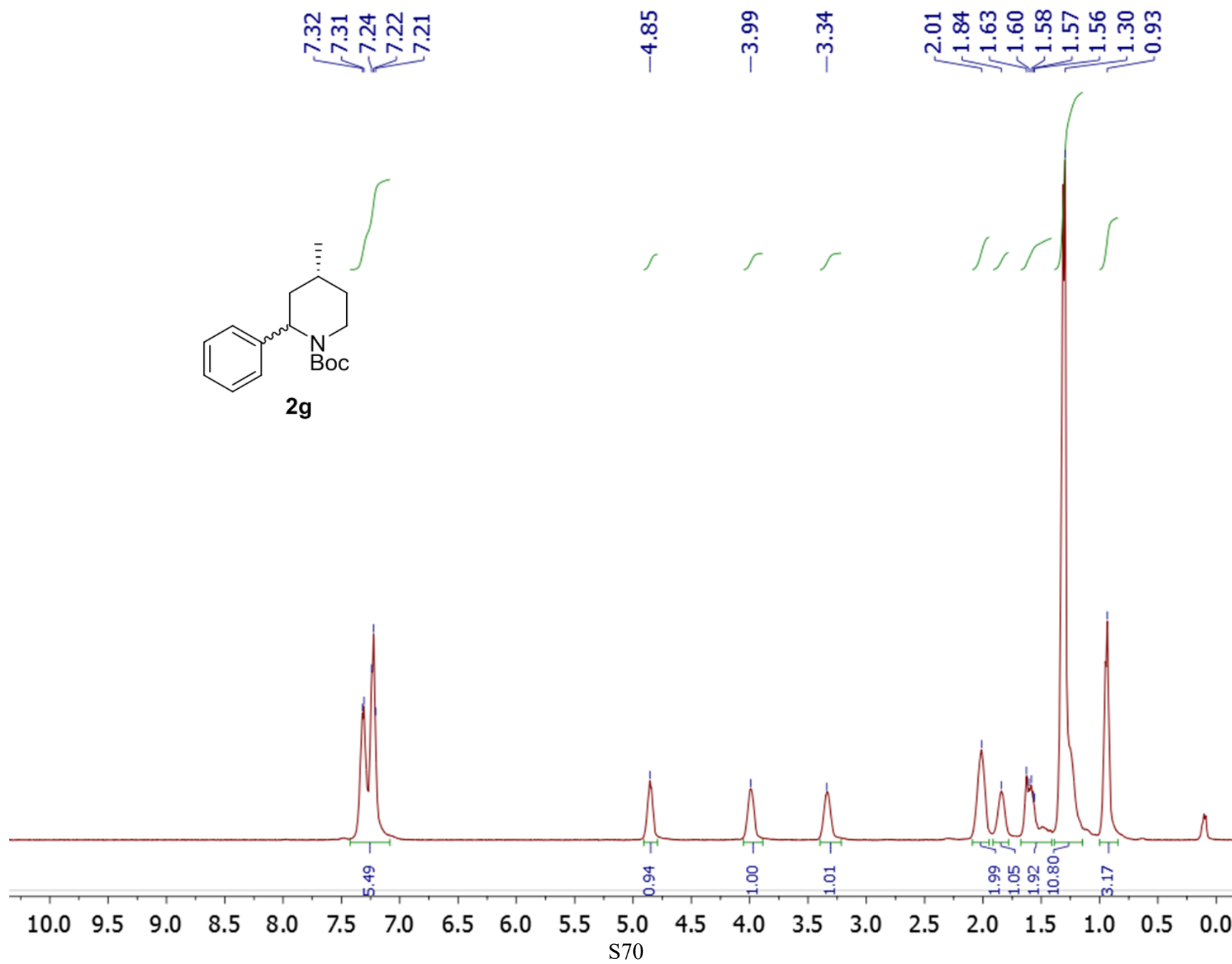
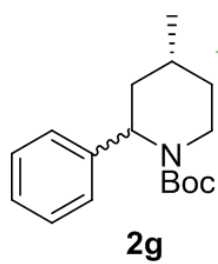


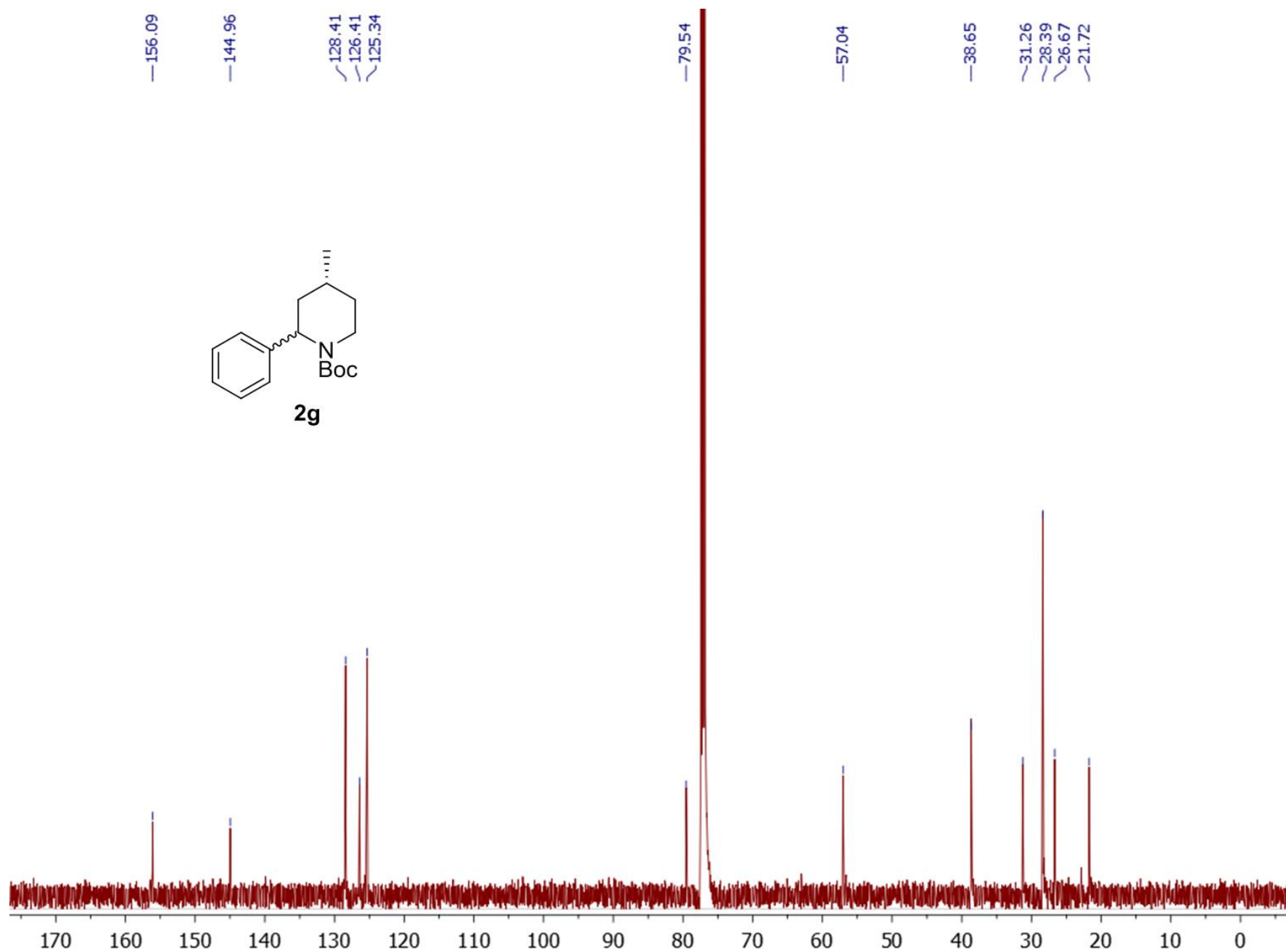
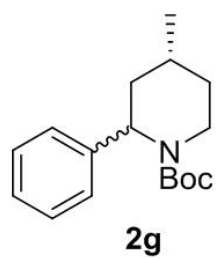


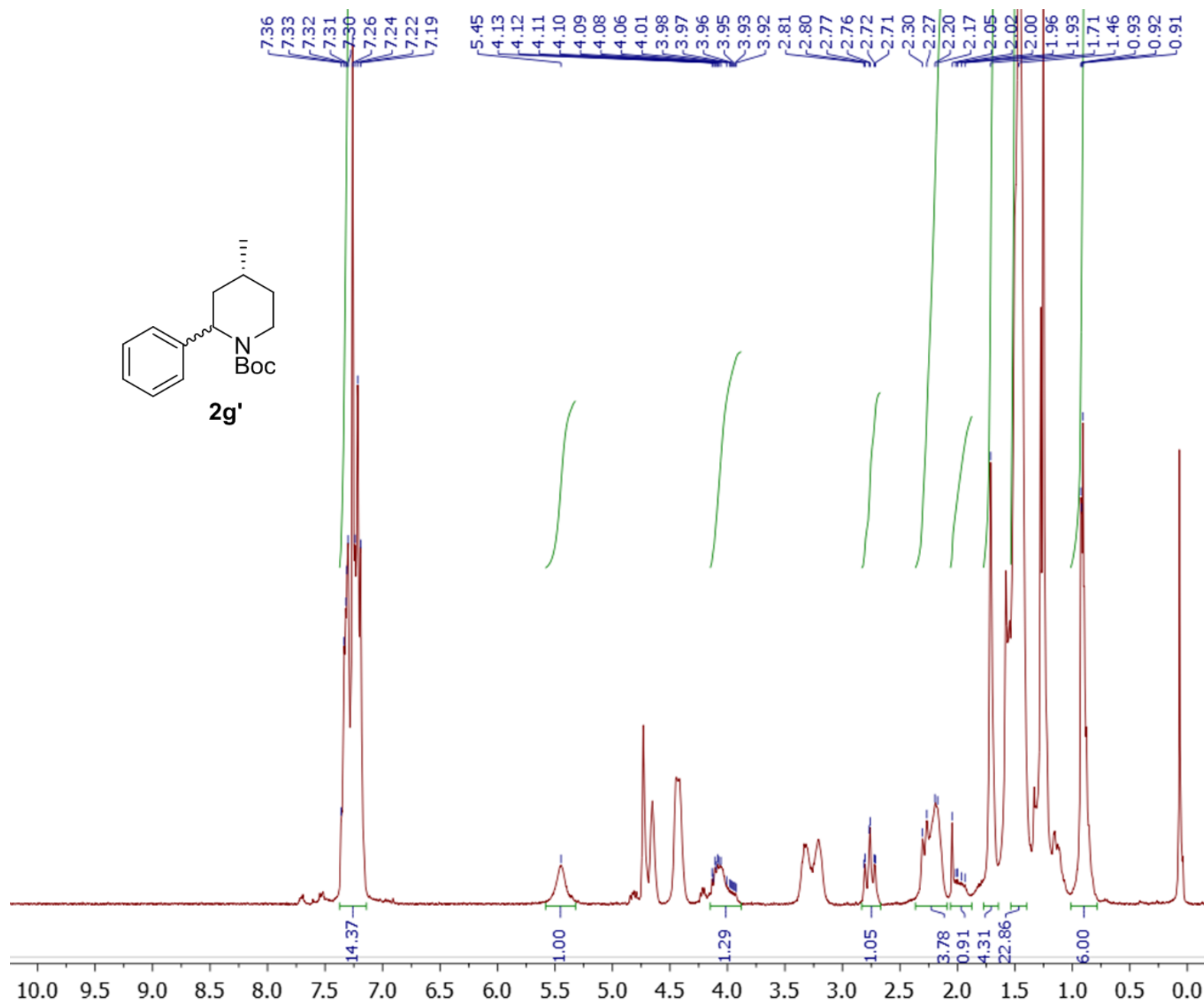
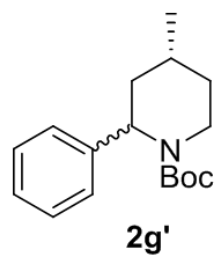


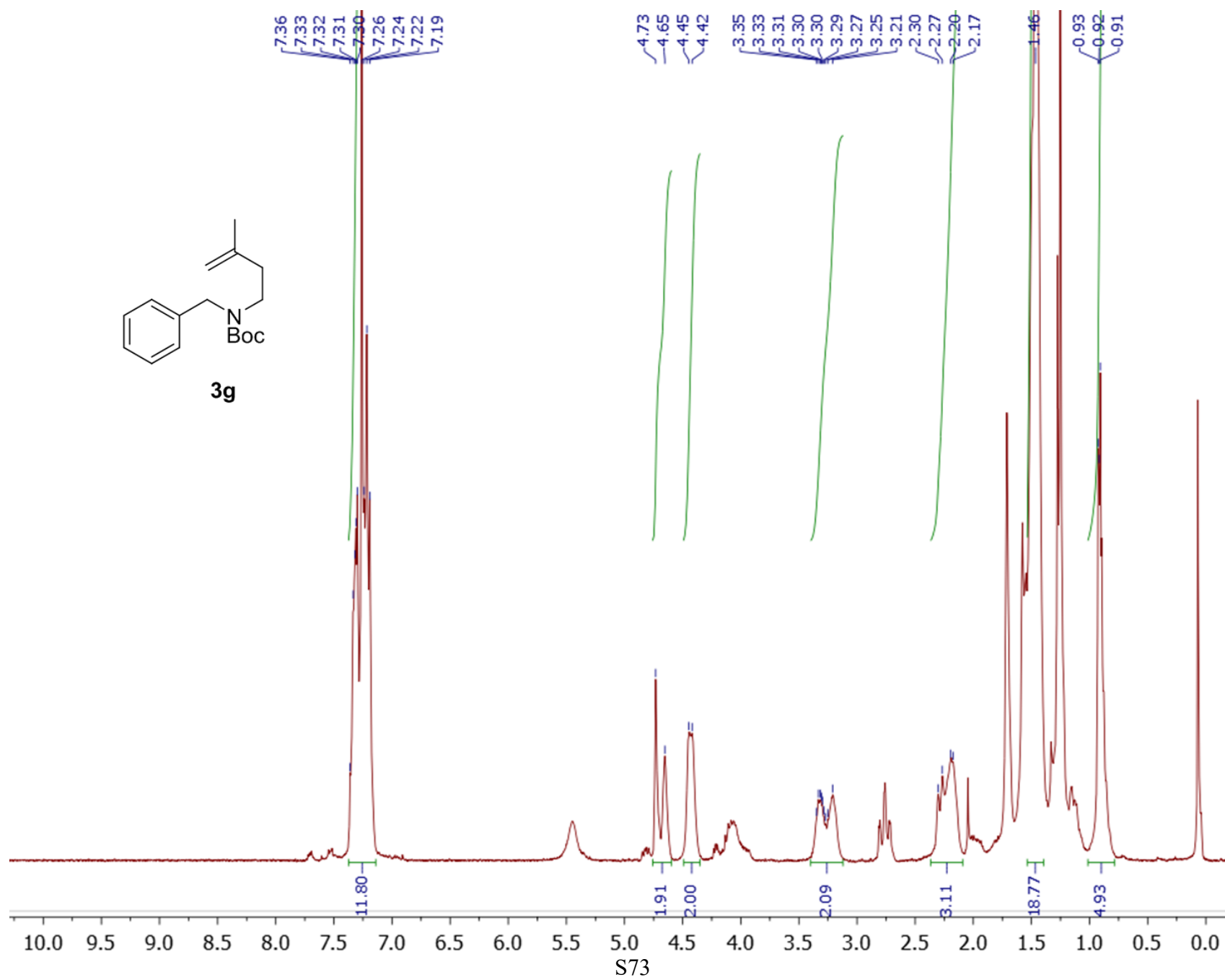
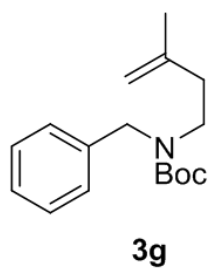


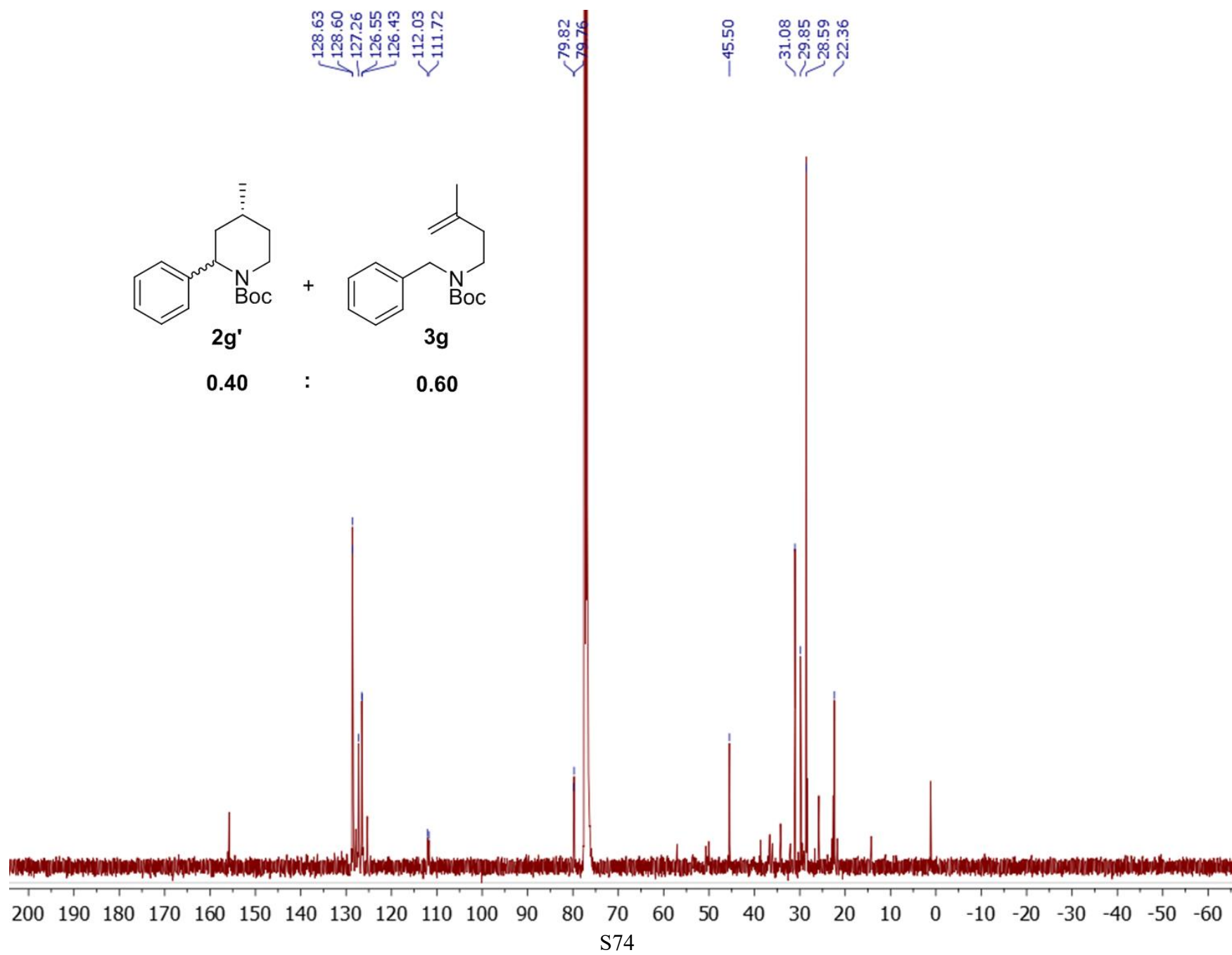


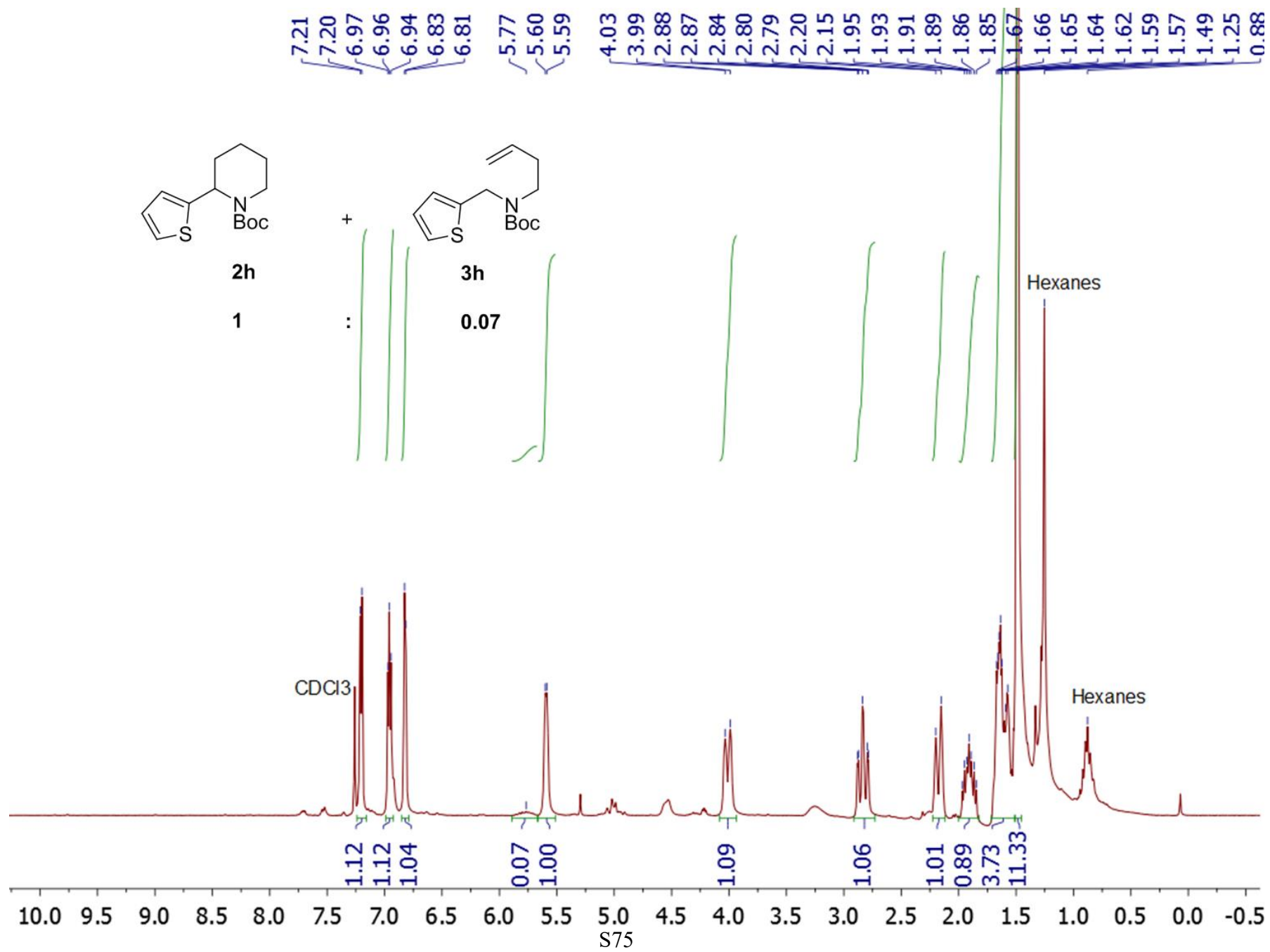


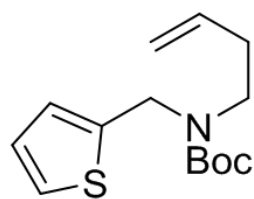




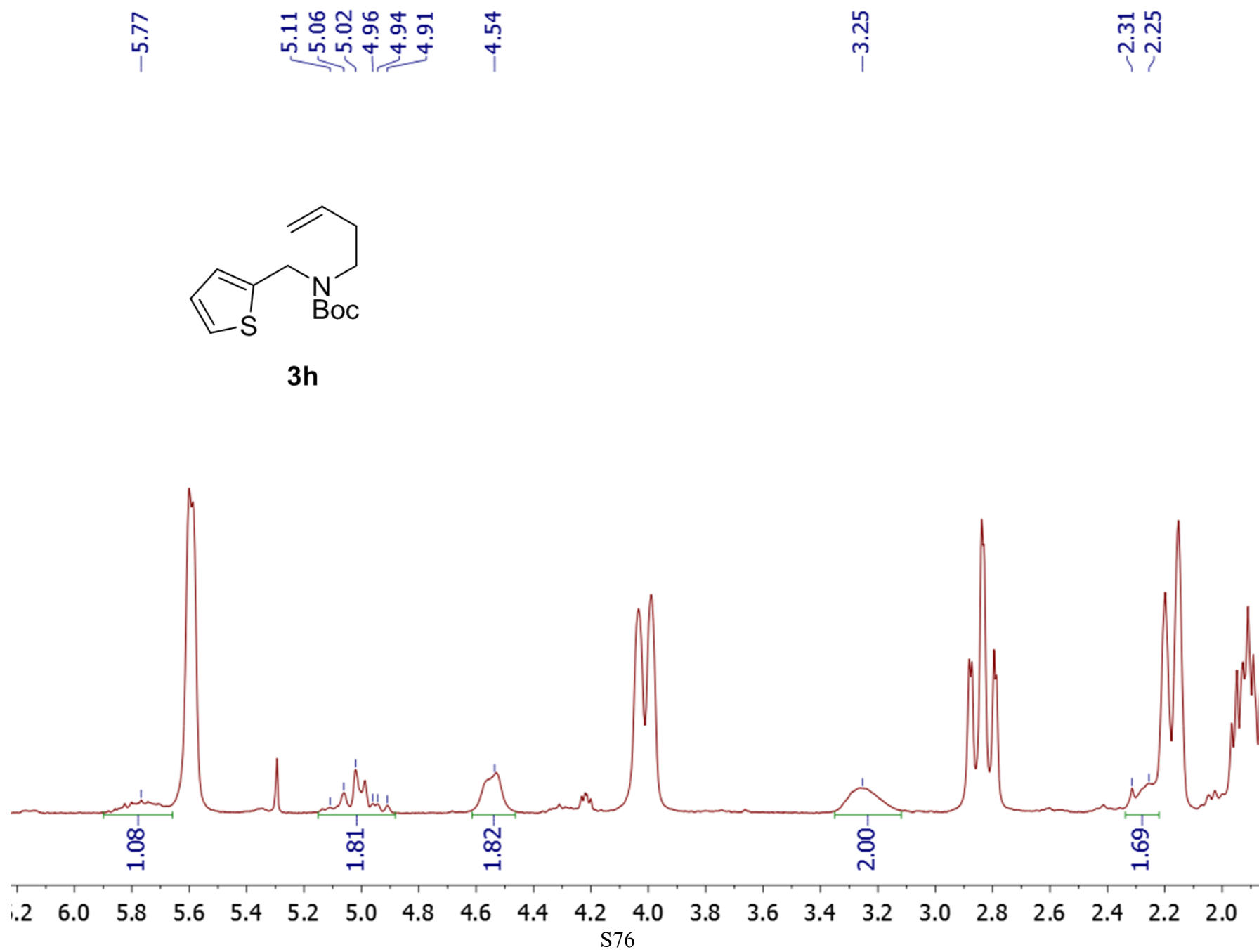


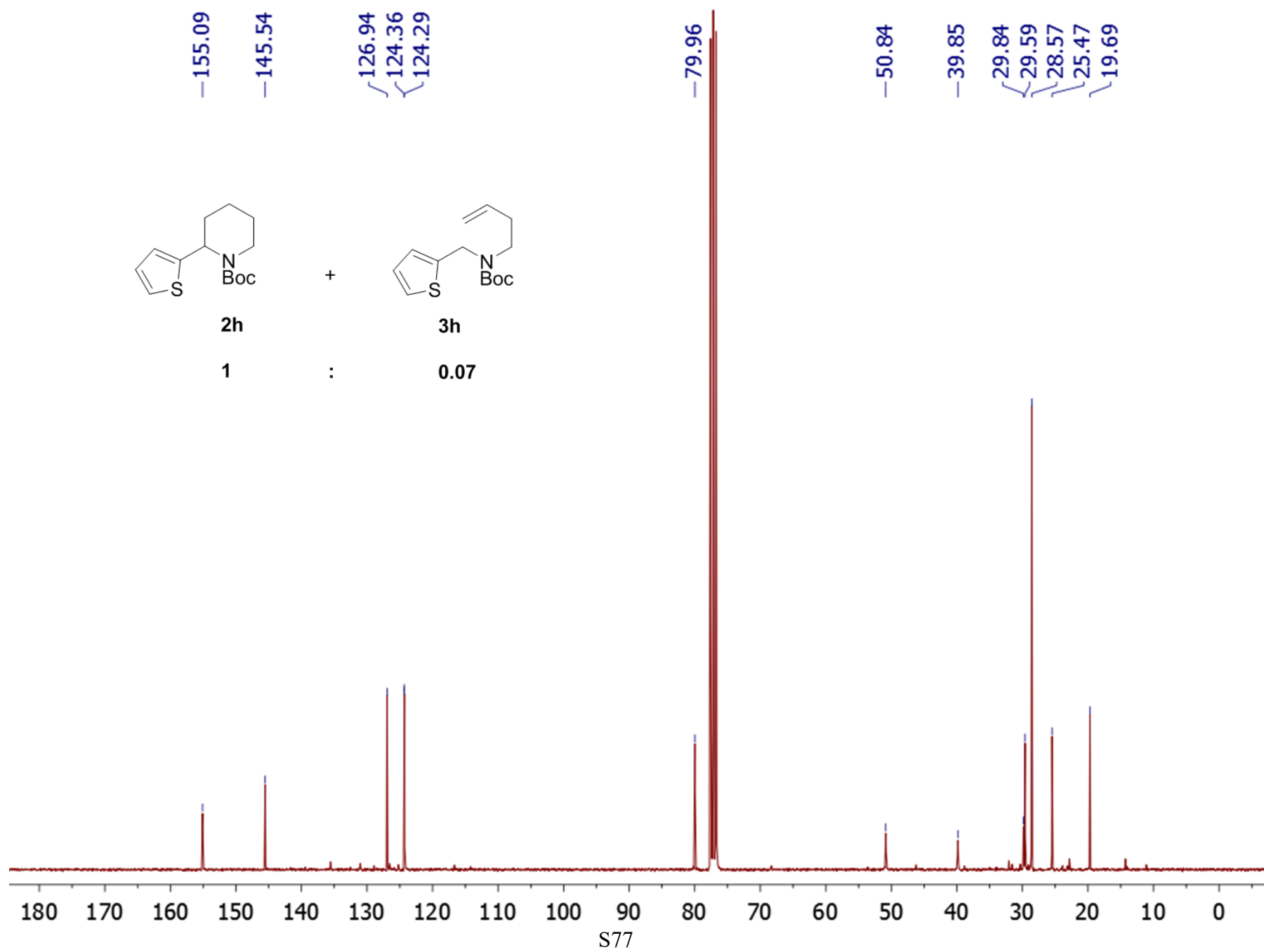


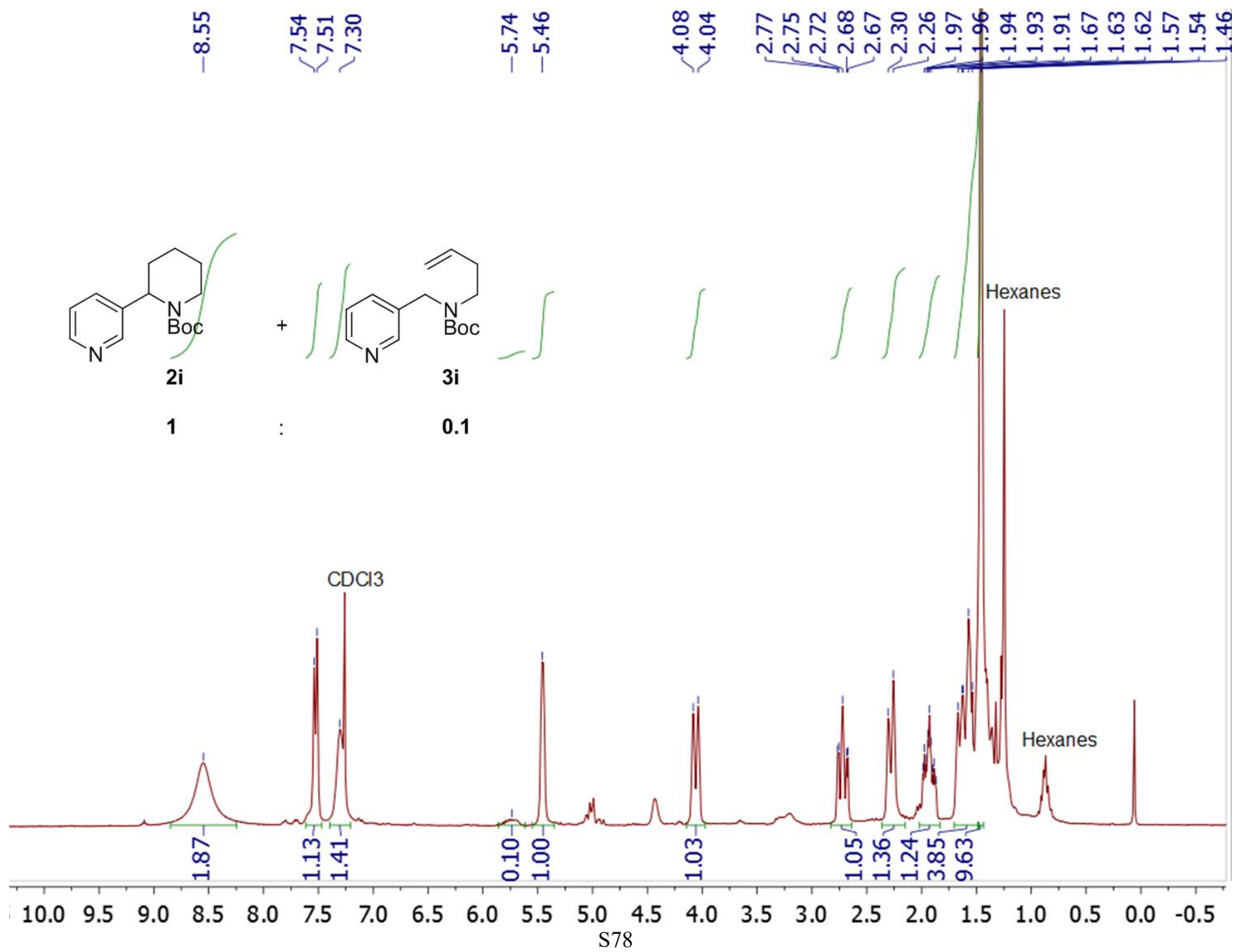


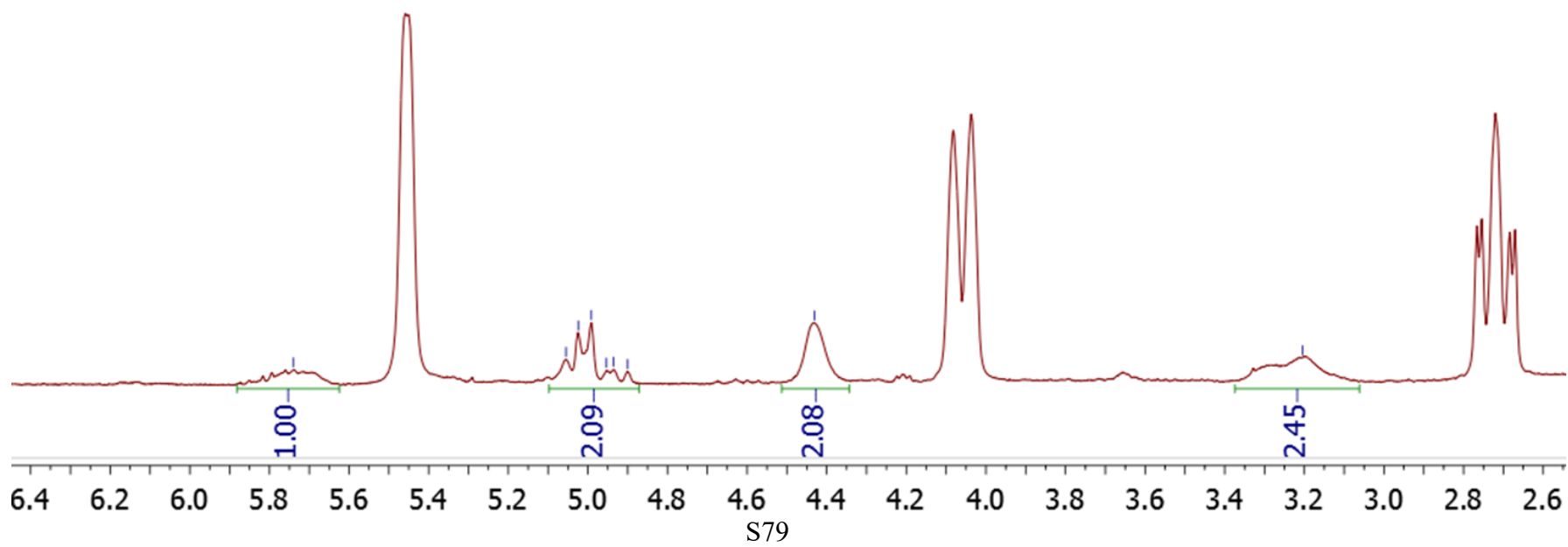
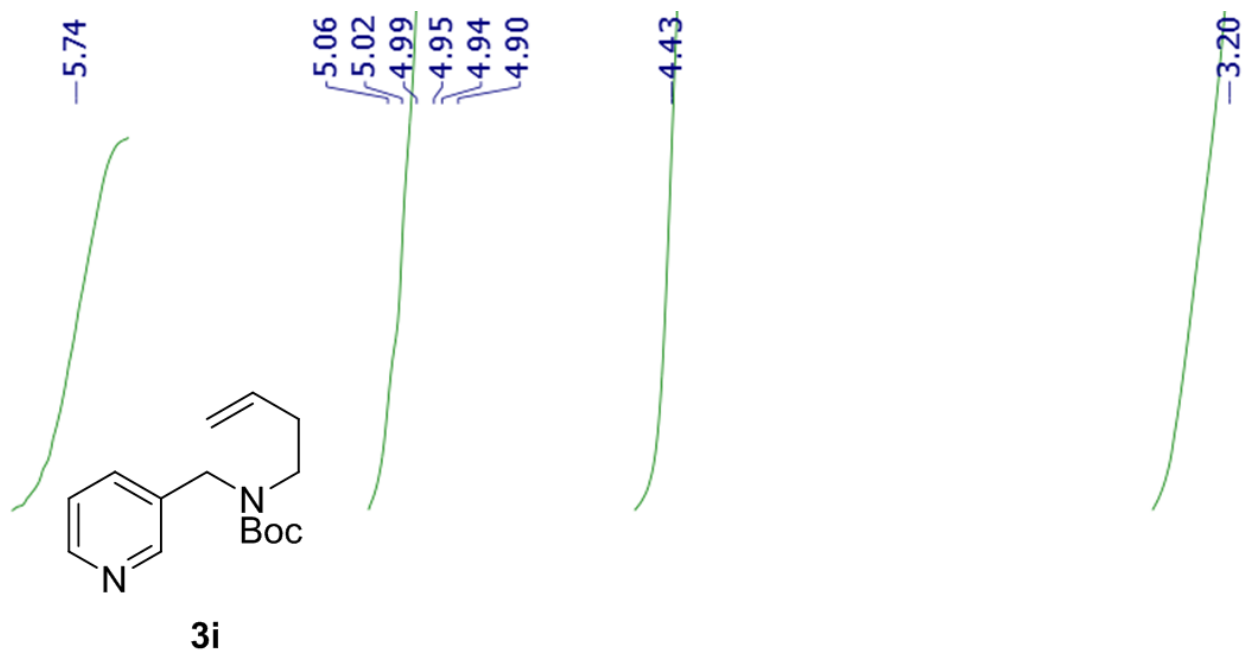


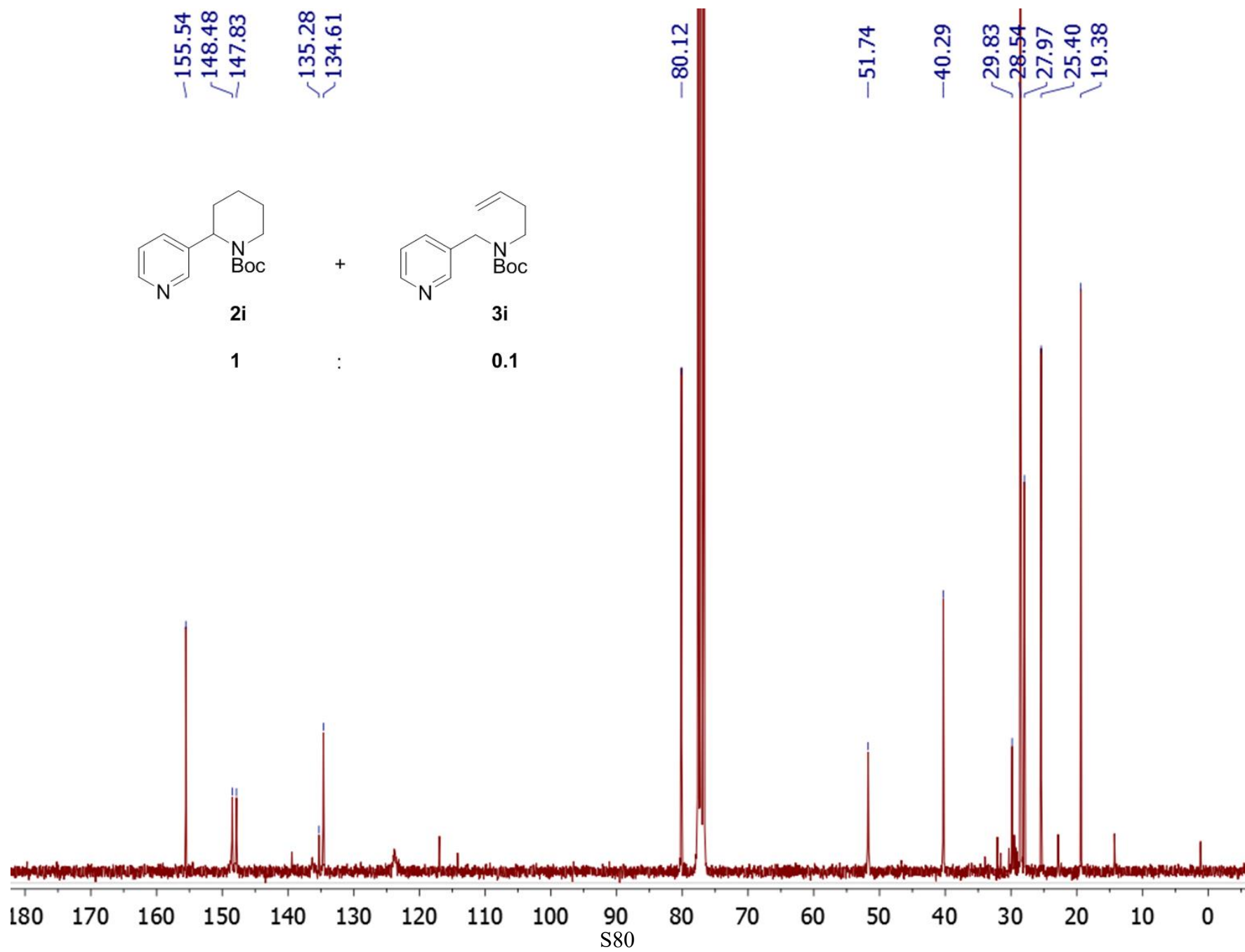
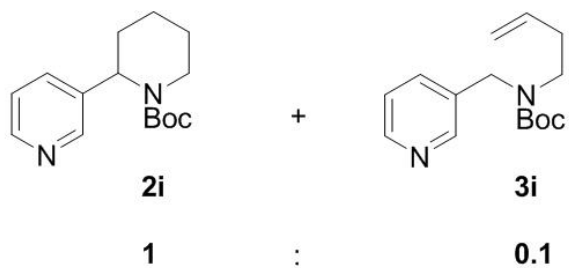
3h

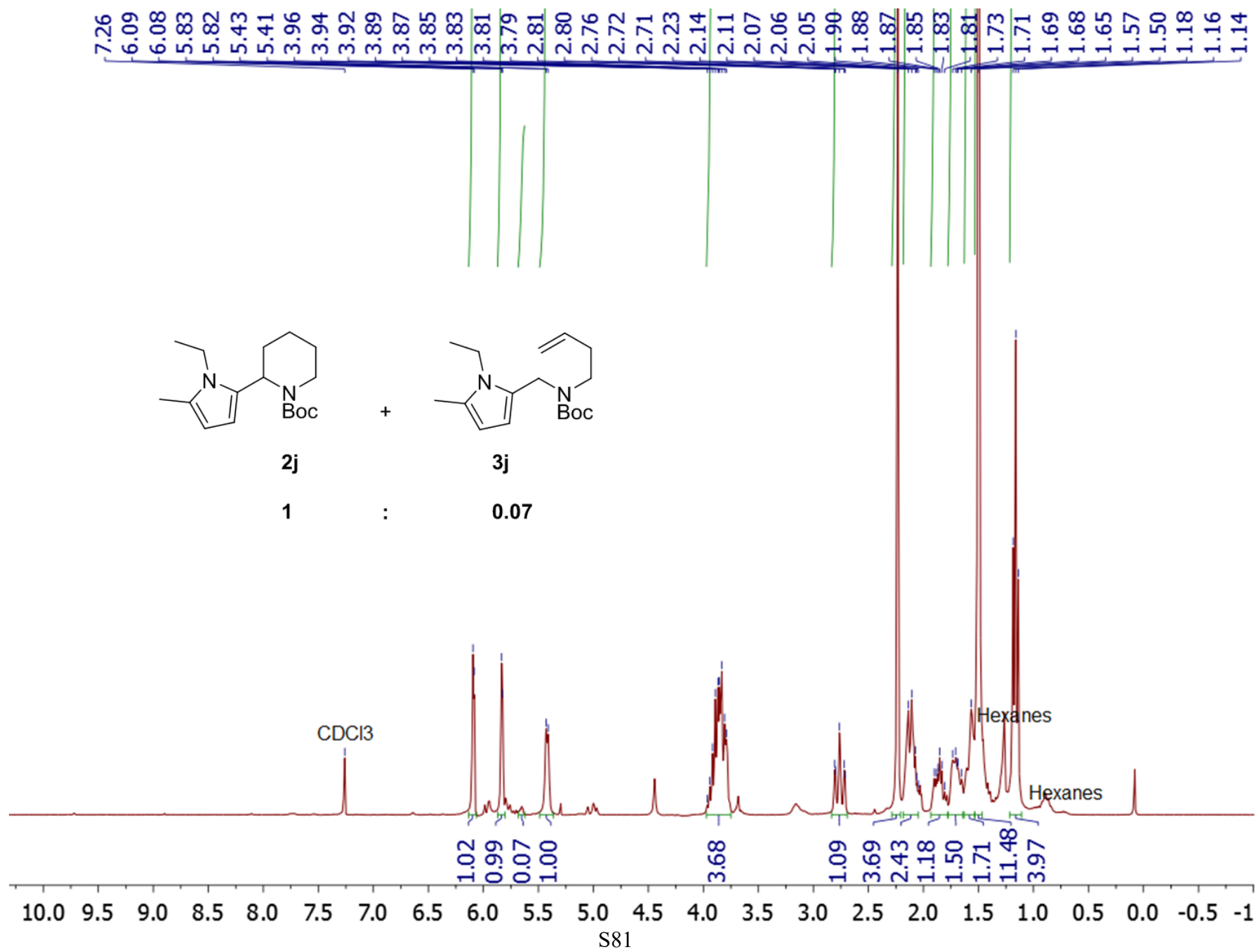


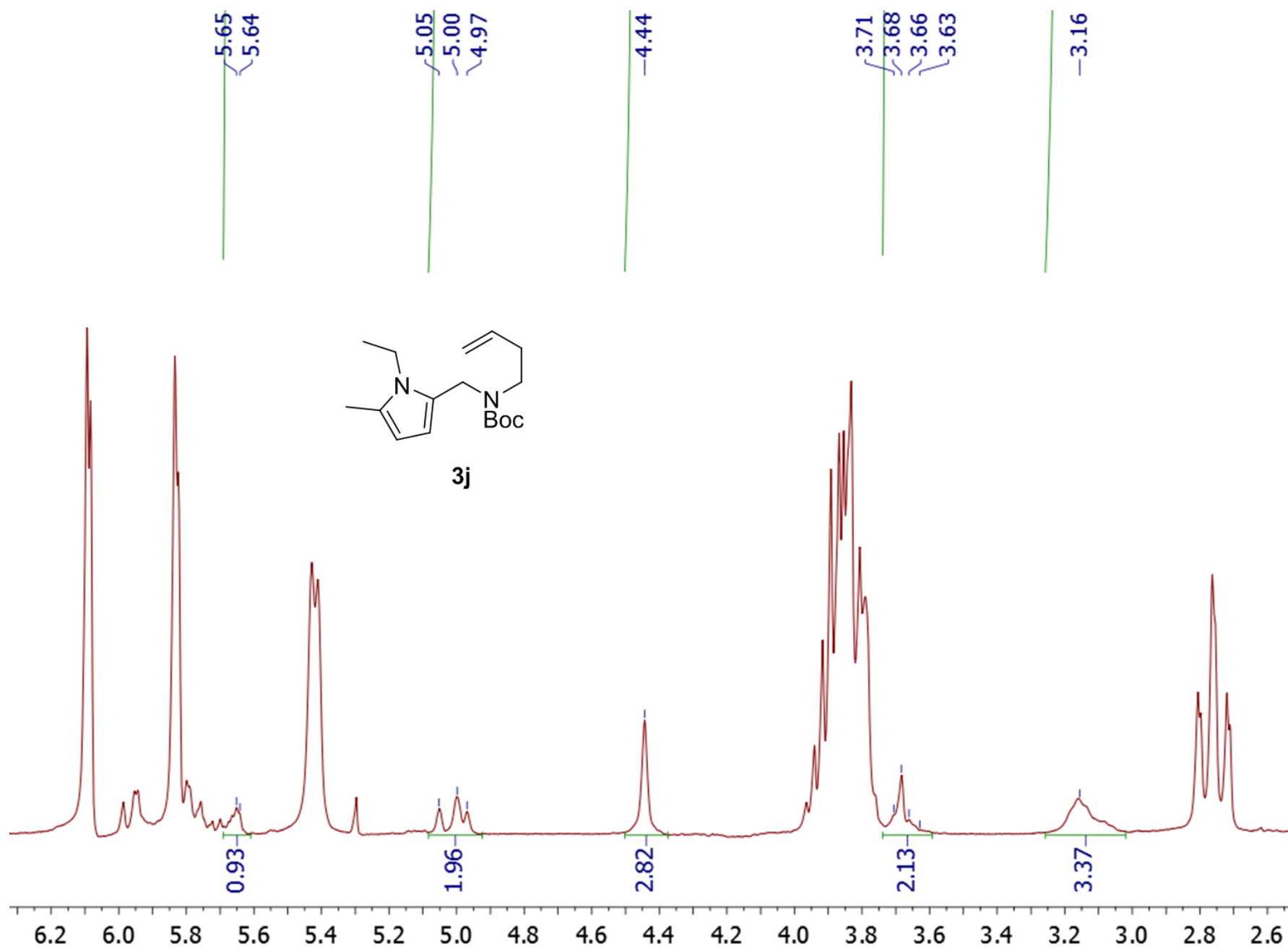


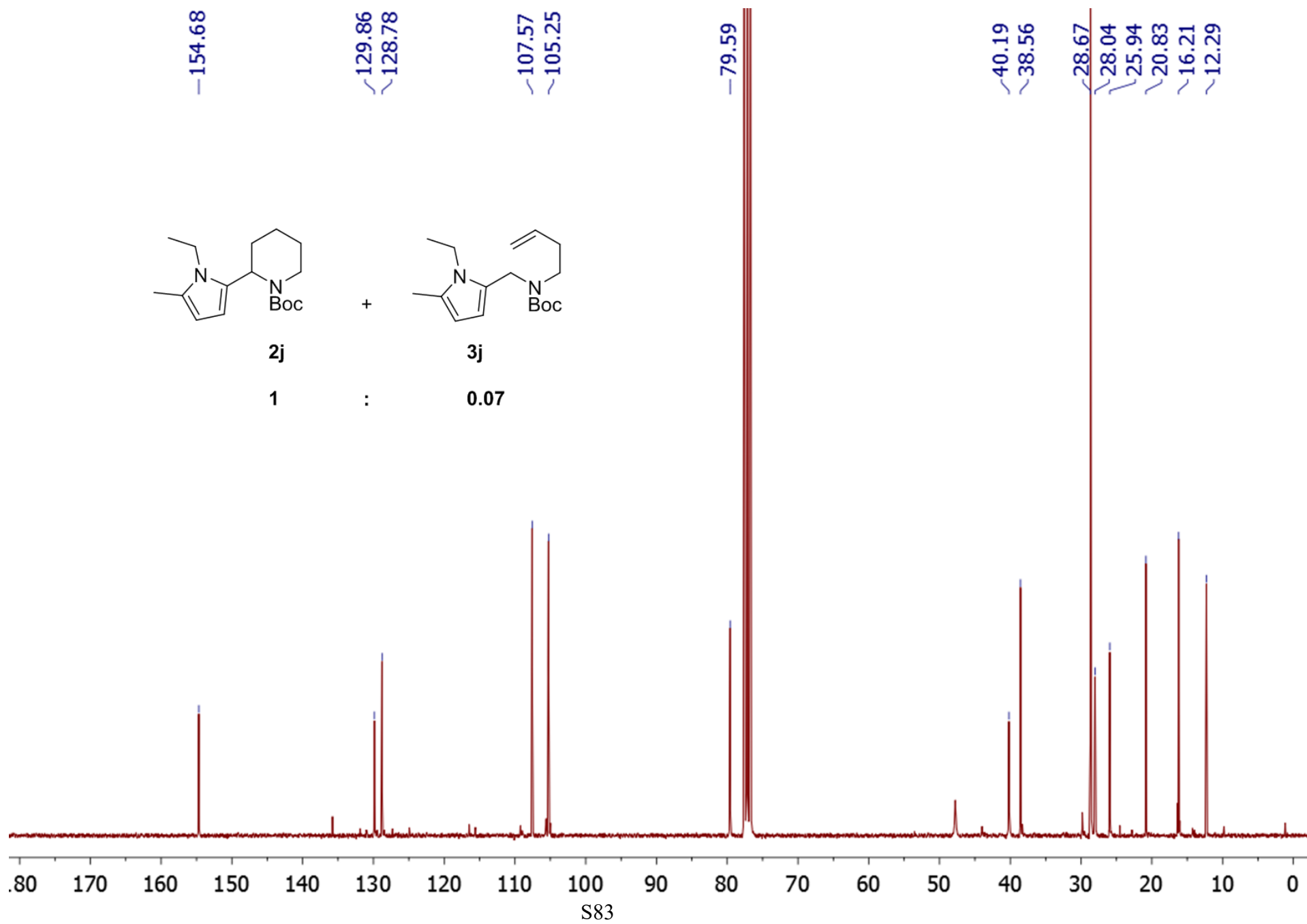


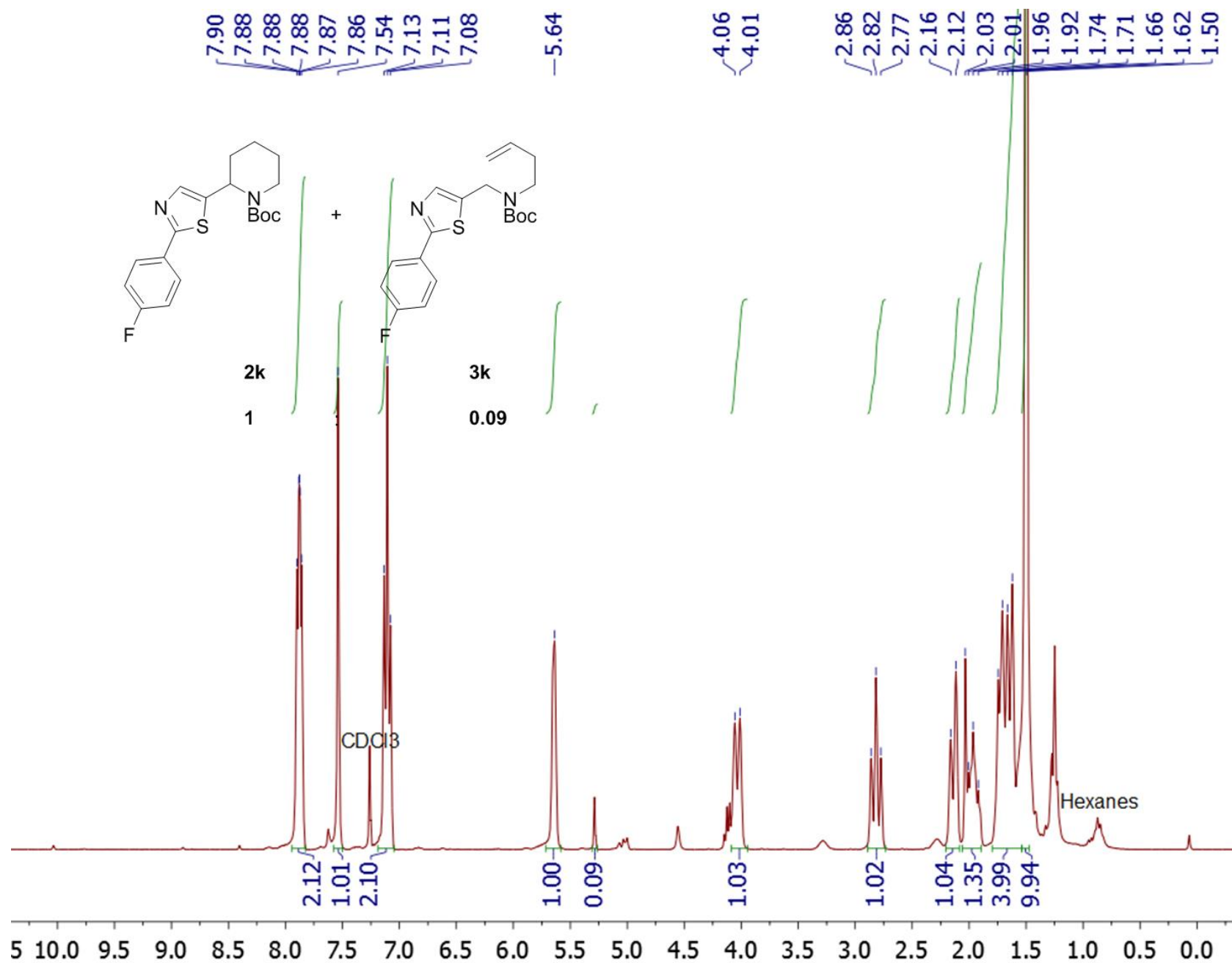


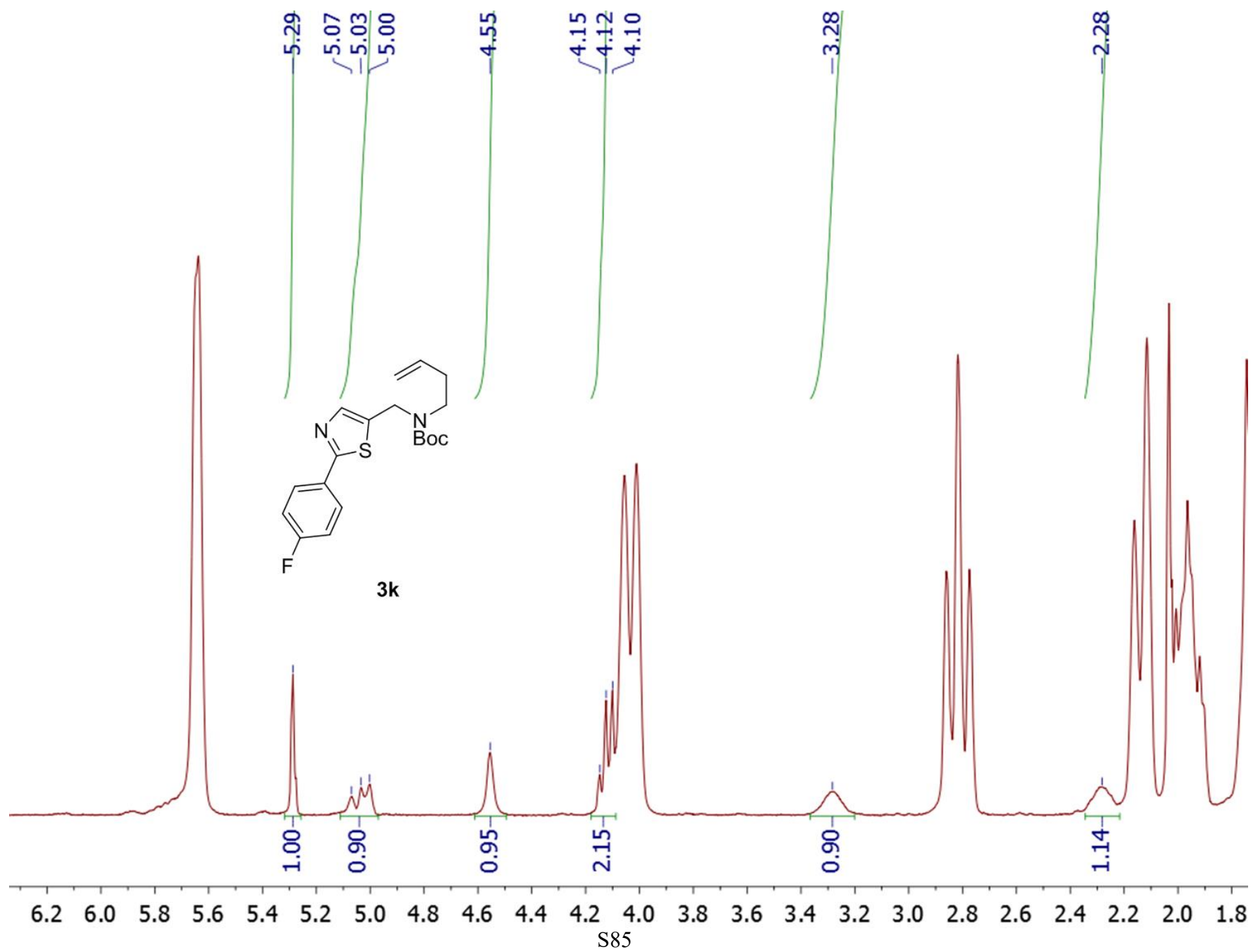


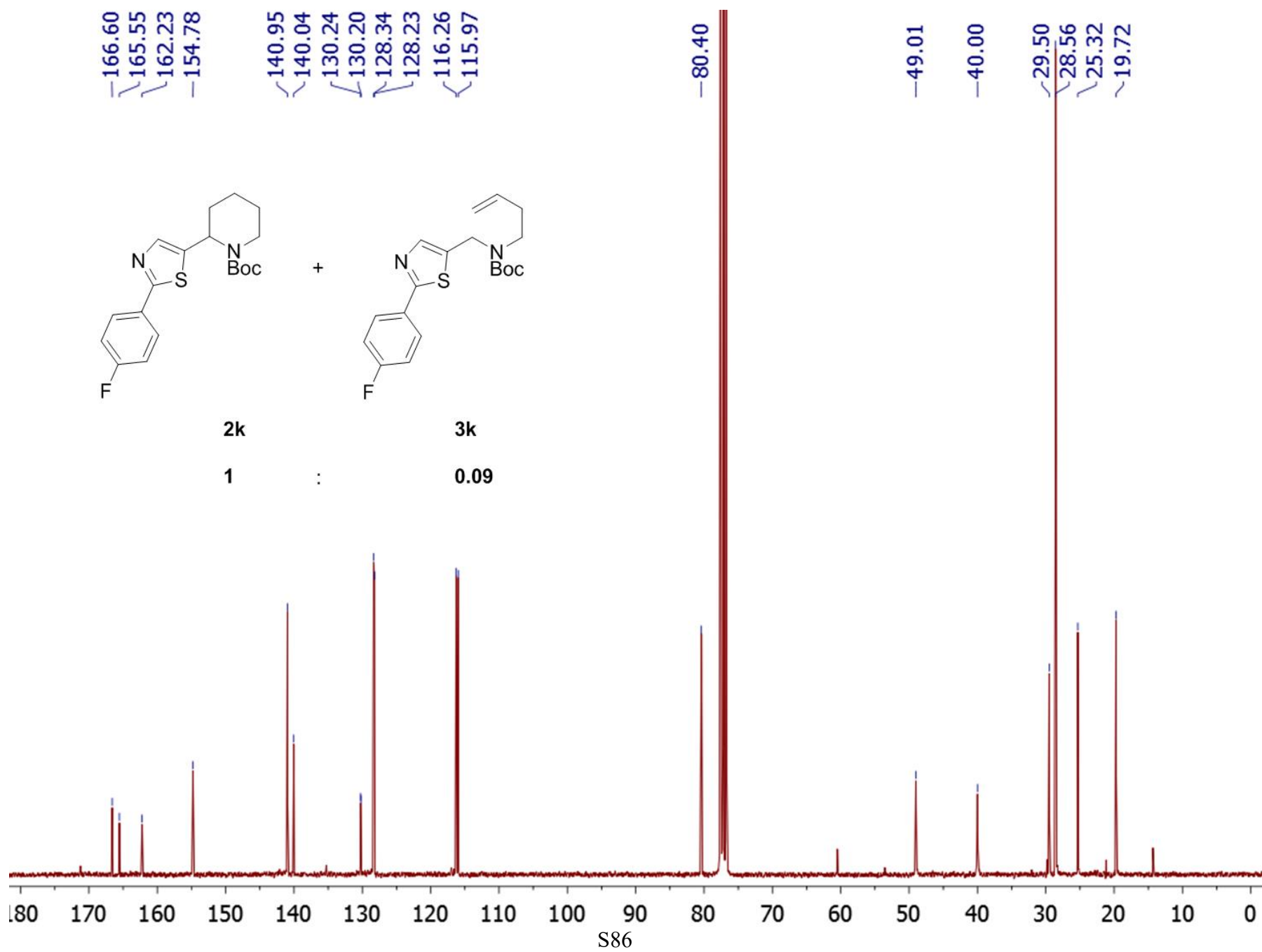


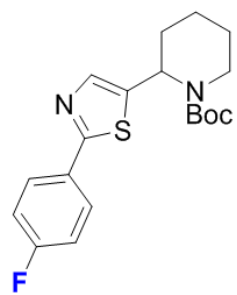








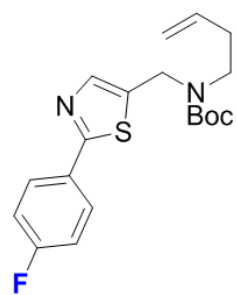




2k

1

+



3k

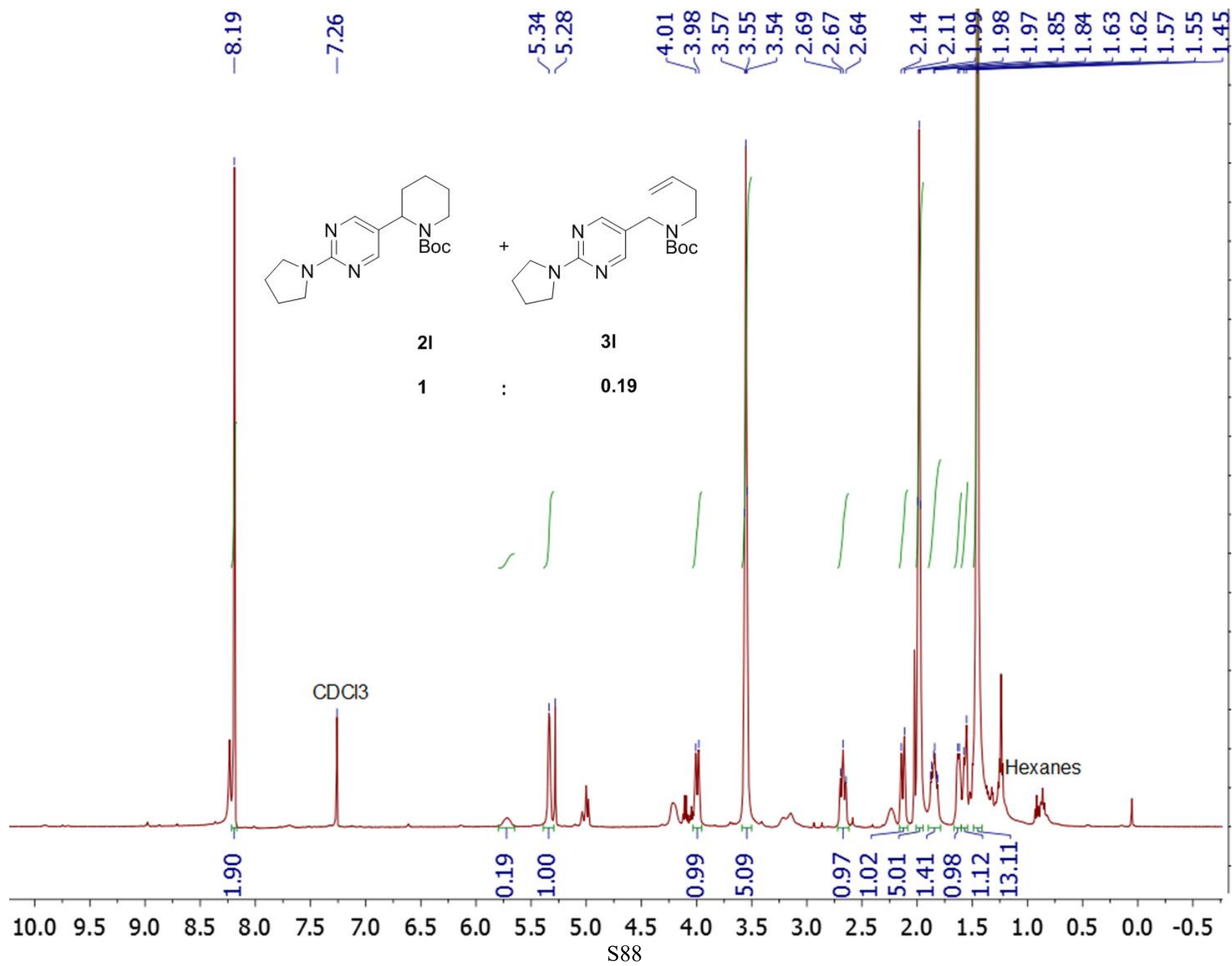
0.09

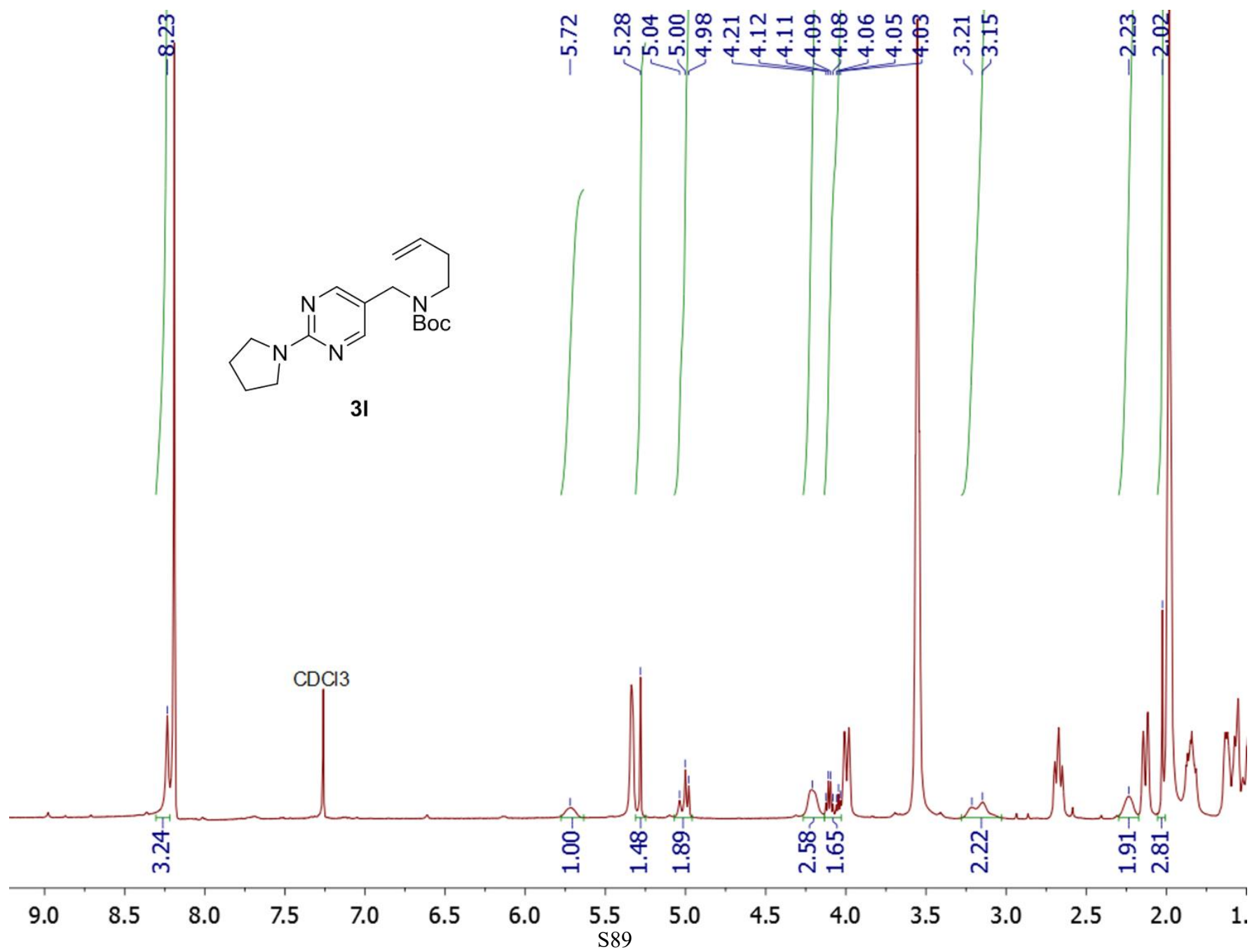
:

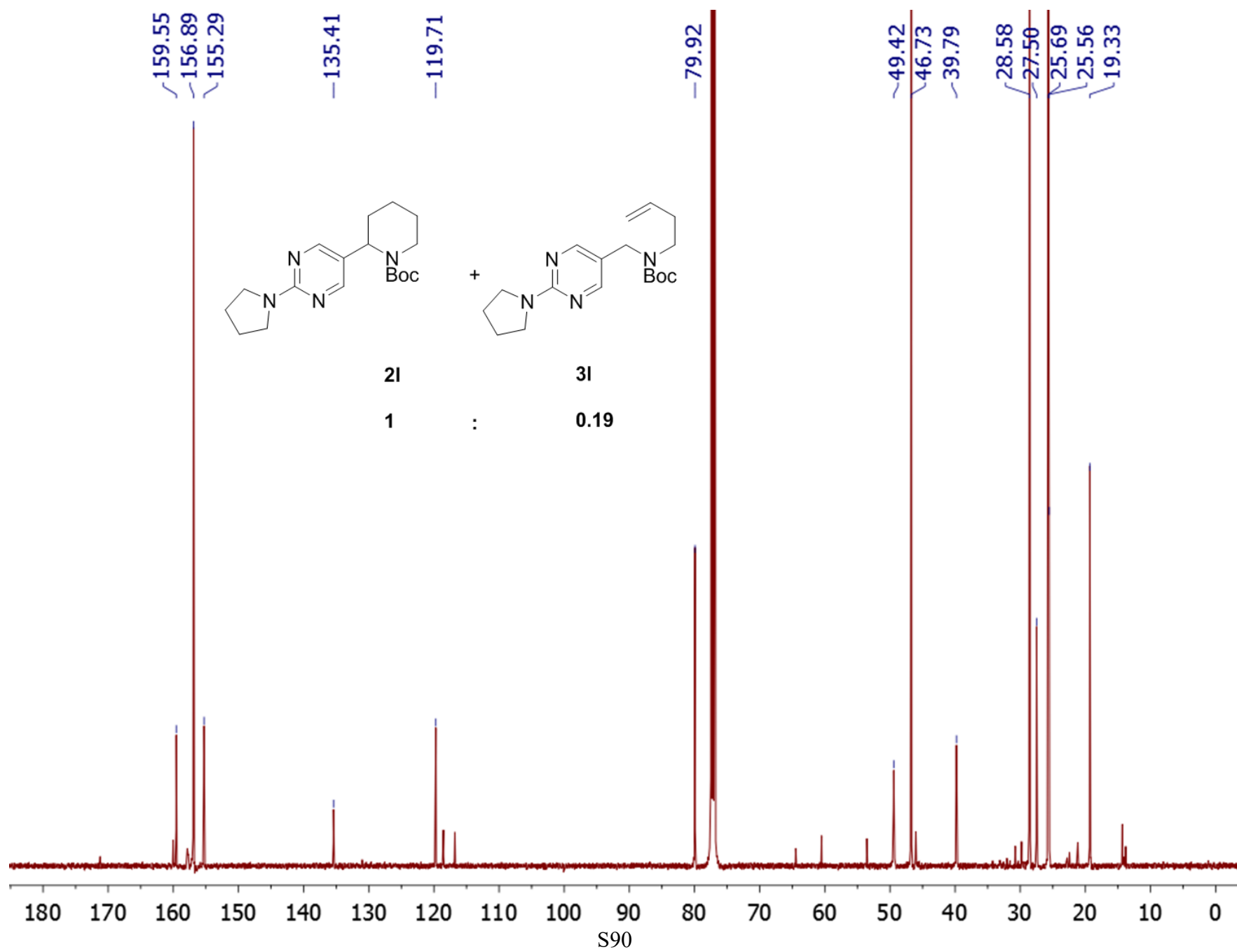
-110.71

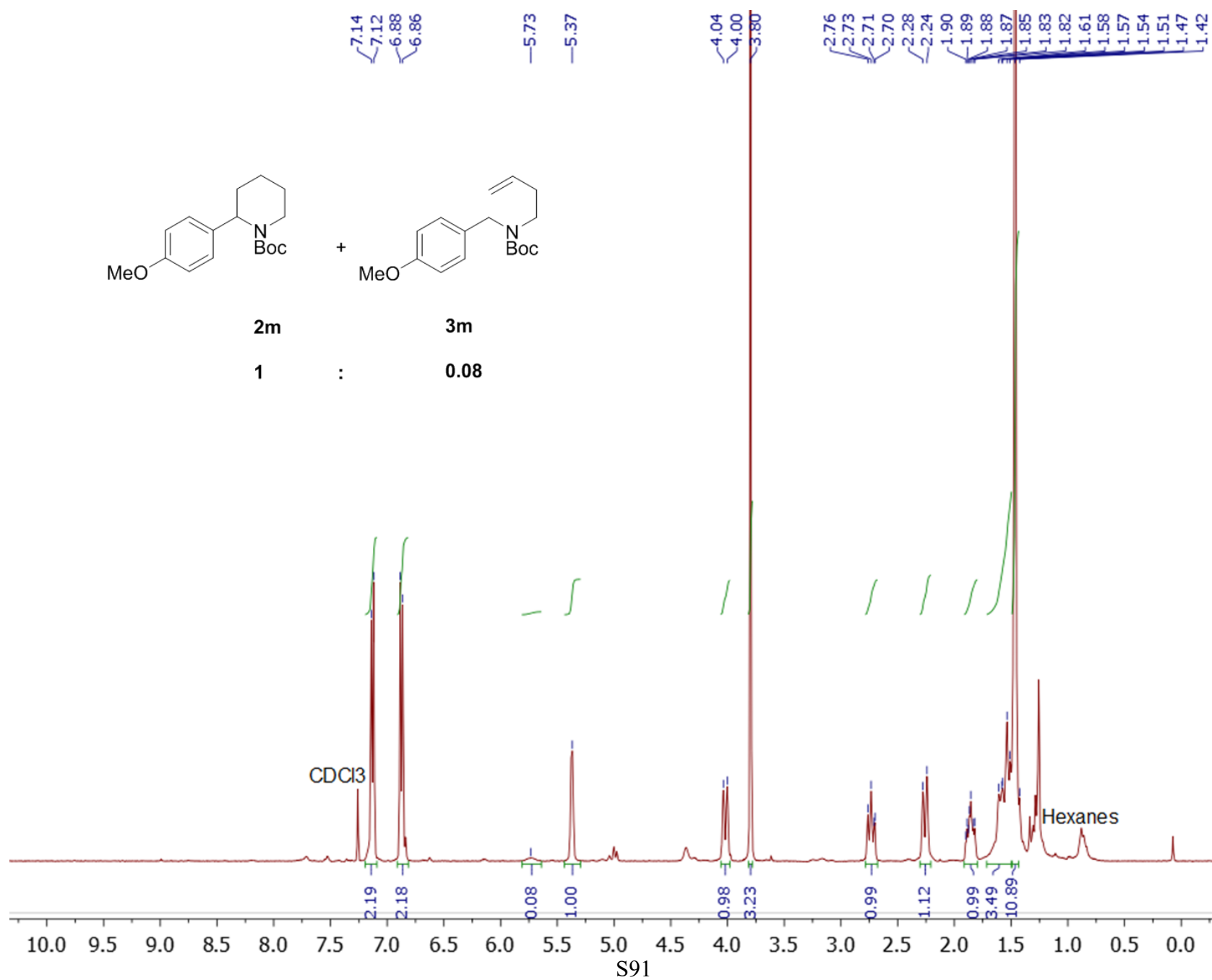
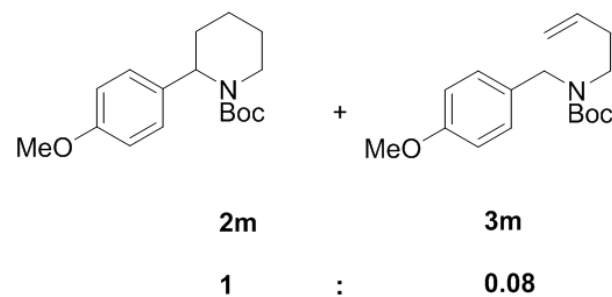


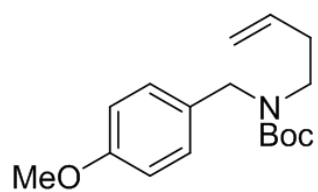
S87



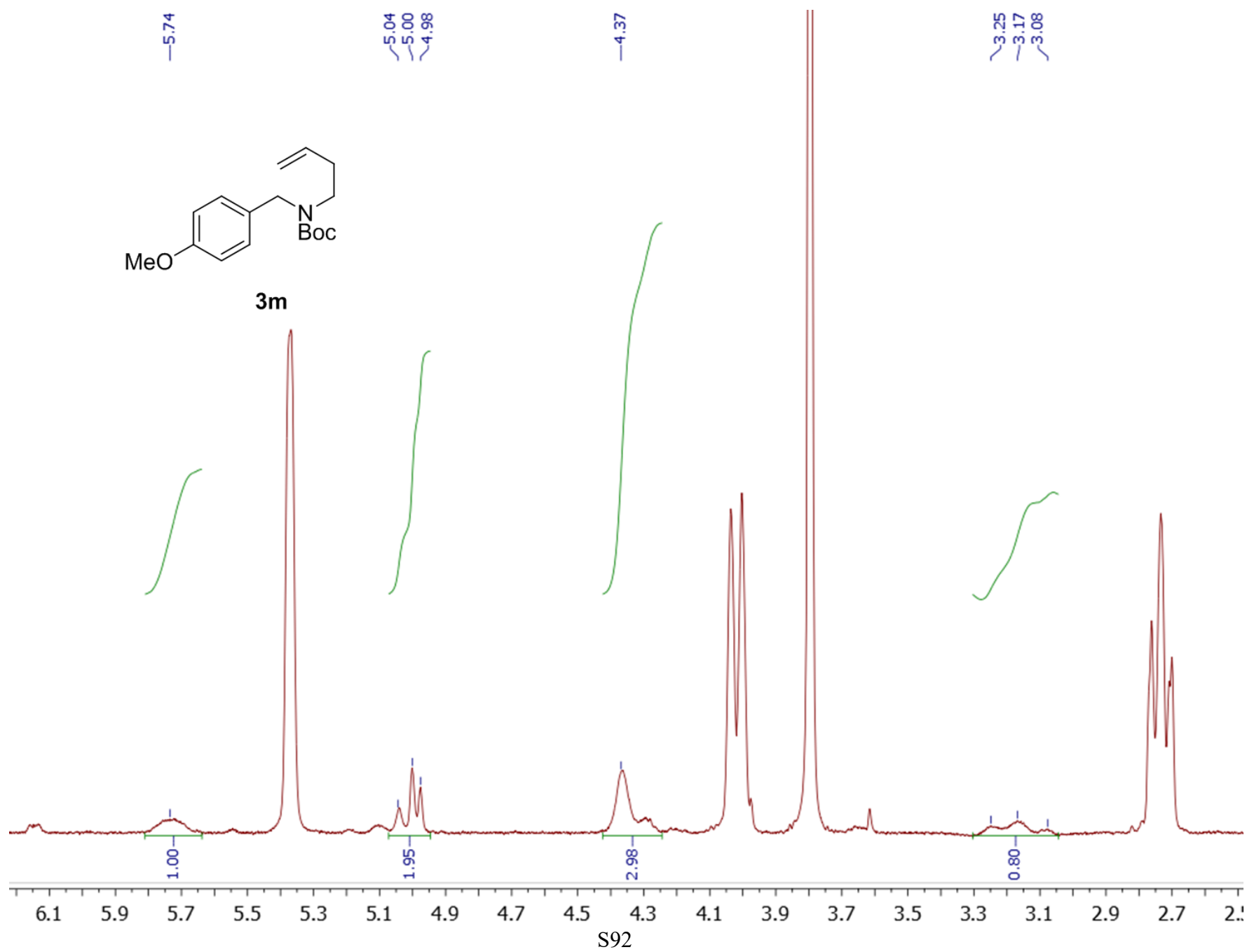


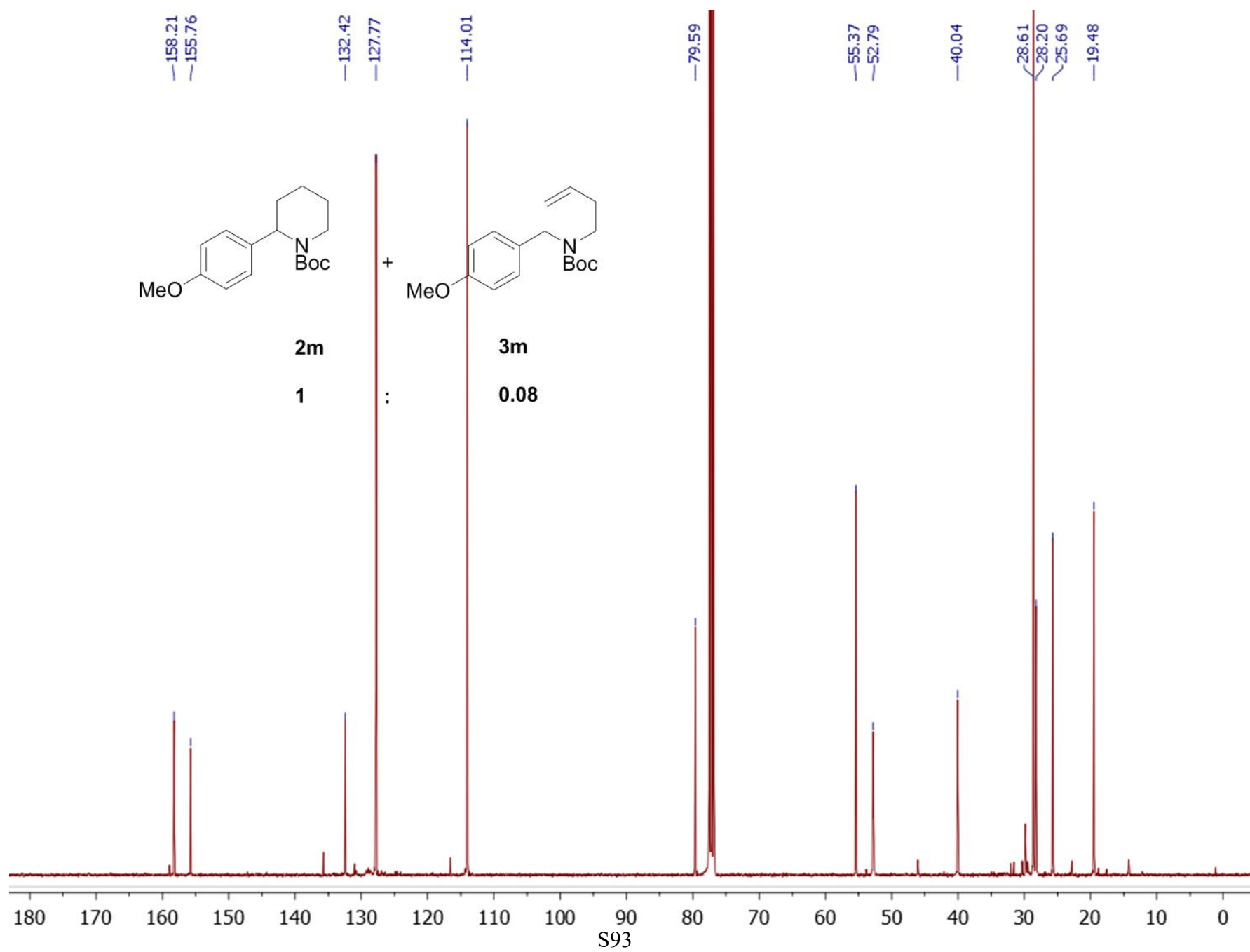


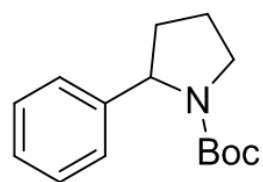




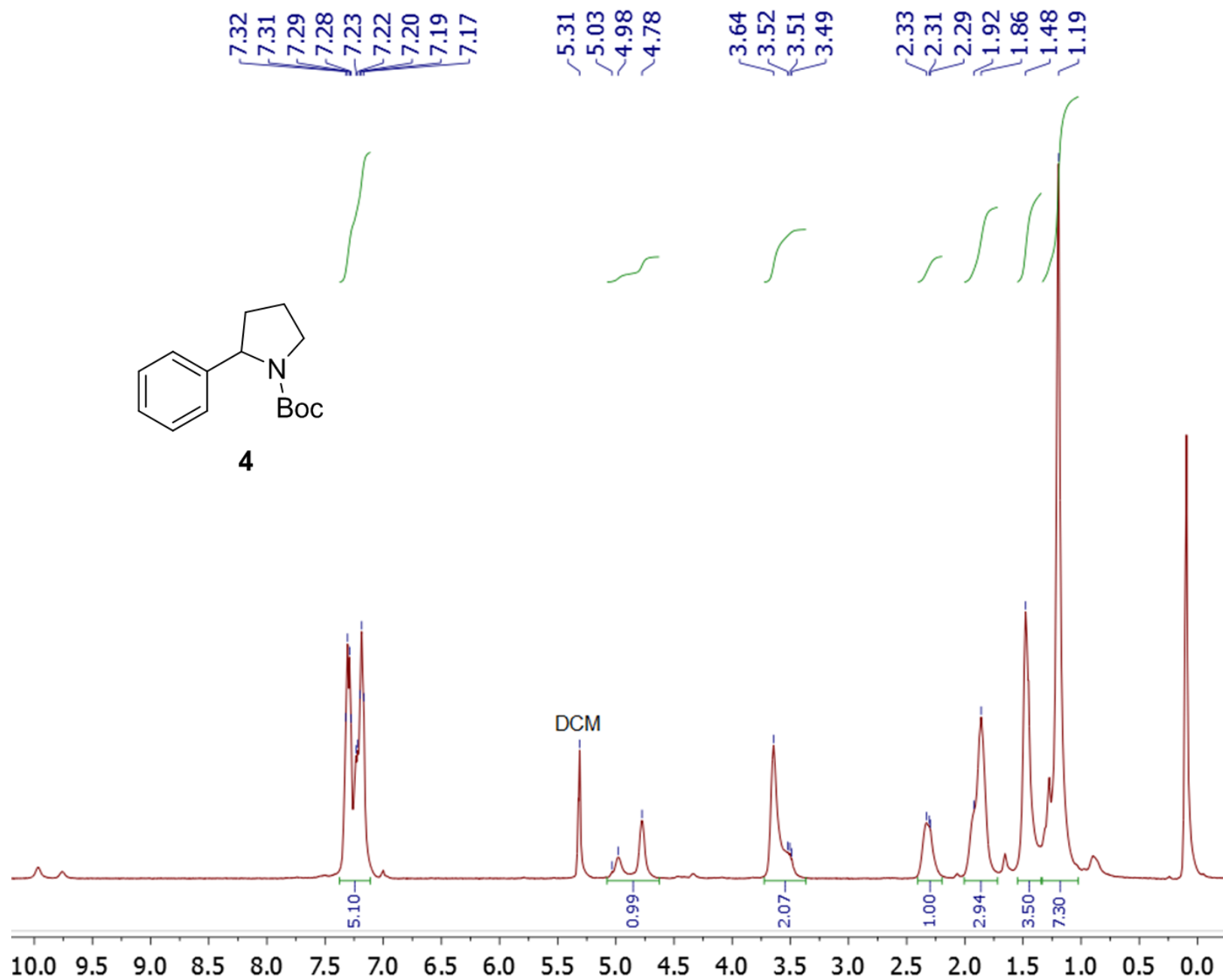
3m

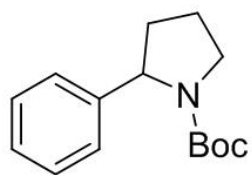




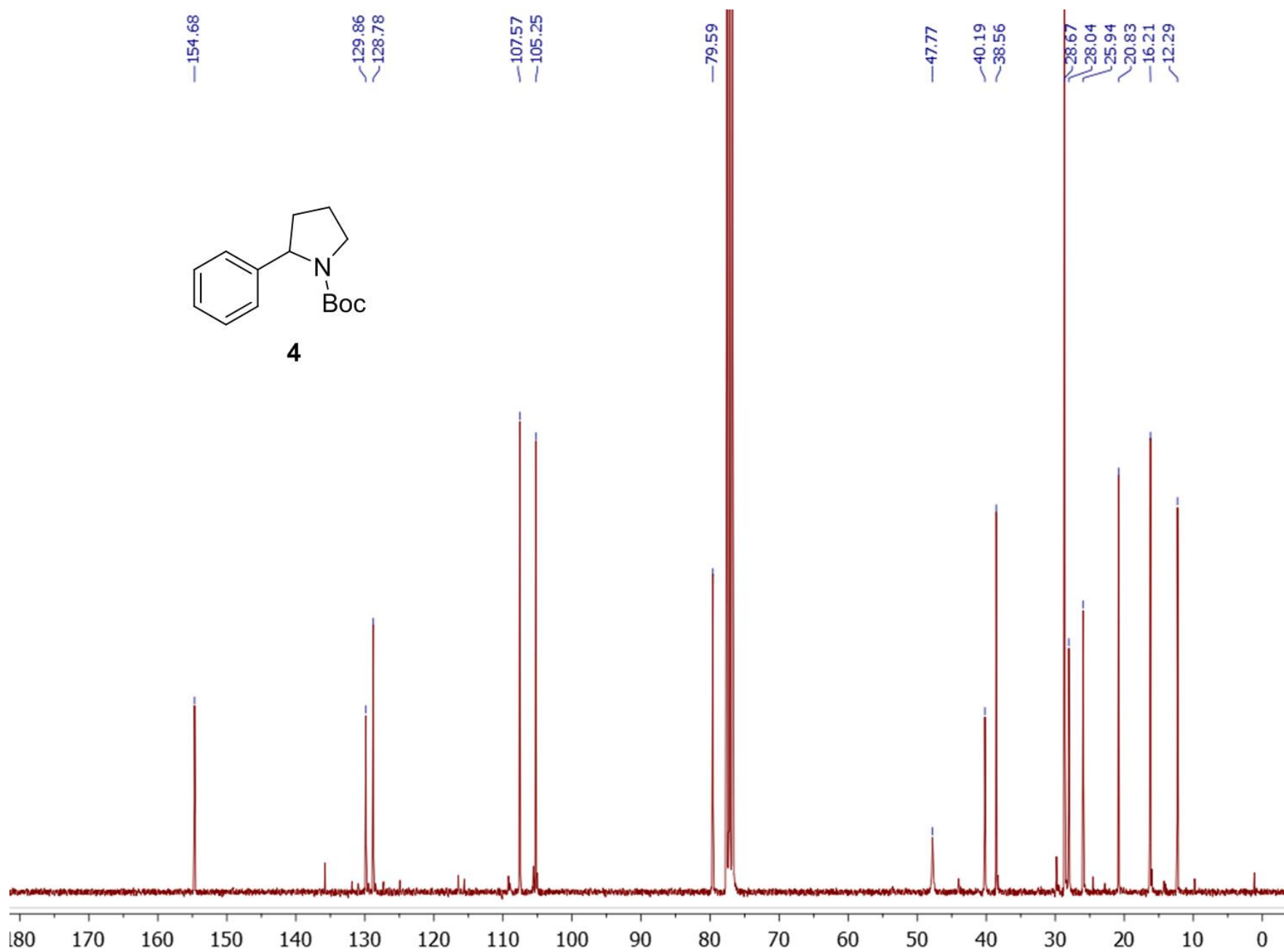


4





4

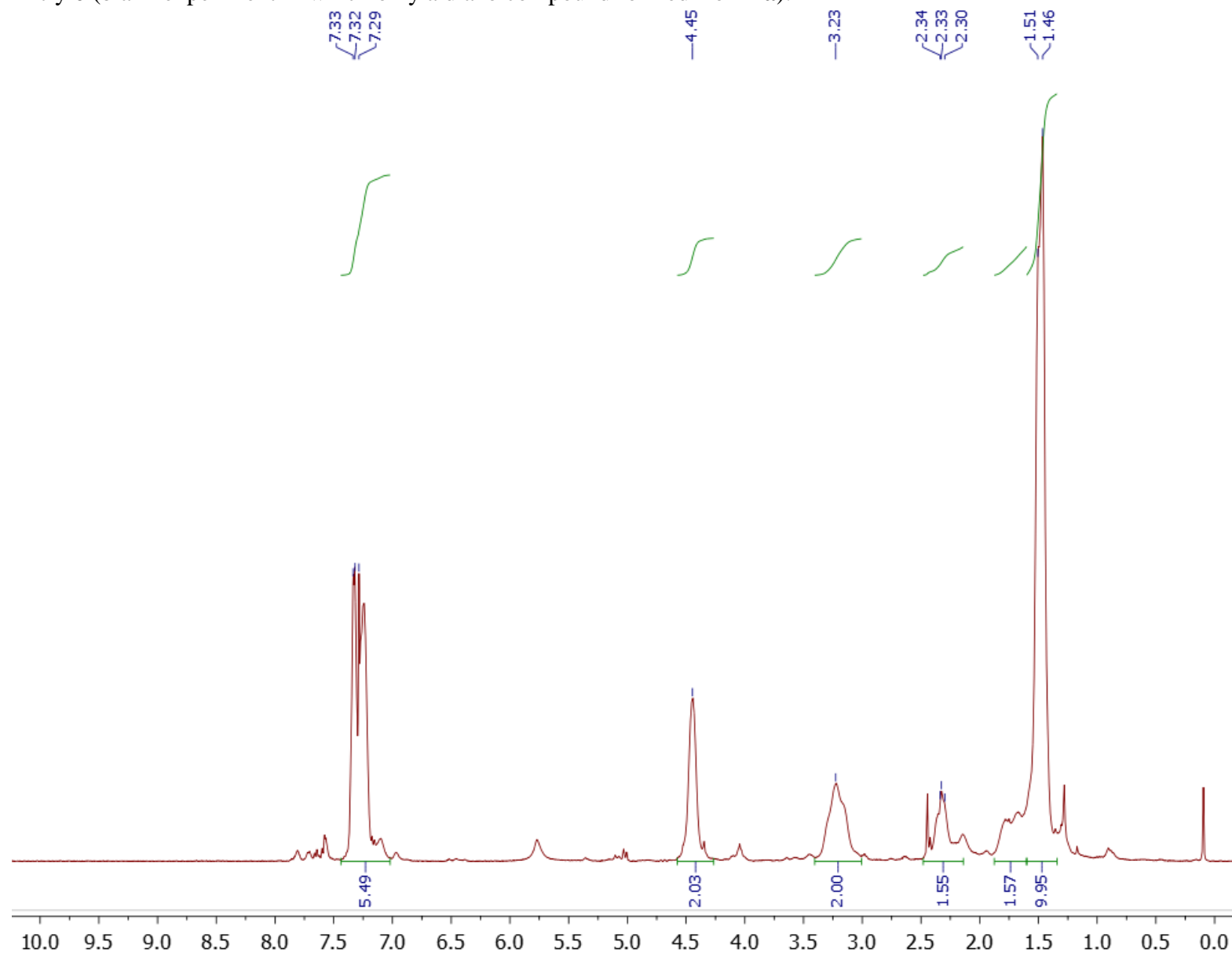


4.4 Copies of ¹H-NMR spectra of the conditions screening and experiments mentioned in the main text

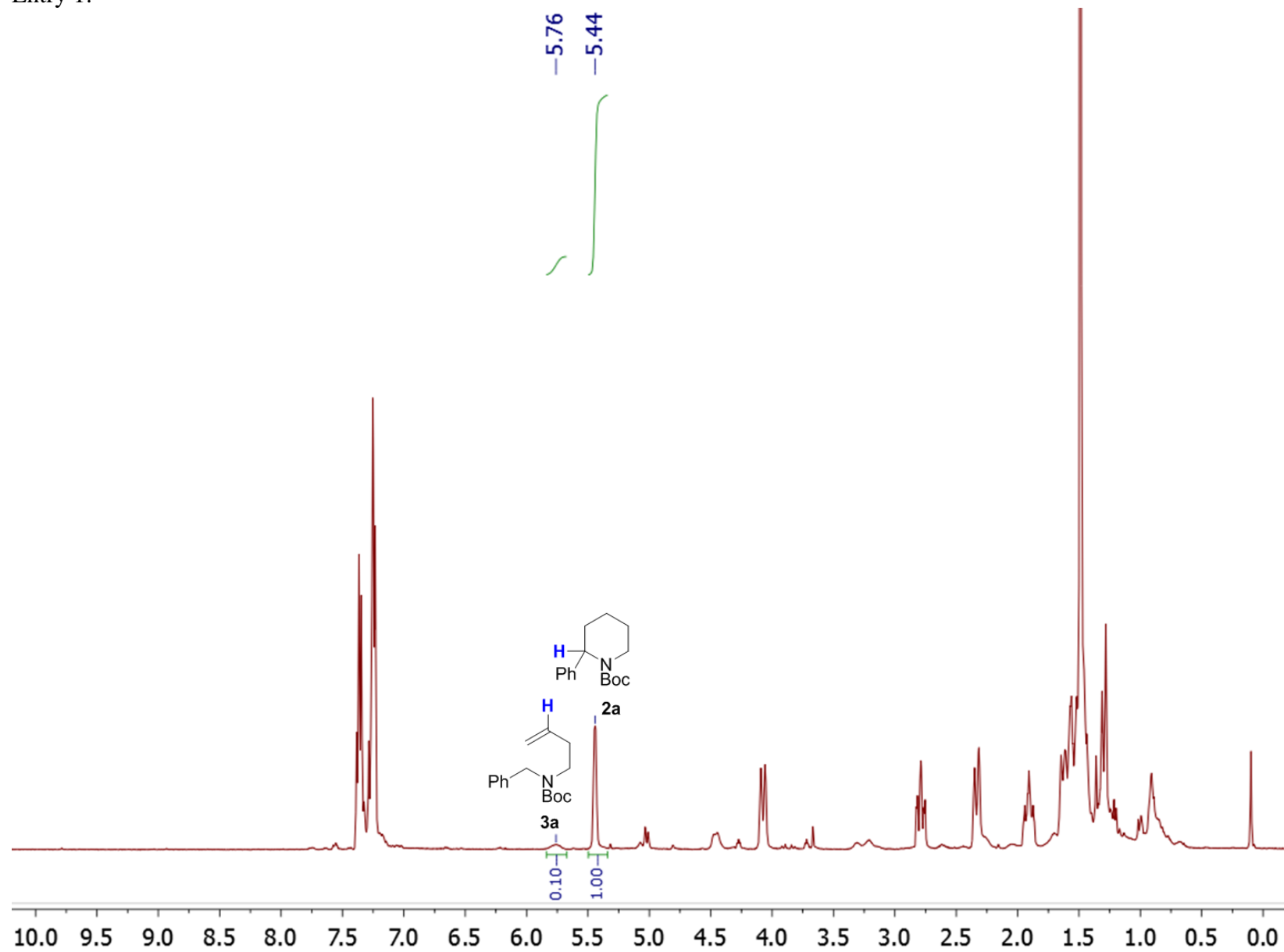
Copy of Table 1:

Entry	[Co(TPP)] (mmol)	<i>p</i> -TsNHNH ₂ (mmol)	Cs ₂ CO ₃ (mmol)	Solvent	Volume (mL)	Temperature (°C)	Time (h)	Yield (%)	Piperidine : alkene ratio
0 ^{a, b}	0	0.12	0.20	Benzene	2	60	24	0	N/A
1 ^a	0.005	0.12	0.20	Benzene	2	60	24	Quant.	1 : 0.10
2 ^a	0.005	0.12	0.20	Benzene	1	60	24	Quant.	1 : 0.08
3 ^a	0.015	0.12	0.20	Benzene	2	60	24	Quant.	1 : 0.14
4 ^a	0.005	0.15	0.20	Benzene	2	60	24	78	1 : 0.40
5 ^a	0.005	0.12	0.22	Benzene	2	60	24	92	1 : 0.42
6 ^a	0.005	0.12	0.20	Benzene	2	80	24	Quant.	1 : 0.28
7 ^a	0.005	0.12	0.20	Toluene	2	105	24	96%	1 : 0.59
8 ^{a, c}	0.005	0.12	0.20	Benzene	1	60	24	Quant.	1 : 0.07
9 ^a	0.005	0.12	0.20	<i>o</i> -dichlorobenzene	2	60	24	85%	1 : 0.11
10 ^a	0.005	0.12	0.20	Toluene	2	60	24	Quant.	1 : 0.51
11 ^a	0.005	0.12	0.20	Cyclohexane	2	60	24	85%	1 : 0.16

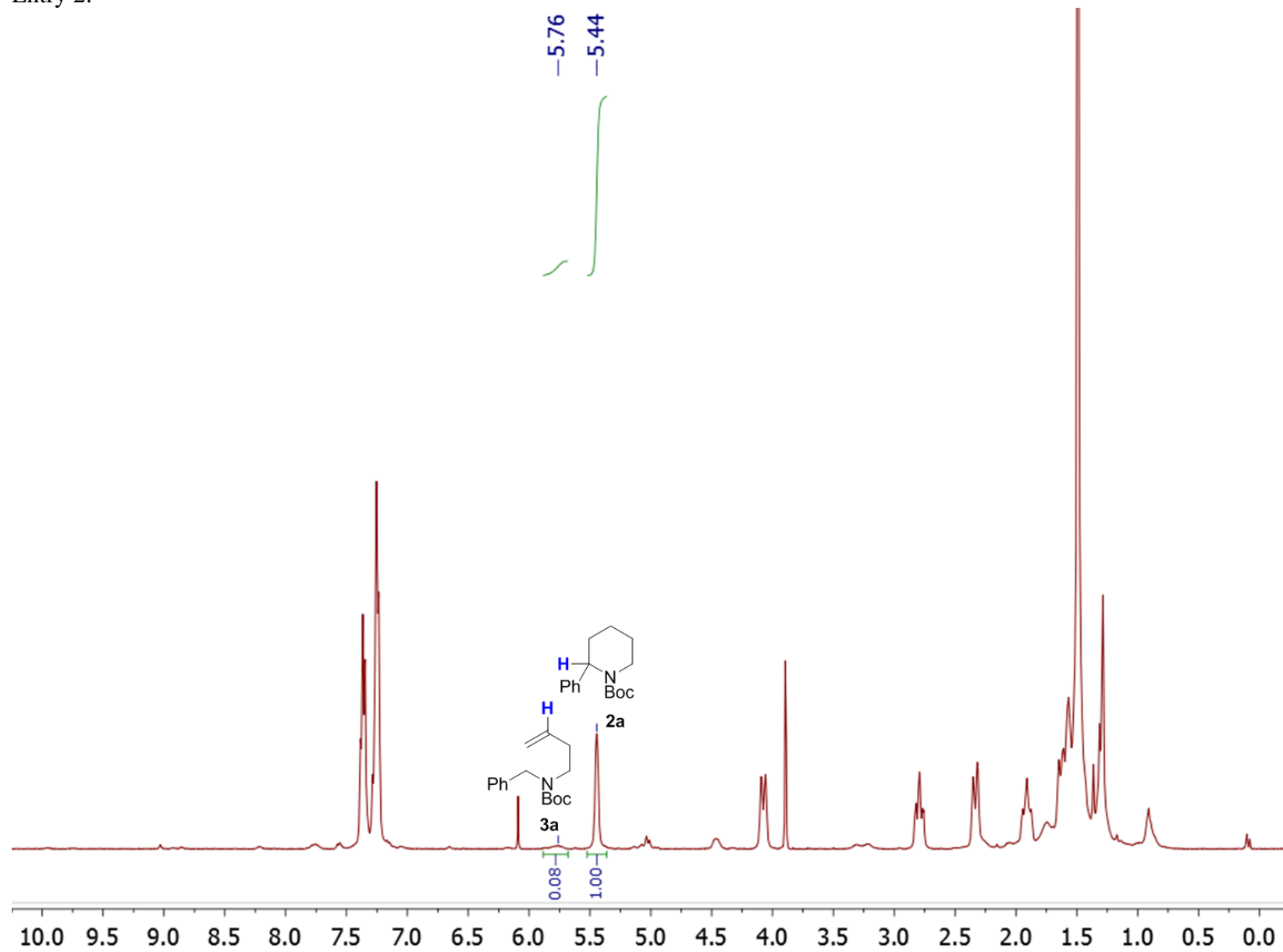
Entry 0 (blank experiment in which only a diazo compound formed from **1a**):



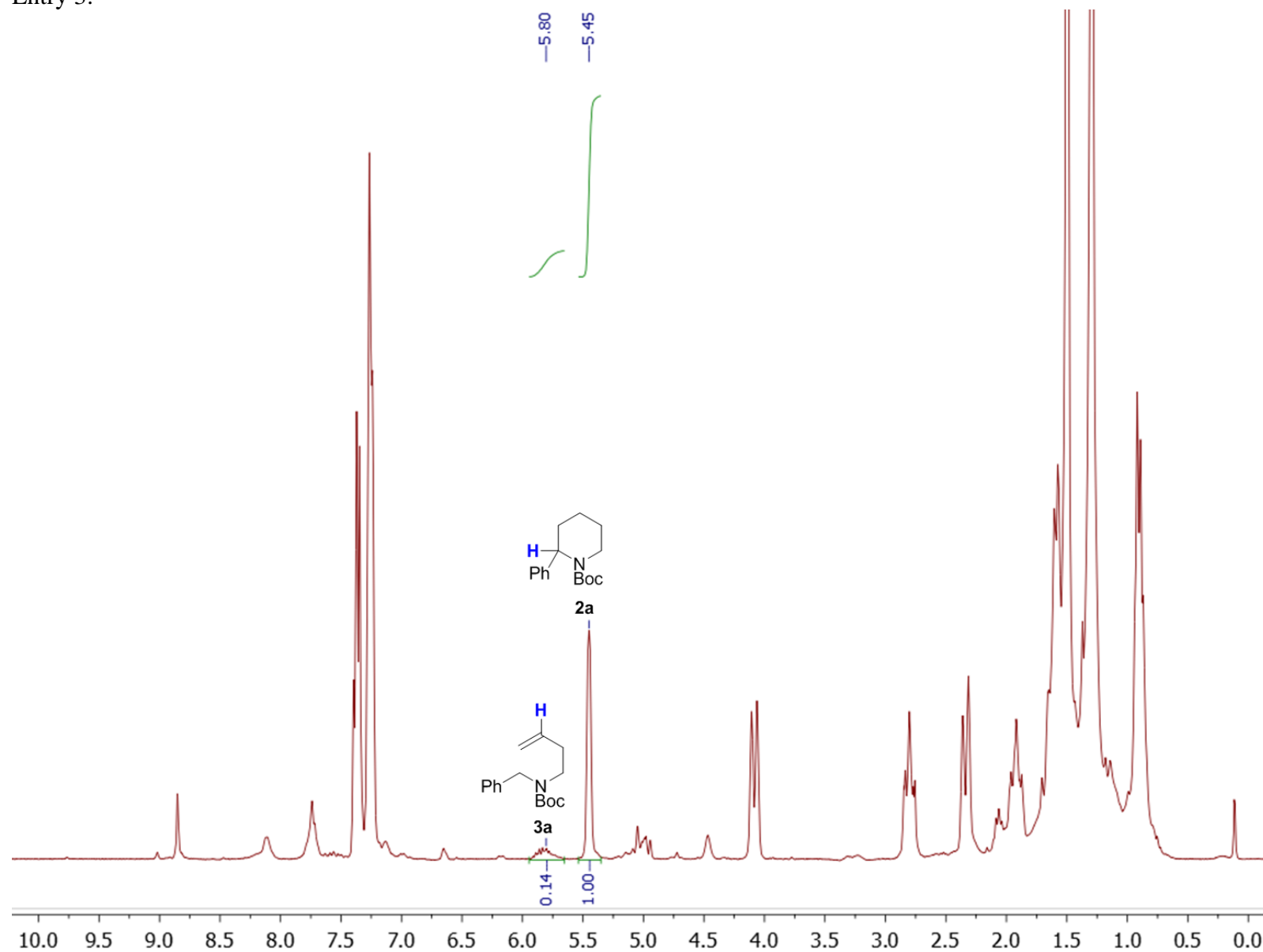
Entry 1:



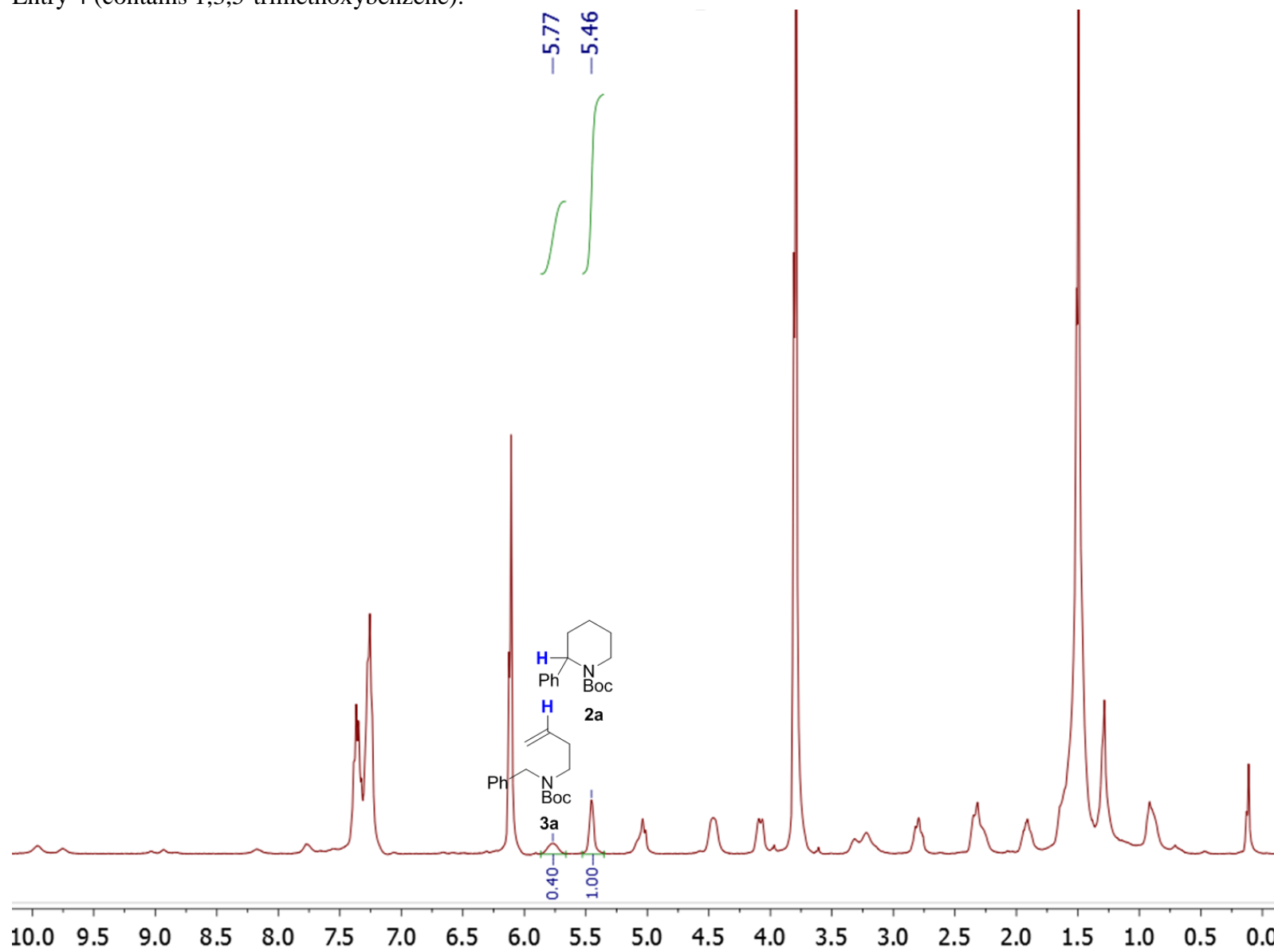
Entry 2:



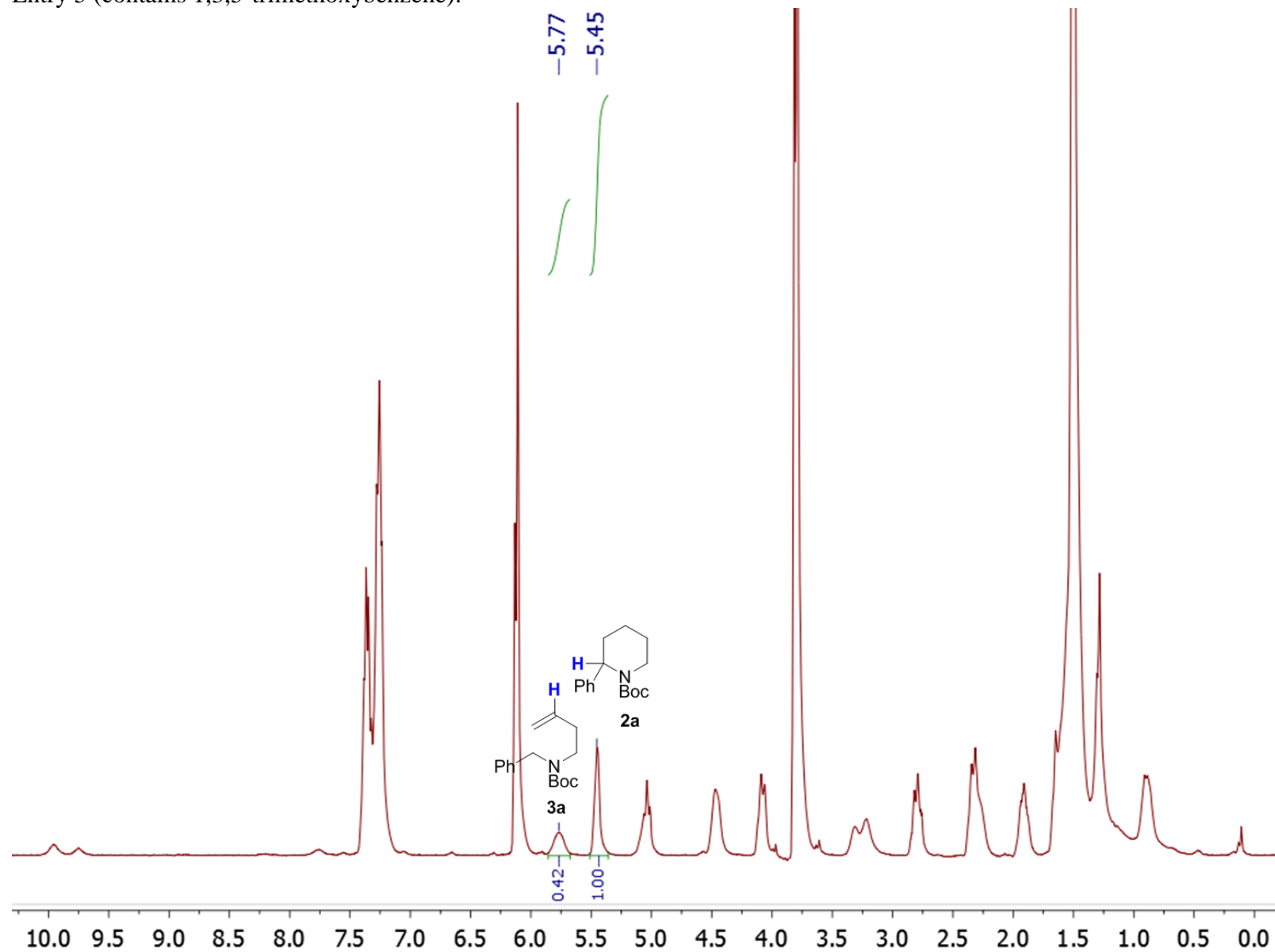
Entry 3:



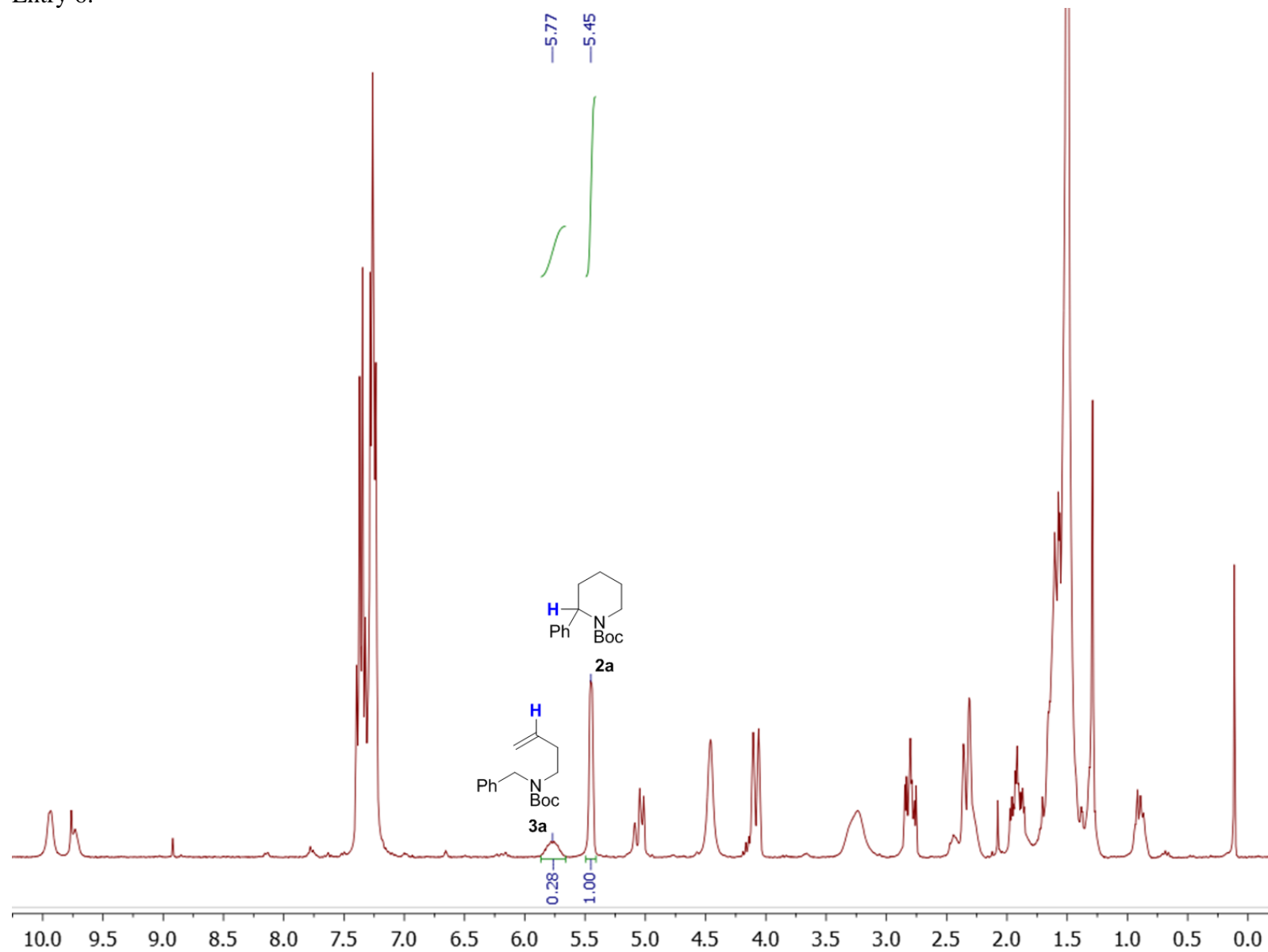
Entry 4 (contains 1,3,5-trimethoxybenzene):



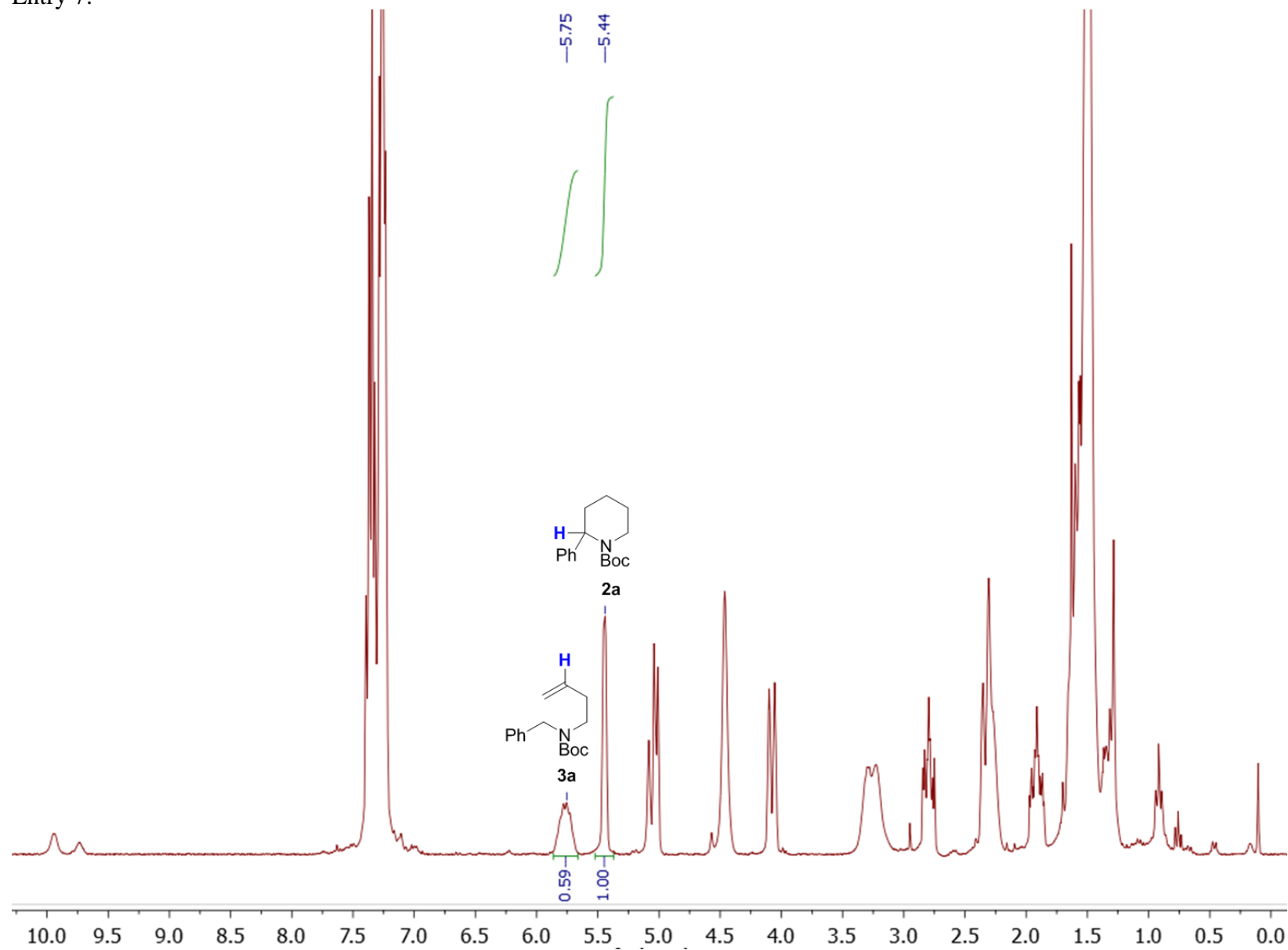
Entry 5 (contains 1,3,5-trimethoxybenzene):



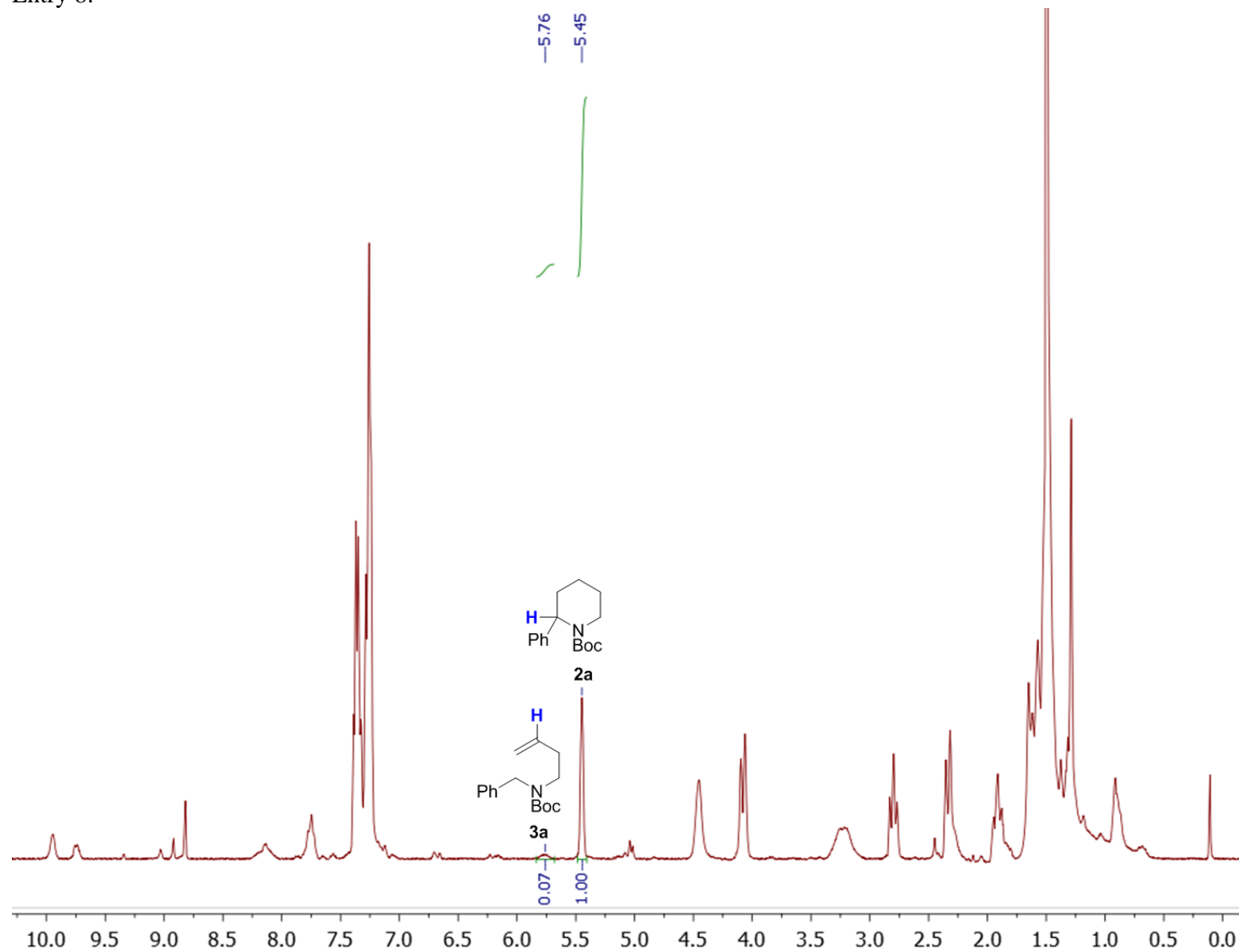
Entry 6:



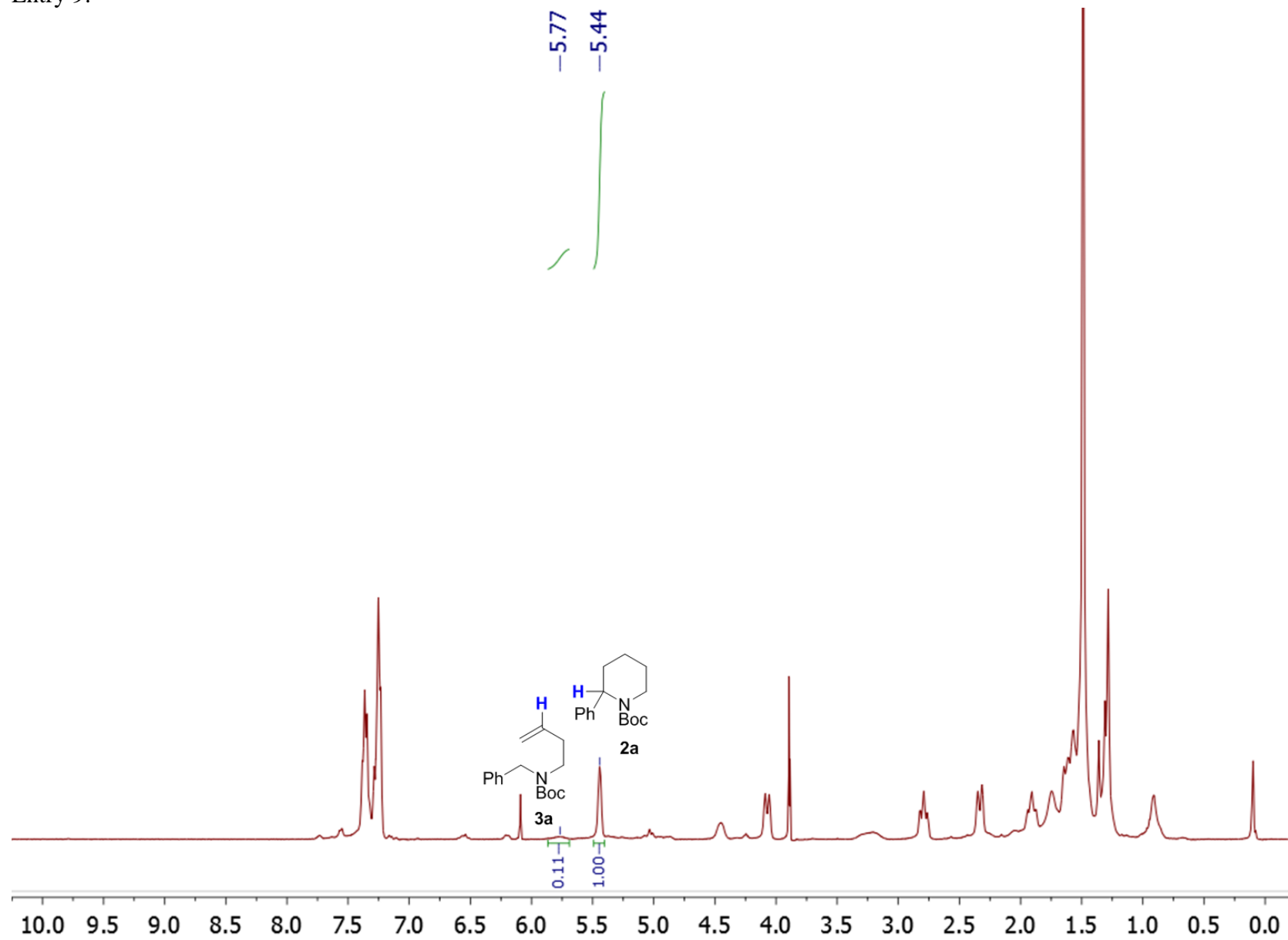
Entry 7:



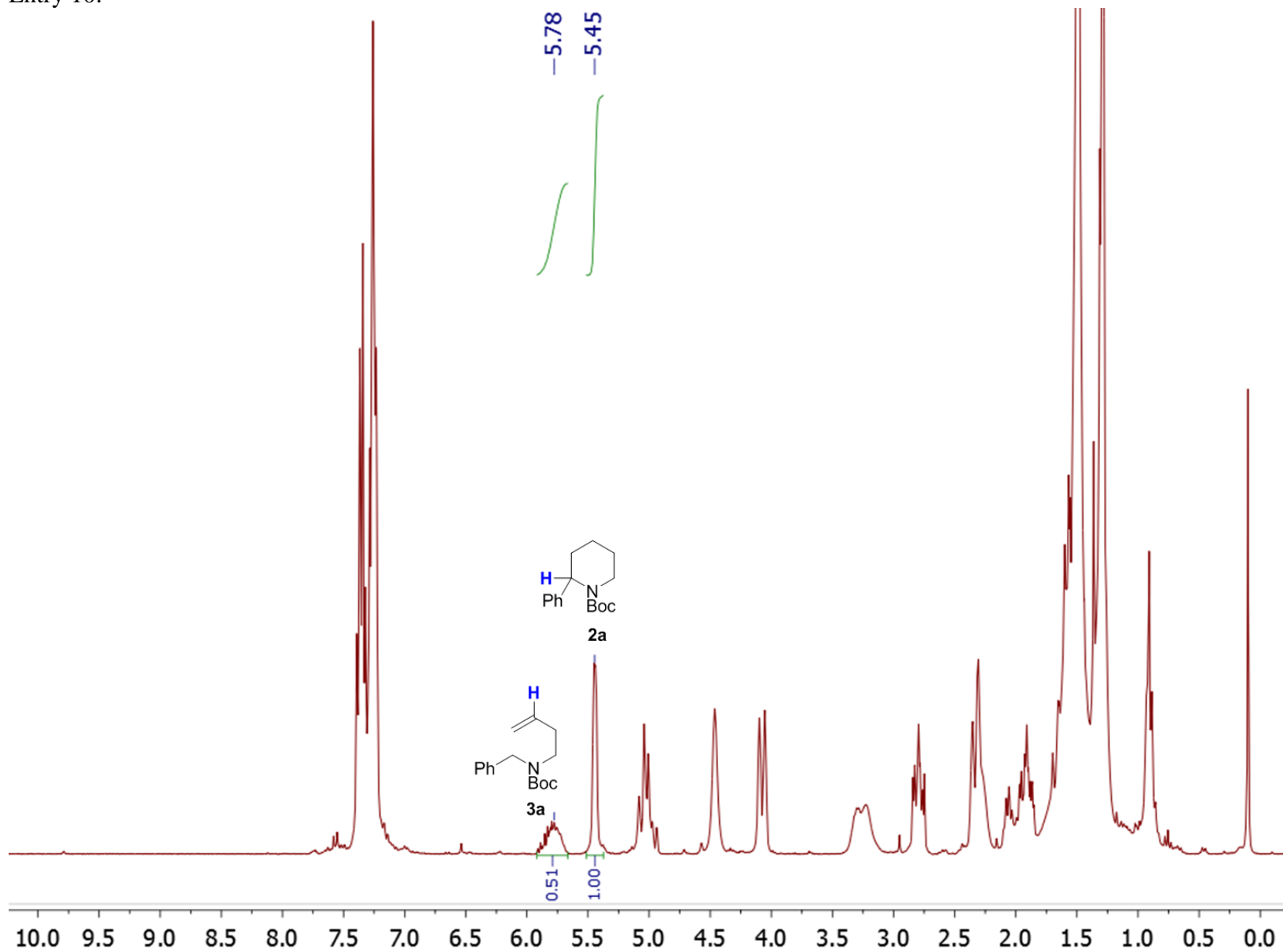
Entry 8:



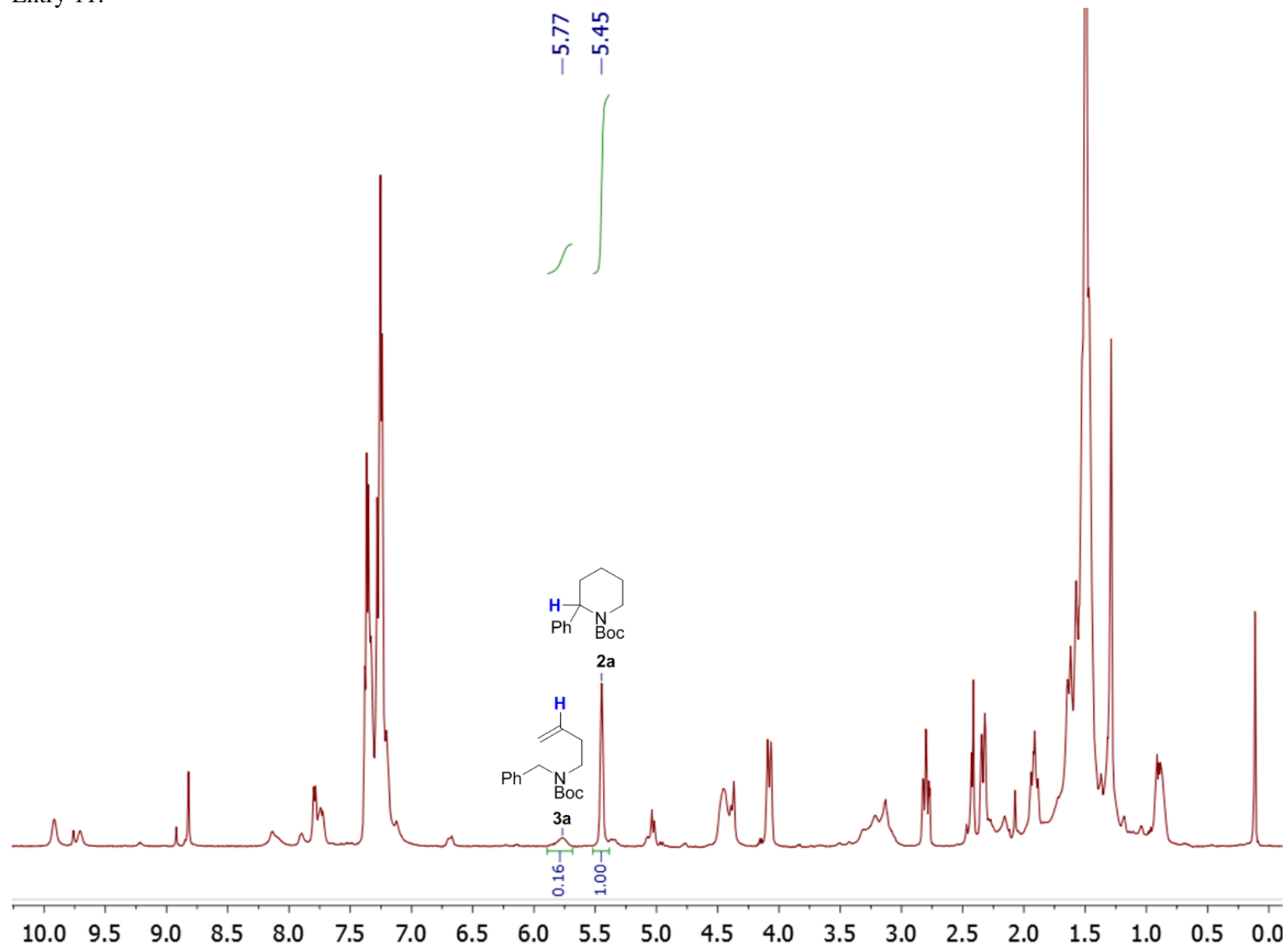
Entry 9:



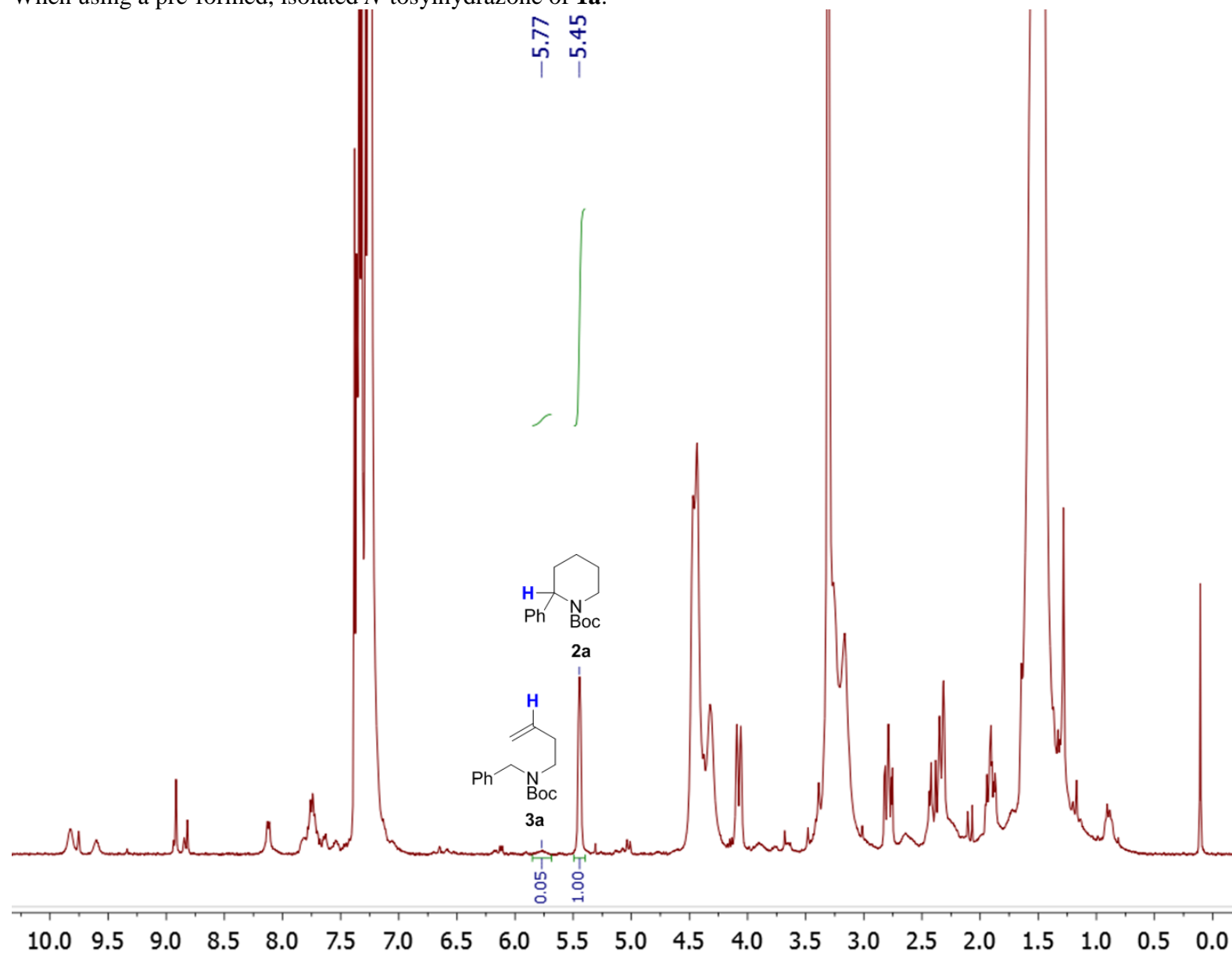
Entry 10:



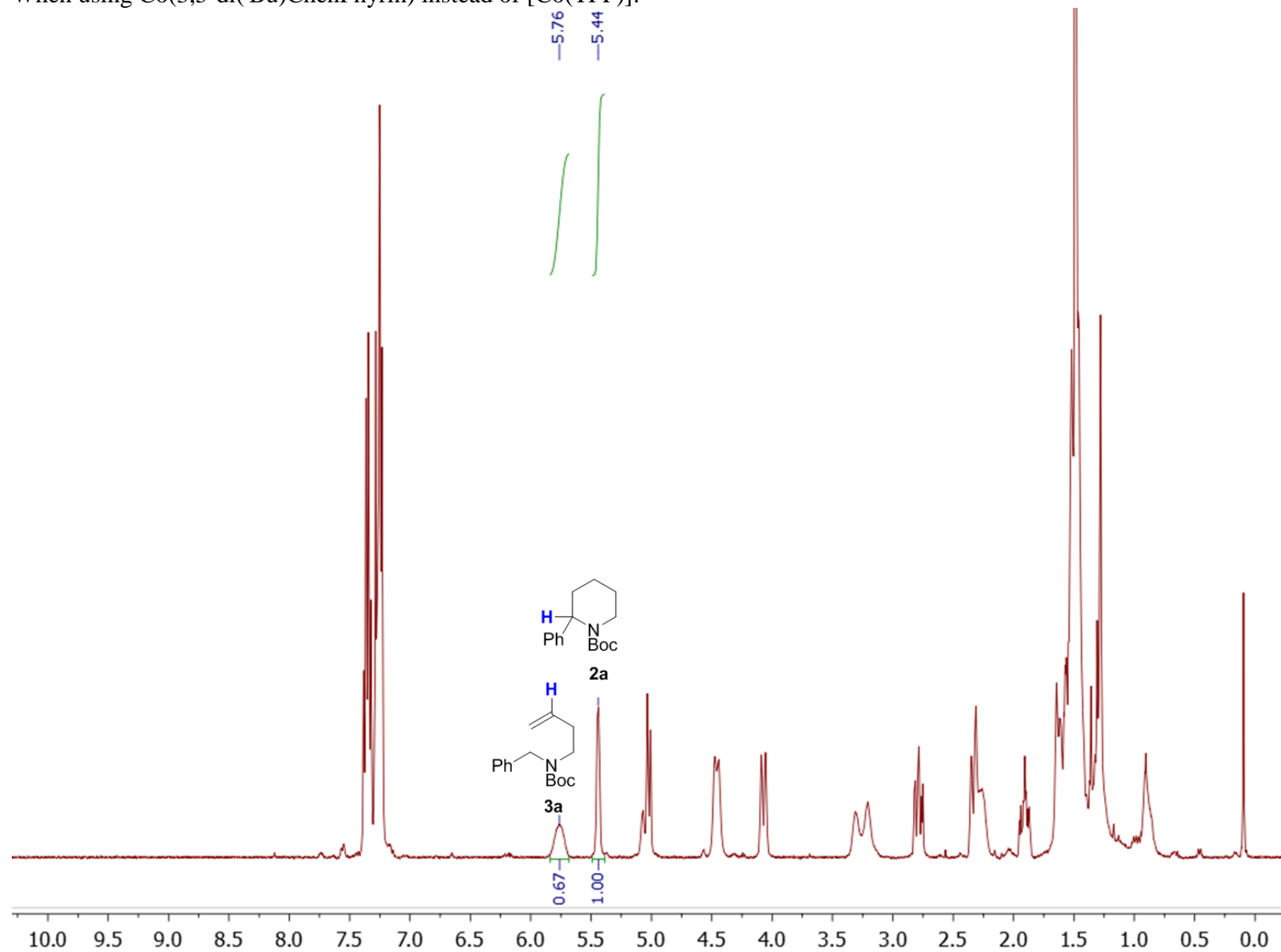
Entry 11:



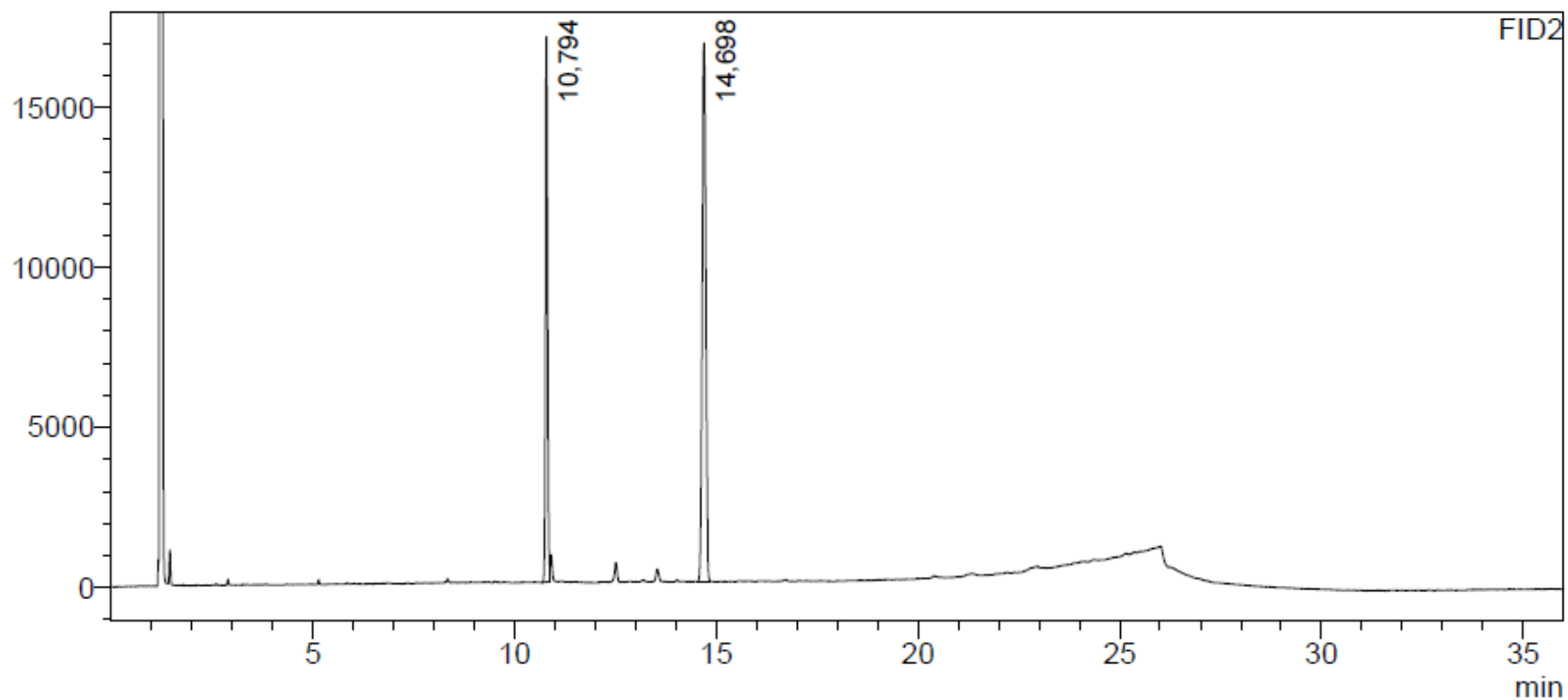
When using a pre-formed, isolated *N*-tosylhydrazone of **1a**:



When using Co(3,5-di(^tBu)ChenPyrin) instead of [Co(TPP)]:



Chromatogram of the reaction mixture obtained upon carrying out General Procedure B with **1a** with [Co(3,5-di(^tBu)ChenPhyrin)] instead of [Co(TPP)]. The products were obtained in 67% yield, in a **2a/3a** ratio of 1 : 0.7 and with an enantiomeric excess of 25%.



<Peak Table>

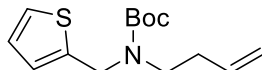
FID2

Peak#	Ret. Time	Area	Height	Conc.	Unit	Mark	Name
1	10,794	62324	17000	0,000			
2	14,698	104253	16816	0,000			
Total		166578	33816				

5. Control experiments

5.1 Addition of alkene **3h** to the reaction of aldehyde **1a**

To fully exclude the possibility that alkenes **3** could be converted to piperidines **2**, aldehyde **1a** was subjected to general procedure B in presence of an equimolar amount of alkene **3h**. From all alkenes formed from the substrates enumerated in Table 2, **3h** was selected based on its ¹H-NMR signature, which was most distinct from the ¹H-NMR signatures of **2a** and **3a**.



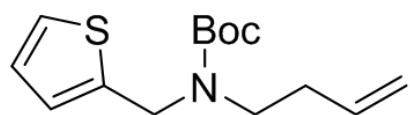
***N*-(thiophen-2-ylmethyl)-*N*-Boc-3-butenylamine (**3h**)**

2-(bromomethyl)thiophene was synthesized following the method of Gopalan and co-workers.^[12] To a suspension of NaH (90%, 171 mg, 6.4 mmol) in DMF (20 mL, Sigma Aldrich, dried over molecular sieves) was added 1-(Boc-amino)-3-butene (Sigma Aldrich, 1 g, 5.8 mmol) at room temperature. The resulting beige suspension was stirred for 40 min, during which only a minor amount of H₂(g) release was observed. Upon dropwise addition of freshly prepared 2-(bromomethyl)thiophene (1.14 g, 6.4 mmol), significant H₂(g) release was observed and the mixture was stirred overnight. The mixture was quenched with water (20 mL) and extracted into Et₂O (3 x 30 mL). The ether layers were dried over MgSO₄ and concentrated to yield pure **3h** as a dark red, brownish liquid (1.54 g, 90%).

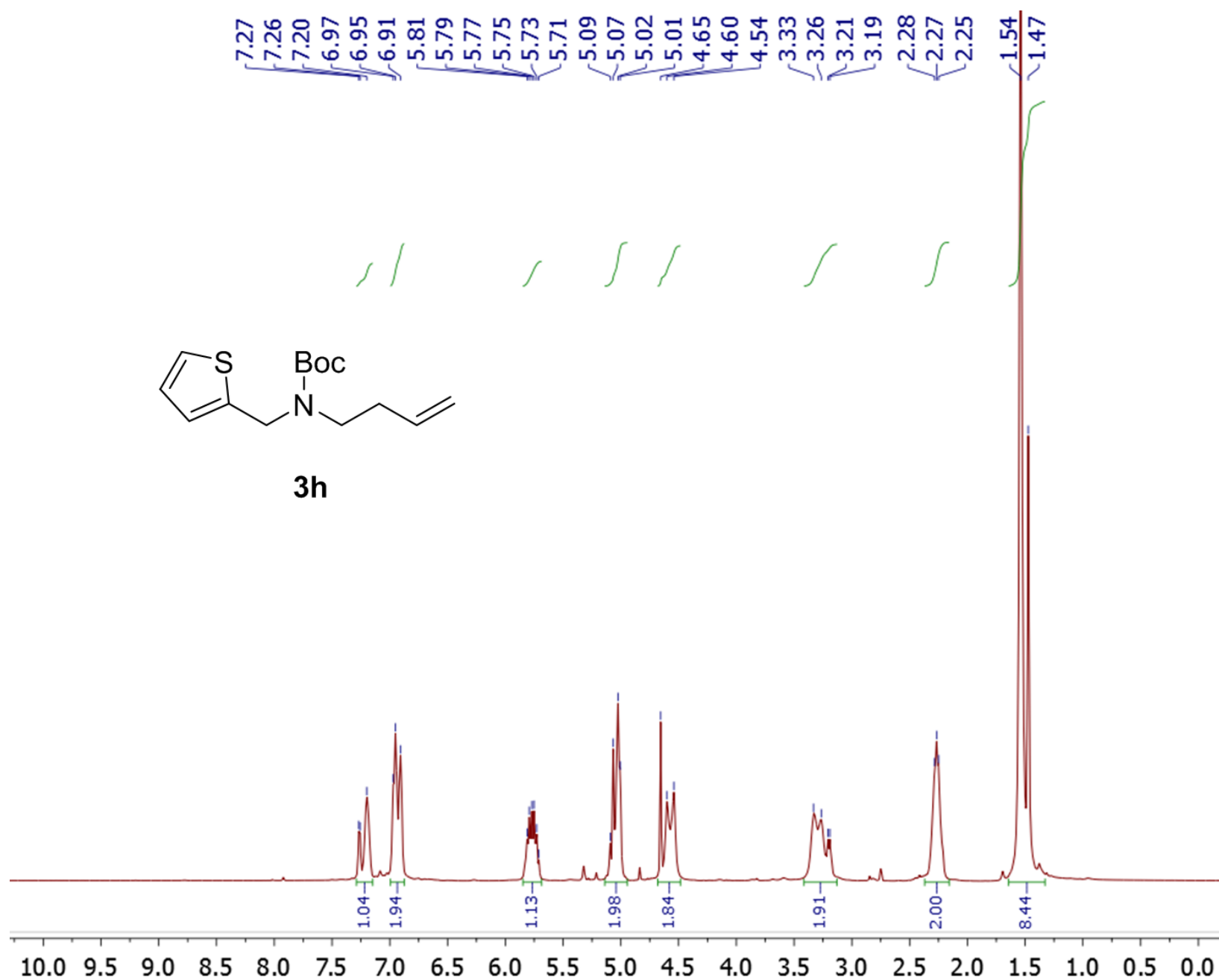
¹H NMR (400 MHz, CDCl₃) δ 7.29–7.15 (m, 1H), 6.99–6.88 (m, 2H), 5.85–5.68 (m, 1H), 5.14–4.94 (m, 2H), 4.68–4.48 (m, 2H), 3.41–3.13 (m, 2H), 2.37–2.16 (m, 2H), 1.64–1.32 (m, 9H).

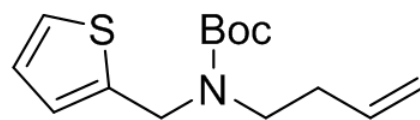
¹³C NMR (101 MHz, CDCl₃) δ 152.30, 151.54, 150.96, 138.25, 137.49, 132.16, 123.16, 123.07, 122.99, 122.42, 121.76, 112.96, 75.94, 75.76, 74.35, 62.27, 42.66, 42.36, 41.76, 36.50, 31.13, 29.77, 29.21, 25.01, 24.91.

HRMS (FD, m/z): Calculated for C₁₄H₂₁NO₂S: 267.1293, found: 267.1304.

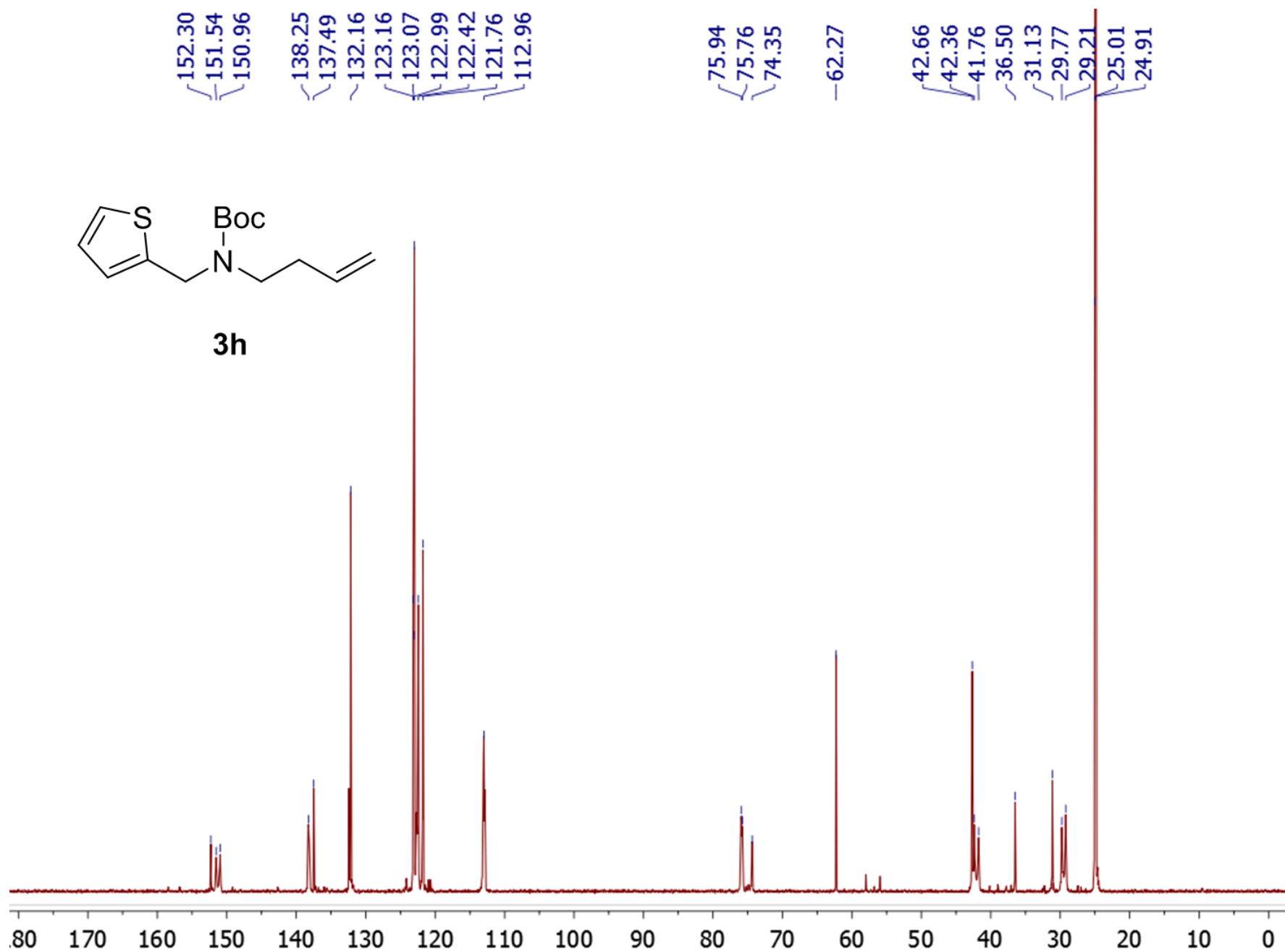


3h





3h

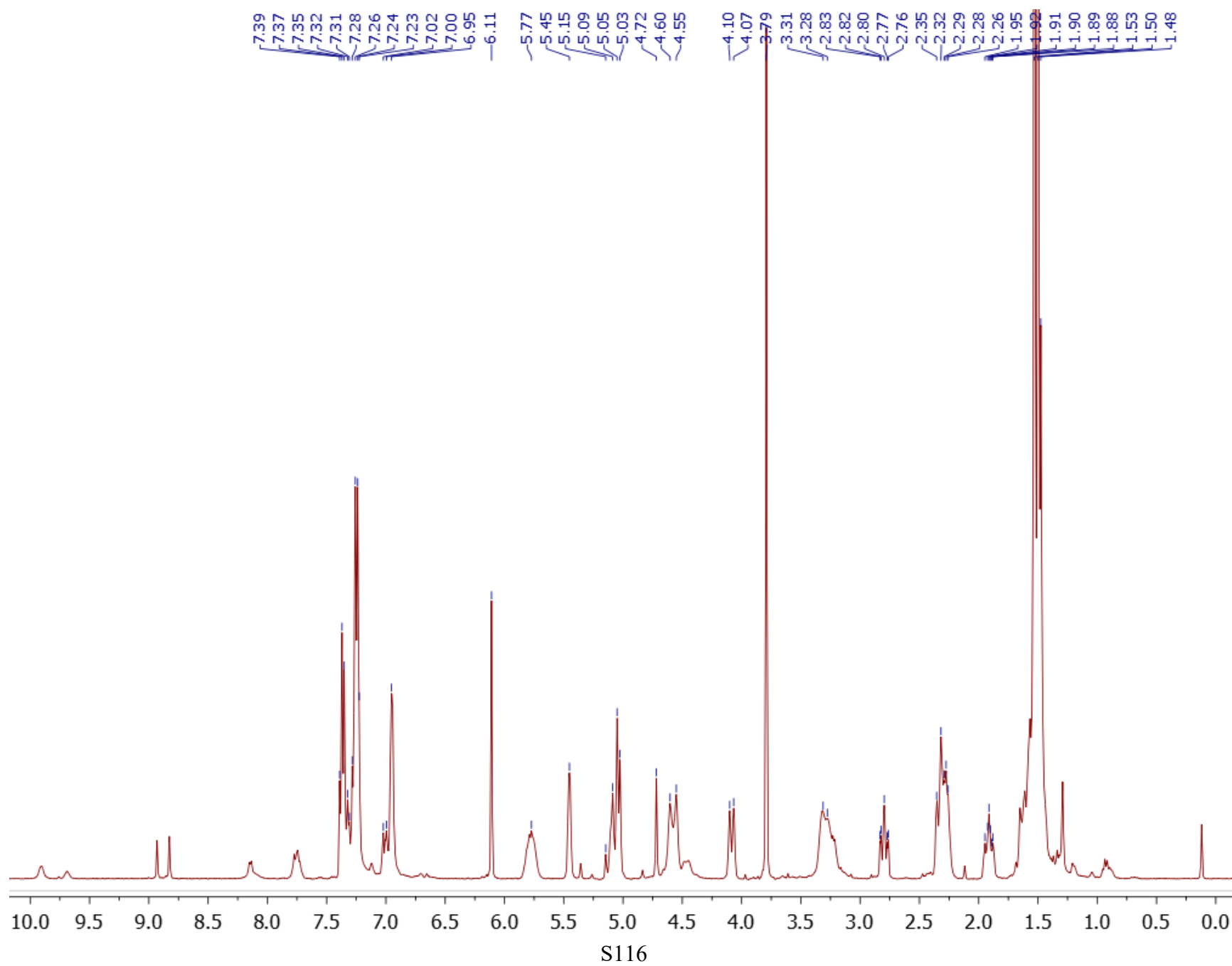


S114

Control experiment to investigate the possibility of conversion of alkenes **3** to piperidines **2**

Inside a nitrogen-filled glove box, an oven-dried 4 mL vial fitted with an oven-dried Teflon-coated stir bar was charged with [Co(TPP)] (0.005 mmol, 3.4 mg), *p*-TsNHNH₂ (0.12 mmol, 22.3 mg), Cs₂CO₃ (0.20 mmol, 65.2 mg) and 1,3,5-trimethoxybenzene (4.3 mg, 0.026 mmol). The liquid aldehyde **1a** (27.7 mg, 0.1 mmol) and alkene **3h** (26.7 mg, 0.1 mmol) were pre-weighed into 1 mL syringes and then weighed into the tared vial by careful deposition onto the inner rim of the vial, thereby avoiding direct solid-liquid contact between the powders and the substrate. Then benzene (2 mL) was quickly added. The vial was tightly capped with a screw cap fitted with a PTFE-faced silicone septum, immediately brought to a pre-heated 60°C metal plate and stirred at 1100 rpm for 24h. The reaction mixture was filtered over a frit to remove the fine powders, which would reduce NMR resolution.

¹H NMR spectroscopy (CDCl₃, below) showed that no piperidine **2h** had formed from alkene **3h** under the reaction conditions; if that had been the case, piperidine **2h** should have been visible at 5.59 ppm. Instead, only signals belonging to **2a**, **3a** and **3h** are visible. For the NMR signatures of **2a** and **3a**, see sections 4.2 and 4.3. For the NMR signature of **3h**, see above. Alkenes **3a** and **3h** overlap under the ¹H multiplet at 5.85–5.68 ppm.



5.2 Monitoring the conversion of **1a** to **2a** and **3a** over time by ¹H-NMR

First, any influence of 1,3,5-trimethoxybenzene on the yield or product ratio was excluded by carrying out General procedure B with substrate **1a** in presence of 1,3,5-trimethoxybenzene (6.7 mg, 0.04 mmol).

Inside a nitrogen-filled glove box, a flame-dried 50 mL Schlenk tube fitted with an oven-dried Teflon-coated oval stir bar was charged with [Co(TPP)] (34 mg, 0.05 mmol), *p*-TsNHNH₂ (223 mg, 1.2 mmol), Cs₂CO₃ (652 mg, 2 mmol) and 1,3,5-trimethoxybenzene (23.6 mg, 0.14 mmol). The liquid aldehyde **1a** (277 mg, 1 mmol) was pre-weighed into a 1 mL syringe and then weighed into the tared Schlenk tube by careful deposition onto the inner rim of the neck, thereby avoiding direct solid-liquid contact between the powders and the substrate. Then C₆D₆ (10 mL) was quickly added, the Schlenk tube was closed with a septum and immediately brought to a pre-heated 60 °C oil bath and stirred at 830 rpm. Samples (0.6 mL) were taken by syringe after 0.5, 1, 2, 3, 4, 5, 6, 8, 9, 10, 11, 12 and 13 hours. Each sample was filtered over a syringe filter containing a hydrophobic PTFE membrane (Ø13 mm, pore size 0.45 µm) to remove the fine powders, which would reduce NMR resolution.

In C₆D₆, the chemical shifts of certain peaks of **2a** and **3a** shifted (vs. their chemical shift in CDCl₃), probably due to anisotropic ring current and π-stacking of benzene with the phenyl ring of the products. In C₆D₆, the 1H peak of the proton of the central tertiary carbon of **2a** and the 1H peak of RCH=CH₂ of **3a** overlap under the broad signal at 5.75 ppm. To account for this, the concentration (mM) of the products was calculated as follows:

$$[\text{piperidine}] = 3 \cdot (Y - (X/2)) \cdot [\text{standard}] \cdot 1000$$

$$[\text{alkene}] = 3 \cdot (X/2) \cdot [\text{standard}] \cdot 1000$$

in which:

X = the integral of the multiplet at 5.12–4.97 ppm (which still corresponds to RCH=CH₂, as in CDCl₃)

Y = the integral of the broad singlet at 5.75 ppm

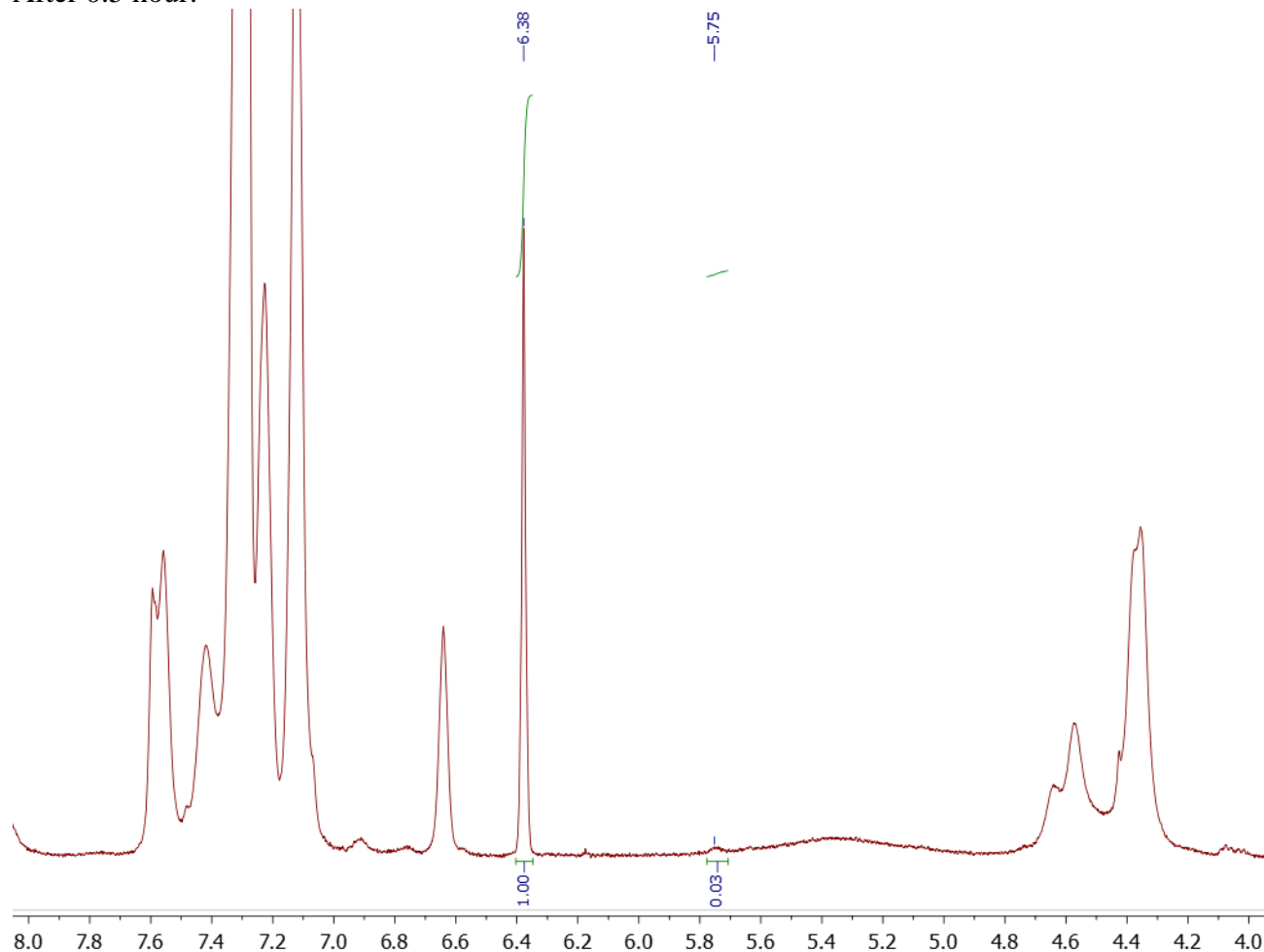
$$[\text{standard}] = 0.14 \text{ mmol} / 10 \text{ mL C}_6\text{D}_6 = 0.014 \text{ M}$$

The integral of the three aromatic protons of 1,3,5-trimethoxybenzene, which shows at 6.38 ppm in C₆D₆, was set at 1H.

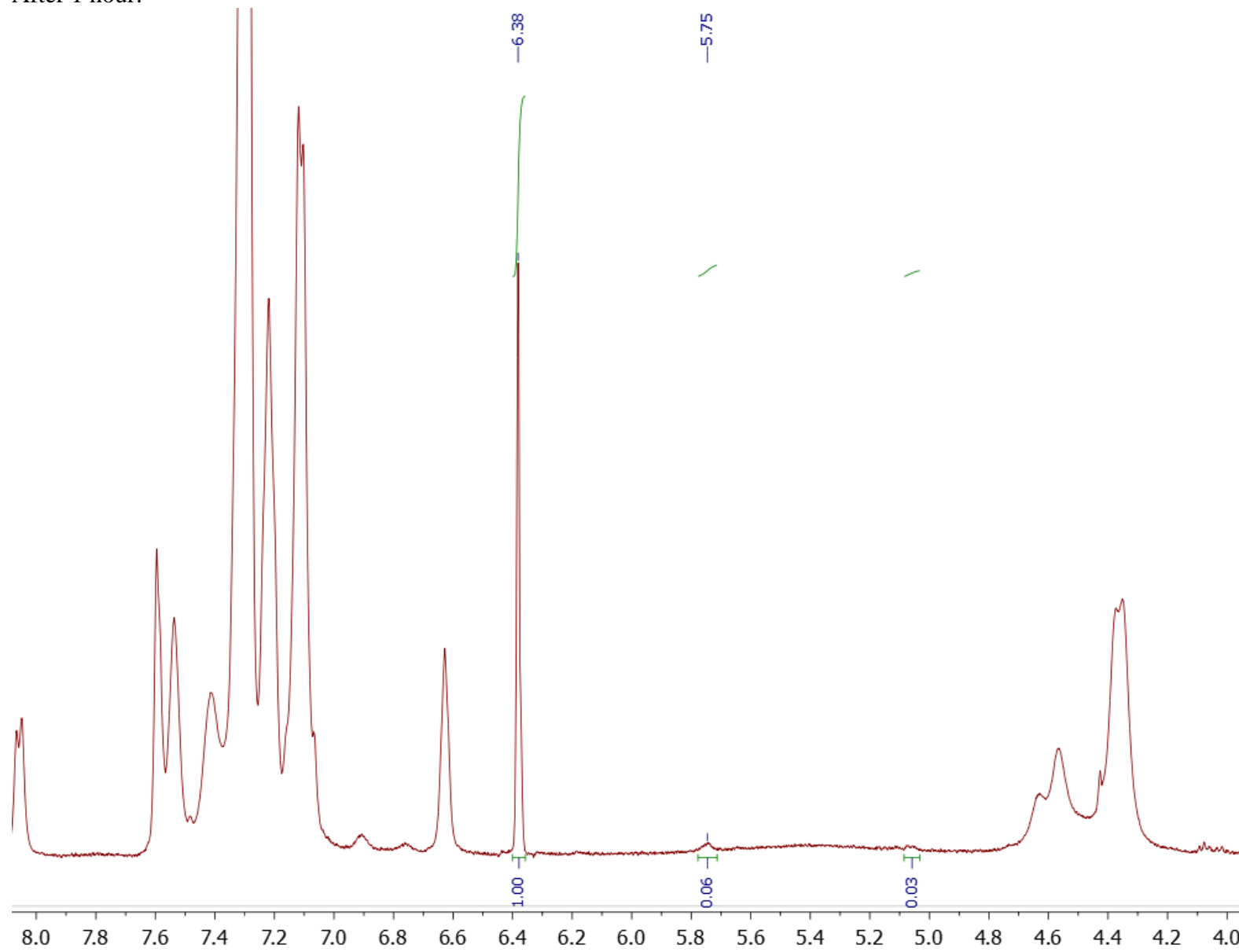
5.3 Copies of the ^1H -NMR spectra of the monitoring experiments

Note: the spectra recorded between 0,5 and 6 hours show shifting of a broad signal, which could correspond to the weighted average of free and coordinated NH_2NHTs (or water, or something else). In the spectra recorded after 4 and 5 hours this broad band complicated proper integration of the alkene and piperidine peaks.

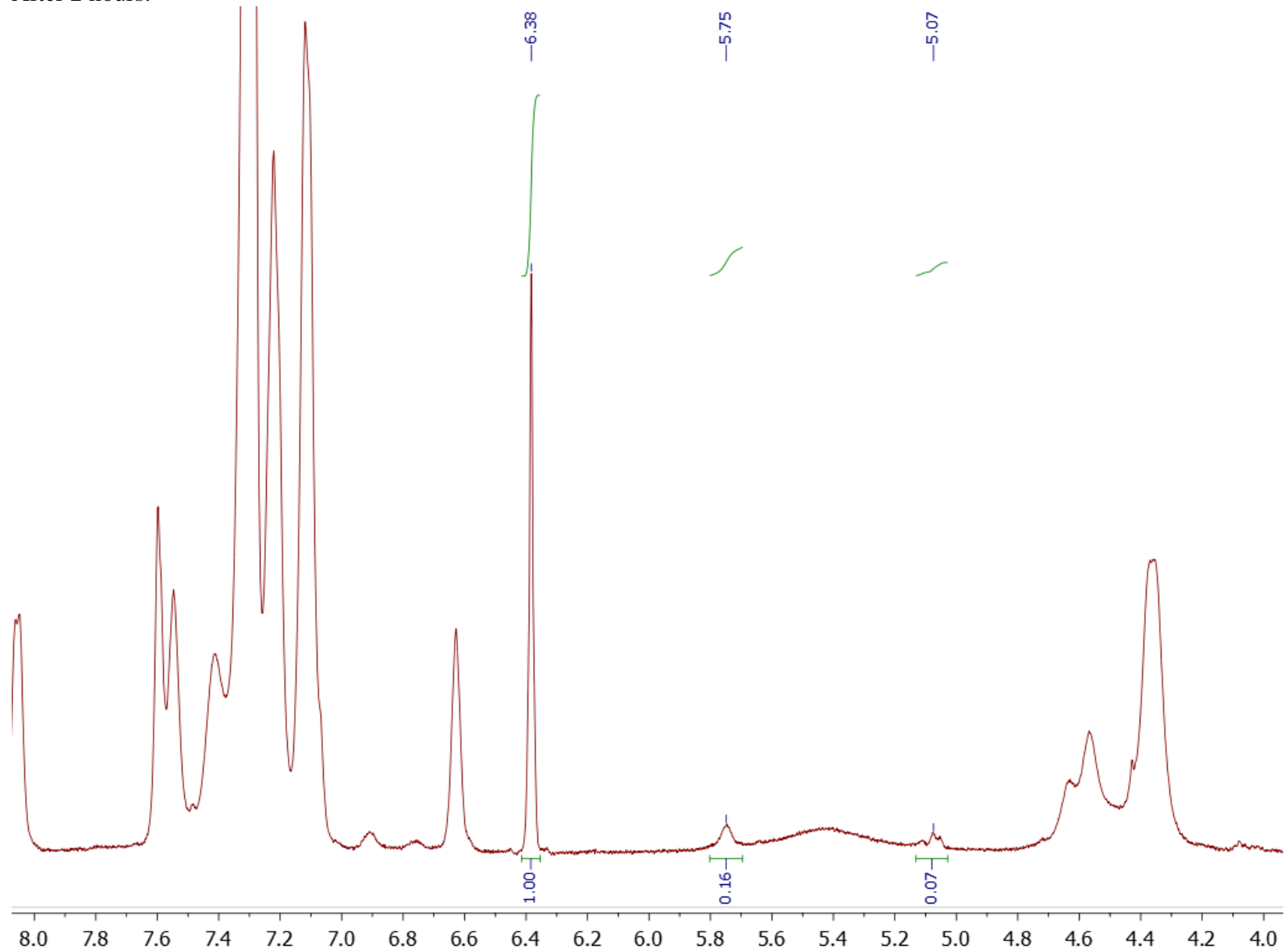
After 0.5 hour:



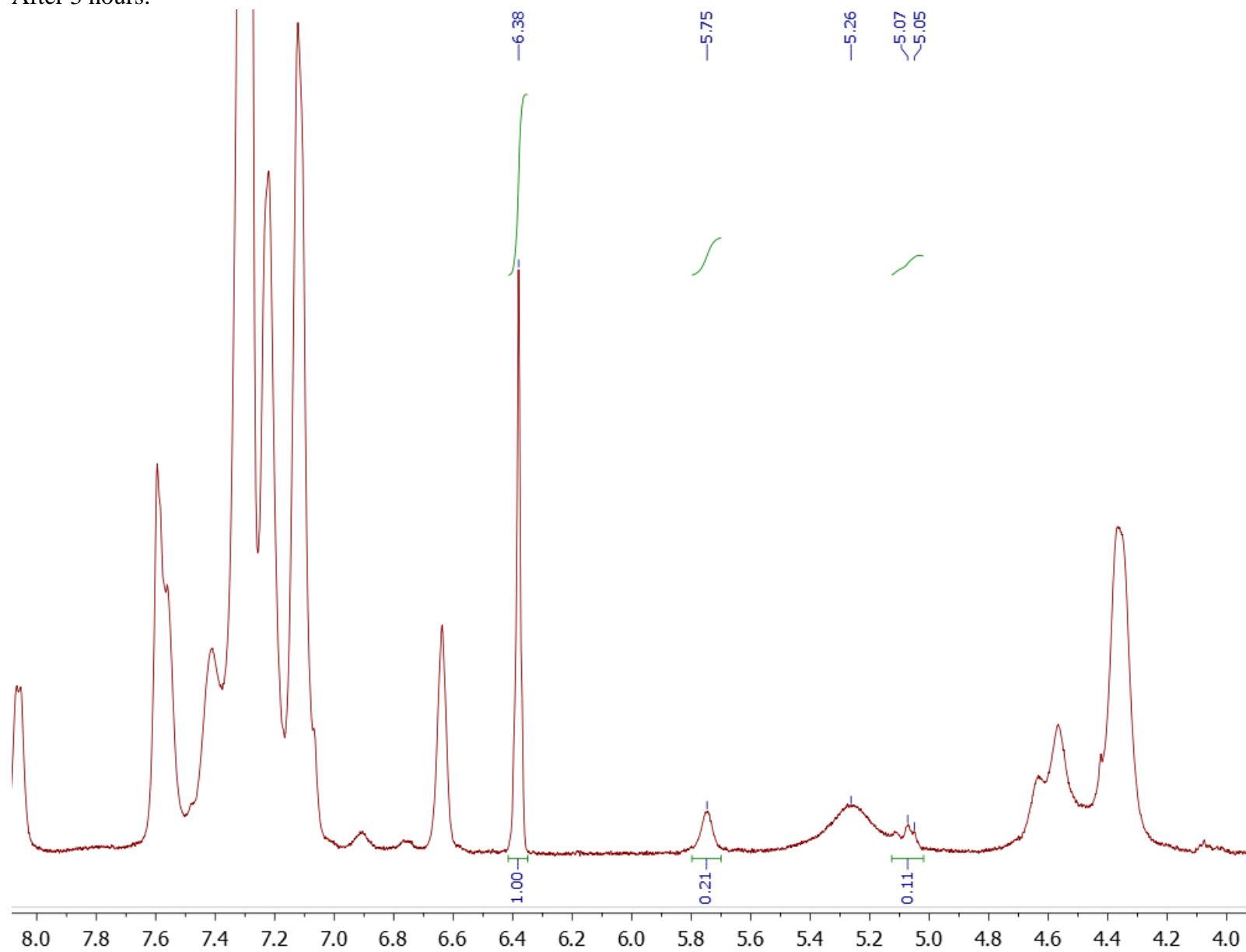
After 1 hour:



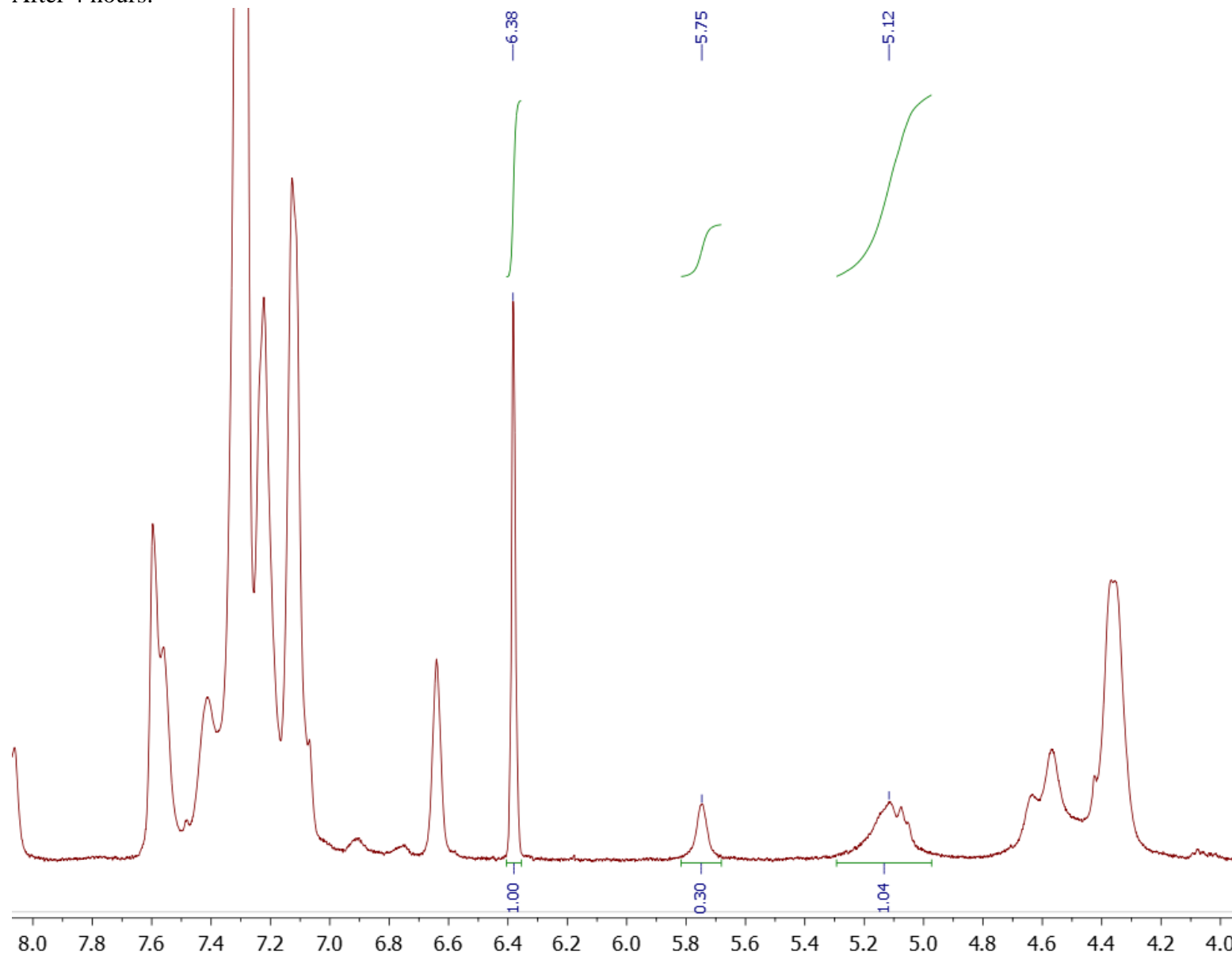
After 2 hours:



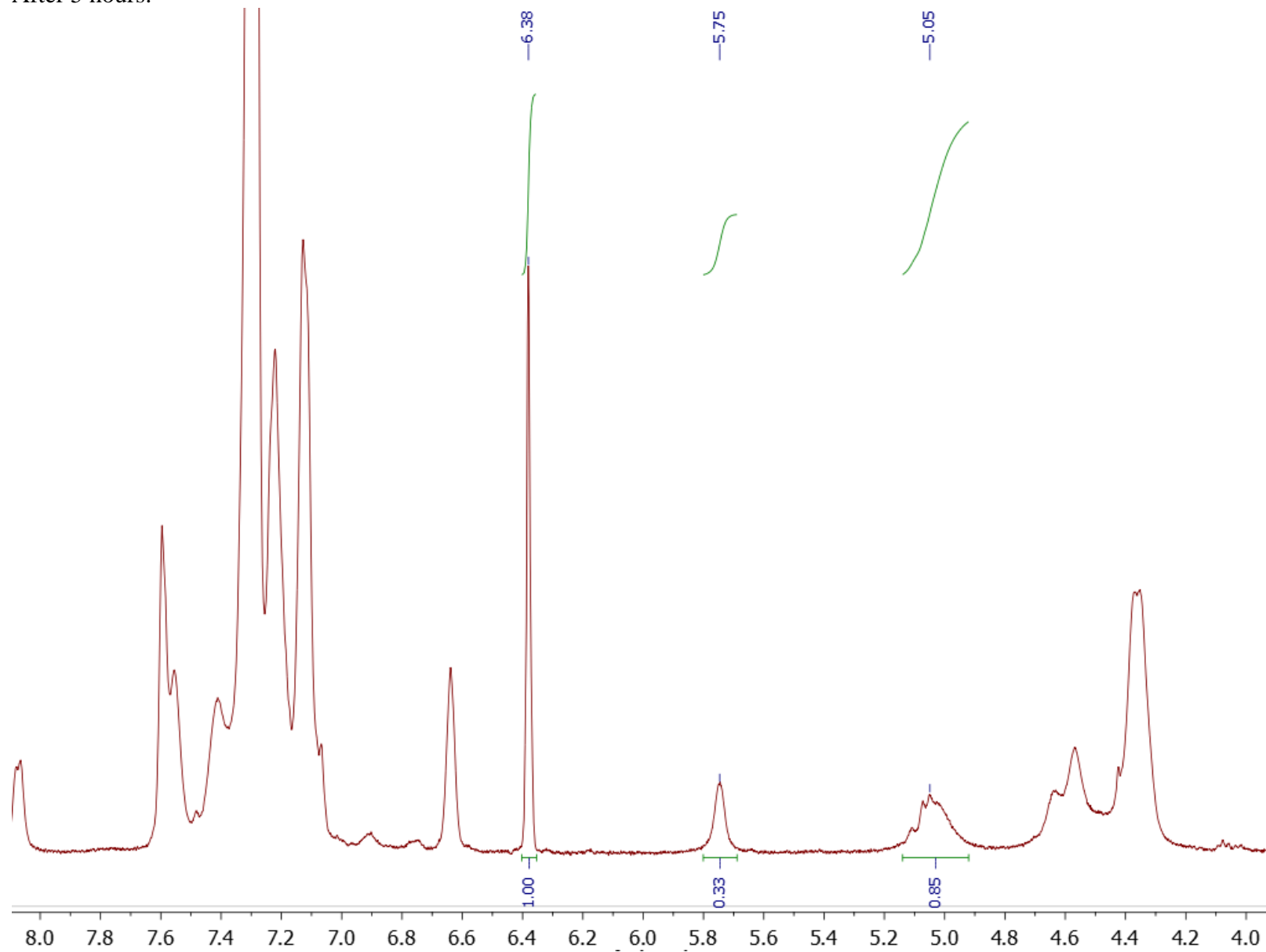
After 3 hours:



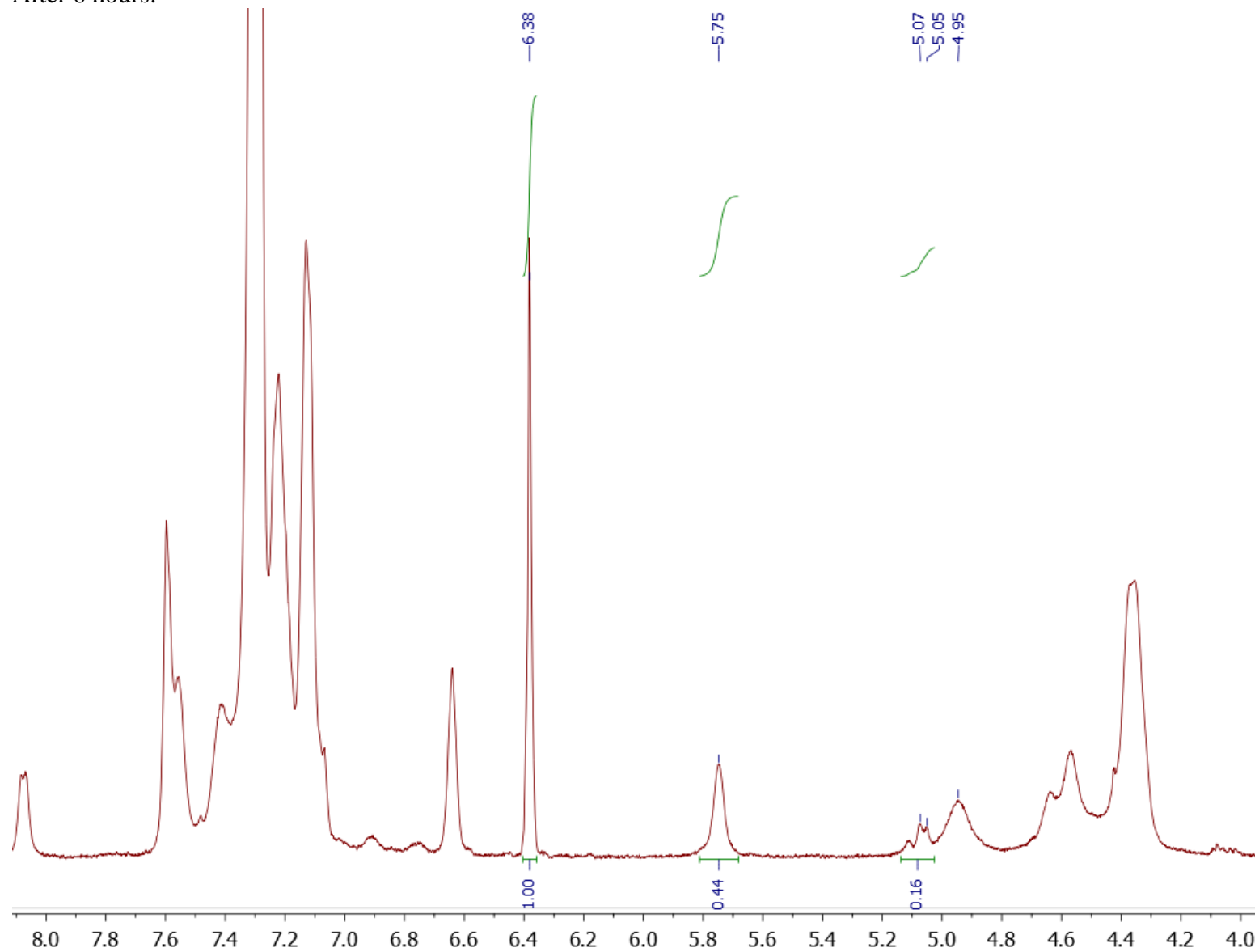
After 4 hours:



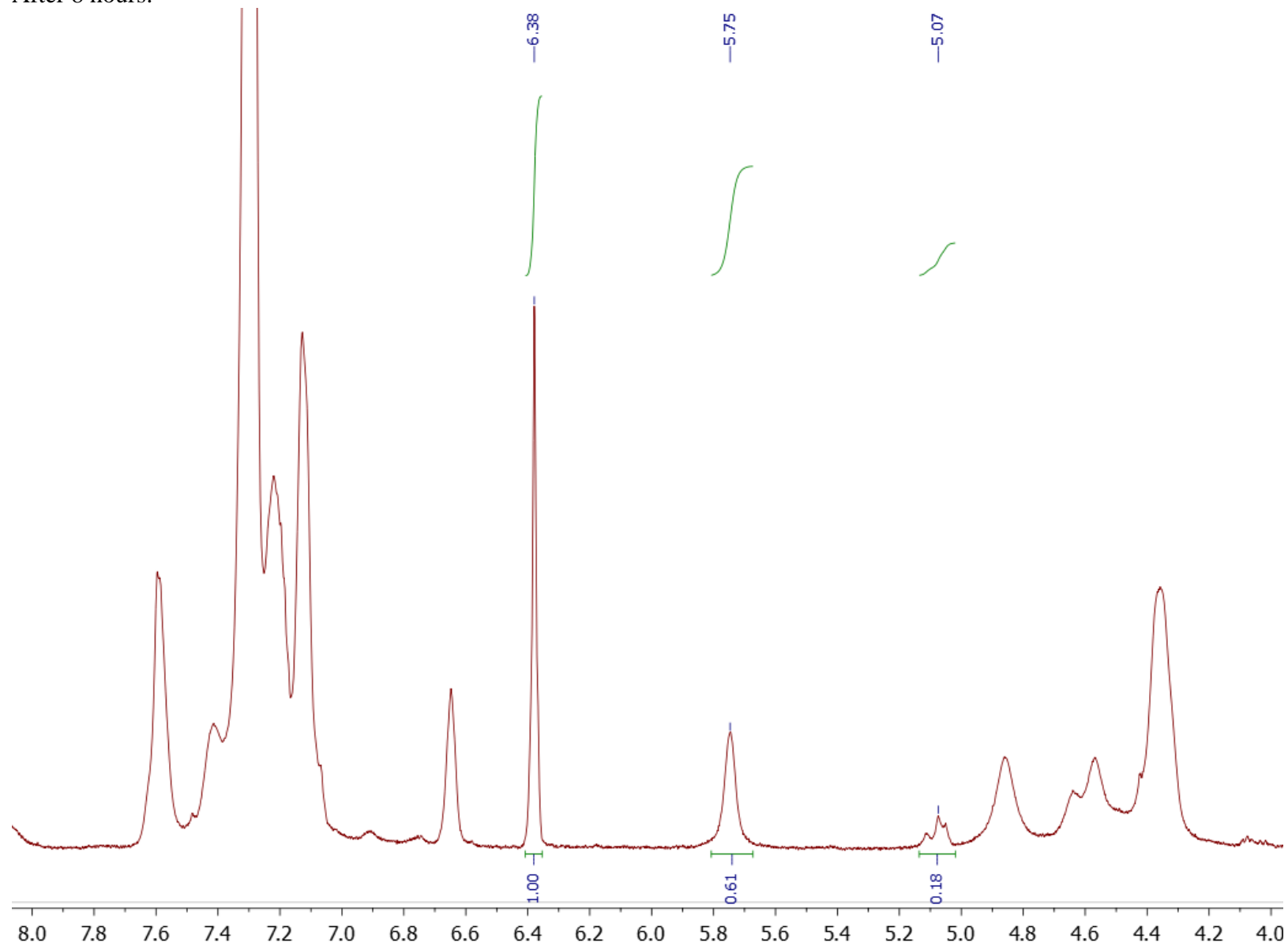
After 5 hours:



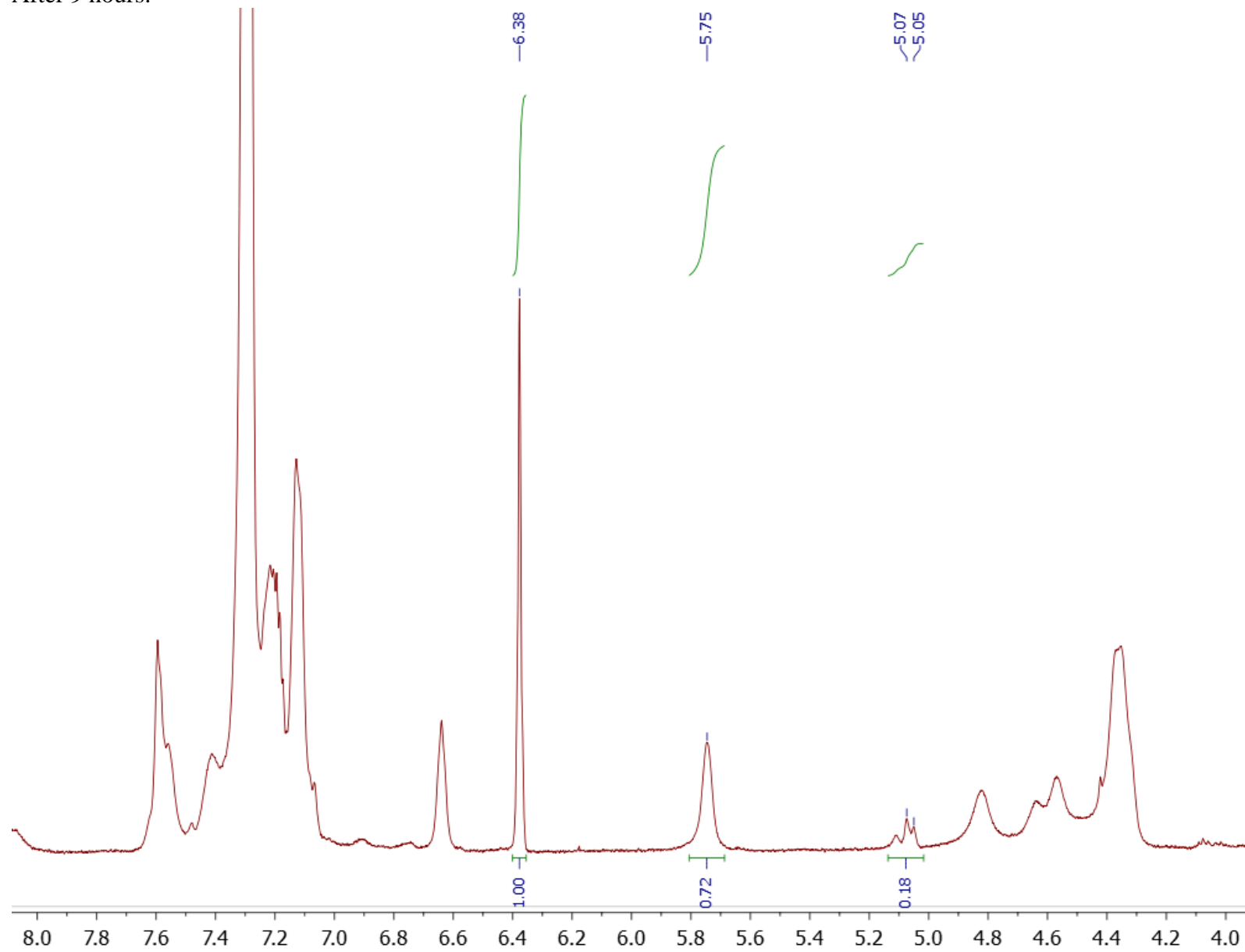
After 6 hours:



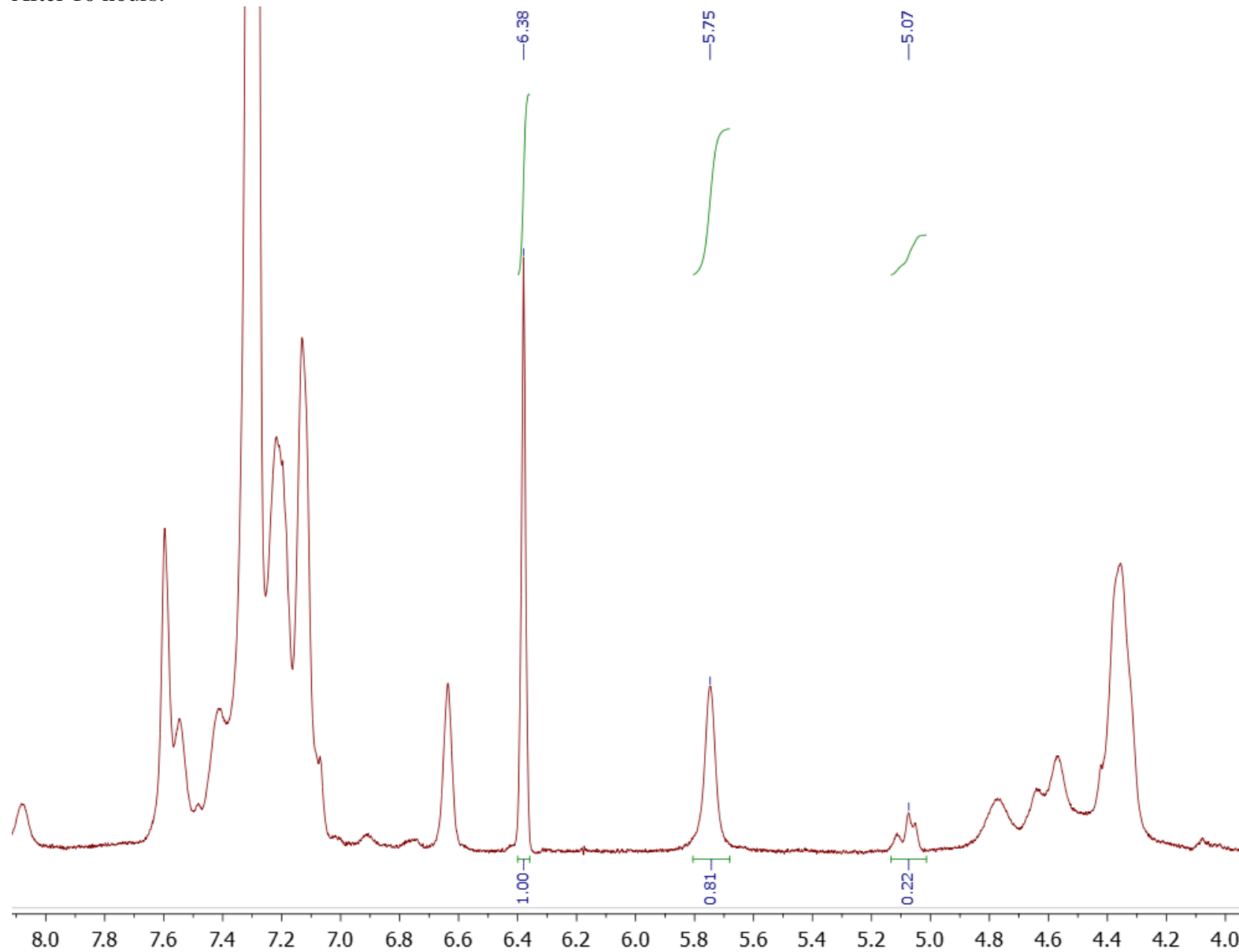
After 8 hours:



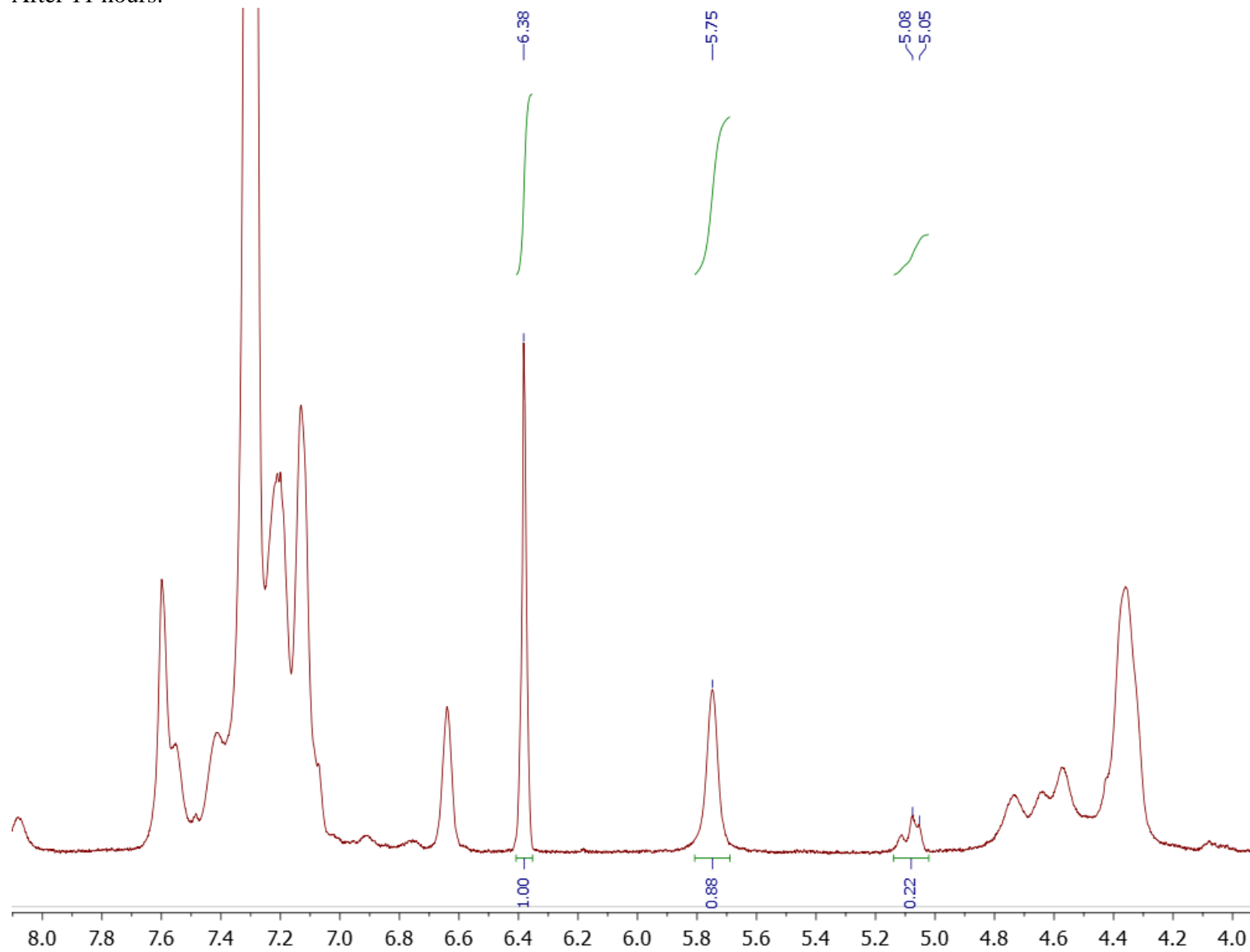
After 9 hours:



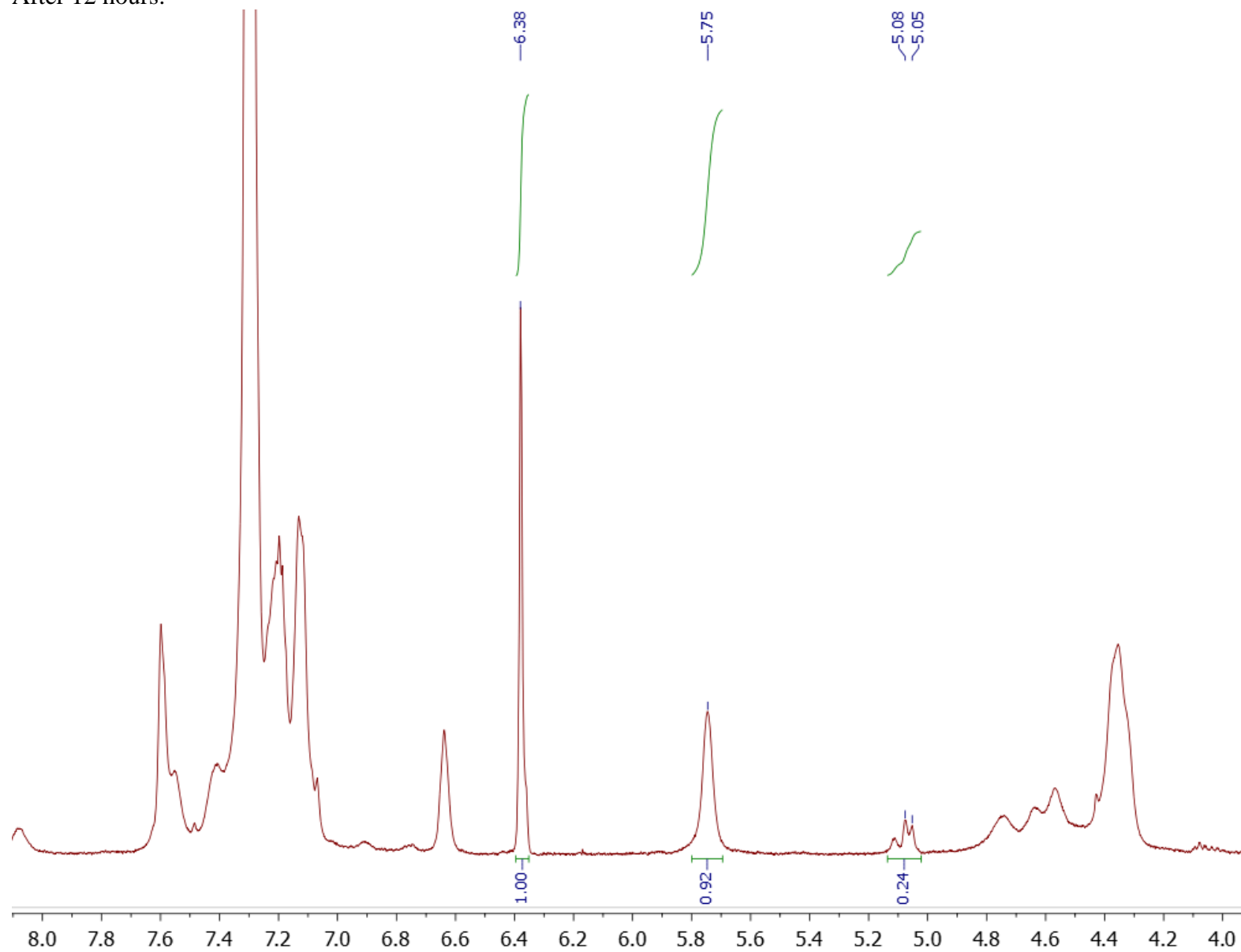
After 10 hours:



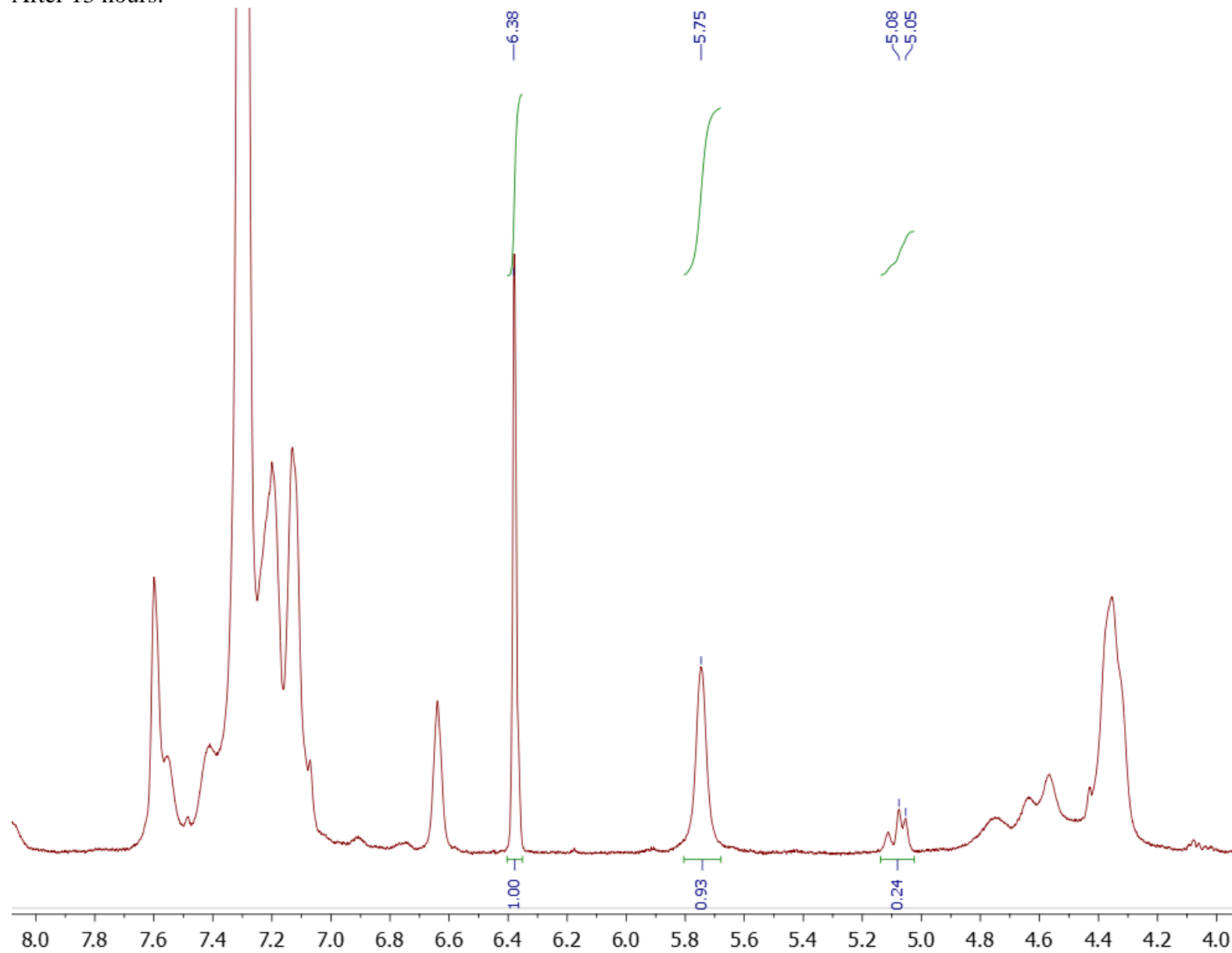
After 11 hours:



After 12 hours:



After 13 hours:

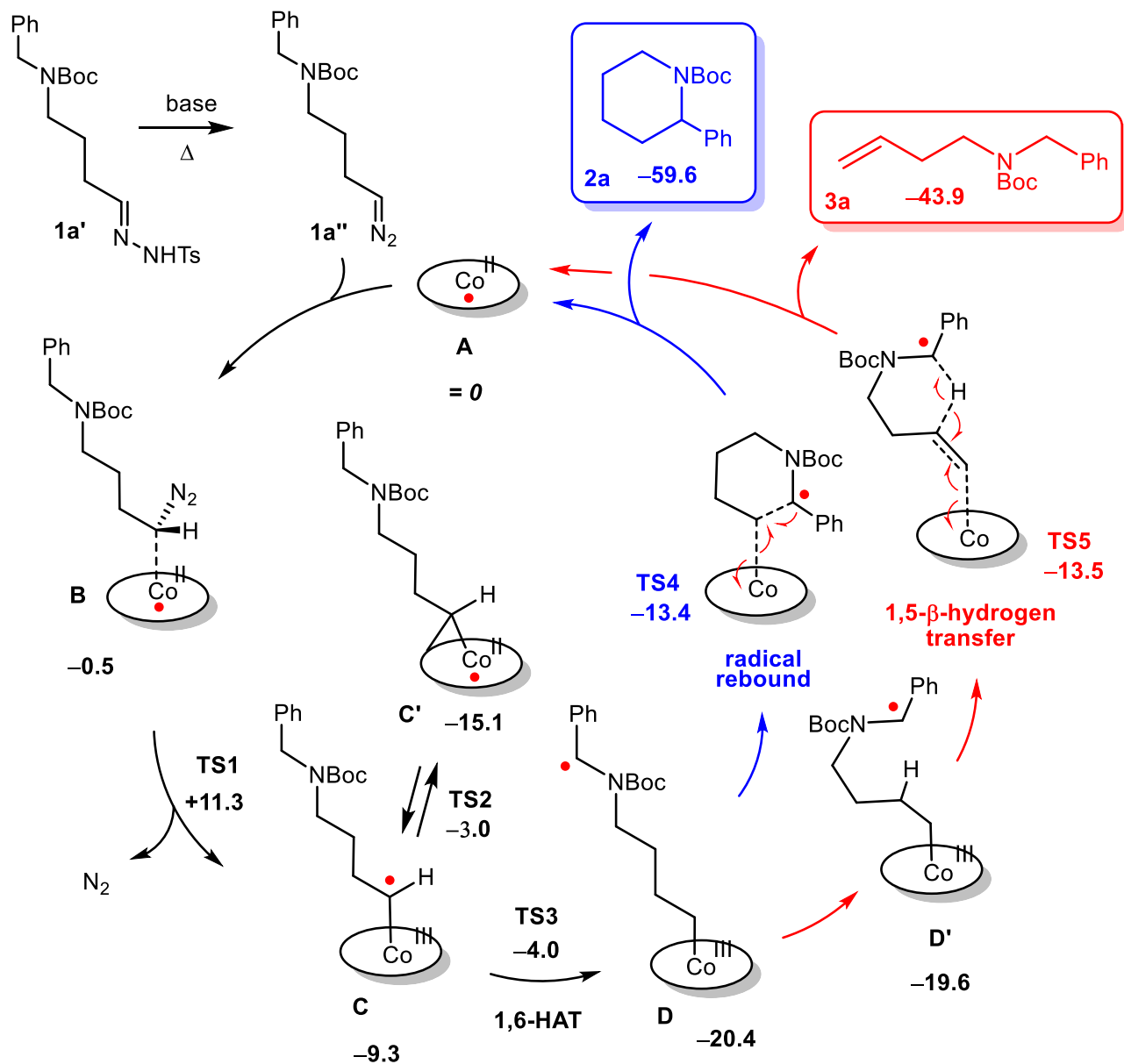


6. Computational methods

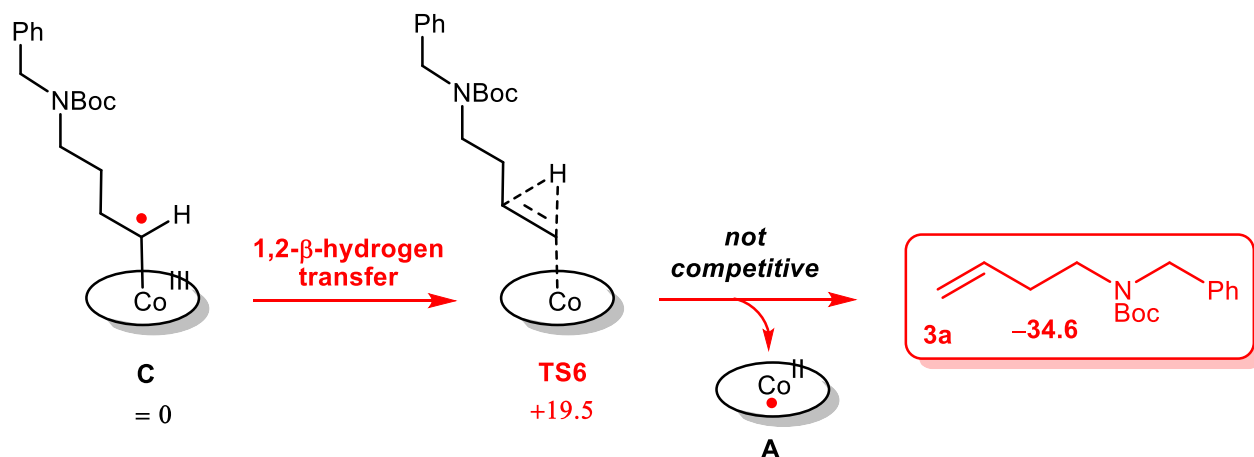
[Co(por)]-catalyzed formation of piperidines and pyrrolidines was investigated computationally using density functional theory (DFT). All geometry optimizations were carried out with the Turbomole program^[13] coupled to the PQS Baker optimizer^[14] via the BOpt package.^[15] All geometries were fully optimized as minima or transition states using the BP86 functional,^[16] the Turbomole def2-TZVP basis set^[17] and a small grid size (m4). To reduce computation time, the resolution-of-identity (ri) approximation^[18] was applied and a simplified porphyrin without phenyl substituents on the *meso*-positions was used (i.e. [Co(por)] instead of [Co(TPP)]). Gas-phase Hessian matrix calculations (BP86/def2-TZVP) were performed to characterize all minima (no imaginary frequencies) and transition states (one imaginary frequency). Thermochemical parameters such as the zero-point energy (ZPE), Gibbs free energy and gas-phase thermal corrections (entropy and enthalpy, 298 K, 1 bar,) were obtained from these analyses. The nature of the transition states was confirmed by following the intrinsic reaction coordinate (IRC). The calculated relative free energies ($\Delta G^\circ_{333\text{K}}$ and $\Delta G^\circ_{298\text{K}}$, in kcal mol⁻¹) are reported in the main text and below. For every transition state, the imaginary eigenvalue was followed in both directions to confirm its connection to the relative reactant and product states. A separate archive file is provided containing Excel sheets with all free energies and enthalpies ($\Delta G^\circ_{333\text{K}}$, $\Delta G^\circ_{298\text{K}}$, $\Delta H_{298\text{K}}$, SCF+ZPE, SCF) and negative eigenvalues of the transition states and all optimized geometries. Optimized geometries of all stationary states and transition states are supplied in .pdb and .xyz format.

A series of test calculations showed that metal-substrate interactions are strongly underestimated when no dispersion corrections are used, therefore Grimme's dispersion corrections (version D3, disp3, zero damping)^[19] were applied to include Van der Waals interactions. A disadvantage of these dispersion corrections is that the dispersion-corrected metal-substrate association/dissociation energies to and from the non-solvated [Co(por)] catalyst **A** are overestimated due to neglected dispersion interactions between cobalt and the solvent. We therefore used the Van der Waals π -complex of [Co(por)] catalyst **A** and an explicit toluene solvent molecule (directly interacting with cobalt) as the energetic reference point in our calculations to prevent overestimation of metal-substrate interactions as a result of such uncompensated dispersion forces. However, this approach also leads to an erroneous cancelation of all translational entropy contributions to the computed free energies. This is because the translational entropy contributions to substrate/product association/dissociation are fully counterbalanced by translational entropy contributions resulting from dissociation/association of the solvent molecule in the DFT calculated thermodynamics ([**A**-solvent complex] + L \rightleftharpoons [**A**-L] + solvent). This is not realistic in comparison to actual solution phase chemistry, for which the translational entropy contributions associated with substrate/product association/dissociation steps can of course not be neglected.^[20] Therefore we applied a translational entropy contribution of 20 cal mol⁻¹ K⁻¹ to the computed free energies of all substrate/product association/dissociation steps in the catalytic cycle (see also the Excel sheets in the separate archive file).

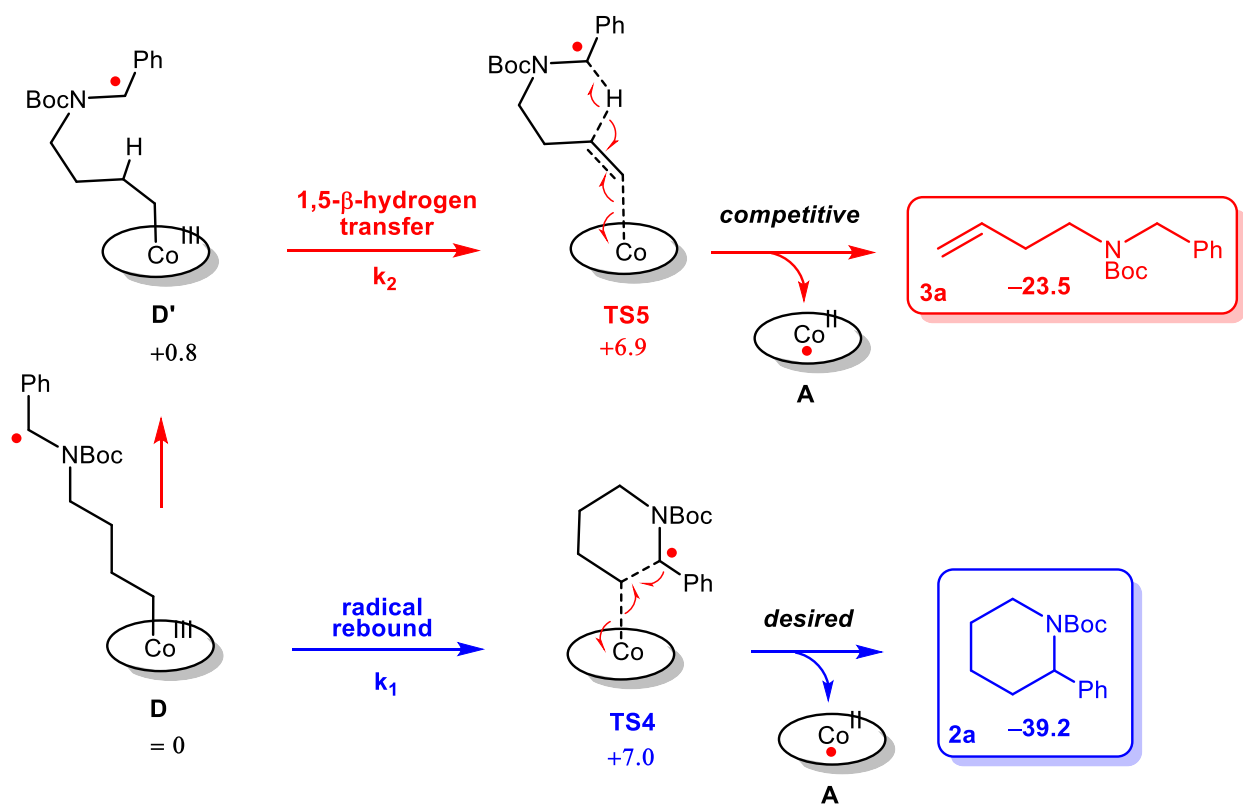
7. Computational studies



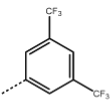
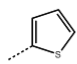
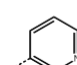
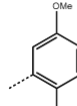
Scheme S1. Proposed mechanisms for [Co(por)]-catalyzed competitive formation of piperidines and alkenes. All Gibbs free energies (ΔG°_{298K} , in kcal mol⁻¹), including those of **TS1-TS5**, are reported relative to **A**.



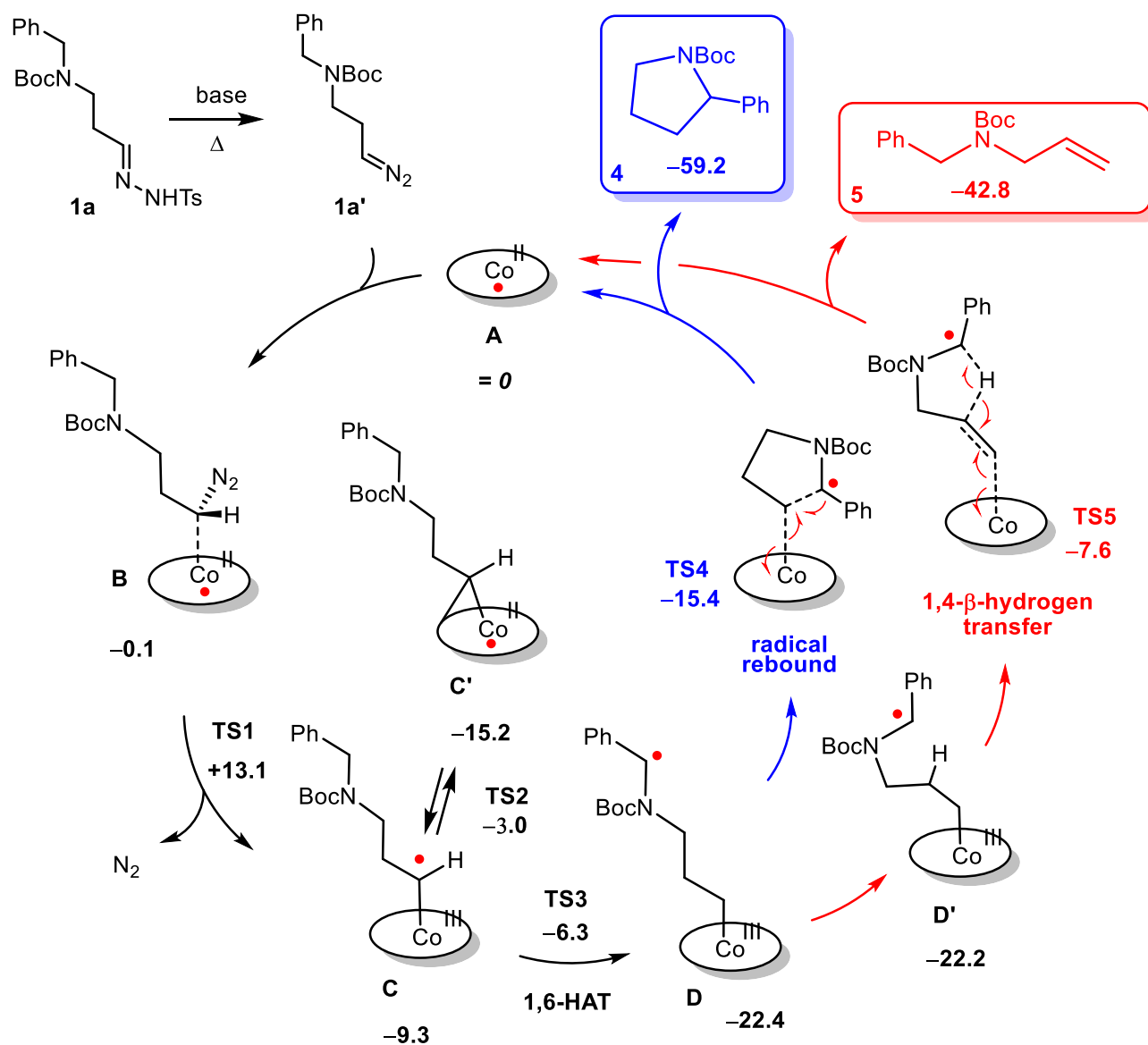
Scheme S2. Direct 1,2-β-hydrogen atom transfer is not in competition with piperidine formation. All Gibbs free energies ($\Delta G^\circ_{298\text{K}}$, in kcal mol⁻¹), including the energy of **TS6**, are reported relative to **C**.



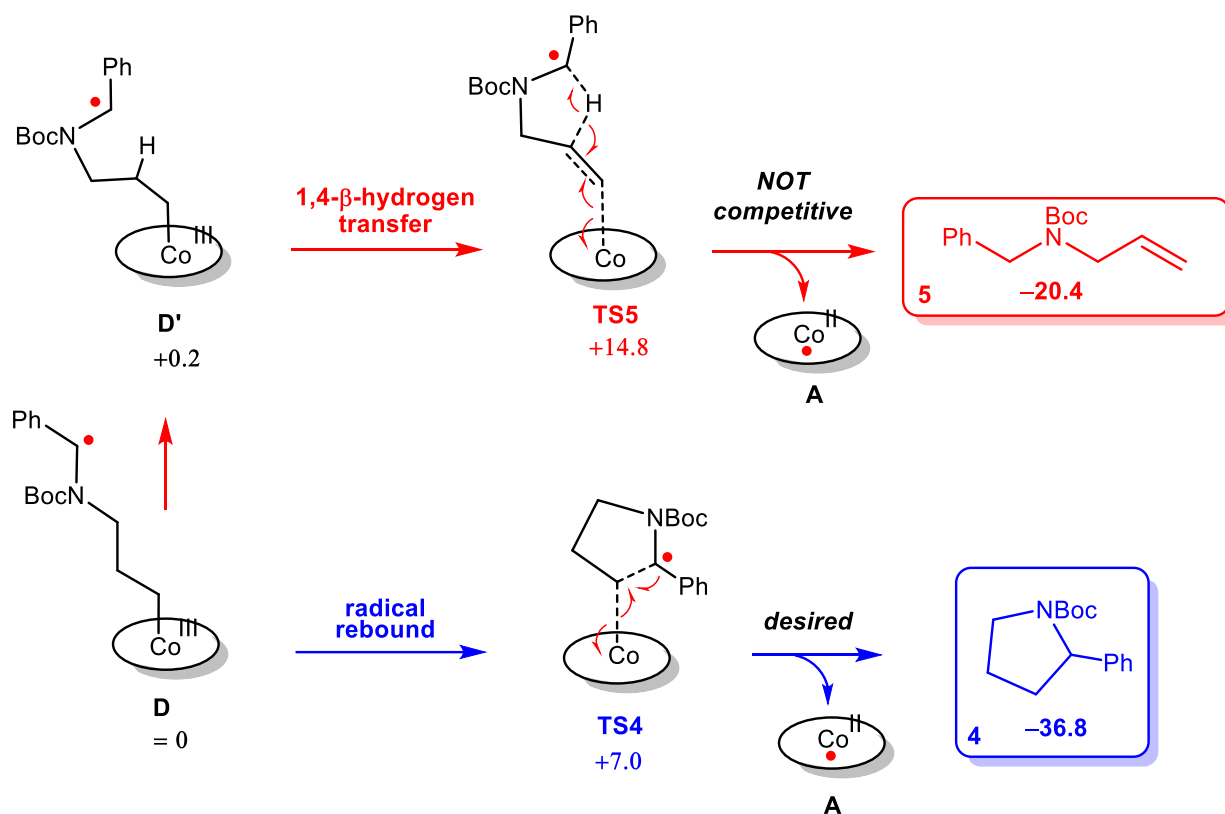
Scheme S3. Piperidine formation is in competition with alkene formation via 1,5-β-hydrogen atom transfer. All Gibbs free energies ($\Delta G^\circ_{298\text{K}}$, in kcal mol⁻¹), including those of **TS4** and **TS5**, are reported relative to **D**.

	k_1/k_2	β -hydrogen 1,5-HAT		Rebound C-C coupling	
		TS5	3	TS4	2
 Y = -C₆H₃(CF₃)₂	2.1	+8.6	-22.7	+8.1	-38.4
 Y = -thiophene	17.7	+11.0 (+11.5)	-19.3	+9.1 (+10.1)	-35.3
 Y = -pyridine	1.6	+8.0 (+8.5)	-23.0	+7.7 (+7.9)	-38.6
 Y = -C₆H₃(Br)(OMe)	0.2	+4.9 (+8.8)	-24.8	+6.1 (+9.9)	-38.0

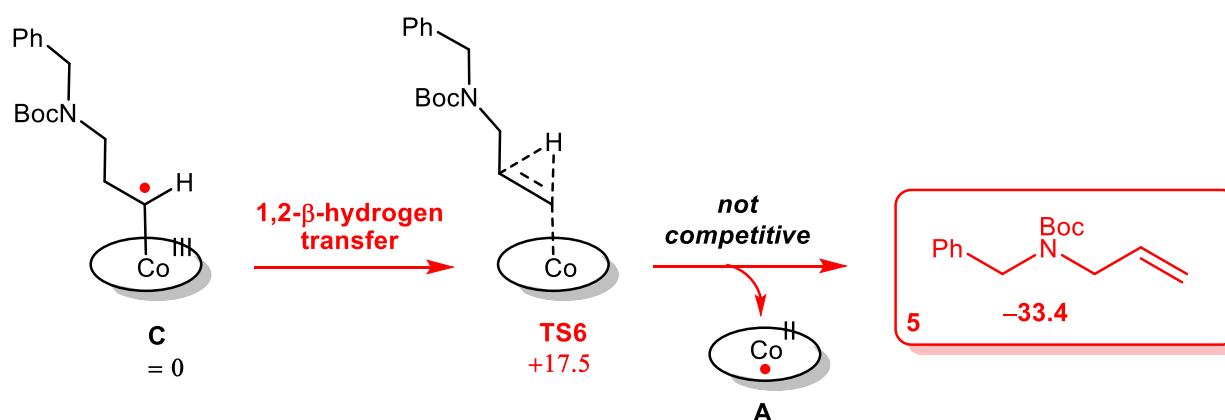
Scheme S4. Dependence of the degree of competition between piperidine and alkene formation on the substitution of the substrate. All Gibbs free energies (ΔG°_{298K} , in kcal mol⁻¹), including those of **TS4** and **TS5**, are reported relative to **D**. For k_1 and k_2 , see Scheme S3. Values between brackets correspond to the energies of transition states that have a higher energy barrier due to a different conformation caused by a different orientation of substituents.



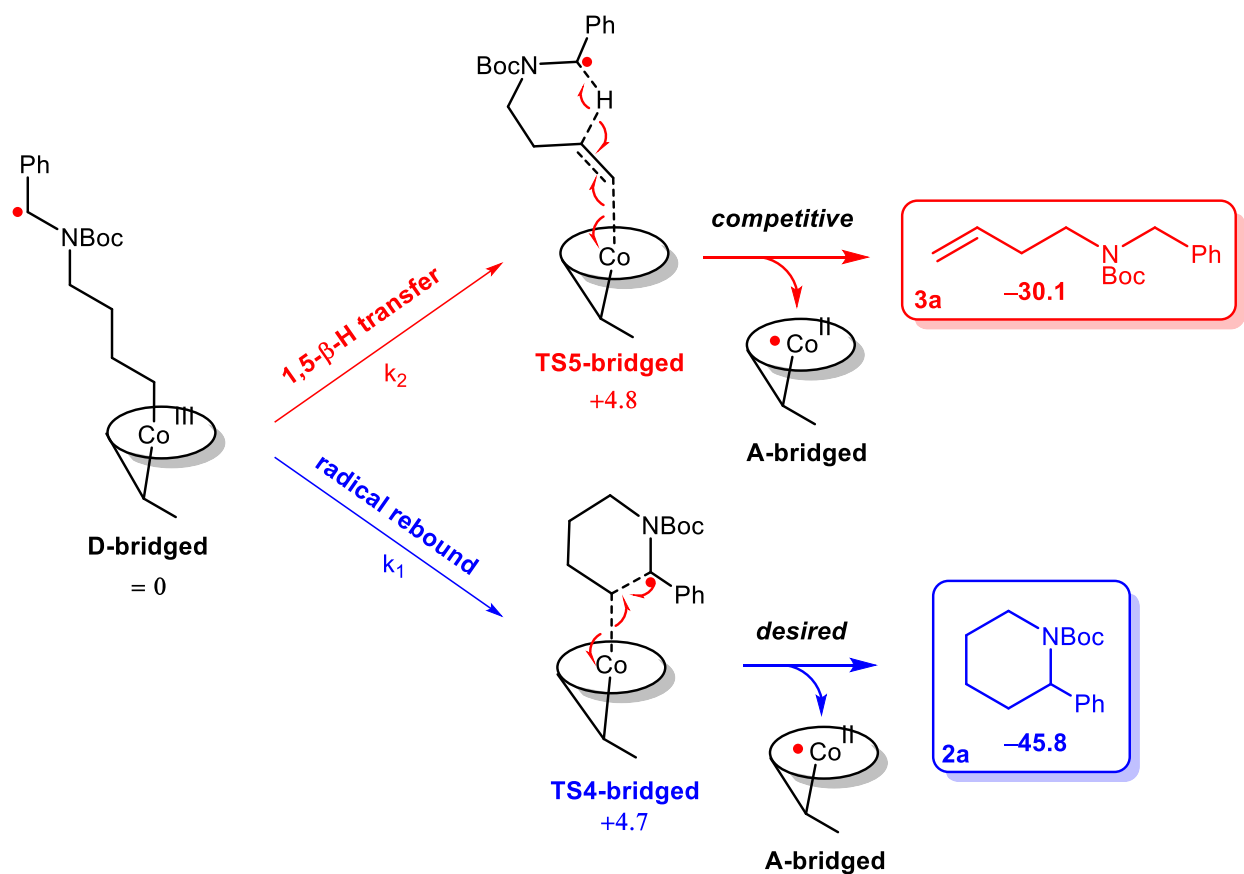
Scheme S5. Proposed mechanism for [Co(por)]-catalyzed formation of pyrrolidines. Because of a significantly higher barrier, alkene formation is *not* in competition with pyrrolidine formation. All Gibbs free energies (ΔG°_{298K} , in kcal mol⁻¹), including those of **TS1-TS5**, are reported relative to **A**.



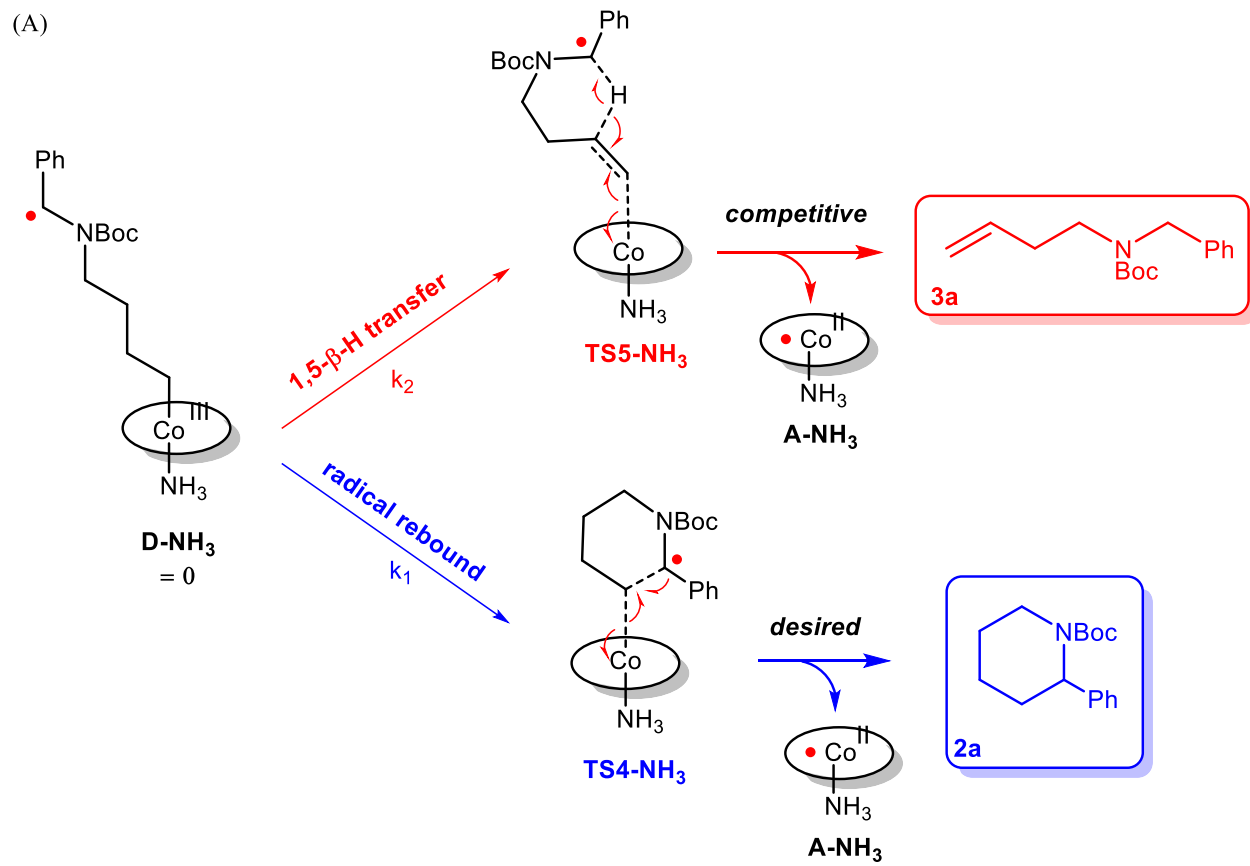
Scheme S6. Because of a significantly higher barrier, alkene formation is *not* in competition with pyrrolidine formation. All Gibbs free energies ($\Delta G^\circ_{298\text{K}}$, in kcal mol⁻¹), including those of **TS4** and **TS5**, are reported relative to **D**.



Scheme S7. Not only alkene formation through 1,4-β-hydrogen atom transfer (Scheme S5–6), but also alkene formation through direct 1,2-β-hydrogen atom transfer is not in competition with pyrrolidine formation. This is similar to the case of the piperidines, but in the case of pyrrolidine formation, the effect is even more pronounced. All Gibbs free energies ($\Delta G^\circ_{298\text{K}}$, in kcal mol⁻¹), including the energy of **TS6**, are reported relative to **C**.



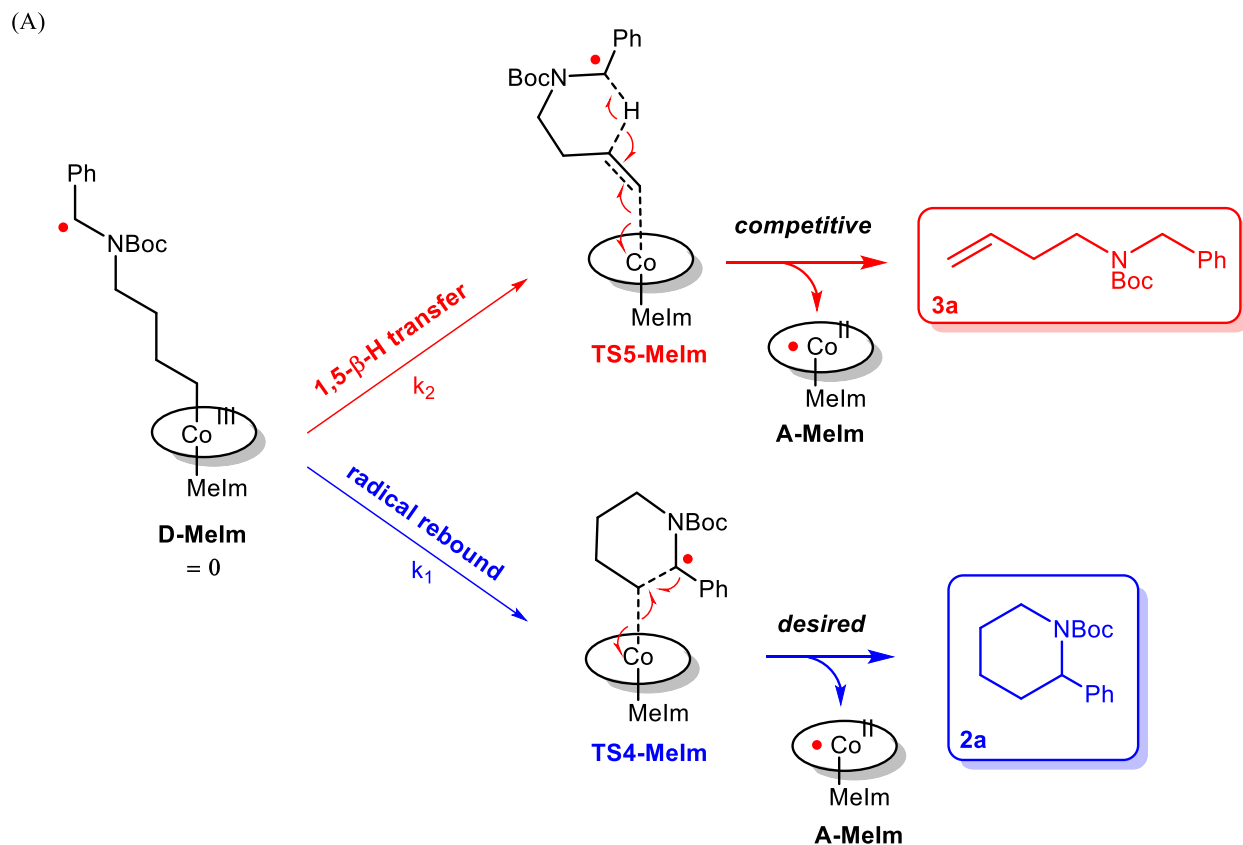
Scheme S8. The effect of coordination of a carbene that is bridging between the metal and a pyrrolato nitrogen of the porphyrin, formed by insertion of the ‘terminal’ carbene into the M–N bond.^[21] All Gibbs free energies ($\Delta G^\circ_{298\text{K}}$, in kcal mol⁻¹), including those of **TS4** and **TS5**, are reported relative to **D-bridged**.



(B)

	TS4-NH_3	TS5-NH_3	k_1/k_2
298 K (25 °C)	9.1	10.5	10.6
333 K (60 °C)	9.3	10.9	10.4
378 K (105 °C)	9.7	11.4	10.1

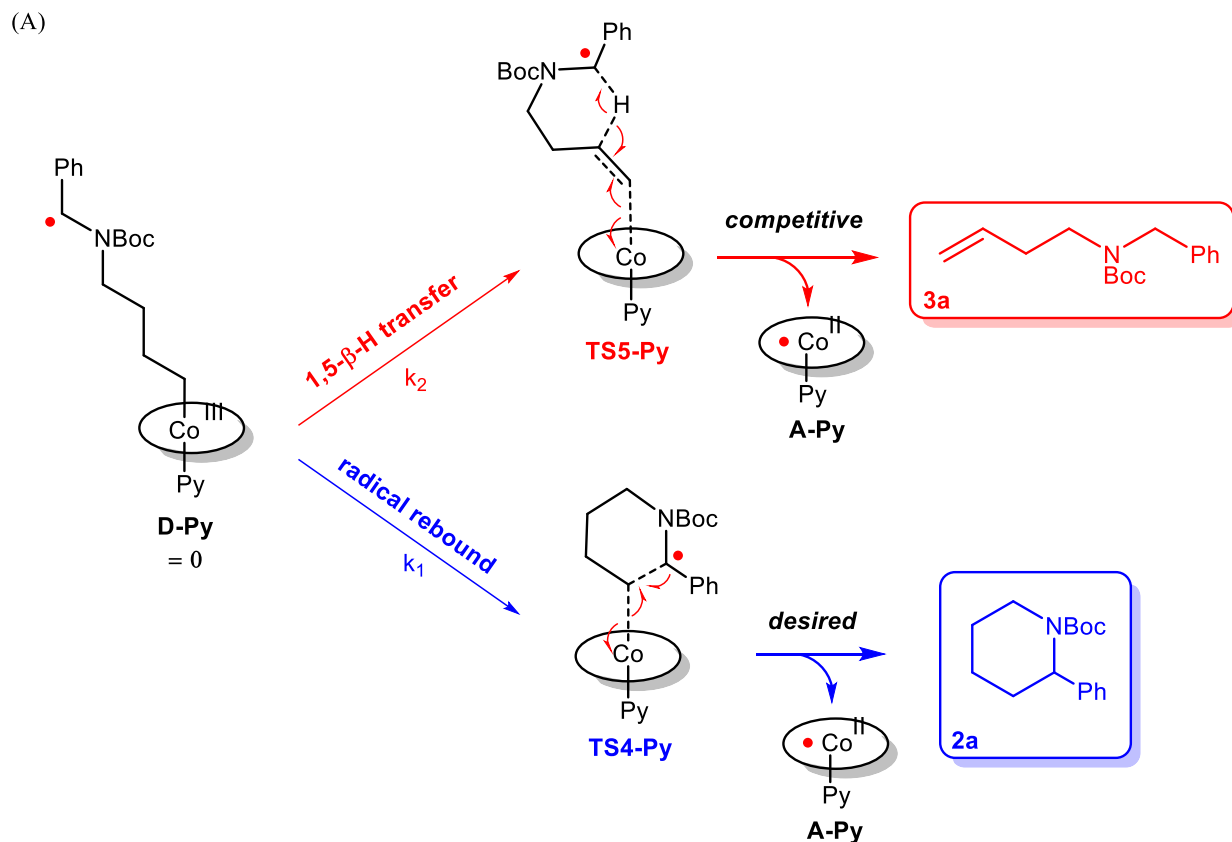
Scheme S9. (A) The effect of axial coordination of NH_3 (as a simplified model for a variety of possible ligands, see main text). All Gibbs free energies ($\Delta G^\circ_{298\text{K}}$, in kcal mol^{-1}), including those of **TS4** and **TS5**, are reported relative to **D-NH₃**. (B) The computed temperature dependence of the effect of NH_3 coordination on the energy barriers for $[\text{Co}(\text{por})]$ -catalyzed piperidine and alkene formation. NH_3 was assumed not to dissociate at the selected elevated temperatures.



(B)

	TS4-MeIm	TS5-MeIm	k_1/k_2
298 K (25 °C)	9.2	10.3	6.2
333 K (60 °C)	9.3	10.5	5.9
378 K (105 °C)	9.6	10.8	5.6

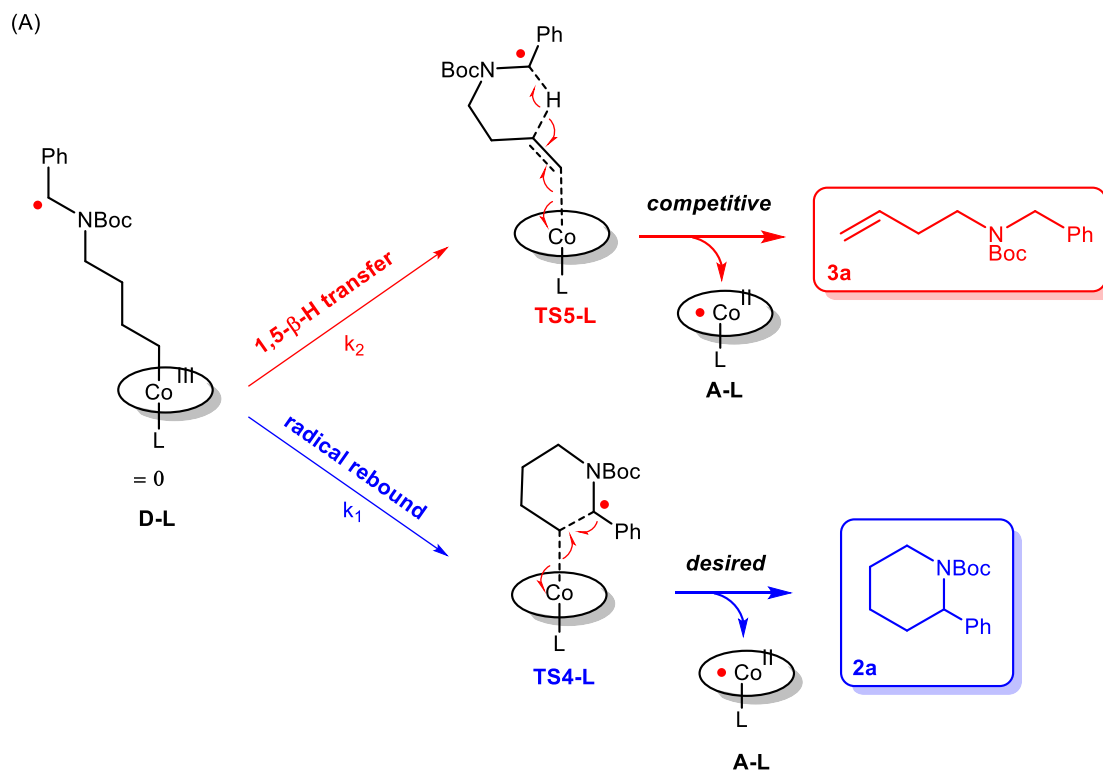
Scheme S10. (A) The effect of axial coordination of methylimidazole (as a simplified model for a variety of possible ligands, see main text). (B) The computed temperature dependence of the effect of methylimidazole coordination on the energy barriers for [Co(por)]-catalyzed piperidine and alkene formation. Methylimidazole was assumed not to dissociate at the selected elevated temperatures. All Gibbs free energies (ΔG° , in kcal mol⁻¹), including those of **TS4** and **TS5**, are reported relative to **D-MeIm**.



(B)

	TS4-Py	TS5-Py	k_1/k_2
298 K (25 °C)	8.8	10.4	15.2
333 K (60 °C)	9.0	10.7	14.4
378 K (105 °C)	9.2	11.2	13.7

Scheme S11. (A) The effect of axial coordination of pyridine (as a simplified model for a variety of possible ligands, see main text). (B) The computed temperature dependence of the effect of pyridine coordination on the energy barriers for [Co(por)]-catalyzed piperidine and alkene formation. Pyridine was assumed not to dissociate at the selected elevated temperatures. All Gibbs free energies (ΔG° , in kcal mol⁻¹), including those of **TS4** and **TS5**, are reported relative to **D-Py**.



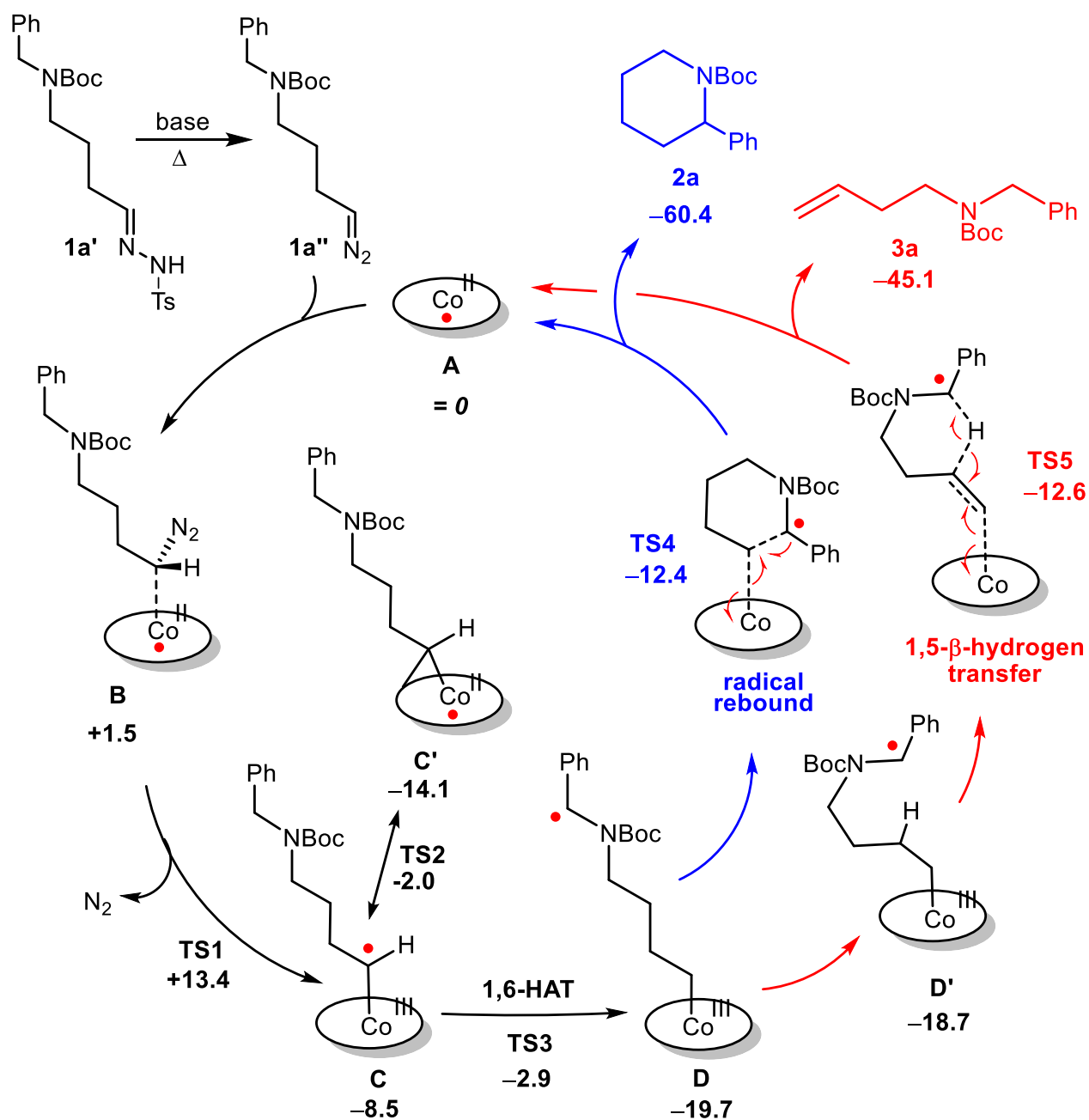
(B)

L	binding energy of ligand L in D-L (kcal mol ⁻¹)	TS4-L	TS5-L	k_1/k_2
-	-	6.9	7.0	1.2
NH ₃	-5.1	9.1	10.5	10.6
MeIm	-7.2	9.2	10.2	6.2
Py	-6.3	8.8	10.4	15.2

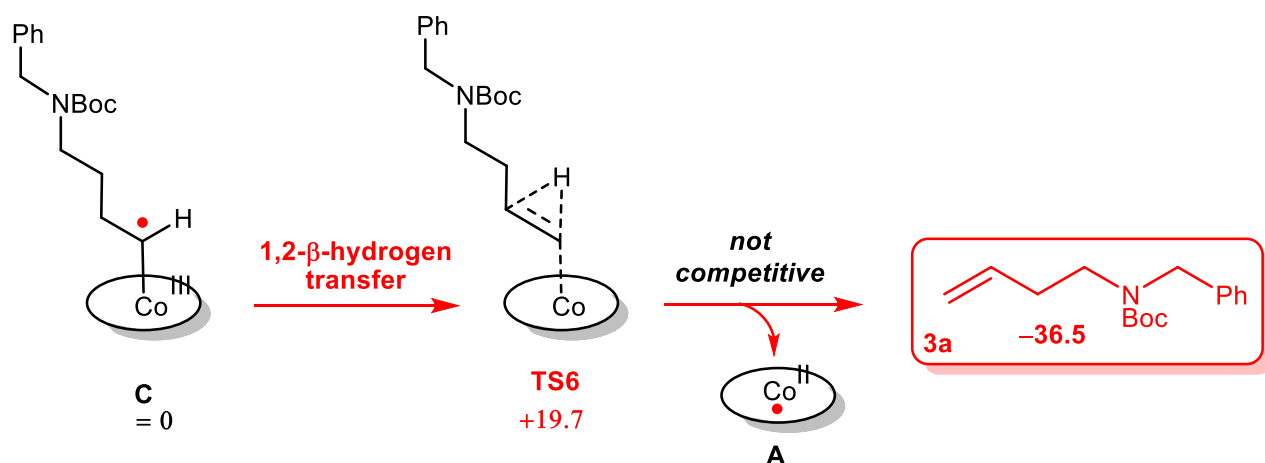
(C)

L	binding energy of ligand L in D-L (kcal mol ⁻¹)	TS4-L	TS5-L	k_1/k_2
-	-	7.1	7.3	1.3
NH ₃	-5.7	9.3	10.9	10.4
MeIm	-8.4	9.3	10.5	5.9
Py	-7.3	9.0	10.7	14.4

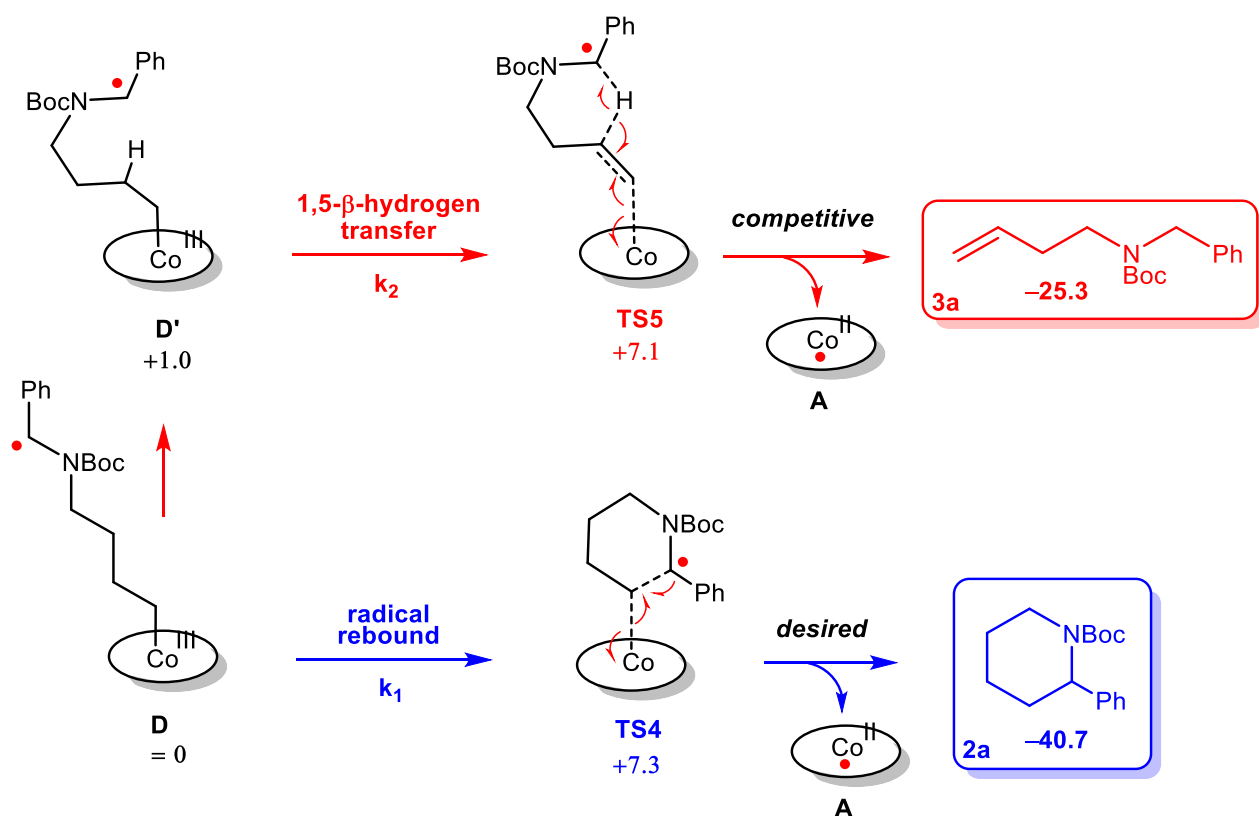
Scheme S12. (A) The effect of axial coordination of different ligands (**L**) to cobalt on the selectivity. (B) and (C) The binding energies of ligands **L** in intermediates **D-L** and the corresponding energy barriers for [Co(por)]-catalyzed piperidine and alkene formation. No clear correlation can be observed between the binding energies and the energy barriers. Ligands **L** were assumed not to dissociate at the selected elevated temperatures. All Gibbs free energies (ΔG° , in kcal mol⁻¹), including those of **TS4** and **TS5**, are reported relative to **D-L**. The energies in table B were calculated at 298K, the energies in table C were calculated at 333K.



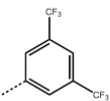
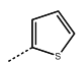
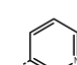
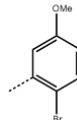
Scheme S13. Proposed mechanisms for [Co(por)]-catalyzed competitive formation of piperidines and alkenes. All Gibbs free energies (ΔG°_{333K} , in kcal mol⁻¹), including those of **TS1-TS5**, are reported relative to **A**.



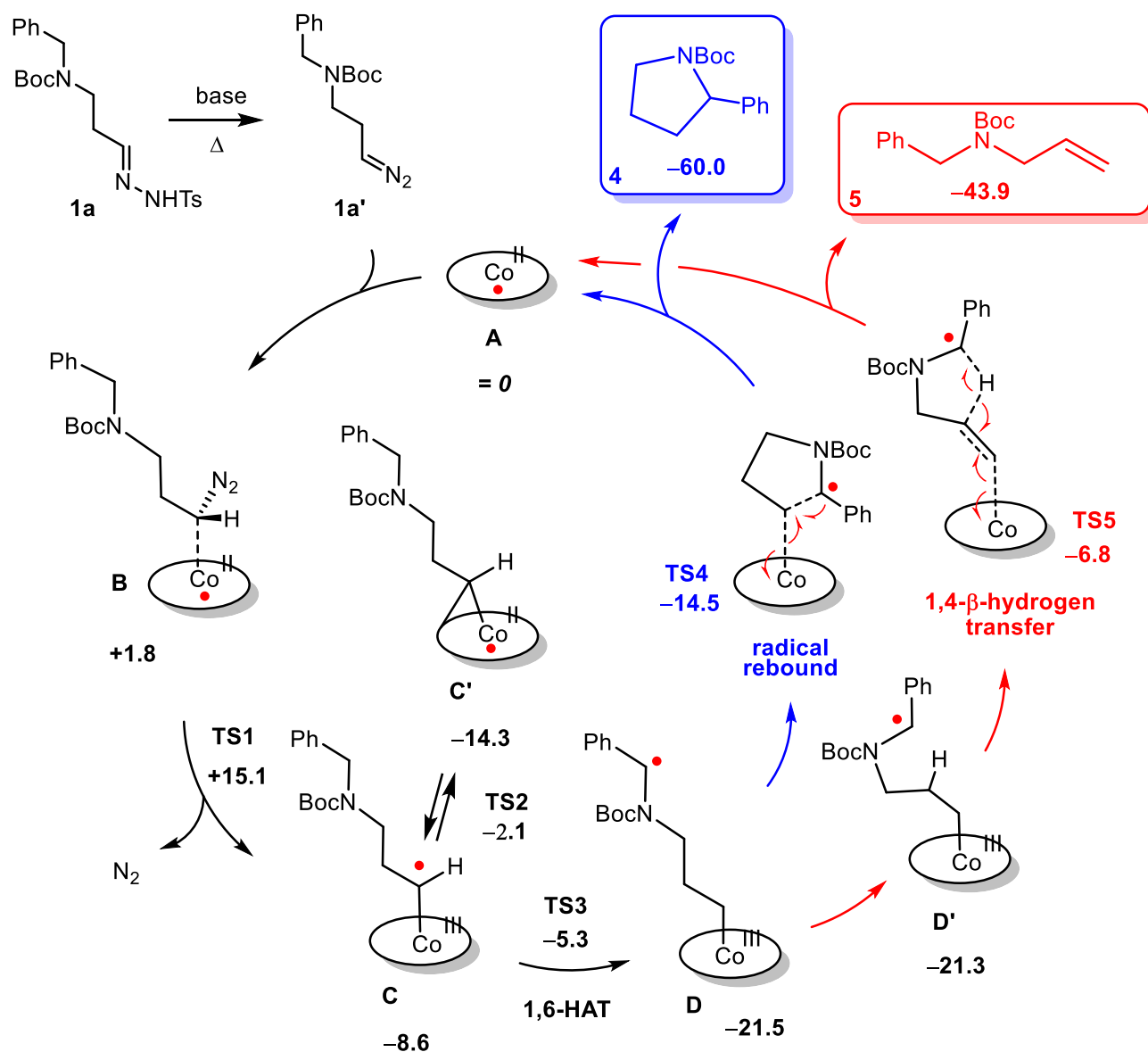
Scheme S14. Direct 1,2-β-hydrogen atom transfer is not in competition with piperidine formation. All Gibbs free energies ($\Delta G^\circ_{333\text{K}}$, in kcal mol⁻¹), including the energy of **TS6**, are reported relative to **C**.



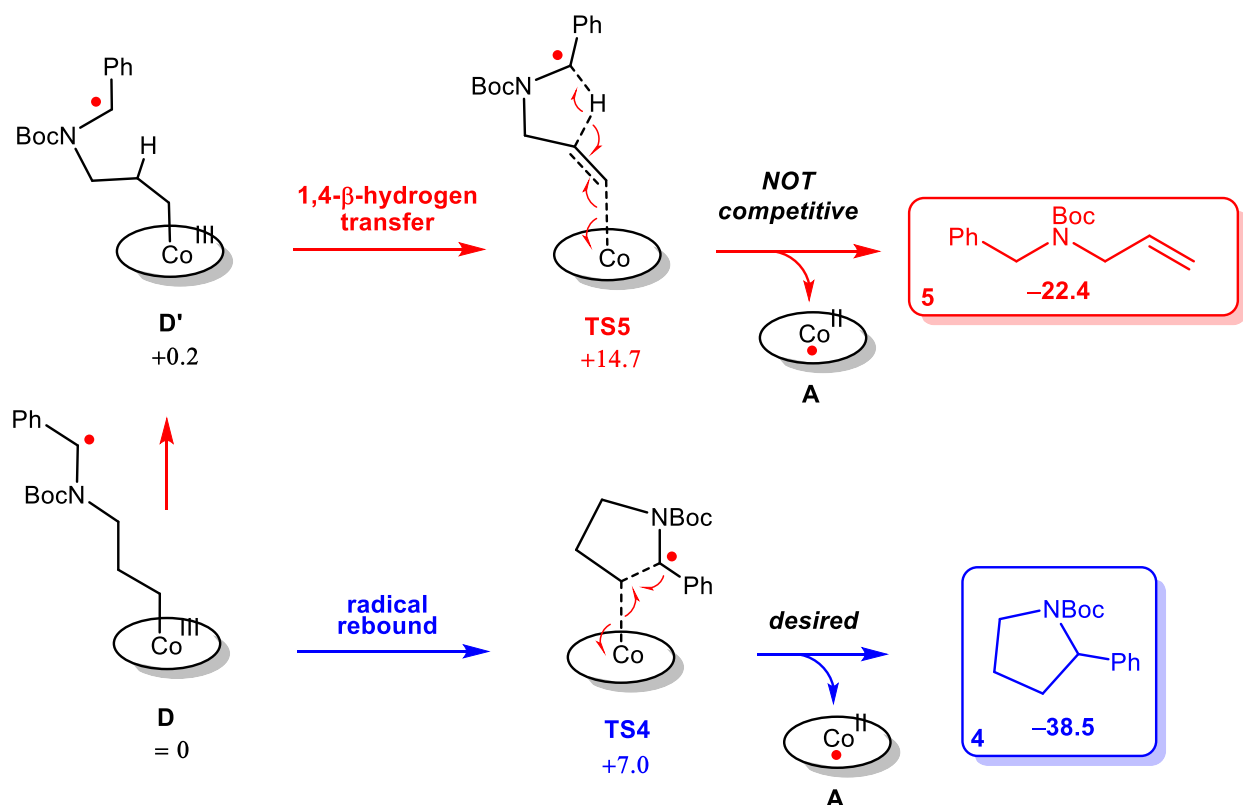
Scheme S15. Piperidine formation is in competition with alkene formation via 1,5-β-hydrogen atom transfer. All Gibbs free energies ($\Delta G^\circ_{333\text{K}}$, in kcal mol⁻¹), including those of **TS4** and **TS5**, are reported relative to **D**.

	k_1/k_2	β -hydrogen 1,5-HAT		Rebound C-C coupling	
		TS5	3	TS4	2
 Y = -C₆H₃(CF₃)₂	1.6	+8.8	-20.4	+8.5	-35.6
 Y = -thiophene	20.5	+11.2 (+11.8)	-17.0	+9.2 (+10.3)	-32.6
 Y = -pyridine	1.8	+8.3 (+8.8)	-20.6	+7.9 (+8.1)	-35.8
 Y = -C₆H₃(Br)(OMe)	0.2	+5.2 (+9.1)	-26.6	+6.4 (+10.3)	-39.4

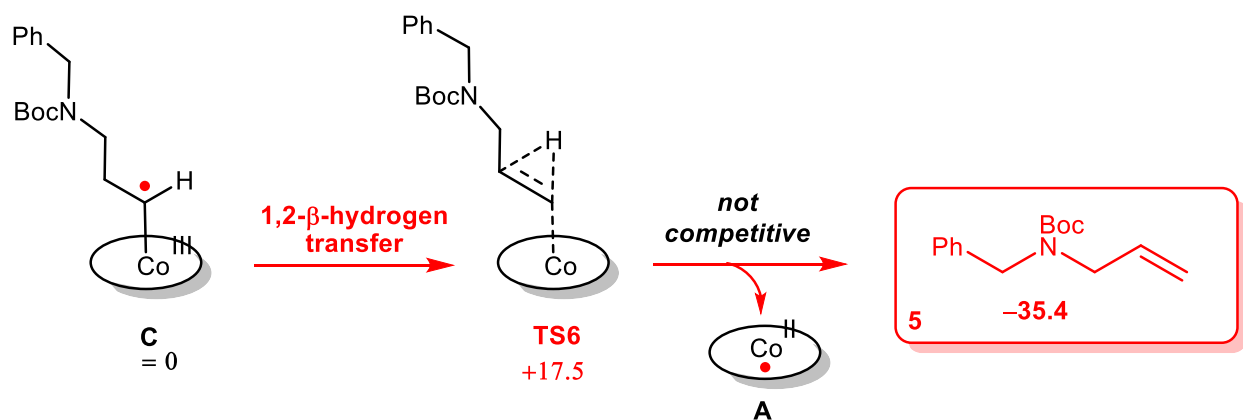
Scheme S16. Dependence of the degree of competition between piperidine and alkene formation on the substitution of the substrate. All Gibbs free energies (ΔG°_{333K} , in kcal mol⁻¹), including those of **TS4** and **TS5**, are reported relative to **D**. For k_1 and k_2 , see Scheme S15. Values between brackets correspond to the energies of transition states that have a higher energy barrier due to a different conformation caused by a different orientation of substituents.



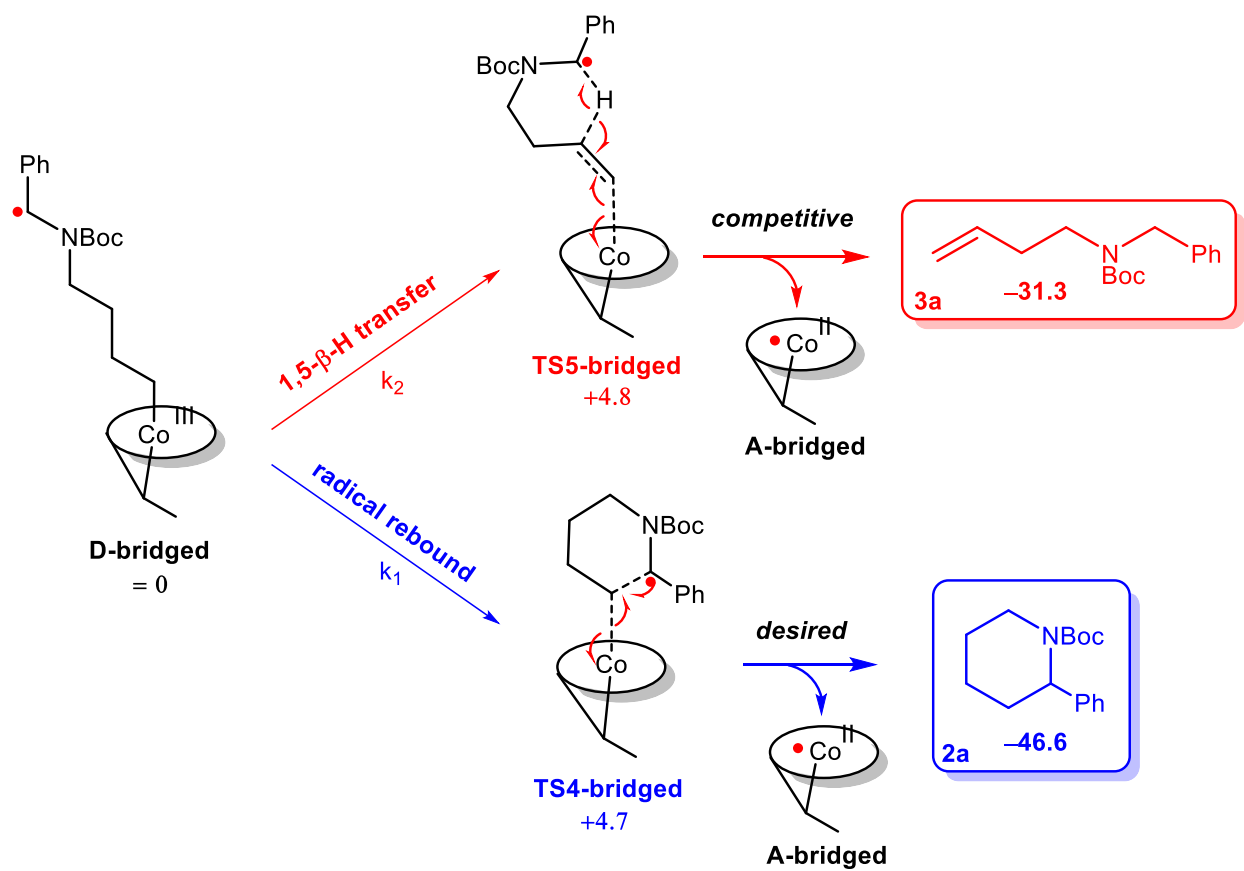
Scheme S17. Proposed mechanism for [Co(por)]-catalyzed formation of pyrrolidines. Because of a significantly higher barrier, alkene formation is *not* in competition with pyrrolidine formation. All Gibbs free energies ($\Delta G^\circ_{333\text{K}}$, in kcal mol^{-1}), including those of **TS1-TS5**, are reported relative to **A**.



Scheme S18. Because of a significantly higher barrier, alkene formation is *not* in competition with pyrrolidine formation. All Gibbs free energies ($\Delta G^\circ_{333\text{K}}$, in kcal mol⁻¹), including those of **TS4** and **TS5**, are reported relative to **D**.



Scheme S19. Not only alkene formation through 1,4- β -hydrogen atom transfer (Scheme S17–18), but also alkene formation through direct 1,2- β -hydrogen atom transfer is not in competition with pyrrolidine formation. This is similar to the case of the piperidines, but in the case of pyrrolidine formation, the effect is even more pronounced. All Gibbs free energies ($\Delta G^\circ_{333\text{K}}$, in kcal mol⁻¹), including the energy of **TS6**, are reported relative to **C**.



Scheme S20. The effect of coordination of a carbene that is bridging between the metal and a pyrrolato nitrogen of the porphyrin, formed by insertion of the ‘terminal’ carbene into the M–N bond.²¹ All Gibbs free energies ($\Delta G^\circ_{333\text{K}}$, in kcal mol⁻¹), including those of **TS4** and **TS5**, are reported relative to **D-bridged**.

8. References

- [1] C.F. Bender, R.A. Widenhoefer *J. Am. Chem. Soc.* **2005**, *127*, 1070.
- [2] S.G. Davies, A.L.A. Figuccia, A.M.F. Paul, M. Roberts, J.E. Thomson *J. Org. Chem.* **2016**, *81*, 6481.
- [3] J.R. Parikh, W. von Eggers Doering *J. Am. Chem. Soc.* **1967**, *89*, 5505.
- [4] D. Crich, K. Ranganathan *J. Am. Chem. Soc.* **2005**, *127*, 9924.
- [5] C.J. Kowalski, A.E. Weber, K.W. Fields *J. Org. Chem.* **1982**, *47*, 5088.
- [6] Y. Wang, X. Wen, X. Cui, X.P. Zhang, *J. Am. Chem. Soc.* **2018**, *140*, 4792.
- [7] K.R. Dieter, J. Li *J. Org. Chem.* **1997**, *62*, 7726.
- [8] I. Coldham, D. Leonori *Org. Lett.* **2008**, *10*, 3923.
- [9] E.J. Cochrane, D. Leonori, L.A. Hassall, I. Coldham *Chem. Commun.* **2014**, *50*, 9910.
- [10] A. Noble, D.W.C. MacMillan *J. Am. Chem. Soc.* **2014**, *136*, 11602.
- [11] K.D. Hesp, D.P. Fernando, W. Jiao, A.T. Londregan, *Org. Lett.* **2014**, *16*, 413.
- [12] M. Leolukman, P. Paoprasert, Y. Wang, V. Makhija, D.J. McGee, P. Gopalan *Macromolecules* **2008**, *41*, 4651.
- [13] University of Karlsruhe and Forschungszentrum Karlsruhe GmbH. *TURBOMOLE* V7.3.1; TURBOMOLE GmbH, 2018.
- [14] J. Baker *J. Comput. Chem.* **1986**, *7*, 385.
- [15] P.H.M. Budzelaar *J. Comput. Chem.* **2007**, *28*, 2226.
- [16] (a) J. P. Perdew *Phys. Rev. B: Condens. Matter Mater. Phys.* **1986**, *33*, 8822. (b) A.D. Becke *Phys. Rev. A: At., Mol., Opt. Phys.* **1988**, *38*, 3098.
- [17] F. Weigend, R. Ahlrichs *Phys. Chem. Chem. Phys.* **2005**, *7*, 3297.
- [18] (a) K. Eichkorn, F. Weigend, O. Treutler, R. Ahlrichs *Theor. Chem. Acc.* **1997**, *97*, 119. (b) K. Eichkorn, O. Treutler, H. Öhm, M. Häser, R. Ahlrichs *Chem. Phys. Lett.* **1995**, *240*, 283. (c) F. Weigend, *Phys. Chem. Chem. Phys.* 2006, *8*, 1057.
- [19] S. Grimme, J. Antony, S. Ehrlich, H. Krieg *J. Chem. Phys.* **2010**, *132*, 154104.
- [20] In solution, the catalyst is completely surrounded by solvent molecules, leading to small translational entropy contributions to the toluene association/dissociation steps. These are of little influence on the translational entropy contributions associated with substrate/product association/dissociation. Hence, the latter are not canceled by the former in toluene solution.
- [21] W.I. Dzik, X. Xu, X.P. Zhang, J.N H. Reek, B. de Bruin, *J. Am. Chem. Soc.* **2010**, *132*, 10891.

De Bruin_piperidines_article_plus_ESI_ChemRxiv.pdf (15.06 MiB)

[view on ChemRxiv](#) • [download file](#)

Other files

De Bruin_piperidines_raw data_7_2_2019.zip (577.49 KiB)

[view on ChemRxiv](#) • [download file](#)
